TU Delft Delft University of Technology

DELTA 21

11.04.2024

# Sustainable Design Development of a Concrete Lock Chamber

REACHING A SUSTAINABLE AND DURABLE DESIGN OF A SHIP LOCK CONCRETE HARD STRUCTURE, ENABLING NAVIGATION THROUGH THE HARINGVLIET STORM SURGE BARRIER AS PART OF THE DELTA21 PROJECT.

SÓLEY HJÖRVARSDÓTTIR

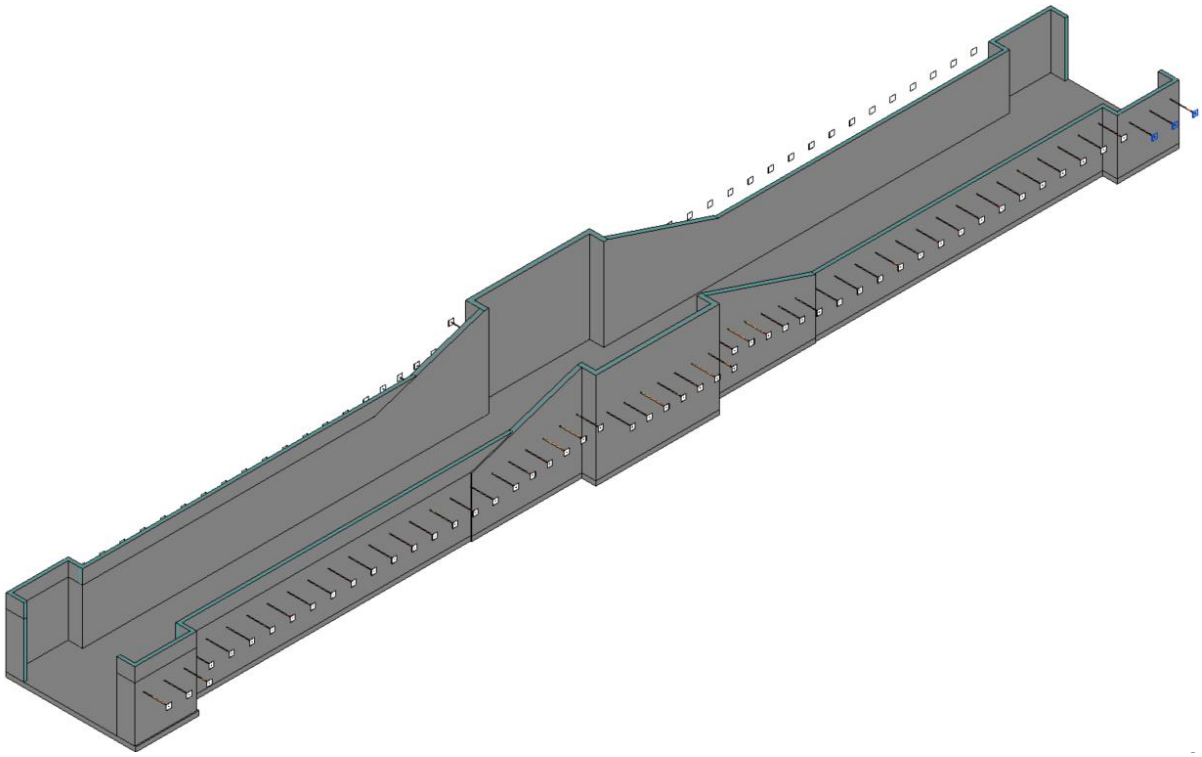

# Abstract

Concrete is the second most used material in the world after water and recent trends show no slowing down of the concrete use around the world. Concrete is also a huge contributor to $CO_2$ emissions as it makes up 8% of emissions. This study investigates the optimization of concrete structures to reduce environmental impact while maintaining structural integrity and cost-effectiveness, e.g. how to make a concrete structure more sustainable. A previous report where quay wall designs of different materials were compared in regard to the $CO_2$-emissions and life cycle assessment found that a concrete quay wall had 43% more emissions than a steel quay wall. The goal of this study is to reduce the overall $CO_2$ equivalent emissions related to a concrete structure by 50% and make the design more sustainable.

A concrete ship lock chamber as part of the Delta21 project is used as a case study. To measure the positive effect of sustainability two chambers are designed; a base case chamber designed based on what is most commonly done in practice in the structural engineering field, and an alternative chamber design with the aim of making the concrete lock chamber more sustainable. A partial life cycle assessment (LCA) is performed on both of the two design alternatives. The optimization of the alternative chamber design focused on minimizing global warming potential (GWP) by adjusting the reinforcement-to-concrete ratio and incorporating structural elements such as plated steel anchors. The two alternatives are analysed comparably as they are designed under the exact same conditions, in the same environment and with the same functionality aspects.

The base case structure is a U-basin concrete chamber with tapered walls. The alternative optimised structure enhances the structural behaviour of the chamber wall by adding anchors. This reduces the moments by 88% and the shear force by 56% compared to the base case design. By changing the structural wall type in the chamber by adding anchors, the concrete volume could be reduced by 47% between the base case design and the optimised design. This also allows for a reduction of concrete strength class, reinforcement volume, underwater concrete floor thickness and the number of tension piles for the construction pit. The LCA reveals a 55% reduction in the GWP for the alternative concrete chamber design, compared to the base case design. An optimum reinforcement ratio for the alternative concrete chamber anchored wall of 2.3% is identified, resulting in a balance between structural performance and environmental sustainability without increasing material costs. This ratio doesn't incorporate labour cost which might affect this optimum ratio by lowering it. This demonstrates the potential for achieving environmentally responsible solutions without compromising the structural integrity of a structure or incurring additional costs.

The study highlights the potential for integrating sustainability objectives into concrete structure design, with recommendations for further research including exploring alternative materials and advanced optimization techniques.

# Table of Contents

Abstract....0
1. Introduction....3
1.1. Problem Analysis....5
1.1.1. Environment and Concrete....5
1.1.2. Delta21 Project....5
1.2. Problem Definition....6
1.3. Objective....7
1.4. Methodology....7
2. Literature Study on Sustainability....9
2.1. Climate Change and Sustainability....9
2.2. Life Cycle Assessment....13
2.3. Summary....15
3. Case Study: Delta21....16
3.1. Infrastructures of Delta21....16
3.2. Water Passing Delta21....20
3.2.1. Storm Surges....20
3.2.2. River Discharge....20
3.3. Location and Layout of a Lock Complex for Delta21....20
3.3.1. Location....21
3.3.2. Layout....22
4. Base Case Design of the Concrete Lock Chamber....27
4.1. Dimensions of Ship, Classification and Sizing of Lock....27
4.1.1. Vessel Classification....27
4.1.2. Intensity of Navigation Volume....28
4.1.3. Size of Ship Lock....31
4.1.4. Construction Methods....33
4.1.5. UWCF Design....33
4.2. Preliminary Design of Chamber; Base Case....41
4.2.1. Governing Load Case....42
4.2.2. Structural Design; U-Basin Chamber....47
4.2.3. Detailing and Material Volumes....59
5. Sustainable Design Optimizations....61
5.1. Sustainable Concrete Structure....61
5.2. Structural Wall Type....62

5.3. Durability and Flexibility ..... 66
5.4. Construction Methods ..... 67
5.5. New Optimized Design ..... 67
6. Design Results: Anchored Wall Lock Chamber ..... 68
6.1. Sizing of the Lock Chamber ..... 68
6.2. Governing Load Case ..... 69
6.3. Structural Design of the Anchored Wall Concrete Chamber ..... 75
6.4. Design Results ..... 90
7. Results: Life Cycle Assessment of the Two Chamber Designs ..... 92
7.1. Inventory Analysis ..... 93
7.1.1. Environmental Product Declarations ..... 93
7.1.2. Bill of Materials ..... 98
7.2. Results ..... 99
8. Discussions ..... 103
9. Conclusion ..... 107
10. Recommendations ..... 108
References ..... 109
Appendix A: Soil properties ..... 115
Appendix B: Dimensioning of the lock complex ..... 117
Appendix C: Base Case Design ..... 120
C.1: Underwater concrete floor ..... 120
C.2: U-Chamber, conceptual design ..... 126
C.2.1: Floor Matlab script ..... 126
C.2.2: Reinforcement ..... 129
C.2.3: Base case volumes ..... 140
Appendix D: Anchored Chamber Design ..... 149
D.1: Matlab; Floor moments and shear forces ..... 152
D.2: Anchored Wall Chamber Reinforcement ..... 153

# 1. Introduction

In this day and age, climate change is starting to have some serious (and visible) consequences on the environment and society. The damage to natural systems all around the world is being driven by human-induced factors. Anthropogenic GHG emission is the main factor contributing to climate change and the construction industry alone is responsible for 25% of the total greenhouse gas (GHG) emissions (KC & Gautam, 2021). Further elaboration on sustainability and the environment is presented in chapter 2.

Delta21 is a project in the Netherlands which aims to protect the Dutch coast from flooding and sea level rise in an environmental friendly manner. The plan includes and open storm surge barrier, a tidal lake, and energy storage lake. Sustainability is key for the solutions proposed in the Delta21 project. Further information about the Delta21 project is available in chapter 3.

Cement is a huge contributor to $CO_2$ emissions and is the main reason why the concrete industry makes up 8% of the overall global emissions. concrete structures should be designed in a sustainable way, where emission is reduced, resources are protected by promoting material efficiency and increasing durability of concrete structures. This report will focus on the sustainable design of the concrete hard structure of a ship lock chamber, using the Delta21 project as a case study. The main goal will be to reduce the overall $CO_2$ emissions connected to the structure by 50% or more.

More detailed information on the problem at hand is presented in chapter 1.1 Problem Analysis, followed by the problem definition in chapter 1.2, objective in chapter 1.3 and the methodology in chapter 1.4.

Sustainability and climate change are defined and discussed in chapter 2 and a life cycle assessment is explained.

In chapter 3 the Delta21 case study is presented and how sustainability is highly related to that project. Chapter 3.3 show the location and layout with the horizontal dimensions of the ship lock complex.

The base case design of the ship lock chamber is found in chapter 4, where the construction method is defined, the governing load case is presented, and the structural design of a U-basin chamber is found (base case). After the base case has been designed and all material volumes have been quantified an alternative sustainable design can be found.

Chapter 5 looks into sustainable design alternatives of the concrete chamber. The first four sub-chapter discuss how the design can be made to be more sustainable considering the effect of concrete strength classes to the overall $CO_2$-eq emission, how different structural wall types can perform better under the soil load, minimizing the moments and shear forces in the wall, how durability and flexibility of a structure affects the sustainability of the structure and how the two sometimes contradict each other, and how different construction methods have a varying effect on the total global warming potential of a structure. In chapter 5.5 a new alternative wall type is chosen to be further designed.

Chapter 6 presents the alternative sustainable chamber design. It is designed in a similar manner to the base case design using NEN-EN 1992-1-1. It is split into four sub-chapters where the first three sub-chapters focus on the structural design of the alternative chamber. Chapter 6.4 presents the design results of the base case chamber and the alternative chamber design side-by-side.

Life cycle assessment of the two chamber designs is performed in chapter 7. It includes an inventory analysis with material quantification and environmental product declarations for all materials used in the design. The results of the LCA study for the two design alternatives are presented in chapter 7.2.

Discussions, conclusions and recommendations are presented in the last three chapters; chapter 8, 9, and 10.

## 1.1. Problem Analysis

### 1.1.1. Environment and Concrete

Due to the looming threat of climate change and finite natural resources, sustainable engineering is becoming increasingly more important to minimize the environmental effects of the construction. The construction industry is one of the top users of natural resources, responsible for more than 30% of total extraction of natural resources and 25% of the total greenhouse gas emissions, including 39% of energy-related emissions (KC & Gautam, 2021). Concrete is the 2nd most consumed material in the world after water, and cement production accounts for roughly 8% of global $CO_2$ emissions (Lehne & Preston, 2018). Since the 1950s, global cement production has increased more than 30-fold (Andrew, 2018) and in 2022 the total volume of cement production was an estimated 4.1 billion tons worldwide in 2022 (US Geological Survey, 2023). The advantages of concrete structures and possible reasons for its popularity are e.g. that the ingredients used in concrete are easily available and relatively cheap, concrete structures are highly durable, and constructing concrete structures does not require highly skilled labour (Gupta, 2017).

It is well known that steel has better tension properties and results in much lighter structures than concrete. Steel has high strength and stiffness per weight and is easy to mass produce. Installation of sheet piles and combi walls is fast and does not need any formwork. In 2010, $CO_2$ emission intensity of steel production was estimated as 1736 kg $CO_2$/tonne crude steel in Germany (Hasanbeigi, Arens, Cardenas, Price, & Triolo, 2016). $CO_2$ emission intensity per tonne of reinforced concrete is estimated to be 80.2 kg $CO_2$/tonne reinforced concrete produced (MPA the Concrete Center, 2022). This is much less than for steel but as steel structures weight is far lower than concrete structures with the same strength and function the final $CO_2$ emission intensity is much higher for a concrete structure. This has been researched by David Dudok Van Heel, et al. in an article called Comparison of infrastructure designs for quay wall and small bridges in concrete, steel, wood and composites with regard to the $CO_2$-emission and the life cycle assessment. The results show that the concrete quay wall resulted in roughly 7000 kg $CO_2$/running meter bridge, while a steel quay wall resulted in roughly 3000 kg $CO_2$/running meter bridge (Van Heel, Maas, De Gijt, & Said, 2011). This is a difference of 43%.

As the choice of using concrete in future construction is unlikely to reduce based on current trends in concrete production, making concrete structures more sustainable is of great importance. Therefore, in this study a concrete ship lock chamber will be designed using Delta21 as a case study as it is situated in a Natura 2000 area hence must be sustainable in order to get permits for construction in that area. The concrete ship lock chamber can be made more sustainable through optimizations of the chamber wall typology, reinforcement volume, durability of structure, flexibility and the type of concrete used, and construction methods. It is very important for future generations that concrete structures will be designed in a sustainable way, where emission is reduced, protecting resources by promoting material efficiency and increasing durability of concrete structures.

### 1.1.2. Delta21 Project

#### *Stake holders*

Delta21 is a very large scale project that affects many sectors. The Delta21 plan includes a tidal lake connected to an energy lake via a spillway, fish migration river, a ship passage, and an open storm surge barrier (SSB) (Delta21, 2021). There are many stakeholders with an interest in the project. A stakeholder is defined as a party that has an interest in the project and can either affect or be affected by the project (Fernando, 2022).

The primary stake holders for the ship lock complex are the Delta21 project (internal stakeholder) and Stellendam and Hellevoetsluis harbours as they will be the primary costumers along with the dutch government (external stakeholder). Other stake holders will include:

- the Natura2000 area as the project has to sustainable to be allowed to be constructed in the allocated area for Delta21
- Society as good access both through the ship lock and over it has to be insured to allow good access to the nature reserves around the energy storage lake.
- Government; the design has to be feasible and attractive to the government to be allowed construction and to avoid as many political conflicts as possible

### *Ship Lock*

For the first 100 functional years of the new Haaringvliet storm surge barrier the barrier can be kept open, with it only closing in extreme flood conditions (storms). due to sea-level rise, after 100 fully functional years of the storm surge barrier where the barrier can be kept open, it will have to be closed permanently m (Verschoor, 2023). Therefore, it is assumed that for approximately the first 50 years there won't be a need for a ship lock. Ships will be able to pass through a ship passage. When the barrier is kept open, strong currents will flow through it during low river discharge. This will not allow for safe navigation through the barrier if a ship passage through the SSB would be chosen. Therefore, only a ship passage adjacent to the SSB on the south side is necessary in the first 50 operational years, with flood gates. After those 50 years the sea level will have risen by 0.82 m (Verschoor, 2023). Therefore, necessary closures of the SSB will become more frequent as extreme water levels will occur for less extreme events. It would therefore be advisable to construct a fully functional ship lock after a 50 year use of the ship passage. This report will thus focus on the design of a ship lock situated south of the storm-surge barrier that will be functional from the year 1100 until the year 2250 (end of functional lifetime for the SSB).

### *Flood defence*

One of the main objectives of the Delta21 project is to protect the Netherlands from flooding. With more extreme rainfall events occurring more frequently due to climate change (extreme) high river discharges are becoming more of a threat. During a river flood, the surplus of water will be pumped into the North Sea. Furthermore, more extreme storms and storm surges are also becoming more frequent. The new Haringvliet storm surge barrier will protect against these extreme conditions by fully closing it gates during extreme storms and river floods. Therefore, the ship lock will also have the main function of serving as flood defence during these extreme conditions. To lower the failure probability of the gates during extreme events, these gates will be kept closed at all times to avoid failure due to closing operations failing. During flood events, the ship lock/passage will be fully closed, and the gates will serve as a flood barrier. Between the two chambers of the ship lock two mitre gates situated in line with the SSB will act as flood gates. They must have the same retaining height as the SSB and be strong enough to resist extreme water heads and wave attacks. The two mitre gates will be pointing away from each other for added security and to minimize the failure probability of the ship lock/flood defence gates. If one gate were to get damaged for instance due to ship collision, there will still be another fully functional gate to close off the lock in case of a flood event. The lock will not have to discharge water during high diver discharges. That access water will be discharged with the pumps in the energy storage lake.

## 1.2. Problem Definition

Sustainable structures are becoming increasingly more important in the fight of mitigating climate change. As concrete is the most used structural material in the world and does not show any trends of decreasing in popularity, concrete structures must be designed in an effective and sustainable way by minimizing the

negative environmental effects originating from those structures. A ship passage at the location of Delta21 will be a necessary service for navigation. The ship passage must provide a safe passage for the ships, and it must also serve as a flood defence during extreme storms. The design must aim for sustainability. The main research question of this master thesis is the following:

*How can a concrete hydraulic hard structure be designed sustainably, using a ship lock chamber as a case study, with the aim of reducing $CO_2$/year by 50%?*

The main focus will be on the sustainable design of the concrete hard structure, using a ship lock adjacent to the new Haringvliet storm-surge barrier as a case study. Several other sub-questions related to the main research question will be answered as well, such as:

- What is a sustainable concrete structure?
- Which aspects of the design are most influential on the sustainability of the structure
- Which aspects of the design are most influential when it comes to the cost of the structure

## 1.3. Objective

The objective of this thesis is to find a sustainable way of designing a concrete lock chamber using Delta21 project as a case study. The lock must be designed in a sustainable, innovative way that works with nature rather than against it and it must be economically feasible. The aim of this study is to investigate the different methods that can be applied to make a concrete hard structure more sustainable, so that kg $CO_2$-eq of the concrete chamber will be reduced by 50% compared to the base design. A 50% reduction was chosen based on LCA study for quay walls constructed out of different materials. As is discussed in chapter **Error! Reference source not found.** the difference in kg $CO_2$-eq/running meter of a steel quay wall and a concrete one was 43%.

## 1.4. Methodology

To accomplish a more sustainable design of a concrete ship lock chamber, a structured methodology is necessary. Throughout the design process the hydraulic engineering design method will be applied. This design method is an iterative cyclic process. This process can be subdivided into several clearly separated phases, working from a general design (case 0) towards a more detailed, sustainable design.

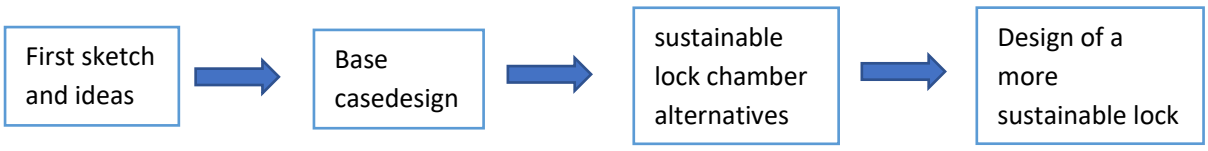


1. **First sketch and ideas**
   First sketches and ideas have been presented in chapter 3.2, where the layout of the ship lock has been sketched. These sketches give a simple overview of the situation; length scales, orientation, harbour and docking stations, approximate distance from the storm surge barrier, etc.
2. **Base case design**
   The design requirements are presented in the problem analysis. With these functions in mind the concrete lock chamber is designed in similar manner as other older hydraulic concrete structures, not focussing on the environmental impact but rather on constructability, durability and what the "norm" has been in the previous years. Structural safety, constructability and maintainability will be taken into account. 2 base case concepts will be discussed that could be a potential solution. These alternatives will be evaluated, taking into account the design requirements, structural

safety, constructability, maintainability, and cost and the most acceptable base design will be elaborated on and later compared to a more sustainable design.

This study will consider the European codes (EN) for the design of the concrete hard structure. The Eurocodes that are considered in the study are as follows

The walls and floors will be designed as a concrete hard structure. For the base (preliminary) design they will be designed with normal concrete (used in most hydraulic structures in the Netherlands) not taking into account sustainability. Loads from the soil and from the water heads will be determined and failure mechanisms for the walls and floors will be defined. All necessary reinforcement to reach structural integrity of the lock chamber will be calculated using excel and Eurocode 2.

3. **Sustainable lock chamber alternatives**

   To reach a more sustainable design of the concrete ship lock chamber the structural design must be optimized. This will mainly be done through the optimisation of the chamber's structural typology. Four different typologies will be discussed and compared in chapter 5.1 using a simplified load for the preliminary comparison. To choose an alternative to proceed with the moments and shear force for each typology will be compared. A lower shear force will result in a smaller wall thickness and a lower moment will reduce the flexural reinforcement necessary for the chamber.

4. **Design of a more sustainable lock**

   After choosing a structural typology to proceed with for the sustainable lock chamber the final design can begin. Moments and shear forces will be calculated by modelling the chamber walls using Diana FEA.

   The structure will be re-designed taking into account sustainability. Concrete and reinforcement volumes will be reduced by changing the structural typology. Different aspects will be explored such as:

   - alternative sustainable concrete mixes.
   - construction methods: Floated in structure or cast in-situ using a construction pit.
   - durability: Not all elements might need to have the same durability.
   - flexibility: Due to sea level rise (+3.88 m in 2250) the final wall height that is necessary in the year 2250 is not needed during the whole lifetime of the structure.
   - cost: explore different construction methods and materials to reduce the cost of the construction without affecting the sustainability of the structure greatly.

   For a detailed design of the hard concrete structure (walls and floors) taking into account sustainability and durability a literature study on sustainable concrete and durable hard structures is necessary. The design of the sustainable concrete hard structure can proceed determining all concrete and reinforcement volumes. The optimized design of the concrete chamber will be compared to the base case design through a life cycle assessment study (LCA) indicating the difference between the design through $CO_2$/year for each structure as is described in the chapter of sustainability (ch. 2.3). When comparing alternatives, costs and natural impact should be included.

The two designs will be compared and analysed through a partial life cycle assessment (LCA) focussing only on the construction phase taking into account all material volumes, types of materials and durability. LCA is a tool used to quantify the degree of sustainability of a product or a process by quantifying aspects of the environmental performance or impact of a product. LCA is further described in chapter 2.2. Using LCA a value for the total global warming potential [kg $CO_2$-eq] value for each structure can be obtained and then compared. The aim is to have the $CO_2$/year value 50% lower for the optimized sustainable design vs the base case design.

# 2. Literature Study on Sustainability

## 2.1. Climate Change and Sustainability

In this day and age, climate change is starting to have some serious (and visible) consequences on the environment and society. The damage to natural systems all around the world is being driven by human-induced factors. Our actions are directly linked to the increased frequency of extreme weather events. Extreme weather events are becoming more extreme and subsequently, the impacts of those events on society and on delicate ecosystems. The resilience of both human and ecological systems is being passed during some of these extreme events, not giving them enough time to adapt before the next weather event hits. Due to the growing urban population, both land, and water are degrading, and important biotopes and biodiversity are being lost (Pathak, et al., 2022). Number of days with extreme precipitation in the Netherlands have increased in the past two decades and in 2018 – 2020 the dry season was very noticeable and begs the question whether these events will occur more aften and more intensely in the future (KNMI, 2021)

Due to the climate changing and the oceans warming, sea-level rise (SLR) poses a serious threat. It has started impacting societies around the world, posing a big threat to low-lying areas. The rate of global mean SLR during 1993 – 2018 was 3.2 mm/yr. This is an acceleration of roughly 140% from the mean SLR of 1.35 mm/yr during 1901-1990 (Le Cozannet , et al., 2022) (Cross-Chapter Box SLR: Sea Level Rise). Around a third of the Netherlands lies below sea level and only around 50% of the country is over 1 m above sea level (Schiermeier, 2010). The IPCC has determined that it is extremely likely that at least 50% of the observed rise in average surface temperature since 1951 is a direct cause of anthropogenic factors. Of these factors, the most important is the emission of greenhouse gasses (GHGs) (KNMI, Satellite observations, 2022). Although it is certain that the sea level will continue to rise in the coming years, it is not known precisely at what speed it will rise. The factor that society can have the most influence on, to mitigate SLR, is the emission of GHGs. Currently, SLR along the Dutch coast is 2 mm/yr. the current assumed (maximum) SLR in the Netherlands is 0.4 m by 2050 and 1.0 m by 2100. These values exclude the possible additional accelerated SLR from the accelerated melting of Antarctica. New studies that include this accelerated rate of Antarctica melting have shown that even if the Paris Agreement target of 2°C of global warming is met in this century, the assumed SLR for 2100 can be between 0.3 m to a maximum of 2.0 m. This can rise to a maximum of 3.0 m by 2100 if a global warming of four°C is assumed. If the accelerated rate of SLR is taken into account the rise per year can increase from the currently assumed 10 mm/yr around 2050 to 14 mm/yr, and it would increase to 20-35 mm/yr around 2070. Figure 1 shows a graph depicting the SLR until 2100 for different scenarios. As extreme weather events are becoming more frequent, extreme floods due to storms (storm surges) and extreme rain events in the Netherlands pose a serious threat to modern society. Hence, a better protected coast of the Netherlands is necessary (Deltares, 2018).

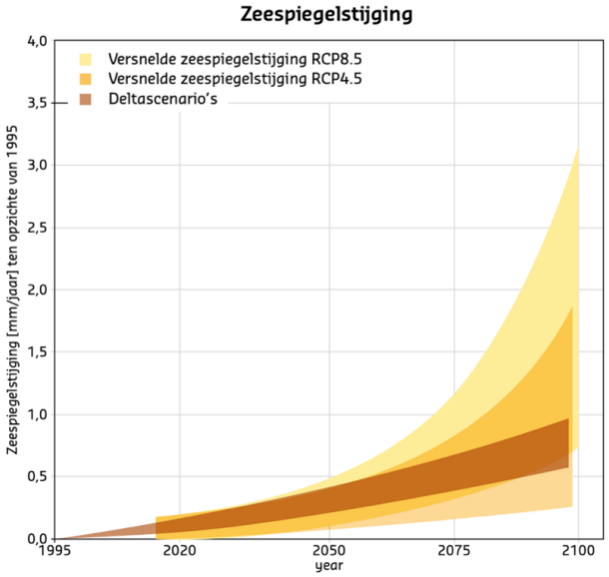


**Figure 1: Accelerated SLR in accordance with the Delta Scenarios as they currently are, a 2°C (RCP4.5) and a 4°C (RCP8.5) warming in 2100.**

Due to the (high probability of) more extreme storm surges and river floods in the Netherlands in the near future, the flood defences are getting more extreme; able to protect from higher water levels and floods. Although the location of the Delta21 project is a Natura 2000 area it would still be in natures favour to protect the coast with a storm surge barrier as the area would be lost underwater in a few years due to the negative development of SLR.

In the Netherlands the tide travels from south to north along its coast and has a tidal period of 12 hours and 25 minutes (44700 s). The tidal pattern is semidiurnal meaning it has two highs and two lows with approximately the same height every lunar day (CRDG University of Hawaii, 2023). Figure 2 shows the tidal signal in January and February 2018 just seaward of the Haringvliet outer delta. These tidal levels are based on the tide for these two months and therefore they may differ when analysing the tidal signal over a longer period (Alonso A. C., 2018).

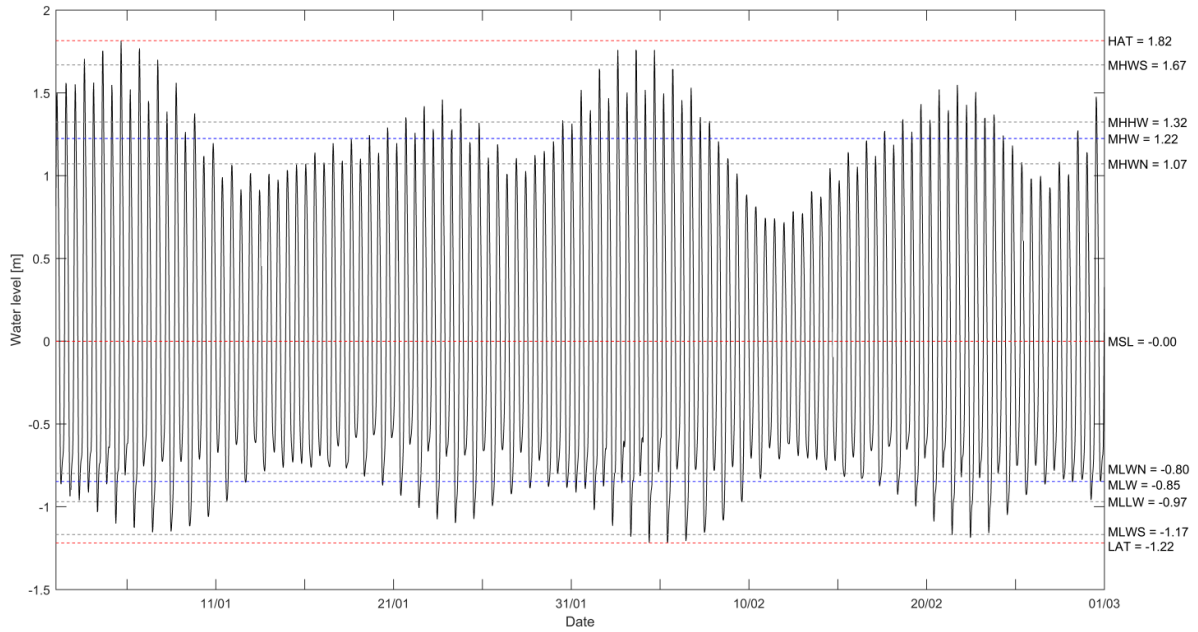


**Figure 2: Tidal signal in front of the Haringvliet outer delta containing 4 spring-neap tidal cycles (Alonso A. C., 2018).**

KNMI has taken the SLR predictions of IPCC and adjusted them to the Netherlands using European models that consider local steric changes, geoidal eustasy etc. KNMI'21 predicts the sea level rise along the Dutch coast for three different climate scenarios: SSP5-8.5; no measures have been taken to lower emissions (emission increases), SSP1-2.6 maximum target of 2°C is held, and SSP2-4.5; a scenario in between SSP5-8.5 and SSP1-2.6. Bob Verschoor has used the indicative values for SLR given in the KNMI'21 report per climate scenario and extrapolated them to the end of design life of the delta barrier (Verschoor, 2023). These predictions along with the SLR according to Hydra-NL is presented in Figure 3.

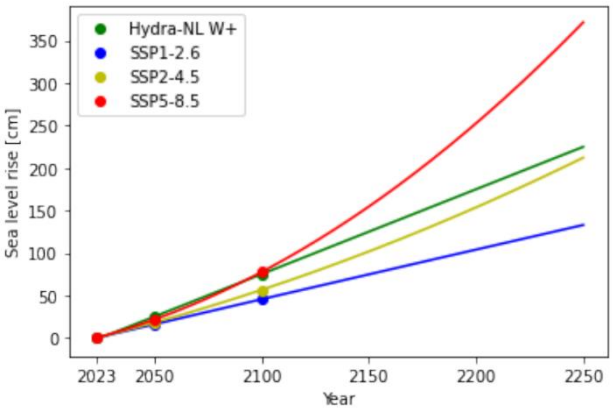


**Figure 3: Forecasted sea level rise for different climate scenarios along the Dutch coast (Verschoor, 2023).**

The United Nations (UN) defined sustainability in 1987 as “meeting the needs of the present without compromising the ability of future generations to meet their own needs”. This means that when designing a new construction, it is just as important to meet the requirements of the present society for that structures use, as it is to make sure that the construction, materials used and demolition or re-use of the structure will also meet the requirements of future generations taking into account the societal-, economical-, and environmental effects. The sustainability aspect of construction nowadays is more important than ever due to the increasing threat of climate change (UN, Sustainability, 2022). To achieve a more sustainable future the UN has formed seventeen sustainable development goals, shown in Figure 4 below. From these 17 goals, three of them are of special interest when it comes to constructing a new ship lock complex:

- Goal 9: Industry, Innovation and Infrastructure. Sustainable industrialization, innovation and infrastructure are important in introducing and promoting new technologies, facilitating international trade and enabling the efficient use of resources. In regard to environmental challenges, Innovation and technology can help find lasting solutions. For the new ship lock complex, new innovative designs of gates will be compared and discussed, and the design will include new innovative and sustainable concrete mixes.
- Goal 12: Responsible Consumption and Production: the natural environment and its resources are finite and thus societal consumption and production rest on the use of these resources in a way that doesn’t overexploit them. This can be achieved by i.e. increasing resource efficiency. For this project, responsible consumption will include locally sourced material. Fine aggregates such as sand can be locally extracted as some sand needs to be dredge for the whole Delta21 project. This will also be accomplished through minimizing the concrete volume of the hard structure.
- Goal 13: Climate action. Climate change is becoming more of a serious problem with every passing year. $CO_2$ levels and other greenhouse gases in the atmosphere are causing the globe to warm, resulting in weather patterns changing, sea levels rising and weather events becoming more extreme (UN, Take Action for the Sustainable Development Goals, 2022). Portland cement is one of the biggest contributors to $CO_2$ emissions. $CO_2$ emission from the design of a new ship lock will be calculated, and optimizations will be made on the design to reduce that emission by making the design more sustainable.


**Figure 4: The 17 Sustainable development goals of the UN.**

When thinking about sustainability in structural engineering, the effect on society has to be taken into account as well as the effect on the environment, what resources and materials are being used, how much the construction industry contributes to total GHG emission, the use phase and how the structure can be demolished or re-used after the use phase in a way that is not harmful to the environment and future generations. Anthropogenic GHG emission is the main factor contributing to climate change. The construction industry alone is responsible for 25% of the total GHG emissions of which the construction and operation sector accounts for 39% of yearly energy related $CO_2$ emissions and 36% of global energy use. The industry is also responsible 30% of all consumed natural resources (KC & Gautam, 2021). Around 20% of a building's initial embodied energy is due to the structural system. Initial embodied energy entails all the energy consumed by processes associated with the construction of the building. This includes mining and processing of raw material, manufacturing, transport and product delivery. As the Delta21 project aims to have turbines and windfarm to produce renewable energy, the operational energy of the ship lock will be minimal. Therefore, minimizing the embodied energy of the structure is important to make the structure more sustainable.

Structural design has an environmental impact as well as an economic and societal impact. For the concrete hard structure of the new ship lock complex these impacts are for example:

- Economic: material and equipment cost, and property damage.
- Environmental: $CO_2$ emission, PM10 emission related to transport of materials, and noise pollution.
- Societal: Risks of injury or death.

There can be conflicts between sustainable practices. An example of such conflict is a that designing a structure with increased use of green materials might lower its $CO_2$ emissions, but it could also result in a shorter life span. The question then becomes; is it more sustainable to have a structure that is more durable with a longer life span or is it better to have a greener structure with a shorter life span.

In the civil engineering sector, Kibert defined the six principles of sustainable construction: "minimize resource consumption; maximize resource reuse; use renewable or recyclable resources; protect the

natural environment; create a healthy, nontoxic environment; and pursue quality in creating the built environment" (Maduka, Greenwood, Osborne, & Udeaja, 2016). These principles can be realized in different ways. For example, by reuse and recycling of resources, switching to a cyclic construction progress where waste is transformed into a resource.

The impact of structural systems on the environment, economy and society can be assessed using sustainable design strategies and assessment tools to achieve a more sustainable structural design (SSD). To start the sustainability assessment a preliminary design of the concrete hard structure of the ship lock will be realized without taking into account any mitigation measures. It will be designed as a gravity wall and a concrete floor system supported with piles. This preliminary design will then be evaluated by calculating the concrete and steel volume used, $CO_2$ emissions of the process including $CO_2$ from cement production, reinforcement manufacturing and transport of the materials. After this a design strategy can be developed that entails the choice of structural material (different types of concrete), structural layout and choice of locally sourced materials. According to Danatzko and Sezen, SSD strategies can be classified as follows:

- Minimizing material use: This can be achieved by shape optimization of the structure .
- Minimizing material production energy: This can be achieved by using locally sourced materials, reused materials and by choosing materials whose production allows for energy and resource savings.
- Minimizing embodied energy: lowering the maintenance need of the structure is one example to how achieve lower embodied energy.
- Lifecycle Assessment/Inventory/Assessment
- Maximizing Structural system reuse: reusing material such at concrete aggregates and/or making the structure demountable.

Sustainability through structural design is more than just concentrating on a single environmental impact. Sustainability can also be implemented through designing durable and flexible structures which ensures the longevity of the structure. This extends the time frame of environmental impacts rather than minimizing them from the start. Hence, SSD assessment should assess the impact of the structure over its entire lifecycle and requires parameters that are both quantitative and as accountable as possible. These parameters should reflect the impact that the strategy aims to address: for the concrete hard structure design, that impact is $CO_2$ emissions. Therefore, the parameter that will be used is the amount $CO_2$ released divided by the lifecycle of the structure, e.g. $CO_2$/year. This way, durability will be accounted for because even though the initial $CO_2$ emission of a durable structure might be higher than a for a structure with less mass and strength, the durable one will last longer and thus have a possibly lover $CO_2$ index. adaptability of the structure will be taken into account in the way that parts of the structure can be reused to increase the lifetime of it and initial environmental impacts are also included.

## 2.2. Life Cycle Assessment

Life Cycle Assessment (LCA) is a tool traditionally used to assess the environmental performance or impact of a product/process associated with its life cycle. In recent years the tool has been developed towards measuring sustainability. It is hard to assess all three aspects of sustainability; social, environmental, and economic impacts. current LCA techniques best suited to assess environmental and certain health impacts of a product during its life cycle. LCA accounts for environmental impacts which are quantifiable in terms of damage such as depletion of finite resources and emission of harmful compounds (Golsteijn, 2022). Social aspects are mostly excluded from LCA but since the navigation lock is not in an urban environment and does not influence many social aspects, it is not of a great importance and won't affect the overall

sustainability of the structure much. Different parts of a products life cycle are referred to as life cycle stages. There are four different life cycle stages of a construction considered in an LCA. The life cycle stages are presented in Figure 5 below (Golsteijn, 2022).

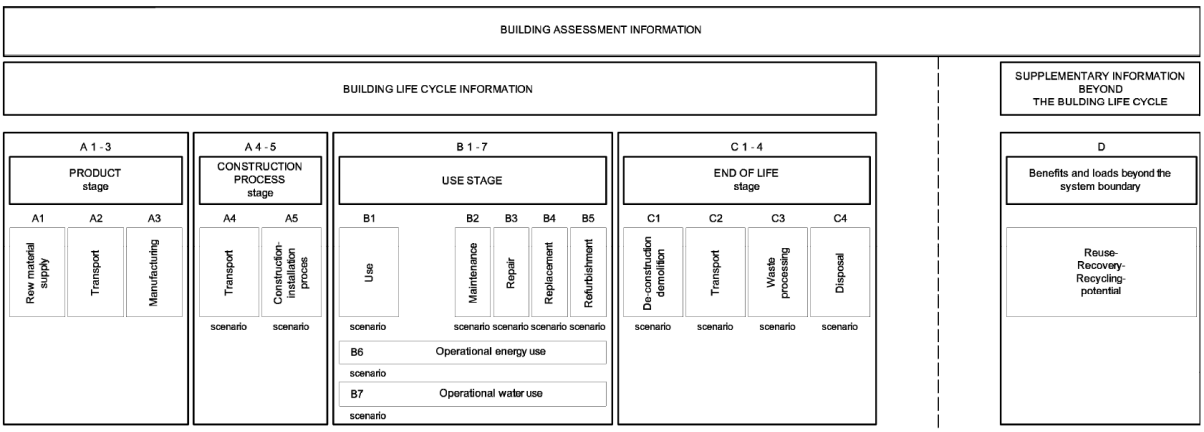


**Figure 5: The specific life cycle stages of a construction considered in LCA according to EN 15978: Product stage; construction process stage; use stage; end of life stage (CEN, 2011).**

With LCA the environmental impact of a product can be determined for its whole life cycle, e.g. from 'cardle to grave'. This includes stages A, B, and C shown in Figure 5. LCA can also be performed for only a certain life cycle stage. Estimations of the environmental effects of all required raw material over the products life stages are made through the LCA procedure including energy ("inputs") and occurring emissions ("outputs") and the effects are presented graphically through so called environmental profiles which can be described as a 'score' list with environmental effects showing which impact categories cause the most environmental problems and at which stage in the designs life cycle (Jonkers, 2019).

LCA is a standardized methodology and the rules of LCA for construction works are defined in EN 15978 (Sustainability of construction works – Assessment of environmental performance of buildings – Calculation method) , ISO 14025, and EN 15804.

When performing LCA there are three main goals:

- Identification of the life cycle stage that is the main contributor to the total environmental impact.
- Identifying so called environmental 'hot spots' over the entire life cycle of the structure. 'hot spots' are the modules within the 3 life cycle stages that contribute the most to the overall environmental impact of each stage. These environmental hot spots can be used to take effective measures to reduce environmental impact in 'next generation' design and optimize it so that the structure will be more sustainable.
- Collection of information required for making environmental product declaration (EPD) of the structure. This information is useful when comparing environmental performance of structures with similar functionality, as will be done here by comparing different designs of a lock chamber.

An LCA is split into 4 main phases; goal and scope definition, inventory analysis, impact assessment, and interpretation of the results (Golsteijn, 2022).

- Goal and scope definition for the structure
- Inventory analysis: this include a process tree and a life cycle inventory analysis
- Impact assessment: Different impacts are assembled into a number of relevant impact categories. Scores can then be calculated for each impact category.

- Interpretation of the environmental impact of the structure using the scores, and discussion on the results.

The goal of the partial LCA study of the ship lock chamber is to get a better view of how the environmental footprint of a large, durable concrete structure can be minimized aiming for a sustainable structural design. The LCA will provide a $CO_2$-eq/year value (amount $CO_2$ released divided by the lifecycle of the relating structural component) as the $CO_2$ impact of the concrete lock design is the most harmful component to the environment. Dividing the $CO_2$ with the lifetime of the relating structural component in the concrete allows for durability to be accounted for because even though the initial $CO_2$ emission of a durable structure might be higher than a for a structure with less mass and strength, the durable one will last longer and thus have a possibly lover $CO_2$ index. adaptability of the structure will be taken into account in the way that not all parts need to be constructed at the same stage in the life cycle.

In this study a partial LCA for the concrete ship lock chamber will be performed considering only stages A1 -A4 (“cradle to gate”). The necessary volume of concrete and steel will be quantified, and the steel grade and concrete classes will be included in the inventory analysis. Product emissions will be gotten from life cycle inventory data extracted from concrete and steel manufacturers reports from a life cycle inventory (LCI) database called EnvironDec.

## 2.3. Summary

As climate change poses a serious threat for the future, it is becoming more important to reduce GHG emissions around the globe. The construction sector can contribute to the reduction GHGs by moving towards a circular design process and more sustainable designs.

For this study two concrete ship lock camber alternatives will be designed with the aim of making the second chamber alternative more sustainable by reducing its global warming potential by 50% compared to the base case alternative. An LCA will be conducted for both alternatives and the results compared and discussed.

# 3. Case Study: Delta21

## 3.1. Infrastructures of Delta21

Southwest of Rotterdam is the former Haringvliet estuary of the Rhine-Meuse delta. As part of the Delta Works it is currently closed off by the Haringvlietdam. The sluices in the current Haringvlietdam only open to discharge river water into the North Sea when the river water levels are too high. It Does however not allow for brackish water to flow into the Haringvliet. This has caused considerable loss of wildlife habitats as the effect of the tide has disappeared and fish migration is no longer possible. Delta21 is a large hydraulic engineering structural system located at the Haringvliet mouth that aims to protect the Dutch coast against floods and sea level rise in a sustainable and eco-friendly way (Delta21, 2021). In Figure 6 below a map of the current layout of the Haringvliet estuary is presented.


**Figure 6: Current View of Haringvliet estuary (Google, 2022)**

The project will redevelop the Haringvliet delta so that it will protect the Netherlands against flooding in a sustainable way. The Delta21 plan includes a tidal lake connected to an energy lake via a spillway, fish migration river, a ship passage, and an open storm surge barrier (SSB). During a storm, the new SSB will be closed. The river water will then be directed through the tidal lake and spillway into the energy storage lake and from there it will be discharged to the North Sea via pumps. During high river discharges the surplus river water will be pumped to the North Sea (Delta21, 2021).

The location of the new storm surge barrier and the Delta21 project as a whole is on the seaside of the Haringvlietdam. This location is classified as a Natura 2000 area; a protected area that shelters the most valuable and threatened species and habitats in Europe. The main goal of Natura 2000 is to ensure long-term survival of Europe's most valuable and threatened habitats and species by protecting core breeding and resting sites for rare and threatened species and rare natural habitats. As can be seen in Figure 7 the location of the Delta 21 project is both a Birds Directive Sites (BDS) and a Habitats Directive Sites (HDS). The Natura 2000 areas at the Delta21 location are the following; Voordelta (BDS & HDS), Voornes Duin (HDS) in the northeast with a small patch of BDS as well, and Duinen Goeree & Kwade Hoek (BDS & HDS) in the south. Natura 2000 areas are not so strictly protected that no human activities can occur there.

Instead, sustainable management of the areas, both ecologically and economically, must be ensured. Therefore, the sustainability aspect of all aspects in the Delta21 project is of high importance where they focus on building with nature while protecting the Dutch coast and preserving as much of the natural habitats and ecological systems as well (Sundseth, 2008).

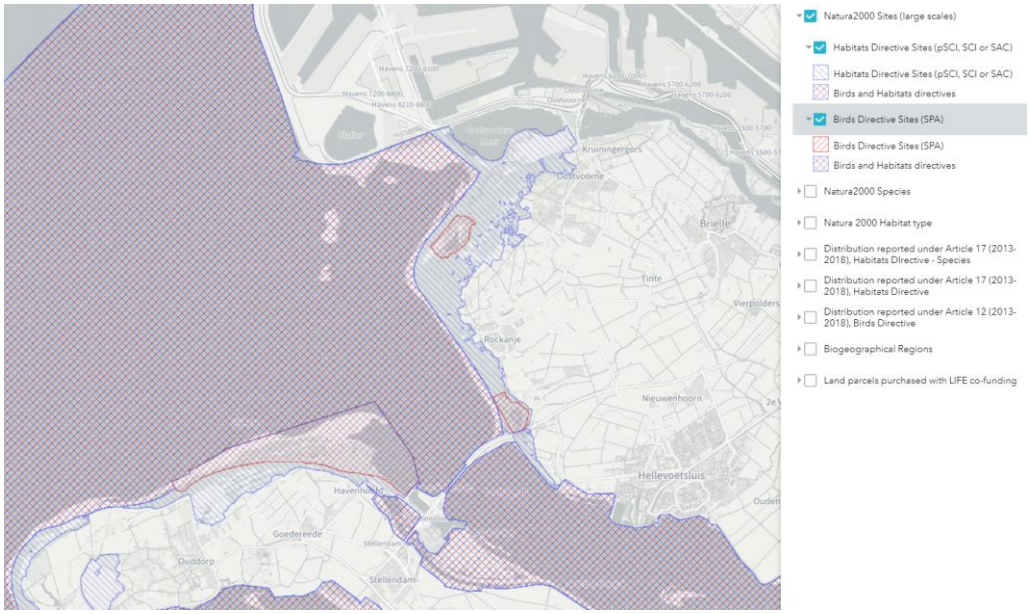


**Figure 7: Map showing the Natura 2000 protected are of the Delta21 Project (Natura 2000 Network Viewer (europa.eu)).**

A new layout of the Delta21 project was designed by Esmée van Eeden. The layout is based on morphological processes along the coastline and the expansion and preservation of wildlife habitats. The new estuary layout is presented in Figure 9 below. The SSB is marked number 3 on the figure. North of the new SSB is the spillway (2) and energy storage lake. South-west of the SSB is a dune area and south-east of the SSB are grasslands with hidden dikes and an intertidal marshland. The intertidal marshland is a low lying area that is flooded during high tide. The hidden dikes on the south end of the SSB are part of the flood defence (van Eeden, 2021). A closer up view of the hydraulic structures is presented in Figure 8.


**Figure 8: Zoomed in view of the hydraulic structures as part of the Delta21 plan, 1 is the energy storage lake outlet to the north sea, 2 is the spillway to the energy storage lake, and three is the new storm surge barrier.**

Hydraulic structures that are part of Delta21 and have a large concrete volume are the following:

- Haringvliet storm-surge barrier
- Tidal lake
- Energy storage lake
- Spillway to the energy storage lake
- Natural reserve and dunes around the energy storage lake
- Ship passage


**Figure 9: New estuary landscape of Delta21 (van Eeden, 2021)**

## 3.2. Water Passing Delta21

The water levels that the ship passage is designed for are taken as the same water levels that were determined for the structural design of the new Haringvliet storm surge barrier. At the Dutch coast the tide has a dominant semi-diurnal tidal pattern with a period of T = 44700 s. The tide propagates from south to north along the Dutch coast. The tidal signal in front of the Haringvliet outer delta during January and February 2018 is presented in Figure 2 (Alonso C. A., 2018). It will be used as a base water level when determining minimum locking levels later on.

### 3.2.1. Storm Surges

The design parameters for the new SSB was collected by Bob Verschoor using Hydra-NL taking into account various effects e.g., fetch, waves, SLR, depth differences, Tidal signal, etc. The Water retaining height of the barrier is 10.5 m where climate scenario SSP5-8.5 is considered for the reference year 2250 (Verschoor, 2023). Therefore, the flood gates and the lock head around them should reach that height as well.

### 3.2.2. River Discharge

The Haringvliet is a part of the Rhine-Meuse estuary. Its discharge comes from the Hollandsch diep which is fed by the Nieuwe Merwede and the Bergsche Meuse (see Figure 10). As the storm surge barrier will be open in normal circumstance the river will be able to discharge water directly through the barrier and into the North Sea.

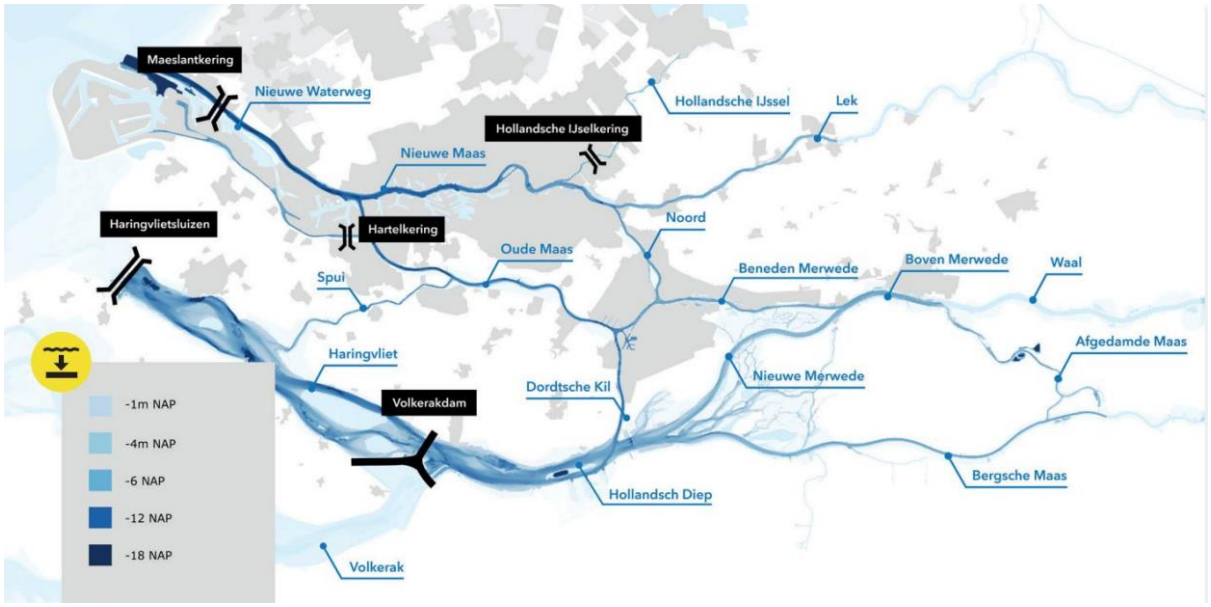


**Figure 10: Rhine-Meuse estuary: Watercourses and the Delta Works.**

When the barrier is closed, excess river water will be discharged via the spillway and pumping stations into the energy storage lake. The water level in the tidal lake will not reach extreme values as it is assumed that given a premature closure of the SSB the water level in the tidal lake will be maintained at a level of NAP +1.0 m by means of the spillway and pumping stations (Verschoor, 2023). Therefore, water level on the riverside of the ship lock is not of a detrimental concern when it comes to the structural design of the ship lock.

## 3.3. Location and Layout of a Lock Complex for Delta21

The Haringvliet will be closed in case of 2 different scenarios; During extreme storm surges with or without high river discharge to prevent flooding, and during a drought. During a drought the river discharge will be

very low and therefore salt intrusion will reach further upstream. The Haringvliet SSB will then be closed to avoid salinization too far upstream in the river. Fish migration will be negatively affected during prolonged closures of the SSB. Therefore, a fish migration river will be implemented parallel to the south bank of the river passing the new SSB to the North Sea. As can be seen in Figure 11, the migration river follows the existing form of the former tidal creeks (van Eeden, 2021). The shortest distance from the migration river to the end of the storm surge barrier is around 1 km.

**Figure 11: Fish migration river in the new Delta plan marked in orange.**

A new ship passage next to the new Haringvliet SSB must be constructed before the construction of the storm surge barrier. This will ensure that recreational and small fishing ships can navigate safely to the North-Sea, with minimum obstruction from the construction of the new SSB.

### 3.3.1. Location

Inland of the Haringvliet barrier are two cities: Stellendam and Hellevoetsluis. The harbours in these cities service recreational boats as well as some smaller fishing ships. It is important to allow access through the new Haringvliet storm surge barrier for ships to ensure that the Goereese ship lock can still be used as a link between the Haringvliet and the North Sea. The choice of location for the new ship lock depends on, among other things, available area for docking station and a small waiting port, and easy navigability through the lock approach. The lock approach should be free of obstacles, not be situated in a bend, and transverse and longitudinal currents should be minimized as well as crosswinds.

North-West of the barrier is the energy storage lake and the spillway. This area is in an inner bend of the river. Due to the proximity to the lake and the spill way the area to construct a ship lock is very limited. Therefore, this location will not be chosen.

South-East of the new storm-surge barrier is a dune area. Positioning the Ship lock in this location gives a more direct access for ships coming from the North-Sea and there is plentiful of available area for the structure and the recreational port mentioned above. Transverse and longitudinal currents as well as crosswinds are also minimized here. The main wind direction is from the south-west towards the northeast, as is depicted in Figure 12. Situating the ship lock on the south-east side of the SSB would therefore give a minimum fetch for the wind and thus minimize the wind waves. Special care needs to be taken in the design of the lock at this location as it will be in a dune area and a big part of the Delta21 project is to restore and preserve the natural environment. This position does provide an area for waiting vessels which will be equipped with mooring facilities (waiting and line-up areas), both on the inland- and the seaside of the lock. On the seaside of the lock a small, sheltered port will be constructed which will allow yachts to moor for recreational purposes without the need to navigate through the lock. It is also a good position with respect to the approach channel. There are better possibilities to keep the approach channel as straight as possible on the south-east side.

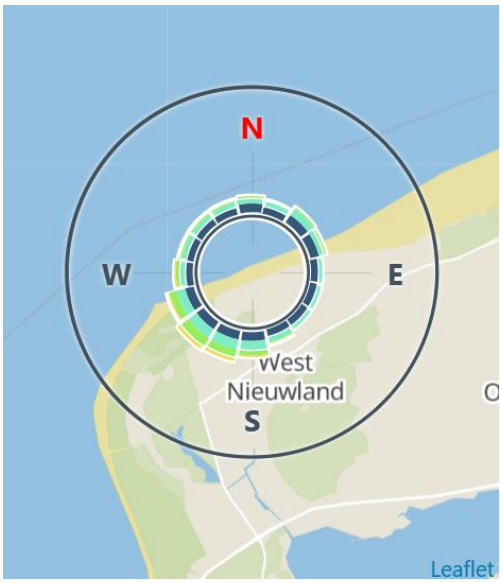


**Figure 12: Wind rose chart showing the occurrence rate of winds at Oudorp uitloop (Windy Weather World Inc., 2023)**

### 3.3.2. Layout

The layout of the ship lock complex was sketched on paper to get an overall idea of the design at hand. A fish migration river will be situated south of the new storm-surge barrier (see Figure 9 & Figure 11). Using the length scale given on Figure 9 the shortest distance from the fish migration river to the SSB is roughly 1 km. If ships get stuck out on sea due to closing of the barrier and the lock during a storm it is important to have a docking port on the seaward side of the ship lock. The port will be designed large enough to also serve as a recreational port for larger yachts and ferries, giving better access to explore the nature reserve surrounding the energy storage lake. It should be well sheltered to prevent wave generation and wave intrusion within the port. As this recreational harbour is located on the seaward side of the lock it will allow for larger recreational vessels to dock and have access to the natural reserves without needing access to the ship lock. Figure 13 below shows a sketch of the greater area around the lock.


**Figure 13: Sketch of the area around the lock**

On the southwest side of the Haringvlietdam is the Goereese ship lock. This lock allows navigation between the North Sea and the Haringvliet for fishing, shipping and recreational shipping. (Hansen, 2022). Goereese sluis is 16 m wide, 144 m long and with a threshold depth of 5 m. It is split into two chambers with three gates in total (Waterkaart, 2022). Figure 14 and Figure 15 are pictures of the Goereese Sluis.

**Figure 14: View of the Goereese Sluis and the waiting port**


**Figure 15: one of the gates in Goereese Sluis (Goereese sluis | Binnenvaart in Beeld).**

The dimensions of the lock chambers in the new ship lock of Delta21 will be the same as for Goereese sluis lock, therefore allowing for navigation of similar ships; 144 m long chamber, split into two chambers this gives a chamber length of 72 m. 4 gates will separate the waterways and chambers; one at the seaward end, one at the landward end, and two in the middle separating the chambers. Mitre gates will be used as they take less space compared to sliding gates and since the lock is relatively narrow (16 m).

A lock approach in necessary to connect the lock chambers to the sea/river. Since the chamber length is 72 m that gives CEMT class between II and III allowing maximum ship length of approximately 65 m in one chamber. Class II and III give a beam width of B = 6.6 – 8.2 m. The approach basin dimensions are calculated and explained in more detail in annex B. Figure 16 and Figure 17 shows the lock basin and the area around it including the harbour.

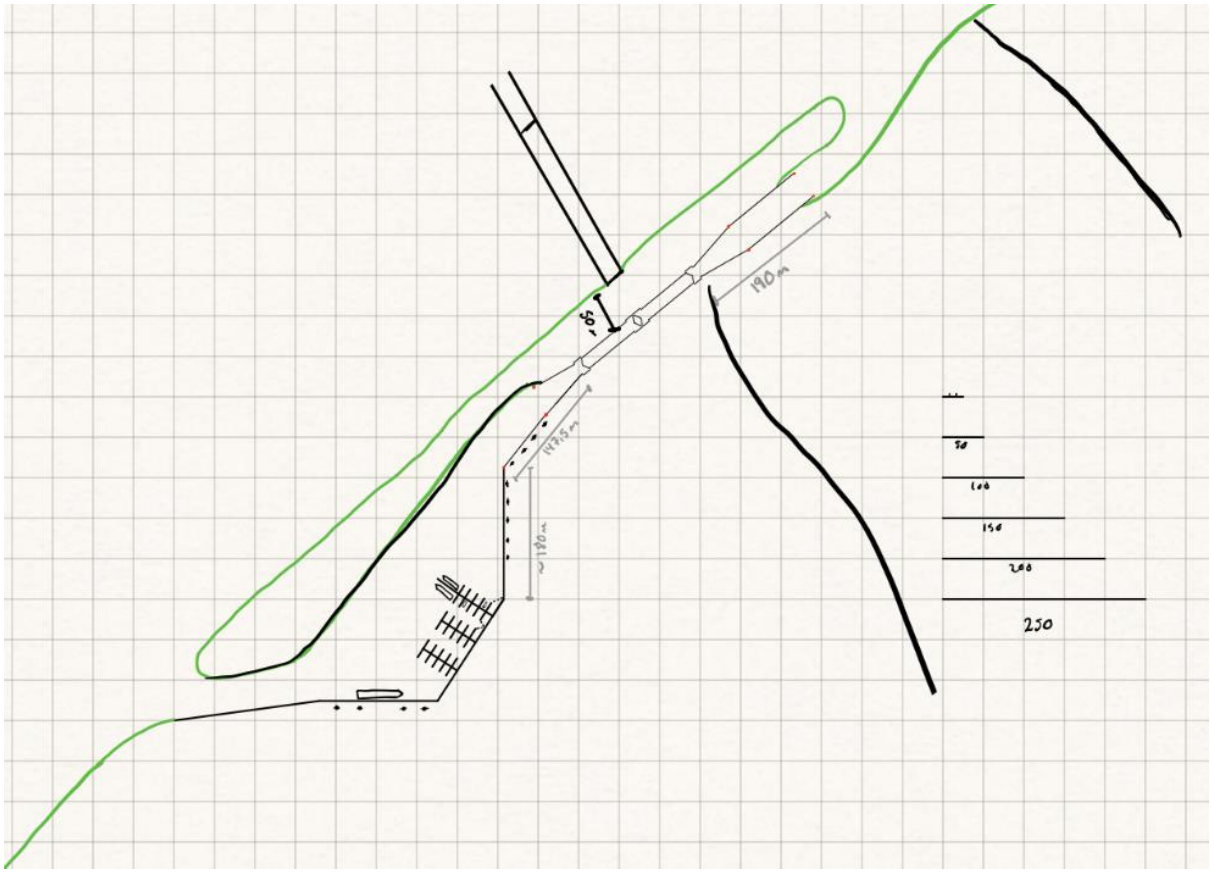


**Figure 16: Sketched overview of the lock basin and the area around it, including the recreational harbour.**

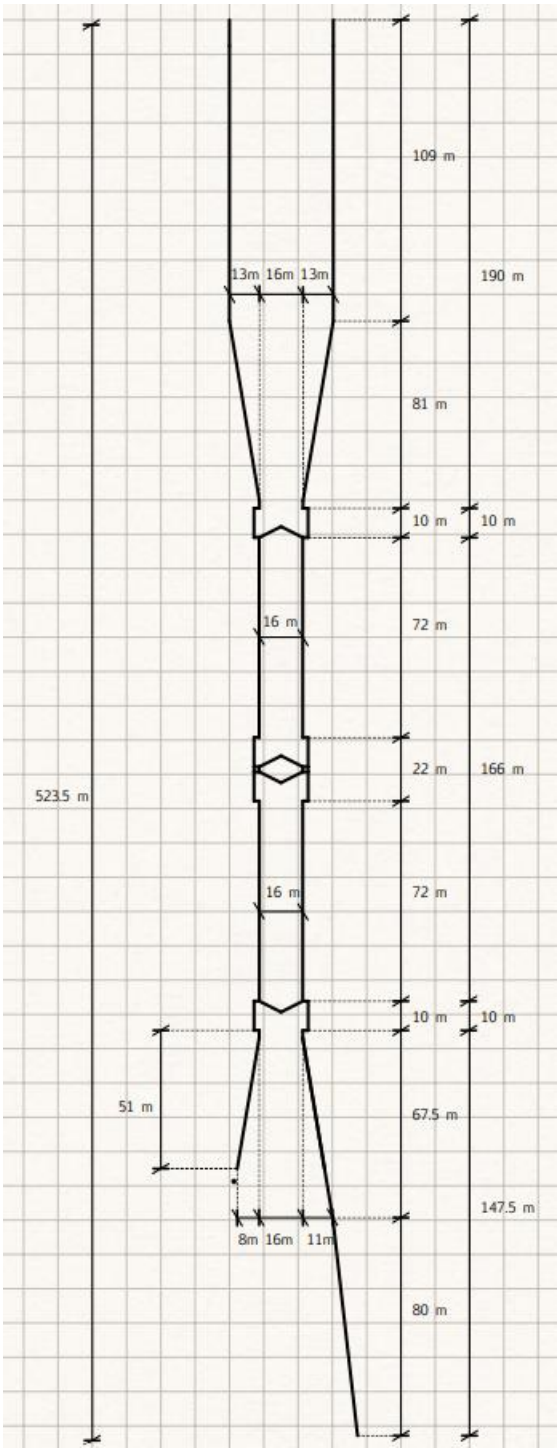


**Figure 17: Lock complex dimensions**

# 4. Base Case Design of the Concrete Lock Chamber

A ship passage at the location of Delta21 will be a necessary service for recreational- and fishing ships, by giving them a navigational connection between the North Sea and the harbours in Stellendam and Hellevoetsluis. This Ship passage needs to be at least large enough so that it can service the same size of ships that pass through the current Goereese sluis and could be bigger if there is a possible demand for a new recreational harbour or if the fishing industry in the Netherlands will grow. The ship passage must provide a safe passage for the ships and thus the location of the ship lock is of high importance. It must also serve as a flood defence during extreme storms.

To start off this chapter, A description of how ship lock dimensions are determined is presented. This will however not be put in practice for this ship lock design as the lock size will be kept the same as the Goereese sluis. In chapter 4.2 the base design of the concrete lock chamber found.

Listed below are some recurring parameters in the coming formulas.

| | | |
|---|---|---|
| $\gamma_{cc}$ | [kN/m$^3$] | Unit weight of reinforced concrete; $\gamma_{cc} = 25\ kN/m^3$ |
| $\gamma_{uwc}$ | [kN/m$^3$] | Unit weight of underwater concrete; $\gamma_{uwc} = 23\ kN/m^3$ |
| $\gamma_w$ | [kN/m$^3$] | specific weight of salt water; $\gamma_w = 10.05\ kN/m^3$ |
| $\gamma_s$ | [kN/m$^2$] | Specific weight of sand; $\gamma_s = 19\ kN/m^2$ |
| $\gamma_{s,sat}$ | [kN/m$^2$] | Specific weight of saturated sand; $\gamma_{s,sat} = 21\ kN/m^2$ |
| $\varphi'$ | [°] | Friction angle of the surrounding soil; $\varphi' = 30°$ |
| $\gamma_{Q,unf}$ | [-] | Variable load safety factor for an unfavourable load; $\gamma_{Q,unf} = 1.5$ |
| $\gamma_{G,unf}$ | [-] | Permanent load safety factor for an unfavourable load; $\gamma_{Q,unf} = 1.35$ |
| $\gamma_{Q,f}$ | [-] | Variable load safety factor for a favourable load; $\gamma_{Q,f} = 1.0$ |
| $\gamma_{G,f}$ | [-] | Permanent load safety factor for a favourable load; $\gamma_{G,f} = 1.0$ |
| $B_{ch}$ | [m] | Width of the lock chamber; $B_{ch} = 16\ m$ |
| $\gamma_c$ | [-] | Partial safety factor for concrete in ULS; $\gamma_c = 1.5$ |
| $\gamma_{s,0}$ | [-] | Partial safety factor for steel in ULS; $\gamma_{s,0} = 1.15$ |

## 4.1. Dimensions of Ship, Classification and Sizing of Lock

A ship lock consists of lock approaches, lock heads, chambers, and the lay out and facilities provided in the lay out. The most important functional requirement of a ship lock is that vessels can pass through it quickly and safely. Safe passage is determined by the degree of certainty that navigational traffic can be dealt with smoothly, without danger and/or damage to people, materials and the environment (Beem, et al., 2000).

### 4.1.1. Vessel Classification

The user group for the waterway classification is maritime navigation for small fishing vessels, transport vessels and recreational navigation. The waterway is a mix of maritime lanes and inland waterways. The vessel classification for the smaller fishing vessels that can be used is PIANC. As the waterway will be new PIANC recommends using larger vessel dimensions such as summarized in the table 1. Table 2 shows the River/Sea classes according to PIANC for smaller sea going vessels that is closely linked to the CEMT classification for inland navigation.

Table 1: River/Sea classes of ships for lock design in new waterways

| R/S klasse (River/Sea) | maximum permitted vessel dimensions (m) | | | minimum bridge passage height (m) |
|---|---|---|---|---|
| | length | width | draught | |
| 1 | 90 | 13.0 | 3.5 of 4.5 | 7.0 of 9.1 |
| 2 | 135 | 16.0 | 3.5 of 4.5 | ≥ 9.1 |
| 3 | 135 | 22.8 | 4.0 of 4.5 | ≥ 9.1 |

Table 2: River/Sea class of ships

| CEMT class | R/S class (River/Sea) | vessel dimensions (m) | | | minimum bridge passage height (m) |
|---|---|---|---|---|---|
| | | length | width | draught | |
| Va | 1 | 80-90 | 11.4 | 3.5-4.5 | 7.0 |
| VIb | 2 | 110-120 | 15.0 | 3.5-4.5 | 9.1 |
| VIb | 3 | 135 | 22.8 | 4.0-4.5 | 9.1 |

Goereese sluis is 16 m wide, 144.5 m long and with a threshold depth of 5 m. Therefore, the ship class for the new lock will be taken as R/S class 2 (table 1) with some limitations to the width, as the Goereese sluis does not allow for 16m wide ships.

For the recreational vessels that will travel through the lock a classification from the CVB guidelines can be used. Table 3 shows a few different classes of recreational navigation vessels. The Netherlands has a lot of traditional and sailing boats. Traditional boats are do not travel much to the open sea but rather belong to small inland navigation. Therefore, category 3 or 4 for sailing boats will be chosen for the design of the ship lock. Tugboats will be available for less experienced vessels (captains that do not use locks often) and for larger vessels.

Table 3: Recreational navigation vessel classes.

| Category | class | height (m) | draught (m) | width (m) | length (m) |
|---|---|---|---|---|---|
| Sailing boats | 1 | 8.50 | 1.25 | 3.00 | 9.00 |
| | 2 | 12.00 | 1.50 | 3.50 | 10.00 |
| | 3 | 12.00 | 1.75 | 3.75 | 11.00 |
| | 4 | >>12.00 | 1.90 | 4.00 | 12.00 |
| Motorboats | 1 | -- | 0.90 | 3.50 | 10.00 |
| | 2 | 2.75 | 1.10 | 3.75 | 12.00 |
| | 3 | 2.75 | 1.40 | 4.00 | 14.00 |
| | 4 | 3.40 | 1.50 | 4.25 | 15.00 |
| Traditional boats | bv1 | >>12.00 | 1.20 | 5.50 | 25.00 |
| | bv2 | >>12.00 | 1.40 | 6.50 | 30.00 |

## 4.1.2. Intensity of Navigation Volume

The number of chambers necessary for a lock is determined by the navigation volume. Navigation volume also determines the required length and width of the chamber, the sill depth and capstone and sometimes the clearance. Fleet composition and the traffic intensity is used to determine the volume of navigation. The number of gate operations for inland-, marine-, and recreational vessels passing through Goereese sluis in 2021 by the month was as follows:

Table 4: Monthly number of lock operations in 2021 – Goereese sluis.

| | |
|---|---|
| **January** | 257 |
| **February** | 218 |
| **March** | 303 |
| **April** | 427 |
| **May** | 604 |
| **June** | 968 |
| **July** | 960 |
| **August** | 896 |
| **September** | 739 |
| **October** | 284 |
| **November** | 176 |
| **December** | 159 |

The total number of lock operations in 2021 were 5991. Ship passages through the Goereese sluis between the year 2015 and 2020, and the split between different type of vessels can be seen in Table 5 below (table in Dutch) (Huizer, 2022):

Table 5: Ship passages through the Goereese sluis in the years 2015-2020

| Goereesesluis | Aantal passages 2015 | Aantal passages 2016 | Aantal passages 2017 | Aantal passages 2018 | Aantal passages 2019 | Aantal passages 2020 |
|---|---|---|---|---|---|---|
| **Visserij schepen** | **749 (13%)** | **747 (13%)** | **596 (12%)** | **712 (12%)** | **283 (22%)** | **348 (6%)** |
| **Zeevisser** | 727 | 710 | 558 | 667 | 261 | 332 |
| **Binnenvaartvisser** | 22 | 37 | 38 | 45 | 22 | 16 |
| **Vrachtschepen** | **515 (9%)** | **495 (9%)** | **516 (10%)** | **602 (11%)** | **449 (36%)** | **498 (10%)** |
| **Vrachtschepen (binnenvaart)** | 472 | 445 | 475 | 557 | 431 | 475 |
| **Vrachtschepen (zeevaart)** | 20 | 12 | 14 | 26 | 0 | 1 |
| **Overige vrachtschepen (zeevaart)** | 23 | 38 | 27 | 19 | 18 | 22 |
| **Recreatieschepen** | **4117 (71%)** | **4098 (72%)** | **3483 (70%)** | **4031 (71%)** | **211 (17%)** | **3630 (71%)** |
| **Vissers** | 133 | 164 | 123 | 187 | 111 | 22 |
| **Passagiersschepen / rondvaartboot / veerboot etc.** | 0 | 1 | 3 | 17 | 3 | 9 |
| **Motorjacht** | 421 | 401 | 405 | 497 | 13 | 648 |
| **Speedboot** | 0 | 0 | 0 | 0 | 0 | 0 |
| **Zeiljacht** | 2850 | 2845 | 2424 | 2707 | 28 | 2246 |
| **Roeiboot/kano etc.** | 608 | 627 | 454 | 544 | 40 | 507 |
| **Grote recreatievaart >20m** | 105 | 60 | 74 | 79 | 16 | 198 |
| **Overige schepen** | **399 (7%)** | **367 (6%)** | **360 (8%)** | **316 (6%)** | **318 (25%)** | **647 (13%)** |
| **Dienstvaartuig (politie etc.): (binnenvaart) en (zeevaart)** | 164 | 155 | 155 | 234 | 82 | 122 |
| **Baggerschepen** | 35 | 6 | 7 | 27 | 19 | 24 |
| **Zeevaart passagiersschip** | 0 | 0 | 0 | 0 | 6 | 5 |
| **Overige zeevaart schepen** | 174 | 188 | 196 | 51 | 31 | 20 |
| **Vaartuig type onbekend** | 0 | 0 | 0 | 0 | 178 | 440 |
| **Overige binnenvaart/ bijzonder transport** | 26 | 18 | 2 | 4 | 2 | 3 |
| **Snel schip draagvleugelboot/catamaran** | 0 | 0 | 0 | 0 | 0 | 33 |
| **Totaal (100%)** | **5780** | **5707** | **4955** | **5661** | **1261** | **5123** |

Due to covid in 2019 and in 2020 the percentage of fishing vessels (Visserij schepen) is skewed. Therefore, in the estimation of the fleet composition that will make use of the new Haringvliet lock, it is assumed that 13% of all vessels that use the lock will be fishing vessels, 11% of the vessels are transport vessels

(vrachtschepen) and 72% of the vessels are recreational (Recreatieschepen). These percentages are taken with regards to table 5 in the years 2015 to 2018. With this fleet composition in mind the number of fishing vessels in 2021 was around 779 vessels, number of transport vessels was 659 vessels and number of recreational vessels was 4314. The rest of the vessels that are not included in these numbers are for example tugboats, dredging vessels and others. June is the busiest month and will thus be chosen with regards to vessel count for the normative intensity (968 gate operations). This is during the summer, so the number of recreational vessels is high. Dividing June's gate operations by 30.5/7 (average month of 30.5 days) results in the normative navigation per week:

$$I_{current,normative} = 968 \frac{navigations}{month} \div \frac{30.5}{7} = 222.17\ navigations\ per\ week$$

The average navigation intensity per week is however:

$$I_{current,average} = I_{total} \frac{navigations}{year} \div \frac{365}{7} = 114.90\ navigations\ per\ week$$

Where $I_{total}$ is the total number of navigations throughout the whole year.

A forecast for the future traffic volume is also needed as the navigational volume is a derivative of transport requirement. The future volume of traffic through the new Haringvliet can depend on a number of things. Some are mentioned here:

- Fishing vessels might be larger in the future; Assuming that the EU aims to keep sustainable fishing by not allowing overfishing, the number of fishing vessels in the fleet composition will be considered to stay similar as to the 2021 numbers (779 vessels).
- Recreational shipping might increase, with climate change increasing the duration of summer; as a first estimate, a 15% increasement of navigation of recreational boats through the new lock is assumed. This increase will be distributed evenly over the summer months when recreational shipping is at its high (from May until the end of September). The total number of recreational navigations in a forecasted year is thus 4962.
- Transport of goods might increase in the future; Due to the constant growth of the population around the globe it can be assumed that Transport of good via waterways will continue to increase. Therefore, as a first estimate the number of transport vessels that will use the lock will be assumed to increase by 10% in the future setting the total number, according to the 2021 estimate, to 725 transport vessels per year.

The rest of the fleet (tugboats, dredgers, etc) will be assumed to stay the same in the future as 239. Therefore, the forecasted total number of navigations in a year is:

$$I_{total,f} = N_{f,fishing} + N_{f,transport} + N_{f,recreational} + N_{f,rest} = 779 + 725 + 4962 + 239$$
$$= 6705 \frac{navigations}{year}$$

Where $N_{f,i}$ is the number of navigations for each vessel type. Since the total number of forecasted vessel passages is over 5000, it is not considered as a small volume of navigation. The forecasted intensity average can now be calculated as:

$$I_{forecast,average} = I_{total,f} \frac{navigations}{year} \div \frac{365}{7} = 128.59\ navigations\ per\ week$$

Where $I_{total,f}$ is the total number of navigations throughout the whole year in the forecasted case. The intensity in the normative forecast week can now be derived as follows:

$$I_{forecast,normative} = \frac{I_{current,normative}}{I_{current,average}} \cdot I_{forecast,average} = 248.64 \approx 249 \text{ navigations per week}$$

Hence, the forecasted navigational intensity during the busiest month of the year is predicted as 249 navigations per week through the new lock complex.

### 4.1.3. Size of Ship Lock

A normative vessel size is used to determine the chamber dimension for a marine navigation lock. Here, the normative vessel dimensions will be taken as the largest vessel allowed through the Goereese sluis. The initial dimensions of the lock will thus be the same as the Goereese sluis with a total length of $L_{lock} = 144$ m (2x 72 m long chambers), a chamber width of $B_{ch} = 16$ m and depth of $d_{ch} = 5$ m with a keel clearance of 1.5 m. This indicates a vessel with a maximum draught of 3.5 m can navigate through the lock. The minimum wet cross-section (c-s) of the chamber is 16 m x 5 m = 80 m$^2$. To ensure sufficiently safe and quick navigation in and out of a marine lock, the wet c-s of the chamber at minimum locking levels should be at least 25 – 30% larger than the c-s of a normative vessel. That means that the c-s of a normative vessel is at most:

$$A_{v,normative} = \frac{80\ m^2}{1.25} = 64\ m^2$$

For the first 50 years (2050 – 2100) there is only need for a single lock head with flood gates as the storm surge barrier will mostly stay open over that period so the water levels on sea and behind the barrier will be the same. The New storm surge barrier was designed for climate scenario SSP5-8.5: continuing rise in greenhouse gas emissions (Verschoor, 2023). The SLR every 50 years until the year 2250 were estimated based on Figure 3 in chapter 2 and the values are given in Table 6 below.

**Table 6: Estimated sea level rise for climate scenario SSP5-8.5**

| ***Year*** | **2050** | **2100** | **2150** | **2200** | **2250** |
|---|---|---|---|---|---|
| *SLR [m]* | 0.32 | 0.82 | 1.50 | 2.60 | 3.88 |

The sill depth is very important in marine locks as it influences the navigation through a lock. A shallow sill depth at the entrance of the chamber can result in higher hydraulic resistance and it can induce translation waves on entry that could result in the hindrance of other vessels. This in return can affect the average passing through time. The sill level can be determined from the minimum locking level. Vessels should be able to navigate through the lock during normal tide conditions and during bad weather (small storms). The lock should also be accessible during low river discharges during the summer. The water level behind the current Haringvlietdam during dry summers such as in 2022 never went under -0.1 m NAP (Rijkswaterstaat, Hellevoetsluis Waterhoogte Oppervlaktewater, 2022) and in 2018 the mean low tide was NAP - 0.85 m. With a sea level rise of 0.82 m in 2100 the minimum locking level is chosen as Min.S = -0.18 m NAP, 0.15 m lower than the estimated mean low tide in 2100, to minimize the wait time of vessels. The sill level will thus be the minimum locking level minus the depth of the chamber, which was chosen as 5 m: $d_{sill} = (NAP - 0.18\ m) - 5m \approx -5.20\ m\ NAP$.

The capstone height (height of the chamber wall) is determined by the nautical requirements in connection with the maximum locking level and by the water retaining function of the lock as it is a part of a flood defence system. The lock head around the center flood gates will have the same length as the dike crest which is 22 m wide. The dike will have the same water retaining height as the SSB with its top level at NAP +10.5 m. For the whole lock the chamber walls will be 0.5 m higher than the soil. Therefore, the wall height for the center lock head will be 16.2 m, e.g. NAP +11 m. the wall height will decrease along with the dike

slope at either side of the center lock head. The height will decrease in steps along the dike slope. The dike has a 1:3 slope and with each step the chamber wall height will decrease by 0.5 m until it reaches the minimum chamber wall height. Therefore, a single step will be 1.5 m long.

The capstone height at the seaside chamber is determined by the maximum locking level and the additional height necessary for visual guidance. The spring mean high water level (MHWS) will be taken as the maximum locking level for the chamber on the seaside of the center lock head. In 2018 this water level was MHWS = NAP +1.67 m, therefore it is estimated to be NAP +5.55 m in 2250 (3.88 m SLR). The walls will be around 1.5 m higher for visual guidance, giving the lowest height of the wall as NAP +7.0 m at the seaward side of the lock. A recreational harbour is situated at the seaward side of the lock complex. The land surrounding the harbour will be at the same level as the wall (NAP + 6.5 m). After the permanent closing of the storm surge barrier the water level withing the tidal lake will be kept at a maximum of NAP +1.0 m. Therefore, the maximum locking level on the riverside of the lock chamber set to a level a bit higher than this. It is assumed that the maximum locking level on the riverside chamber is +3.0 m. the capstone height for the riverside chamber is therefore set to NAP +4.5 m (1.5 m additional height for visual guidance).

Lock heads will allow for 2.5 m additional width for the mitre gates. Assuming that the rotating mechanism positioned 1.5 m away from the chamber wall the gates must be able to close an 18 m wide opening. The extra 1.5 m behind the gates will be used for maintenance of the gates. Two sets of mitre gates (4 gates in total) are provided at the crest of the dike. Using the optimum angle of 18.4° for load transfer and material use (Vrijburcht, et al., 2000), the total length of a single gate is:

$$L_{gate} = \frac{18\ m/2}{\cos\left(18.4°\right)} \approx 9.5\ m$$

Allowing for 1.0 m space between the two mitre gates for rotating mechanisms the total width of the lock head will be:

$$L_{center,head} = 2t_{wall,t,center} + L_{gate} \cdot 2 + 1.0\ m = 2t_{wall,center} + 20\ m$$

Where $t_{wall,t,center}$ is the top wall thickness of the tapered wall at the center lock head, $t_{wall,t,center}$ = 1.0 m. the lock heads at the end of the seaside and riverside chamber will each have one set of mitre gates. Allowing for a 0.5 m additional length of the lock head for the gate moving mechanisms the total width of the smaller lock heads will be:

$$L_{small,head} = 2t_{wall,t,sea/river} + L_{gate} + 0.5\ m = 2t_{wall,center} + 10\ m$$

Where $t_{wall,t,sea/river}$ is the top wall thickness of the chamber walls at the seaside and riverside chamber.

Table 7 presents the dimensions of the base case lock chamber.

**Table 7: main dimensions of the base case concrete lock chamber**

| | Description | Value | Unit |
|---|---|---|---|
| $L_{lock}$ | Lock length | 144.0 | m |
| $L_{ch}$ | Chamber length | 72.0 | m |
| $B_{ch}$ | Chamber width | 16.0 | m |
| $d_{ch}$ | Chamber min. water depth | 5.0 | m |
| $L_{center,head}$ | Center lock head length | 20.0 | m |
| $L_{river-sea,head}$ | Smaller lock head length | 10.0 | m |
| $L_{step}$ | Length of one step along the dike slope | 1.5 | m |
| $H_{step}$ | Height of one step along the dike slope | 0.5 | m |

| | | | |
|---|---|---|---|
| $n_{step,sea}$ | Number of steps along the dike at the seaside of the center lock head | 8 | [-] |
| $n_{step,river}$ | Number of steps along the dike at the riverside of the center lock head | 13 | [-] |
| $L_{slope,sea}$ | Length of chamber wall along the dike slope on the seaside of the center lock head | 10.5 | m |
| $L_{slope,river}$ | Length of chamber wall along the dike slope on the riverside of the center lock head | 18.0 | m |
| $Min.S$ | Minimum locking level | -0.18 | NAP m |
| $Max.S_{sea}$ | Maximum locking level for the seaside chamber | +5.55 | NAP m |
| $Max.S_{river}$ | Maximum locking level for the riverside chamber | +3.00 | NAP m |
| $H_{wall,center}$ | Wall height at the center lock head | 16.2 | m |
| $H_{wall,sea}$ | Minimum wall height for the seaside chamber | 12.2 | m |
| $H_{wall,river}$ | Minimum wall height for the riverside chamber | 9.7 | m |

### 4.1.4. Construction Methods

When constructing a lock chamber, different construction methods are available. In this report two construction method alternatives are considered:

1. Immersed lock chamber elements: the lock chamber elements are split into segments and each segment is constructed on ground level and then immersed at the site. This method would save both time and resources as no building pit is necessary.
2. Built in-situ: An open building pit (cofferdam) will be built using sheet piles and an underwater concrete floor (UWCF) to retain water or soil. This will be done over the summer months to avoid large water heads from winter storms. This can be done two ways. If there is a deep impermeable layer sheet piles can be used as a seepage screen and the U-basin can be constructed on top of the soil. If there is no impermeable layer or it is too deep underground, an underwater concrete floor can be built with or without tension piles to resist the uplift pressure from the ground water (see Figure 18).

   From the CPT results in appendix A it can be seen that from -10 m NAP to -12.2 m NAP (-6.5 to -8.7 m NAP on Figure 63) the friction ratio is around 3%, which is representable for silty-clay soil (Apriyono & et al., 2018). How ever it does not constantly stay above 3% meaning that this layer is mixed with some sand and is therefore not completely impermeable. Therefore, a construction pit with sheet pile walls and a piled underwater concrete floor would be opted for.

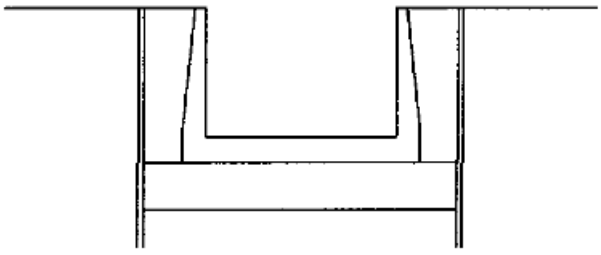

**Figure 18: Simple demonstration of a construction pit and with an underwater concrete flooring**

### 4.1.5. UWCF Design

To Ensure water tightness of the construction pit, an underwater concrete floor (UWCF) will be constructed. hydrostatic water loads will cause loading on the floor in the form of uplift force from an upward water pressure. After the lock chamber is constructed there will also be compression on the floor. Circular prefabricated concrete foundation piles will be used as they can perform in both tension and

compression. These piles can reach a length of maximum 35 m and are suitable for both tension and compression forces. They can be driven down using vibrations (Voorendt & Molenaar, 2020). As the ship lock is not located near older buildings or any industry the driving of the piles should not lead to any damages to nearby structures.

The bottom of the chamber is at -6.9 m NAP assuming 1.7 meter thick chamber floor (see chapter 4.1). With some iterations of the equations below a UWCF thickness of $t_{uwc} = 1.4$ m was chosen for the base case design putting the bottom of the UWCF at level of NAP -8.3 m. The construction pit will allow for 1.2 m margin on either side of the Chamber. With 2.8 m thick walls (see chapter 4) the width of the UWCF will be $B_{uwc} = 24$ m. With the ground water level at $h_{gwl}$ = NAP + 2.0 m the hydrostatic uplift force at $h_{bot,uw}$ = NAP -8.3 m is calculated as:

$$P_{hydro} = \left(h_{gwl} - h_{bot,uw}\right) \cdot \gamma_w = 103.57\ kN/m^2 \tag{4.1}$$

Where $\gamma_w$ is the specific weight of salt water.

Forces that will counteract this uplift force to avoid floatation of the floor are the weight of the UWCF, the weight of the piles and the attached clump weight pulled up by the piles. The UWCF is made of unreinforced concrete with a unite weight of $\gamma_{uwc} = 23\ kN/m^3$.

The top of the piles that is not within the UWCF slab is at -8.3 m NAP. The CPT test in appendix A (offset by 3.5 m for the chosen location) shows that from -8.3 m NAP to -16.2 m NAP is a sand layer. From -16.2 m NAP to -22.5 m NAP is a gravely sand layer (see Appendix A). Therefore, the Piles should reach at least 7.9 m below the floor so that they reach through the sand layers. With a 0.8 m anchoring length into the UWCF the minimum length of the piles will be 8.7 m. This length might not provide enough resistance and thus the pile might have to reach into the sand-gravel layer. A pile length of 13 m will be assumed. Therefore, the pile tip will reach a depth of -20.5 m. A pile diameter of $D_{pile}$ = 500 mm is chosen.

**Tension loads**

Tension piles will resist the upward water pressure when the construction pit is still empty. The total uplift force ($F_{uplift}$) causing tensile loads is the upwards buoyancy force counteracted by the weight of the 1.4 m thick uwc slab with the added weight of the plies:

$$F_{uplift} = A_{uw}\left(P_{hydro} - \gamma_{uwc} \cdot t_{uw}\right) - n_p \cdot V_{pile} \cdot \left(\frac{\gamma_{cc}}{1.1} - \gamma_w\right) = 123{,}325.8\ kN - 32.35 n_p \tag{4.2}$$

Where:

| | | |
|---|---|---|
| $A_{uw}$ | [m²] | Area of the underwater concrete floor under one chamber; $A_{uw} = 1728\ m^2$ |
| $P_{hydro}$ | [kN/m²] | Hydrostatic uplift force at NAP -8.3 m calculated in equation 4.1 |
| $t_{uw}$ | [m] | Thickness of UWCF; $t_{uw} = 1.4\ m$ |
| $n_p$ | [-] | Total number of piles in the UWCF |
| $V_{pile}$ | [m³] | Volume of a single pile; $V_{pile} = \frac{\pi D_{pile}^2}{4} h_{pile} = \frac{\pi \cdot (0.5m)^2}{4} \cdot 13\ m = 2.55\ m^3$ |

The required number of tension piles can be determined using the cone resistance method which checks for failure due to sliding. The maximum tensile forces that a single pile can resist can be determined through the following equation:

$$F_{r,tension,d} = \int_{z=0}^{L} q_{c,z,d} \cdot f_1 \cdot f_2 \cdot O_{p,mean} \cdot \alpha_t\ dz = O_{p,mean} \cdot \alpha_t \cdot L = 749.33\ kN \tag{4.3}$$

Where:

| | | |
|---|---|---|
| $q_{c,z,d}$ | [MPa] | Design value for the tensile strength of the soil, equation 4.4 |
| $f_1$ | [-] | Pile installation factor $\geq 1$. Here taken as $f_1 = 1$ |
| $f_2$ | [-] | Cone resistance reduction factor $\leq 1$. Hare taken as $f_2 = 1$ |
| $O_{p,mean}$ | [m] | Average circumference of the circular pile shaft. $O_{p,mean} = \frac{2\pi D}{2} = 1.57$ m |
| $\alpha_t$ | [-] | Pile class factor depending on soil type. gives values for different piles driven in sand. $\alpha_t = 0.007$ |
| L | [m] | Pile length under the UWCF; L = 12.2 m |

**Table 8: Maximum values for the pile class factor in sand and sand containing gravel (Voorendt & Molenaar, 2020)**

| Pile class/type | $\alpha_t$ |
|---|---|
| • Ground displacing installing methods: | |
| ○ driven smooth prefab concrete pile and steel tube pile with closed tip[1)] | 0,007 |
| ○ pile made in the soil, whereby the concrete column directly presses onto the ground and the tube is driven back (*teruggeheid*) out of the soil[2)] | 0,012 |
| ○ ditto, in case the tube is removed by vibration | 0,010 |
| ○ tapered wooden pile | 0,012 |
| • Screwed piles: | |
| ○ with grout injection or mixing | 0,009 |
| • Piles with little ground displacement: | |
| ○ driven steel profiles | 0,004 |
| • Soil removing piles: | |
| ○ drilled piles (and auger piles) | 0,0045 |
| [1)] The base of a tube pile with a closed tip shall not exceed 10 mm beyond the tube protruding. [2)] For this type of pile the diameter of the base may in principle be 30-50 mm larger than the outside diameter of the casing. | |

The design value for the cone resistance is then:

$$q_{c,z,d} = \frac{q_{c,z,rep}}{\gamma_{m,b,4} \cdot \gamma_{m,var,qc}} = 5.59\ MPa \tag{4.4}$$

Where:

| | | |
|---|---|---|
| $q_{c,z,rep}$ | [MPa] | Representative value for the cone resistant at depth z. Calculated in Appendix C.1: Under water concrete floor; $q_{c,z,rep} = 11.31\ MPa$ |
| $\gamma_{m,b,4}$ | [-] | Resistance factor for tension piles; $\gamma_{m,b,4}$ =1.35 |
| $\gamma_{m,var,qc}$ | [-] | Load factor conservatively taken as the maximum value of the material factor; $\gamma_{m,var,qc} = 1.5$ |

The uplift force must be resisted by the tension piles. Hence the number of tension piles necessary to resist the uplift force is found iteratively using equation 4.2 and 4.3:

$$n_{tension} = \frac{F_{uplift}}{F_{r,tension,d}} = \frac{123{,}325.8\ kN - 32.35 n_{piles}}{749.33\ kN} \approx 158\ piles$$

The second check for the tension piles is the clump criterion, considering the surrounding soil. It indicates that the tensile force on a pile cannot surpass the weight of the pile and the weight of the clump of soil effected by the pile, hence $F_{tension} < F_{clump}$. The resisting clump force is computed using the following equation:

$$F_{clump} = V_{clump}\gamma_{d,soil} + V_{pile}\gamma_{d,cc} = \left(V_{cone} + V_{cylinder} - V_{pile}\right)\gamma_{d,soil} + V_{pile}\gamma_{d,cc} \tag{4.5}$$

Where:

| | | |
|---|---|---|
| $F_{clump}$ | [kN] | Maximum tensile force the soil can absorb |
| $V_{clump}$ | [m³] | Volume of the clump of soil affected by the pile |
| $V_{cone}$ | [m³] | Volume of the cone-shaped soil at the tip of the pile |
| $V_{cylinder}$ | [m³] | Volume of the cylinder-shaped soil above the cone |
| $V_{pile}$ | [m³] | Volume of the pile shaft that is underground |
| $\gamma_{d,soil}$ | [kN/m³] | Design value for the effective specific weight of the soil; $\gamma_{d,soil} = \gamma_{s,sat} - \gamma_w = 21 - 10.05 = 10.94$ kN/m³ |
| $\gamma_{d,cc}$ | [kN/m³] | Design value for the underwater weight of the pile. $\gamma_{d,cc} = 25 - 10.05 = 14.95$ kN/m³ |

The zones of each pile cannot overlap as the soil can only absorb tensile load once. The maximum influence area of a pile is a cylindrical with a diameter $D_c = 2R_c = 6D$, e.g. $D_c = 3.0$ m. When the pile is driven into the ground soil is displaced and at the top angle is formed. The top angle depends on the pile type and the position of the pile (in the middle of the pile group or on the edge). The piles used here are installed with a ground displacing method and thus the half top angle of piles within a group of piles is 45°. Figure 19 shows the clump and the top angles for an inner pile and an outer pile.

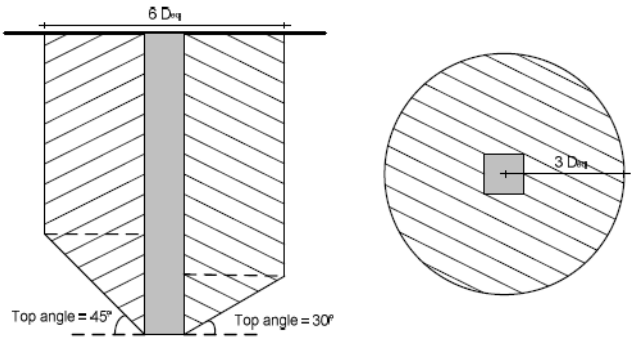


**Figure 19: Clump volume of a tension pile**

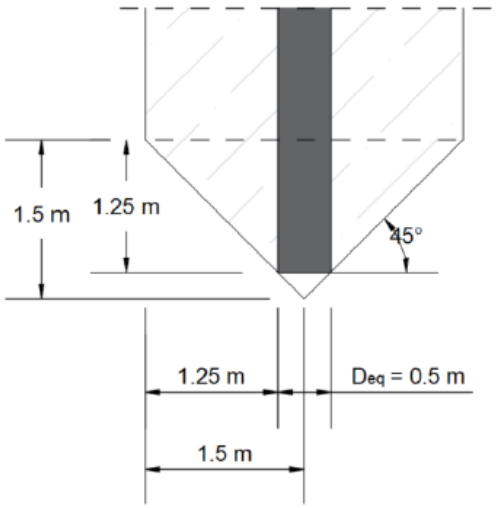


**Figure 20: schematization of a cylindrical clump cone around a tension pile**

The volume of the cone shaped clump around the end of the pile, the cylinder-shaped clump and the pile under the UWCF is calculated according to Figure 20 as:

$$V_{cone} = \pi R_c^2 \frac{h_c}{3} - \pi R_{c,tip}^2 \frac{h_{c,tip}}{3} = 3.52\ m^3$$
$$V_{cylinder} = \pi R_c^2 h_{cil} = 77.40\ m^3 \quad (4.6)$$
$$V_{pile} = \pi RL = 2.40\ m^3$$

Where:

| | | |
|---|---|---|
| $R_c$ | [m] | Radius of the clump cylinder; $R = 1.5$ m |
| $h_c$ | [m] | Height of the cone. With a 45° angle $h_c = 1.5$ m |
| $R_{c,tip}$ | [m] | Radius of the tip of the cone underneath the pile; $R_{c,tip} = R = \frac{D}{2} = 0.25$ m |
| $h_{c,tip}$ | [m] | Height of the tip of the cone underneath the pile; $h_{c,tip} = R_{c,tip} = 0.25$ m |
| $h_{cil}$ | [m] | Height of the cylinder-shaped clump; $h_{cil} = L - h_{tip} = 10.95$ m |
| $h_{tip}$ | [m] | Height of the cone shaped tip; $h_{tip} = 1.25$ m |
| L | [m] | Pile length under the UWCF; L = 12.2 m |
| R | [m] | Radius of the pile; $R = \frac{D}{2} = 0.25$ m |

Inserting equations 4.6 into equation 4.5 gives:

$$F_{clump} = (3.52\ m^3 + 77.40\ m^3 - 2.40\ m^3) \cdot 10.94 \frac{kN}{m^3} + 2.40\ \ m^3 \cdot 14.95 \frac{kN}{m^3} = 895.22\ kN$$

Since $F_{clump} > F_{r,tension,d}$ the cone resistance of the pile is the determining factor for the number of piles needed and thus 165 tension piles are necessary. With an underwater concrete floor area of $A_{uw} = 1728$ m$^2$ (length of 72 m and width of 24 m) and a minimum of 158 piles the piles will be distributed in 23 rows over the length of the chamber and 7 rows of the width of the chamber giving a total number of 161 piles. This also fulfils the spacing requirements for the piles in the clump criterion as a minimum spacing between piles can be kept as 3 m.

**Compression loads**

The strength of the pile and the bearing capacity of the activated soil around the pile will resist compression loads. The critical load condition for the compression piles is when the ship lock chamber is at maximum locking level. The spring mean high water level (MHWS) will be taken as the maximum locking level. In 2018 this water level was MHWS = NAP +1.67 m, therefore it is estimated to be NAP +5.55 m in 2250 (3.88 m SLR), e.g. the water depth in the chamber will be $d_{water} = +5.55\ m - (-5.2\ m) = 10.75\ m$. The weight of the water within the chamber is thus:

$$W_{water} = \gamma_{Q,unf} \gamma_w d_{water} B_{ch} L_{ch} = 1.5 \cdot 10.06\ kN/m^3 \cdot 10.75\ m \cdot 16\ m \cdot 72.25\ m = 187{,}434.89 kN$$

The weight of the chamber itself is:

$$W_{ch} = \gamma_{G,unf} \big(W_f + 2W_w\big) L_{ch} = 1.35 \cdot (918\ kN/m + 2 \cdot 769.5\ kN/m) \cdot 72m = 239{,}649.64\ kN$$

Where:

| | | |
|---|---|---|
| $W_f$ | [kN/m] | Weight of the floor calculated in chapter 4.2.2 Stability of the chamber |
| $W_w$ | [kN/m] | Weight of a single chamber wall calculated in chapter 4.2.2 Stability of the chamber |
| $L_{ch}$ | [m] | Length of a chamber; $L_{ch} = 72$ m |

The total compression force is therefore:

$$F_{comp} = W_{water} + W_{ch} = 427{,}084.53\ kN \tag{4.7}$$

The Koppejan method is used to determine the bearing capacity of a compression pile. The bearing capacity in ULS is determined by the tip bearing capacity and the shaft bearing capacity:

$$F_{r;max} = F_{r;max;tip} + F_{r;max;shaft} \tag{4.8}$$

Where:

| | | |
|---|---|---|
| $F_{r;max}$ | [kN] | Bearing capacity of the pile |
| $F_{r;max;tip}$ | [kN] | Maximum tip resistance force; $F_{r;max;tip} = p_{r;max;tip}A_{tip}$ |
| $F_{r;max;shaft}$ | [kN] | Maximum shaft friction force; $F_{r;max;shaft} = O_{p;avg}\int_0^{\Delta L} p_{r;max;shaft}dz$ |
| $p_{r;max;tip}$ | [kN/m²] | Maximum tip resistance according to a cone penetration test |
| $p_{r;max;shaft}$ | [kN/m²] | Maximum pile shaft friction according to a cone penetration test |
| $A_{tip}$ | [m²] | Area of the tip of the pile; $A_{tip} = \frac{\pi D^2}{4} = 0.1963$ m² |
| $O_{p;avg}$ | [m] | Average circumference of the pile; $O_{p;avg} = 1.57$ m² |
| $\Delta L$ | [m] | Length of the pile; $\Delta L = 12.2$ m |

For the bearing capacity in SLS the maximum shaft friction force is reduced by a maximum negative shaft friction force.

The maximum tip resistance according to a cone penetration test is calculated accordingly:

$$p_{r;max;tip} = \frac{1}{2}\alpha_p \beta s \left(\frac{q_{c;I;avg} + q_{c;II;avg}}{2} + q_{c;III;avg}\right) \quad (4.9)$$

Where:

| | | |
|---|---|---|
| $q_{c;I;avg}$ | [MPa] | The average value of the cone resistance $q_{c;z;corr}$, along section I from the start of the tip of the pile down to a level that is $0.7D_{eq}$ to $4D_{eq}$ deeper. The bottom of section I is selected so that $p_{r;max;tip}$ is minimal. |
| $q_{c;II;avg}$ | [MPa] | The average value of the cone resistance $q_{c;z;corr}$, along section II from the bottom of section I to the tip of the pile. The chosen value of the cone resistance may never exceed that of a lower level. |
| $q_{c;III;avg}$ | [MPa] | The average value of the cone resistance $q_{c;z;corr}$, along section III from the tip of the pile up to a level that is $8D_{eq}$ above the tip. The chosen value of the cone resistance may never exceed that of a lower level, starting with the value of the cone resistance at the top of section II |
| $\alpha_p$ | [-] | Pile class factor, determined using Table 9; $\alpha_p = 0.7$ |
| $\beta$ | [-] | Influence factor for the shape of the foot of the pile determined using Figure 21. Where $A_1 = A_2$ as $D_{eq} = d_{eq}$ so $A_1/A_2 = 1$; $\beta = 1$ |
| $s$ | [-] | Shape factor for the shape of the cross-section of the foot of the pile determined using Figure 22 where b/a = 1 as it is a circle; $s = 1$ |

**Table 9: Values of the pile class factor $\alpha_p$**

| pile class / type | $\alpha_p$ |
|---|---|
| • **soil displacing placement methods** | |
| - driven piles | 0,70 |
| - driven piles, formed in the soil | 0,70 |
| - screwed piles, formed in the ground | 0,63 |
| - prefabricated screwed piles | 0,56 |
| • **piles with little soil displacement, such as steel profiles and open steel tubes** | 0,70 |
| • **piles made with soil replacement** | |
| - auger piles | 0,56 |
| - drilled piles | 0,35 |
| - pulsated piles | 0,35 |

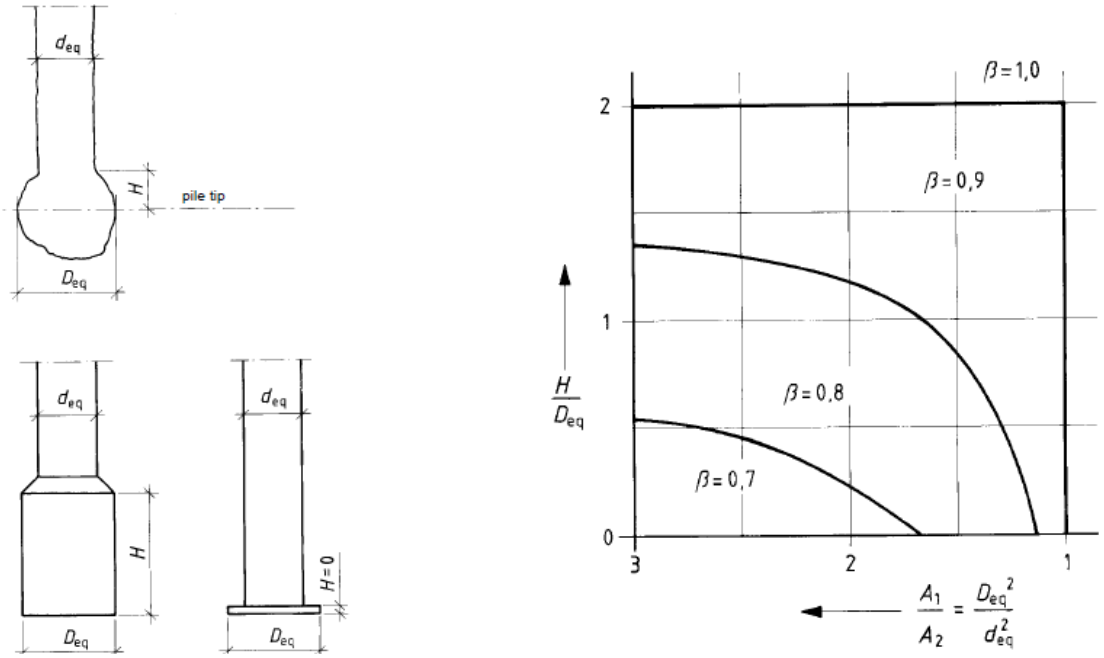


**Figure 21: Left; Shape of the plie footing. Right; Factor for the shape of the pile footing, β**

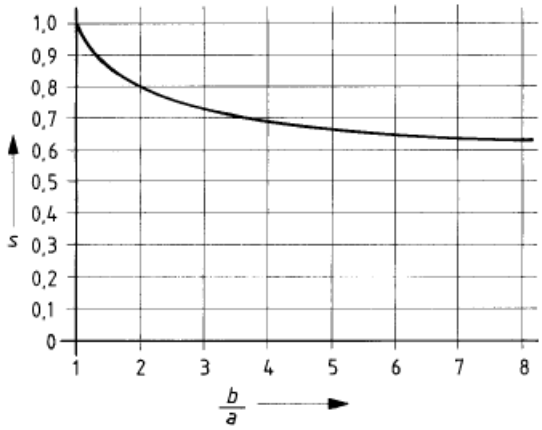


**Figure 22: Values of s; the pile footing shape factor**

The average values of the cone resistance are determined using the cone penetration test. The results are shown on Figure 23.

**Figure 23: cone resistance sections**

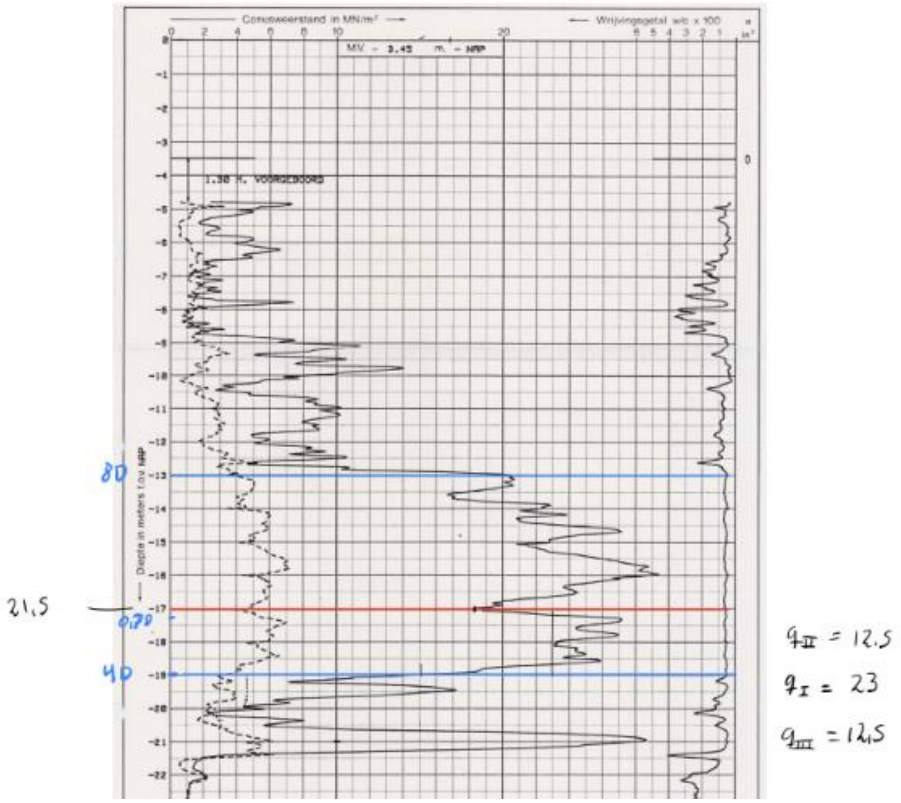


$$q_{c;I;avg} = 23.0\ MPa$$

$$q_{c;II;avg} = 12.5\ MPa$$

$$q_{c;III;avg} = 12.5\ MPa$$

Inserting this in equation 4.9 gives:

$$p_{r;max;tip} = \frac{1}{2} \cdot 0.7 \left( \frac{23 + 12.5}{2} + 12.5 \right) = 10.59\ MPa$$

Therefore, the maximum tip resistance force is

$$F_{r;max;tip} = p_{r;max;tip} A_{tip} = 10.59\ MPa \cdot 0.1963\ m^2 \cdot 10^3 = 2078.85\ kN \quad (4.10)$$

The maximum pile shaft friction at depth z is now determined through the following equation:

$$p_{r;max;shaft,z} = \alpha_s q_{c;z;a} \quad (4.11)$$

Where:

| | | |
|---|---|---|
| $q_{c;z;a}$ | [MPa] | Cone resistance, where the peaks in the sounding diagram with values larger than 15 MN/m$^2$ are removed if these values occur over sections of at least 1 m and otherwise at values of 12 MN/m$^2$. |
| $\alpha_s$ | [-] | Pile factor that considers the influence of the pile installation method determined through Table 10 that applies for fine to coarse sand. 0.010 |

Table 10: Maximum values of $\alpha_s$ in sand

| Pile class / type | $\alpha_s$ |
|---|---|
| • **ground displacing placement methods**: | |
| - driven smooth prefab concrete pile and steel tube pile with closed tip | 0,010 |
| - pile made in the soil, whereby the concrete column presses directly onto the ground and the tube was driven back out of the ground | 0,0014 |
| - in the case of a tube removed by vibration | 0,0012 |
| - tapered wooden pile | 0,0012 |
| - screwed piles | |
| with grout injection or grout mix | 0,009 |
| without grout | 0,006 |
| • **piles with little ground displacement** | |
| - steel profiles | 0,0075 |
| • **piles made with ground replacement** | |
| - auger piles | 0,006 |
| - drilled piles | 0,006 |
| - pulsated piles | 0,005 |

In The cone resistance calculations for the tension piles $q_{c;z;rep}$ was calculated (Appendix C.1:). in zone V all the peaks exceed 15 MN/m$^2$ and therefore the average value for zone V is reduced to 15 MN/m$^2$, resulting in:

$$q_{c;z;a} = 8{,}73\ MPa$$

Inserting this into equation 4.11 gives:

$$p_{r;max;shaft,z} = 0.01 \cdot 8.73\ MPa = 0.0873\ MPa$$

Therefore the maximum shaft friction force becomes; $F_{r;max;shaft} = O_{p;avg} \int_0^{\Delta L} p_{r;max;shaft} dz$

$$F_{r;max;shaft} = O_{p;avg} \int_0^{\Delta L} p_{r;max;shaft} dz = O_{p;avg} \cdot p_{r;max;shaft} \cdot \Delta L \tag{4.12}$$

$$F_{r;max;shaft} = 1.57\ m \cdot 0.0873\ MPa \cdot 12.2\ m \cdot 10^3 = 1672.90\ kN$$

Inserting equations 4.10 and 4.12 into equation 4.8 results in a bearing capacity of:

$$F_{r;max} = 3751.75\ kN$$

The number of compression needed is therefore:

$$n_{comp} = \frac{F_{comp}}{F_{r;max}} = \frac{427{,}084.53\ kN}{3751.75\ kN} = 114\ piles$$

The required number of compression piles are fewer than the required number of tension piles (159 piles) therefore no additional piles need to be added for the compression.

## 4.2. Preliminary Design of Chamber; Base Case

Two alternatives were explored when it came to the chamber typology for the base case; a u-basin structure that and a gravity type structure that would not have any reinforcement. The bottom wall thickness for the gravity structure was found to be over 6 m wide and was therefore not chosen for the base case design as that would require an enormous amount of concrete for the whole structure. Therefore, the base case structure will be a u-basin concrete chamber with a tapered semi-gravity wall design.

The flood gates and lock head will have to be operational until 2250 alongside the SSB. When the ship lock will be constructed in 2100 the sea level will have risen by 0.82 m resulting in the minimum locking level at NAP -0.18. The top of the floor is at NAP -5.2 m.

As the location of the ship passage is currently in water, see Figure 24, the ground water level (GWL) for the new dike and land that will surround the ship lock is assumed to be similar to the GWL of nearby land. According to data from DINOloket most tests on the south side of the Haaringvliet show that the groundwater lies at +1.5 m NAP. The GWL will also rise with the sea level but as the barrier should protect the hinterland the ground water level will be assumed to be at a maximum NAP +2.0 m for the design of the lock chamber. During a storm the water level in the tidal lake will be maintained at NAP +1 m. This water level will also be kept as a maximum after the barrier has been permanently closed.

The ship lock chamber will be constructed in a construction pit consisting of sheet pile walls and an underwater concrete floor. After the chamber has been constructed the backfill soil will be added, and the sheet pile walls will be removed. First, a part of the backfill will be installed and the chamber will be flooded with water. To avoid large internal forces on the lock floor the back fill will be added in a controlled way, equally at the same time on either side of the chamber to avoid asymmetric loads. In the use-phase of the structure, the chamber will never be fully emptied (maintenance will be realized underwater if necessary). Therefore, the governing load case for the chamber walls is when the water level inside the lock is at minimum locking level (NAP -0.18 m in for the year 2100).

### 4.2.1. Governing Load Case

The governing load case demonstrated in this chapter is the load case surrounding the flood gates where the walls are the highest with a top level of NAP +11 m.

The walls of the lock chamber must be able to bear the pressure from the soil, the hydrostatic pressure from the groundwater (1025 kg/m$^3$ for seawater), surcharge load on the surface, and its self-weight. The water within the chamber will act as a passive load. The walls can be schematized as a cantilever beam. The floor of the lock must be able to withstand the uplift water pressure and the moment asserted from the walls on to the floor.

the lock will be constructed where the current topography lies at around -7.5 m NAP. There are not many CPT tests around that area, therefore the CPT test S3-85-963 will be used as a reference to lower layers as it is also located in the Haringvliet near to the location of the new lock complex. Figure 24 shows the location of that test. The CPT test can be seen in appendix A and the subsoil profile is shown in Figure 25. As can be seen the subsoil profile starts at around -4 m depth at this location. Since the depth at the location where the lock will be constructed is at -7.5 m depth, it is assumed that the same soil profile holds but offset by 3.5 meters.

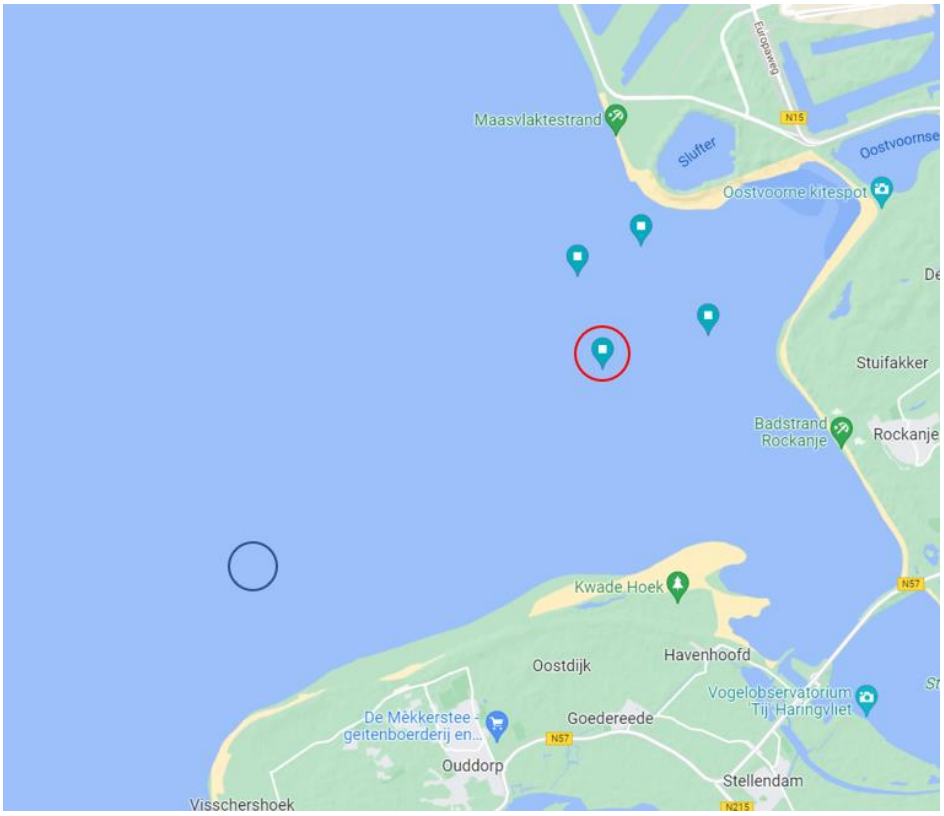


**Figure 24: Red circle indicates the location of CPT test S3-85-963. Blue circle indicates the approximate location of the ship lock.**

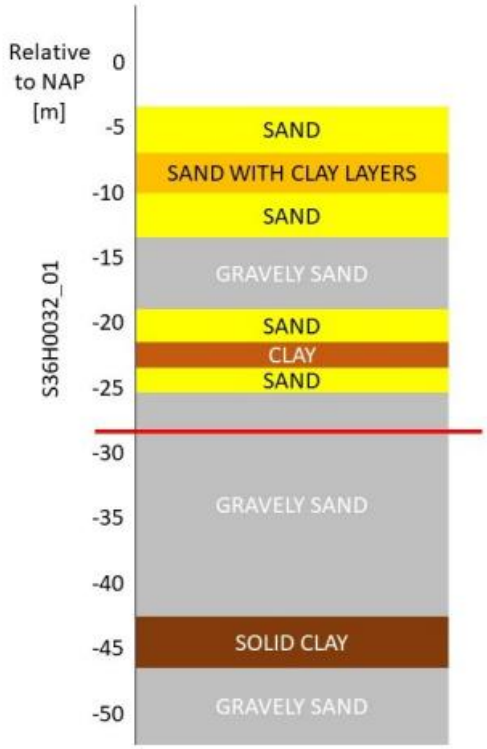


**Figure 25: Soil profile of CPT S3-85-963 (Paasman, 2020), lowered by 3.5 m for the location of the ship lock.**

Since the lock will be constructed where there is currently no land, landfill will be used to build up the land around the Delta21 project. The land fill will be assumed to be well graded sand. Hence, that will be the

soil type surrounding the chamber walls. The soil properties for each soil type are presented in Table 11 below:

**Table 11: Soil types and their properties (abg, 2022)**

| Soil type | Dry [kN/m$^2$] | Saturated [kN/m$^2$] |
|---|---|---|
| **Sand** | $\gamma_s$ = 19 | $\gamma_{s,sat}$ = 21 |
| **Sand and gravel** | $\gamma_g$ = 19 | $\gamma_{g,sat}$ = 21.5 |
| **Clay** | - | $\gamma_{c,sat}$ = 22 |

The height of the chamber around the center flood gates are:

$$H_{chamb} = h_{soil} - d_{lock} + t_f + 0.5\,m = +10.5\,m\,NAP - (-5.2\,m\,NAP) + 1.7\,m + 0.5\,m = 17.9\,m$$

Where:

| | | |
|---|---|---|
| $h_{soil}$ | [m] | Elevation of the dike |
| $d_{lock}$ | [m] | Bottom level of the chamber (top of the chamber floor); $d_{lock} = NAP - 5.2$ m |
| $t_f$ | [m] | Floor thickness; $t_f = 1.8$ m |

As concrete is the main structural material the lock chamber will be a fairly rigid structure. Hence, very little deformation will occur, and the soil can be assumed to be at rest. Therefore, the neutral soil stress will be used for the calculations of the load from the soil acting on the wall. The neutral soil coefficient is calculated using Jáky's theory:

$$K_0 = 1 - \sin\phi' \approx 0.5$$

Here, $K_0$ is the neutral soil pressure and $\phi'$ is the friction angle (30°).

The water within the chamber will provide some resistance to the horizontal load from the soil. As this is a passive load (beneficial to the design) the water level within the chamber is taken as the minimum locking level in the year 2100 (NAP -0.18 m). On top of the surrounding soil will be some machinery, roads, and trucks, and therefore a distributed load of q = 20 kN/m$^2$ on top of the soil is considered. The lock chamber is $H_{wall}$ = 16.2 m deep in proximity to the flood gates. The governing load case for the gravity wall is presented in the Table 25 below. It shows the chamber in proximity to the flood gates, where the wall height is at its maximum, as it is the most unfavourable load case. The soil will lie half a meter below the top level of the chamber wall.

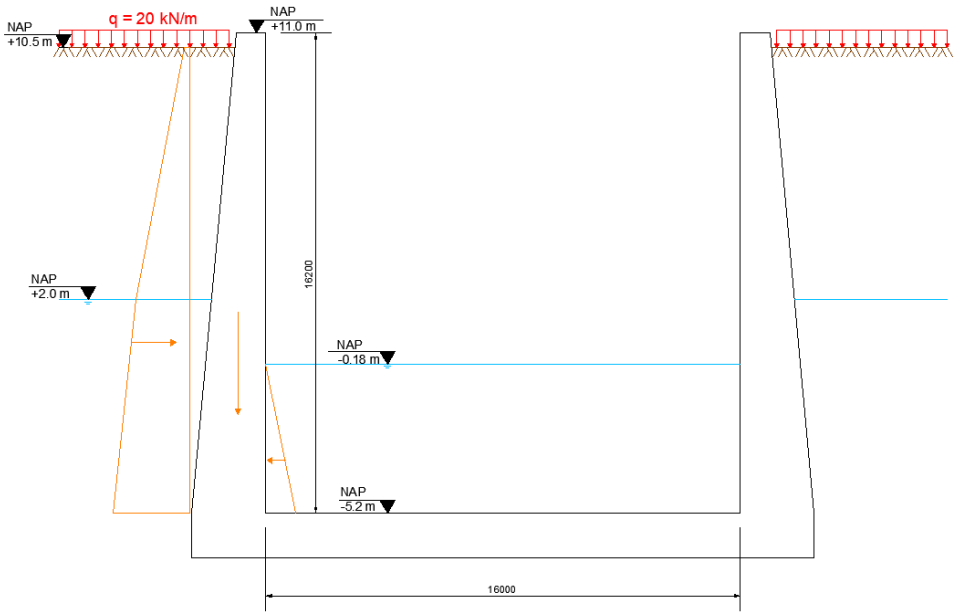


**Figure 26: governing load case**

The vertical soil pressure, $\sigma_{v,n}$ [kN/m$^2$] is calculated using the following equation:

$$\sigma_{v,n} = \gamma \cdot d \tag{4.13}$$

Where γ is the unit weight of the soil and d is the depth of the soil layer. n will represent the level of each layer relative to NAP. For the calculations of the soil pressures acting on the wall a soil height of 15.7 m will be used (from NAP +10.5 m; top of soil, down to NAP -5.2 m; top of chamber floor). The 1.7 m thick floor will resist all the soil pressures at the bottom. The vertical effective pressure, $\sigma'_{v,n}$, for a soil system with n layers is determined with:

$$\sigma'_{v,n} = \sigma_{v,n} - p_n \tag{4.14}$$

Where $p_n$ [kN/m$^2$] is the water pressure in the considered plane, $p_n = \gamma_w \cdot d$. The water within the chamber at minimum locking level (NAP -0.18 m) acts as a resisting force (passive). Results of equations 4.13 and 4.14 are shown in Table 12 and a sketch of the vertical soil stresses and the water pressures are shown in Figure 27

**Table 12: Vertical stresses acting on the wall**

| Level n [m NAP] | Layer thickness [m] | $\sigma_{v,active}$ [kN/m$^2$] | $p_{v,active}$ [kN/m$^2$] | $p_{v,passive}$ [kN/m$^2$] | $\sigma'_{v,active}$ [kN/m$^2$] | $\sigma'_{v,passive}$ [kN/m$^2$] |
|---|---|---|---|---|---|---|
| **10.5** | 0 | 20 | 0 | 0 | 20 | 0 |
| **2** | 8.5 | 181.5 | 0 | 0 | 181.5 | 0 |
| **-0.18** | 2.18 | 227.3 | 21.9 | 0 | 205.4 | 0 |
| **-5.2** | 5.02 | 332.7 | 72.4 | 50.5 | 260.3 | -50.5 |

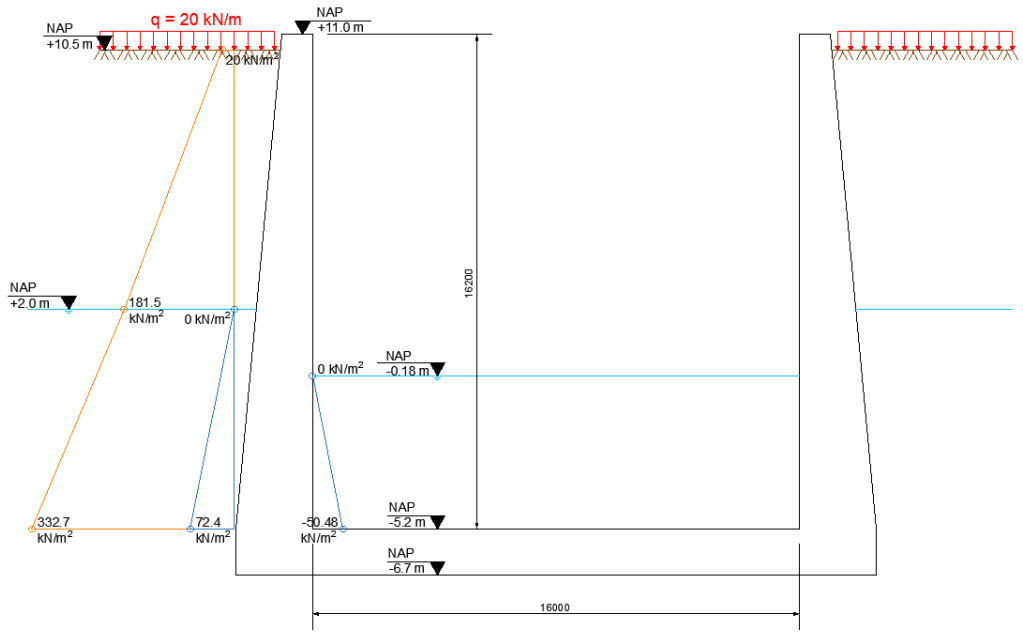


**Figure 27: vertical soil pressures**

The effective horizontal soil pressure can be found through its relation to the effective vertical soil pressure as the relation is assumed to be constant. On the active side this relation gives:

$$\sigma_h' = K_0 \cdot \sigma_v' \tag{4.15}$$

As there is only water on the passive side the effective passive horizontal pressure is equal to the water pressure at the bottom of the chamber. The effective horizontal pressures are calculated with equation 4.15 and the results are shown on Figure 28:

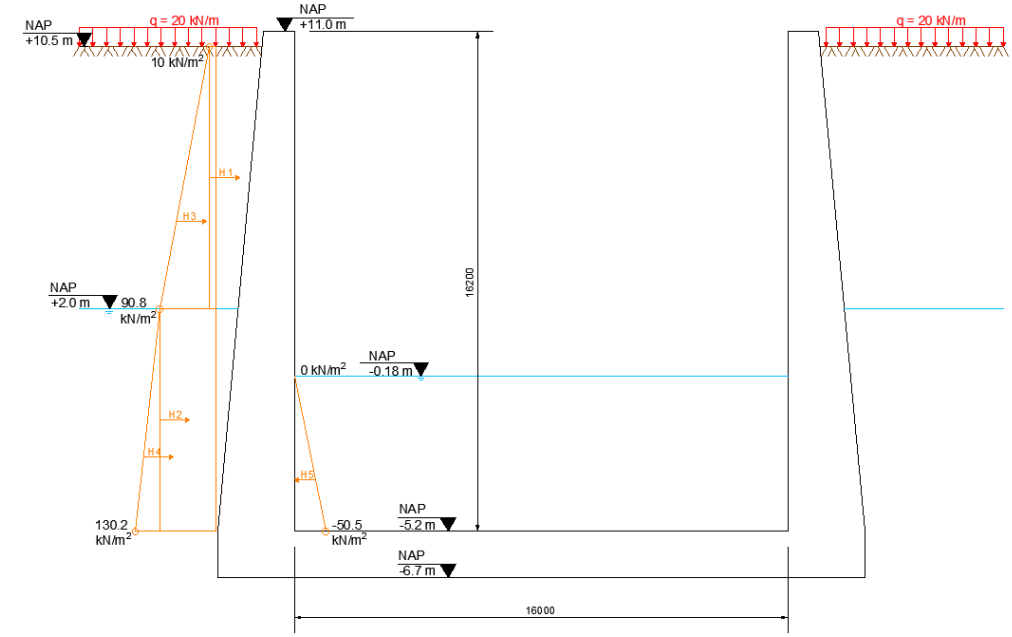


**Figure 28: horizontal pressures and resulting horizontal point loads**

The soil pressure is a permanent unfavourable action and thus, the resulting horizontal forces on the active side must be multiplied with a partial factor $\gamma_{G,unf}$ = 1.35. The resulting horizontal force on the passive side is multiplied with $\gamma_{Q,f}$ = 1.0. The horizontal forces are determined as:

$$H_1 = \gamma_{G,uf} \cdot \sigma'_{h,a,10.5} \cdot (10.5 - 2)$$
$$H_2 = \gamma_{G,uf} \cdot \sigma'_{h,a,2.0} \cdot (2 - (-5.2))$$
$$H_3 = \gamma_{G,uf} \cdot (\sigma'_{h,a,2.0} - \sigma'_{h,a,10.5}) \cdot \frac{10.5-2}{2}$$
$$H_4 = \gamma_{G,uf} \cdot (\sigma'_{h,a,-5.2} - \sigma'_{h,a,2.0}) \cdot \frac{2-(-5.2)}{2}$$
$$H_5 = \gamma_{Q,f} \cdot \sigma'_{h,p,-5.2} \cdot \frac{-0.18-(-5.2)}{2}$$

The horizontal loads, moments, and lever arms are given in Table 13. The moment is taken around the center of gravity of the wall at a level NAP -5.2 m.

**Table 13: horizontal point loads on U-chamber walls and resulting moments**

| | Load [kN/m] | Lever arm [m] | Moment, $M_i$ [kNm/m] |
|---|---|---|---|
| **H1** | 114.75 | 11.45 | 1313.89 |
| **H2** | 882.09 | 3.60 | 3175.52 |
| **H3** | 463.30 | 10.03 | 4648.47 |
| **H4** | 191.49 | 2.40 | 459.57 |
| **H5** | -126.70 | 1.67 | -212.01 |
| **Total ($V_{Ed}$)** | 1524.93 | | 9385.45 |

Using the horizontal point loads the maximum moment can be found at the bottom of the wall as:

$$M_{max} = \sum M_i = 9385.45\ kNm/m \quad (4.16)$$

## 4.2.2. Structural Design; U-Basin Chamber

A concrete U-basin chamber constructed in-situ will be used as the base case for the sustainability study. In a u-basin structure the wall is reinforced into the concrete floor to avoid member failure where the wall meets the floor, e.g. the walls will be cast on top of the floor with a stiff connection. A sheet pile construction pit will be used during the construction phase of the chamber.

The side walls of the chambers will not have the same height along the length of the chamber. In the center, where the flood gates will be situated, the walls will have a level 0.5 m higher than the retaining height of the storm surge barrier of NAP + 10.5 m. The wall level will then decline with the slope of the dike (assumed to have a top level equal to the retaining height of the SSB, a 25 m crest width, and a 1:3 slope) on either side until it reaches its minimum. The minimum wall height is determined by the maximum locking level and the additional height necessary for visual guidance in chapter 4.1.3 as 12.2 m with a top level at NAP +7.0 m at the seaward side of the dike and 9.7 m with a top level at NAP + 4.5 m at the riverside of the dike. A recreational harbour is situated at the seaward side of the lock complex. The land surrounding the harbour will be at the same level as the wall (NAP + 6.5 m).

**Wall thickness**

Due to the fact that no shear reinforcement is normally present in a concrete lock structure (Vrijburcht, et al., 2000), Shear force at the foot of the wall will determine the width of the footing of the wall, e.g. the base of the wall must be wide enough to resist the shear without shear reinforcement. To increase the shear resistance the bottom width can be increased, further flexural reinforcement can be increased locally

until the reinforcement percentage reaches 1% or the concrete strength class can be increased. The Shear at the bottom of the wall that must be resisted is $V_{Ed} = 1524.93\ kN$. Using the formula for the design shear resistance and adjusting mentioned wall properties a bottom width of 2.8 m was found. The design shear resistance, $V_{Rd,c}$, is determined with eq. 6.2 from EN 1992-1-1:2004, 6.2.2(1):

$$V_{Rd,c} = \left[C_{Rd,c}k(100\rho_l f_{ck})^{1/3} + k_1\sigma_{cp}\right]b_w d_e \geq \left(v_{min} + k_1\sigma_{cp}\right)b_w d_e \quad (4.17)$$

Where:

| | | |
|---|---|---|
| $C_{Rd,c}$ | [-] | Recommended value by Eurocode; $C_{Rd,c} = 0.18/\gamma_c = 0.12$ |
| $\gamma_c$ | [-] | Partial safety factor for concrete; $\gamma_c = 1.5$ |
| $k$ | [-] | $= 1 + \sqrt{200/d_e} \leq 2.0$ |
| $d_e$ | [mm] | Effective depth of the section; $d_e = 2539\ mm$ (eq. 4.26) |
| c | [mm] | Concrete cover. Concrete covers for different parts of the lock chamber are given in appendix C.2.2. for the wall against the soil, it is c = 45 mm |
| $\theta$ | [mm] | Reinforcement bar diameter; $\theta = 32$ mm (see appendix C.2.2) |
| a | [mm] | Center-center spacing between rows of longitudinal reinforcement if more than one row; a = 200 mm (2 rows of flexural reinforcement in the wall) |
| $\rho_l$ | [-] | $= \frac{A_{sl}}{b_w d_e} \leq 0.02$ |
| $A_{sl}$ | [mm$^2$] | The area of tensile reinforcement which extends ≥ ($l_{bd}$+d) beyond the section considered. Lapping length into the floor will be provided so this requirement is fulfilled. |
| $b_w$ | [mm] | Smallest width of the cross section in the tensile area. Since this is a wall, we assume a 1 m wide beam and take $b_w$ = 1000 mm |
| $\sigma_{cp}$ | [MPa] | $= \frac{N_{Ed}}{A_c} < 0.2 f_{cd} = 0.36$ MPa |
| $N_{Ed}$ | [N] | Axial force in the cross-section due to loading |
| $A_c$ | [mm$^2$] | Area of the concrete cross section; $A_c = 2800 \cdot 1000 = 2{,}800{,}000$ mm$^2$ |
| $f_{ck}$ | [MPa] | Characteristic compressive cylinder strength of concrete. $f_{ck}$ = 50 for C50/60 |
| $k_1$ | [-] | Recommended value by Eurocode; $k_1 = 0.15$ |
| $v_{min}$ | [-] | $= 0.035k^{3/2}f_{ck}^{1/2} = 0.36$ |

The axial force, $N_{Ed}$, is the sum of the walls self-weight and the soil weight on top of the wall as these are permanent favourable load, they are multiplied with a factor $\gamma_{G,f} = 1.0$. The walls self-weight is calculated as:

$$W_{wall} = H_{wall}\gamma_{cc}\left[b_{top} + \frac{(b_{bot} - b_{top})}{2}\right] = 16.2m \cdot 25\ kN/m^3 \cdot \left[1m + \frac{2.8m - 1m}{2}\right] = 769.50\ kN/m$$

The weight of the soil on top of the wall is calculated using trigonometry, considering the dry and saturated layer of soil. For the saturated layer the submerged unit weight is used; $\gamma_{sub} = \gamma_{s,sat} - \gamma_w$. The resulting soil weight is $W_{soil} = 236.99\ kN/m$. Therefore, the axial force in the cross section due to loading is:

$$N_{Ed} = W_{wall} + W_{soil} = 1{,}006{,}485\ N$$

The provided area of flexural reinforcement at the bottom of the wall was determined in appendix C.2.2: Reinforcement as $A_{s,prov} = 8936.1\ mm^2/m$, using 2 rows of K32 bars, a center-to-center distance (c/c) of 180 mm, and a 200 mm distance between the 2 rows. However, this amount of tensile reinforcement

would result in a very wide bottom profile of the wall. The tensile reinforcement is thus locally increased to 3 rows of K32 bars with c/c = 100 mm and a 100 mm distance between rows, thus keeping the same effective depth. This results in the local tensile reinforcement area of:

$$A_{sl} = \frac{\pi \emptyset^2}{4} \cdot \frac{b_w}{c/c} \cdot rows = 24{,}127.4\ mm^2/m$$

The length of these local bars must reach $l_{bd}$+d beyond the section considered. The anchorage length was calculated in appendix C.2.2 as $l_{bd} = 815$ mm. hence the bars must extend at least 3324 mm into the bottom slab of the chamber. As the bottom slab is only 1700 mm thick the rebars will be L shaped, bent into the slab. The design shear resistance can now be calculated with equation 4.17 as:

$$V_{Rd,c} = 1549.42\ kN < V_{Ed} = 1524.93\ kN$$

Thus, a C50/60 concrete wall with a bottom width of 2.8 m and a local tensile reinforcement of K32 – 100 mm in three rows provides sufficient shear resistance to resists the horizontal forces acting on the wall.

**Floor thickness**

The floor thickness is also checked against shear. The floor of the ship lock chamber will be impermeable and therefore, hydrostatic water loads will cause loading on the floor in the form of uplift force from an upward water pressure. The floor will also have to resist the weight of water when the ship lock is in use. A watertight joint will be designed between the wall and the floor, hence, the floor will also be loaded with a normal force due to the floor-wall interaction. The Chamber lays on top of a soil and the reaction of the soil, and the chamber floor is calculated via MATLAB. To model the floor the Winkler – Pasternak model is used. With the Winkler model the floor is modelled as a beam on a continuous spring support. Pasternak adds shear deformation in the elastic support to create horizontal linkage between the Winkler springs. The ordinary differential equation is:

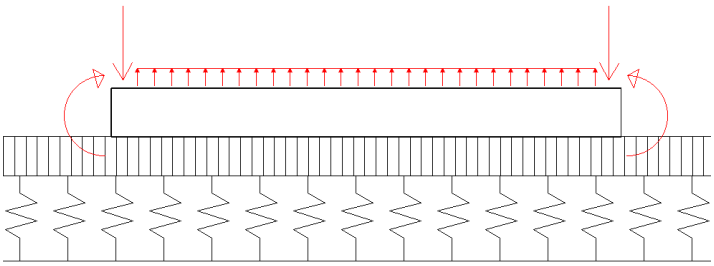

**Figure 29: Winkler-Pasternak model of the chamber floor. The bottom layer depicts the Winkler springs and the layer directly below the slab depicts the 1.4 m thick Pasternak shear layer.**

$$EI\frac{d^4w}{dx^4} - k_s\frac{d^2w}{dx^2} + kw = q \qquad (4.18)$$

Where:

| | | |
|---|---|---|
| $w$ | [mm] | Displacement of the beam |
| $k_s$ | [kN/m] | Shear modulus of the sub layer; $k_s = G \cdot d_{eff}$ |
| $k$ | [kN/m/m] | Winkler constant; $k = k_0 b$ |
| $k_0$ | [kN/m²/m] | Soil modulus of subgrade reaction |
| $q$ | [kN/m] | Distributed load on the floor slab. In this case it is the force from the uplift pressure and the downward pressure from the water within the chamber; $q = -(89.49 - 50.47) = -39.02$ kN/m² |
| $E$ | [kN/m²] | $= 37 \cdot 10^6$ kN/m²; Elastic modulus for C50/60 concrete |
| $I$ | [m⁴] | Moment of inertia for the slab; $I = \frac{bt^3}{12} = \frac{1 \cdot 1.7^3}{12} = 0.41\ m^4$ |

| | | |
|---|---|---|
| $G$ | [kN/m²] | Shear modulus of the shear layer; here the shear layer is taken as the cracked concrete; $G = \frac{E_{uwc}}{2(1+\nu)} = 5 \cdot 10^6$ kN/m² |
| $d_{eff}$ | [m] | Effective depth of shearing in the soil, $d_{eff} = 1.4\ m$ |
| $E_{uwc}$ | [kN/m²] | $= 10 \cdot 10^6$ kN/m²; Elastic modulus for cracked concrete |
| $\nu$ | [-] | =Poisson's ratio. For cracked concrete $\nu = 0.0$ |

Under the floor slab is a 1.4 meter thick UWCF with a bottom level at NAP -8.3 m. To include the effect of the UWCF in the Winkler foundation it is assumed that the modulus of subgrade reaction is higher than for only a sandy soil. The modulus of subgrade reaction is assumed to be similar to that of crushed stone, e.g. $k_0$ = 200,000 kN/m²/m. The floor is modelled as a 1 m wide beam, hence the Winkler constant is equal to $k_0$ (k = $k_0$). The effect of shear layer is assumed to come from the cracked UWCF as the cracked parts of the floor will rub against each other thus creating a shear force resisting the displacement of the floor slab. The effective depth of shearing in the soil is thus taken as the UWCF thickness; $d_{eff} = 1.4$ m. The shear modulus of the sublayer is therefore:

$$k_s = 5 \cdot 10^6\ kN/m^2 \cdot 1.4\ m = 7 \cdot 10^6\ kN/m$$

As the chamber is symmetric, symmetry condition can be applied to the model and thus only half of the floor slab is analysed. Four boundary conditions are applied. The end of the slab modelled as a beam (x = 0) supports the chamber wall. Therefore, the two boundary conditions at the end are an applied moment and an applied shear force. In the center of the chamber (x = L/2) the shear force and the curvature will be 0.

$$M(0) = 9385.45\ kNm$$

$$V(0) = 1038.83\ kN$$

$$\varphi(L/2) = 0$$

$$V(L/2) = 0\ kN$$

The ODE presented in equation 4.18 is solved via MATLAB. The length of the whole beam is taken as the length between the center of gravity of the walls which is calculated to be 1.78 m from the outer edge of the chamber.

$$L = B_{ch} + 2 \cdot \left(B_{w,b} - 1.78\ m\right) = 18.04\ m$$

After the ODE is solved the moment and shear force can be calculated through:

$$M = EI\frac{d^2w}{dx^2}$$

$$V = EI\frac{d^3w}{dx^3}$$

The MATLAB script is shown in appendix **Error! Reference source not found.**. The resulting bending moment and shear force diagrams over half of the beam are shown in Figure 30. From the shear force

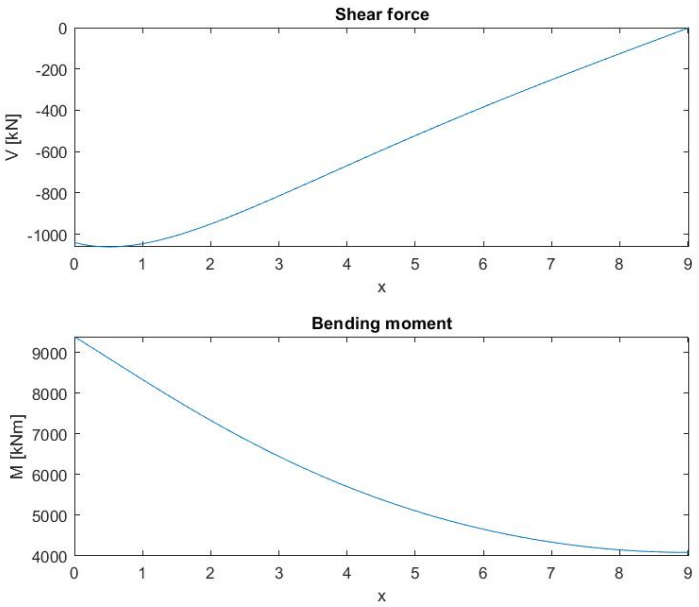


**Figure 30: Shear and moment diagrams over half of the floor width, for the center lock head**

diagram, the maximum shear force occurs at the inner edge of the wall:

$$V_{Ed} = 1060.65\ kN$$

The design shear resistance, $V_{Rd,c}$, is determined in the same manner as for the wall; through equation 4.17. The effective depth is now $d = 1514$ mm (taken from appendix C.2.2). The longitudinal steel in the floor is adjusted locally so that the shear resistance suffices. The axial force is taken as the horizontal forces from the soil: $N_{Ed} = 1524.93$ kN. Table 14 shows the values and results for the shear resistance of the 1.7 m thick floor.

**Table 14: Shear resistance calculations for the 1.7 m thick floor slab**

| **Shear** | | |
|---|---|---|
| $V_{Ed}$ | 1060.65 | kN |
| $C_{Rd,c}$ | 0.12 | [-] |
| $d$ | 1514.00 | mm |
| $k$ | 1.36 | [-] |
| $f_{ck}$ | 50.00 | MPa |
| $A_{sl}$ | 14622.69 | mm$^2$ |
| $\rho_l$ | 0.0097 | [-] |
| $b_w$ | 1000.00 | mm |
| $N_{Ed}$ | 1524.93 | kN |
| $\sigma_{cp}$ | 0.90 | MPa |
| $v_{min}$ | 0.39 | [-] |
| $V_{Rd,c}$ | 1105.78 | kN |

The reinforcement needed locally to resist the shear force is two rows of K32 with a center-to-center distance between rows of 110 mm.

$$V_{Rd,c} = 1105.78\ kN < V_{Ed} = 1060.65\ kN$$

Thus, a C50/60 concrete floor with a thickness of 1.7 m and a local tensile reinforcement of K32 – 110 mm in two rows provides sufficient shear resistance.

**Stability of the chamber**

The Chamber must be safe against floating. In the use-phase of the structure the UWCF will start to crack. Therefore, the weight of the chamber and the water level inside the chamber at minimum locking level must counteract the uplift water pressure directly under the chamber floor to avoid floating of the structure. During the time period where the minimum locking level is NAP -0.18 m the ground water level in the area will be lower. Therefore, the G.W.L. is assumed to be at NAP +1.5 m for the calculations of floating. The following equilibrium for the uplift should be met:

$$F_{uplift} \leq W_f + 2 \cdot W_w + W_{water} \qquad (4.19)$$

Where the uplift force is:

$$F_{uplift} = \gamma_w \cdot (B_{ch} + 2 \cdot B_{w,b}) \cdot \Delta h_w$$

$$F_{uplift} = 10.05 \frac{kN}{m^3} \cdot (16\ m + 2 \cdot 2.8\ m) \cdot 8.4\ m = 1823.47\ kN/m$$

Where:

| | | |
|---|---|---|
| $\Delta h_w$ | [m] | Water depth from the G.W.L. to the bottom of the chamber floor |
| $W_f$ | [kN/m] | Weight of the floor per meter: $W_f = (B_{ch} + 2 \cdot B_{w,b}) \cdot t_f \cdot \gamma_{cc} = 918\ kN/m$ |
| $t_f$ | [m] | Floor thickness; $t_f = 1.7$ m. |
| $W_w$ | [kN/m] | Weight of the walls per mete |

| | | |
|---|---|---|
| $W_{water}$ | [kN/m] | Weight of water within the chamber at minimum locking level; $W_{water} = d_{water} \cdot B_{ch} \cdot \gamma_w \cdot \gamma_{Q,f} = 807.63\ kN/m$ |
| $d_{water}$ | [m] | Water depth within the chamber; $d_{water} = -0.18\ m - (-5.2\ m) = 5.02$ m |
| $B_{w,b}$ | [m] | Bottom with of the wall stem; $B_{w,b} = 2.8$ m |
| $B_{w,t}$ | [m] | Top with of the wall stem; $B_{w,t} = 1.0$ m |
| $H_w$ | [m] | Wall height; $H_w = 16.2$ m |
| $A_w$ | [m²] | Cross sectional area of the wall; $A_w = \left(B_{w,b} - B_{w,t}\right) \cdot \frac{H_w}{2} + B_{w,t} \cdot H_w = 30.78$ m² |

The wall weight around the flood gates is:

$$W_w = A_w \cdot \gamma_{cc} = 769.5\ kN/m$$

The counter acting force is thus:

$$W_f + 2 \cdot W_w + W_{water} = 918\frac{kN}{m} + 2 \cdot 769.5\frac{kN}{m} + 807.63\frac{kN}{m} = 3264.64\frac{kN}{m}$$

As this is greater than the uplift force (2899.53 kN/m) the structure is safe against floating (criteria in equation 4.19 is satisfied)

It is necessary to verify that no tension forces are acting on the soil. In order to have no tension acting on the soil the minimum load acting on the subsoil ($\sigma_{k,min}$) must be larger than 0 and the maximum load acting on the subsoil ($\sigma_{k,max}$) needs to be less than the bearing capacity of the soil itself:

$$\sigma_{k,min} = \frac{F}{A} - \frac{M}{W} = \frac{\sum V}{b \cdot l} - \frac{\sum M}{1/6 \cdot l \cdot b^2} > 0 \quad (4.20)$$

$$\sigma_{k,max} = \frac{F}{A} + \frac{M}{W} = \frac{\sum V}{b \cdot l} + \frac{\sum M}{1/6 \cdot l \cdot b^2} < Bearing\ capacity \quad (4.21)$$

Where:

| | | |
|---|---|---|
| $\sum V$ | [kN] | Total vertical force from the u-basin chamber. |
| $\sum M$ | [kNm] | Total moment acting on the soil. |
| $b$ | [m] | Width of the chamber. |
| $l$ | [m] | Length of the chamber segment. |

Assuming that the U-shaped chamber is a rigid structure the bearing capacity of the soil is calculated for the width of the whole chamber, and the moment is disregarded as it is fully transmitted to the bottom slab of the chamber via reinforcement. It is assumed that the underwater concrete floor is cracked. Therefore, the uplift water pressure lifting the structure up is taken at a depth of NAP -6.9 m. the outer width of the chamber is:

$$b = B_{ch} + 2 \cdot b_{bot} = 16\ m + 2 \cdot 2.8\ m = 21.6\ m$$

As the moment is neglected the minimum load acting on the subsoil, $\sigma_{k,min}$, will always be greater than zero and is thus the criteria given in equation 4.20 is automatically fulfilled without further calculations. The critical vertical force is the weight of the whole chamber, full of water. The water level within the chamber is thus taken as +10.5 m NAP as the SSB is designed to resist this water height. The sum of vertical forces is thus:

$$\sum V = \left(V_{wall} + V_{soil} + V_q\right) \cdot 2 + V_{floor} + V_{uwcf} + V_{w,ch} + V_{up} = 6589.17\ kN/m \quad (4.22)$$

Where:

| | | |
|---|---|---|
| $V_{wall}$ | [kN/m] | Self-weight of a single wall; $V_{wall} = W_{wall} \cdot \gamma_{G,uf} = 1038.83$ kN/m |
| $V_{soil}$ | [kN/m] | vertical soil force acting on an inclined wall; $V_{soil} = W_{soil} \cdot \gamma_{G,uf} = 319.93$ kN/m |
| $V_q$ | [kN/m] | Vertical load from surcharge; $V_q = q\left(B_{w,b} - B_{w,t}\right)\gamma_{Q,uf} = 54$ kN/m |
| $V_{floor}$ | [kN/m] | Self-weight of the chamber floor; $V_{floor} = B \cdot t_{floor}\gamma_{cc}\gamma_{G,uf} = 1385.10$ kN/m |
| $V_{uwcf}$ | [kN/m] | Self-weight of the uwc floor over the width of the chamber; $V_{uwcf} = B \cdot t_{uwc}(\gamma_{uwc} - \gamma_w)\gamma_{G,uf} = 566.20$ kN/m |
| $V_{w,ch}$ | [kN/m] | Weight of the water inside the chamber; $V_{w,ch} = \left(+10.5 - (-5.2)\right)m\ NAP \cdot B_{ch}\gamma_w\gamma_{Q,uf} = 3788.82\ kN/m$ |
| $V_{up}$ | [kN/m] | Uplift force under the chamber floor; $V_{up} = -\gamma_{Q,f}\left(h_{gwl} - d - t_{floor}\right)\gamma_w B = -1976.46\ kN/m$ |

Therefore equation 4.21 gives;

$$\sigma_{k,max} = \frac{\sum V}{b \cdot l} = \frac{6589.17\ kN/m}{21.6\ m\ \cdot 1\ m} = 305.05\ kN/m^2/m$$

To guarantee that there will be no tension force acting on the soil the maximum load acting on the subsoil ($\sigma_{k,\,max}$) should be lesser than the bearing resistance of the soil. EN 1997-1 is used to determine the bearing capacity of the soil. To compute the bearing resistance of the subsoil, Equation D.2 from EN 1997-1 for drained conditions is used as the subsoil consists of sand:

$$bearing\ resistance;\ R/A' = c'N_c b_c s_c i_c + q'N_q b_q s_q i_q + 0.5\gamma' B' N_\gamma b_\gamma s_\gamma i_\gamma \quad (4.23)$$

The bearing resistance depends on cohesion (c), the surcharge pressure at the level of the foundation (q) and the specific weight of the soil below the foundation (γ). Form table 31-4 in *Manual: hydraulic structures 2020*, the cohesion factor c' is 0 for sand. Thus, the bearing resistance only depends on the surcharge pressure and the specific weight of the soil. The bearing resistances are determined as:

$$N_q = e^{\pi \cdot tan\varphi'} \tan^2(45 + \frac{\varphi'}{2}) = 18.40$$

$$N_\gamma = 2\left(N_q - 1\right)\tan(\varphi') = 20.09$$

Where ϕ' is the internal friction angle for sand taken as 30°. The inclination angle of the foundation of the gravity wall is α=0°:

$$b_q = b_\gamma = (1 - \alpha \cdot \tan\varphi')^2 = 1$$

To determine the shape factors for the foundation the effective width and length needs to be determined. As the u-basin is a stiff structure the effective width and length are equal to the actual width and length of the chamber segment around the center flood gates:

$$B' = B = 21.6\ m$$

$$L' = L = 25\ m$$

The shape factors for a rectangular shape are therefore:

$$s_q = 1 + (B'/L')sin\varphi' = 1.43$$

$$s_\gamma = 1 - 0.3(B'/L') = 0.74$$

The inclination of the load, caused by a horizontal load H is:

$$i_q = [1 - H/(V + A'c'cot\varphi')]^m = 1$$

$$i_\gamma = [1 - H/(V + A'c'cot\varphi')]^{m+1} = 1$$

Where H is the total horizontal load (The global structure is being considered and therefore H is taken as 0), V is the total vertical load calculated above (ΣV), and as the load H acts in parallel direction to the width B, $m = m_B = \frac{2+(B'/L')}{1+(B'/L')} = 1.54$.

The surcharge on top of the soil is q' = 20 kN/m$^2$ and the design effective weight density of the soil is:

$$\gamma' = \gamma_{s,sat} - \gamma_w = 21 - 10.06 = 10.94\ kN/m^2$$

With all the factors determined they can be inserted into equation 4.23. Thus, the bearing resistance of the soil is:

$$R/A' = 2286.46\ kN/m^2 > \sigma_{k,max} = 305.05\ kN/m^2$$

The bearing resistance of the soil is greater than the maximum load acting on the subsoil, e.g. the criterion in equation 4.21 is fulfilled. Therefore, no tension forces will be acting on the soil.

**Wall reinforcement**

As the gravity wall is subjected to out of plane bending it can be designed as a cantilever slab according to EN 1992-1-1:2004, 9.6.1. Concrete of class C50/60 will be used in the base design and the reinforcement will be S500. Material factors for the concrete and reinforcement are depicted in Table 15

**Table 15: Material factors of concrete strength class C50/60 and reinforcing steel S500**

| **Concrete class C50/60** | | | |
|---|---|---|---|
| *Characteristic cylinder compressive strength* | $f_{ck}$ | 50.00 | MPa |
| *Mean cylinder compressive strength* | $f_{cm}$ | 58.00 | MPa |
| *Mean tensile strength* | $f_{ctm}$ | 4.07 | MPa |
| *Elastic modulus* | $E_{cm}$ | 37278 | MPa |
| *Design compressive strength* | $f_{cd}$ | 33.33 | MPa |
| *Design tensile strength* | $f_{ctd}$ | 1.90 | MPa |
| *Minimum longitudinal tension reinf. ratio* | $\rho_{min}$ | 0.212 | % |
| *Minimum shear reinf. ratio* | $\rho_{w,min}$ | 0.113 | % |

| *Reinforcement S500* | | | |
|---|---|---|---|
| *Characteristic yield strength* | $f_{yk}$ | 500 | MPa |
| *Design yield strength* | $f_{yd}$ | 435 | MPa |
| *Strain at maximum force* | $\varepsilon_{uk}$ | 3.25 | [-] |
| *Elastic modulus* | $E_s$ | 20000 | MPa |

Minimum area of steel in the main direction (vertical reinforcement) is:

$$A_{s,min} = 0.26\frac{f_{ctm}}{f_{yk}}b_t d = \mathbf{5373.5\ mm^2} \geq 0.0013 b_t d = 3300.7\ mm^2$$

This equation usually applies for beams. Therefore, $b_t$ is taken as 1000 mm and d is the effective depth of the wall from equation 4.26: $d = 2539\ mm$

Maximum area of steel is 4% of the concrete cross section $A_c$:

$$A_{s,max} = 0.04A_c = 0.04 \cdot 1000\ mm \cdot 2800\ mm = 112{,}000\ mm^2$$

In order to determine the necessary reinforcement in the U-chamber all concrete covers must be known. The concrete covers for each part of the concrete chamber are found in appendix C.2.2 and presented in the Table 16 below.

**Table 16: Concrete cover for different parts of the ship lock chamber**

| Chamber part | Exposure class | Concrete cover; c [mm] |
|---|---|---|
| *Wall Outside of the chamber (soil contact)* | XC2 | 45 |
| *Wall, inside chamber, submerged* | XS2 | 60 |
| *Wall, inside chamber, above minimum locking level* | XS3 | 65 |
| *Top of wall* | XC4 | 50 |
| *Top of floor slab* | XS2 | 60 |
| *Bottom of floor slab* | XC2 | 50 |

The necessary area of flexural reinforcement that will resist tension can be calculated with:

$$A_{s1} = \frac{M_{Ed}}{f_{yd} z} \tag{4.24}$$

Where:

| | | |
|---|---|---|
| $f_{yd}$ | [MPa] | design tensile capacity of the steel reinforcement |
| $M_{Ed}$ | [Nmm] | design bending moment. At the bottom of the wall it is; $M_{Ed} = 9385.45$ kNm/m |
| $z$ | [mm] | lever arm between the tension and compression stresses within the element |

The lever arm is calculated through the following quadratic equation:

$$z = d_e \left[1 - \frac{f_{yd} A_s}{2\eta f_{cd} b d_e}\right] = 2480.69\ mm > 0.95 d_e = \mathbf{2412.05\ mm} \tag{4.25}$$

Where:

| | | |
|---|---|---|
| $d_e$ | [mm] | Effective depth of the concrete cross section |
| $f_{yd}$ | [MPa] | design yield strength |
| $f_{cd}$ | [MPa] | Design compressive strength |
| $A_s$ | [mm²] | Area of steel in the cross section |
| b | [mm] | Width of the cross section; $b = 1000$ mm |
| $\eta$ | [-] | Factor defining the effective strength. $\eta = 1.0$ for $f_{ck} \leq 50\ MPa$ |

The lever arm given in equation 4.25 was found iteratively using the provided flexural reinforcement area found below in equation 4.27. it is traditionally limited to $0.95d_e$ to avoid issues with the quality of concrete (mpa The Concrete Centre, 2023).

With two rows of reinforcement bars with a diameter of 32 mm, 200 mm between rows, and a concrete cover of 45 mm the effective depth will be:

$$d_e = B_{w,b} - c - a/2 - \emptyset/2 \tag{4.26}$$

Where:

| | | |
|---|---|---|
| $B_{w,b}$ | [mm] | Bottom width of the wall; $B_{w,b} = 2800$ mm |

| | | |
|---|---|---|
| $c$ | [mm] | Concrete cover. Here $c = 45$ mm |
| $a$ | [mm] | Distance between the two rows of rebar. Here $a = 200$ mm |
| $\emptyset$ | [mm] | Rebar diameter. Here $\emptyset = 32$ mm |

$$d_e = 2800 - 45\ mm - \frac{200\ mm}{2} - \frac{32\ mm}{2} = 2639\ mm$$

The required reinforcement area calculated with equation 4.24 is:

$$A_{s1,b} = \frac{9385.45 \cdot 10^6\ Nmm}{435\ MPa\ \cdot 2412.05\ mm} = 8606\ mm^2/m$$

This is satisfied with K32 bars, a center-to-center spacing of s = 170 mm and the number of rows n = 2, the provided steel area is:

$$A_{s1,provided} = \pi \cdot \frac{\emptyset^2}{4} \cdot \frac{b}{s} \cdot n \tag{4.27}$$

$$A_{s1,b,provided} = \pi \cdot \frac{32^2}{4} \cdot \frac{1000}{170} \cdot 2 = 9461.7\ mm^2/m$$

The secondary transverse reinforcement may not be less than 20% of the primary reinforcement. This is fulfilled using two rows of K16 bars with a center-to-center distance of 220 mm.

$$A_{s2,b,provided} = \pi \cdot \frac{16^2}{4} \cdot \frac{1000}{220} \cdot 2 = 1827.8\ mm^2/m > 0.2A_{s1} = 1789.0\ mm^2/m$$

To determine if compression reinforcement is needed the following criteria needs to be checked:

$$K = \frac{M}{f_{ck} b d^2} = 0.029 < K'$$

If the following criterion holds no additional compression reinforcement will be necessary and only the minimum reinforcement needs to be installed ($A_{s,min}$). K is the normalised bending resistance. The limit K' is at its minimum 0.120 and therefore no additional compression reinforcement is necessary (mpa The Concrete Centre, 2023). In the compression zone of the wall (The phase of the wall inside the chamber) a minimum reinforcement will be provided using one rows of K32 c/c-140 mm:

$$A_{s,b,comp} = \pi \cdot \frac{32^2}{4} \cdot \frac{1000}{140} = 5744.6\ mm^2/m > A_{s,min} = 5373.5\ mm^2/m$$

And a transverse reinforcement at least 20% of $A_{s,min}$ resulting in one row of K16 c/c 180 mm giving a reinforcement area of 1117.0 mm$^2$/m.

Production and transport of reinforcement rebars limits the length of the bars. The length is mostly limited by the maximum hauling length for the transport. Usually, the maximum length of rebars is 10 m - 12 m (Autodesk Support, 2019). The reinforcement that is calculated above is designed to resist the maximum moment occurring at the bottom of the 16.2 m high chamber wall. As the length of a rebar is limited due to production and transportation reasons, two vertical bars will be needed to reinforce the whole height of the wall. The moment reduces significantly over the height of the wall and therefore the area of the top row of reinforcement can be reduced compared to the one resisting the moment occurring at the bottom of the wall. The moment line over the height of the wall is depicted in Figure 31 where the wall is depicted as a fixed beam and rotated 90° to the right. 6 m from the base of the wall (NAP +0.8 m) the moment $M_{+0.8} = 2590$ kNm/m.

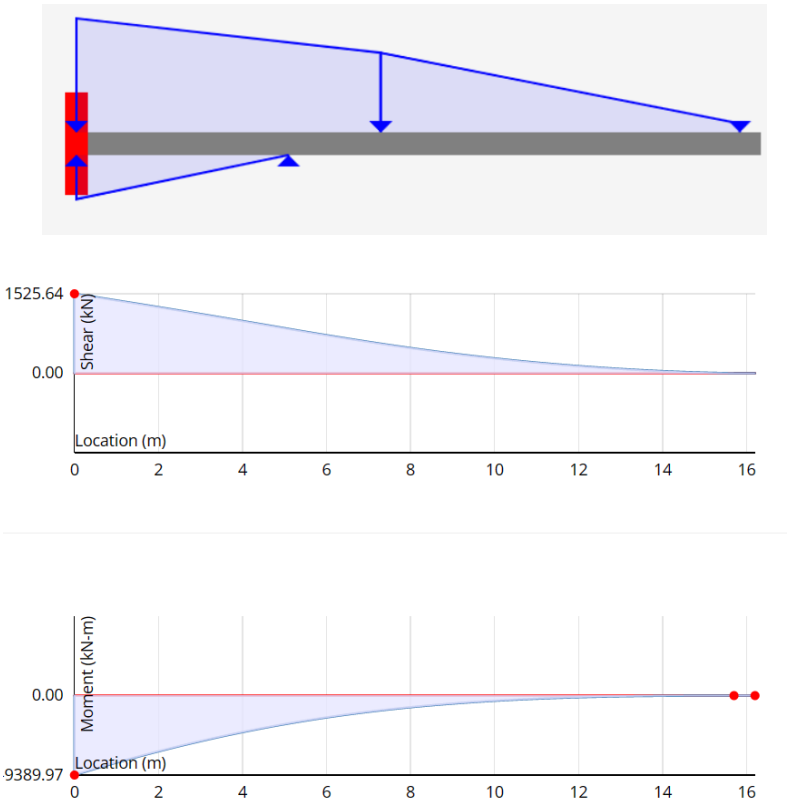


**Figure 31: 6 m from the base of the wall (NAP +0.8 m) the moment $M_{+0.8} = 2590$ kNm/m. The effective depth of the cross section at NAP +0.8 m must be found. The angle of the wall near the flood gates is**

The effective depth of the cross section at NAP +0.8 m must be found. The angle of the wall near the flood gates is:

$$\theta = \tan^{-1}\left(\frac{2.8\ m - 1\ m}{16.2\ m}\right) = 6.34°$$

The depth of the wall cross section at NAP +0.8 m is therefore:

$$d_{+0.8} = \tan(\theta) \cdot (H_W - 6\ m) + B_{w,t} = 2133.3\ mm$$

The effective depth of the cross section at NAP +0.8 m is calculated with equation 4.26 but the rebar diameter is now smaller (see equation 4.28) and instead of $B_{w,b}$, $d_{+0.8}$ is used:

$$d_{e,+0.8} = 2133.3 - 45\ mm - 200\ mm - \frac{25\ mm}{2} = 1875.8\ mm$$

The lever arm between the tension and compression stresses are calculated with equation 4.25.

$$z_{+0.8} = 1782.04\ mm$$

The minimum reinforcement is:

$$A_{s,min} = 0.26\frac{f_{ctm}}{f_{yk}} b_t d = 4515\ mm^2/m$$

The required flexural reinforcement is then calculated using equation 4.24 with a moment $M_{+0.8} = 2590$ kNm/m:

$$A_{s1,t} = \frac{2590 \cdot 10^6\ Nmm}{435\ MPa\ \cdot 1843.8\ mm} = 3341.1 \frac{mm^2}{m} < A_{s,min} = \mathbf{4515\ mm^2/m}$$

Therefore, the minimum required flexural reinforcement for the top half of the chamber wall is $A_{s1,t} = A_{s,min} = 4515$ mm²/m. The vertical reinforcement for the top half of the chamber wall will be two rows of K25 c/c-210 mm. Using equation 4.27 that gives:

$$A_{s1,t,provided} = \pi \cdot \frac{25^2}{4} \cdot \frac{1000}{210} \cdot 2 = 4675.0\ mm^2/m$$

The secondary transverse reinforcement may not be less than 20% of the primary reinforcement. This is fulfilled using two rows of K12 c/c-220 mm which results in $A_{s2,t,provided} = 1028.2$ mm²/m.

The bottom compression bars will reach 9 meters height from the bottom slab to NAP +3.8 m. At NAP + 3.8 m the depth of the wall cross section is 1800 mm and $A_{s,min} = 3809.5$ mm²/m. Therefore, the compression reinforcement for the top part of the chamber wall will be a single row of K32 c/c-210 mm:

$$A_{s,t,comp} = \pi \cdot \frac{32^2}{4} \cdot \frac{1000}{210} = 4021.24\ mm^2/m$$

And a transverse reinforcement at least 20% of $A_{s,min}$. Here it will be kept the same as the transverse reinforcement in the compression zone of the bottom of the wall to minimize the chance of errors during the construction of the lock.

The floor of the lock is 21.6 m wide in proximity to the flood gates in the lock chamber. On Figure 30 the moment and shear are shown for half of the floor. The floor is symmetric, so the same graph applies for both sides of the chamber floor. x = 0 is the center of gravity of the wall and therefore x=1 is the inner side of the wall. Due to length limitations of rebars and to save material the floor will be split into 3 zones; the 1st zone where the maximum moment occurs is from the outer edge of the wall until 2 meters inside the chamber measured from the inner side of the wall (x=3 on Figure 30), the 2nd zone is from 2 meters inside the chamber (x = 3) until 5 m inside the chamber (x = 6), and the 3rd zone is the center part of the chamber floor where 6 m long bars will be placed. The maximum shear and moment for each of these zones are taken from the graphs on Figure 30 and presented in the Table 17.

**Table 17: maximum moments and shear forces for the floor design at the center lock head of the base case concrete chamber design**

| Zone | Coordinate on Figure 30Figure 55 | Maximum moment $M_{max}$ [kNm/m] | Maximum shear force $V_{max}$ [kN/m] |
|---|---|---|---|
| **1 (edges)** | 0 | 9385.45 | 1060.65 |
| **2** | 3 | 6446.55 | 814.50 |
| **3 (center)** | 6 | 4656.41 | 384.29 |

The flexural, compression and transverse reinforcement were found in the same manner as for the wall above using equations 4.24 to 4.27. the compression reinforcement will need two 10 m bars to span the whole width of the chamber. The spacing between rows of bars in the floor is 120 mm. The reinforcement in the chamber wall and floor are summarized in Table 18.

**Table 18: Reinforcement for the chamber walls and floors at the center lock head.**

| | *L [mm]* | *Ø [mm]* | *volume [m³]* | *no. Rows* | *c/c [mm]* | *no bars long* | no. Walls | *tot no. bars* |
|---|---|---|---|---|---|---|---|---|
| **Shear longitudinal** | 2825 | 32 | 0.0023 | 1 | 100 | 219 | 2 | 438 |
| | 2300 | 32 | 0.0018 | 1 | 100 | 219 | 2 | 438 |
| | 4225 | 32 | 0.0034 | 1 | 100 | 219 | 2 | 438 |

| | | | | | | | | |
|---|---|---|---|---|---|---|---|---|
| **tension bottom** | 7100 | 32 | 0.0057 | 2 | 170 | 129 | 2 | 516 |
| **tension top** | 10000 | 25 | 0.0049 | 2 | 200 | 110 | 2 | 440 |
| **transv. Tens. Bottom** | 7730 | 16 | 0.0016 | 2 | 220 | 84 | 2 | 336 |
| **transv. Tens. Top** | 7200 | 12 | 0.0008 | 2 | 320 | 96 | 2 | 384 |
| **comp. Long. Bottom** | 9000 | 32 | 0.0072 | 1 | 140 | 139 | 2 | 278 |
| **comp. Long. Top** | 8000 | 25 | 0.0039 | 1 | 100 | 199 | 2 | 398 |
| **transv. comp. Bottom** | 7380 | 16 | 0.0015 | 1 | 180 | 153 | 2 | 306 |
| **transv. comp. Top** | 7380 | 16 | 0.0015 | 1 | 260 | 81 | 2 | 162 |
| **U-loops top** | 2975 | 25 | 0.0015 | 1 | 100 | 199 | 2 | 398 |
| **U-loops top** | 2775 | 25 | 0.0014 | 1 | 100 | 199 | 2 | 398 |
| **anchor bar** | 8060 | 32 | 0.0065 | 3 | [-] | 3 | 2 | 18 |
| **U-loop floor** | 4725 | 32 | 0.0038 | 1 | 120 | 183 | 2 | 366 |
| **anchor bars** | 8060 | 32 | 0.0065 | 3 | [-] | 3 | 2 | 18 |
| **anchor bars** | 8480 | 32 | 0.0068 | 2 | [-] | 3 | 2 | 12 |
| **L-bar bottom** | 5200 | 32 | 0.0042 | 1 | 140 | 139 | 2 | 278 |

The reinforcement calculations are performed for every wall height segment within the chamber and the resulting reinforcement is given in appendix C.2.3:.

### 4.2.3. Detailing and Material Volumes

Figure 32 Shows a 3D view of the concrete lock chamber design.

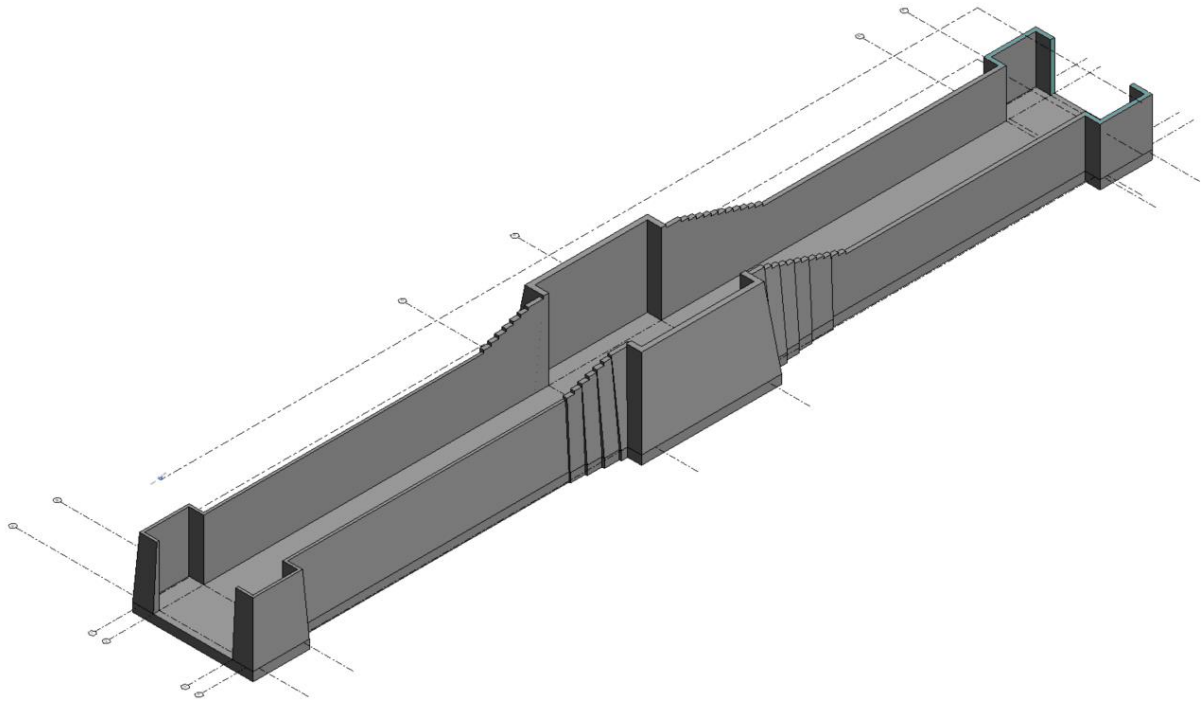

**Figure 32: 3D view of the concrete lock chamber design. The left section of the chamber is on the seaside of the ship lock and the right section of the chamber is on the riverside of the ship lock.**

The Base case design of the chamber will have a step like design of the wall along the dike. The dike will have the same top level as the storm surge barrier of NAP +10.5 m and a 22 m crest width. The dike is assumed to have a 1:3 slope. The minimum wall height on the seaside of the chamber is determined by the maximum locking level and the additional height necessary for visual guidance. This was determined in

chapter 4.1.3 where the lowest height of the wall at the seaside is at NAP + 7.0 m (necessary height for the year 2250) and at NAP +4.5 m at the riverside. On the seaside of the lock the chamber wall height will decrease in 8 steps following the slope of the dike. Each step has a height of 0.5 m and a length of 1.5 m, e.g. the wall height will decrease by 500 mm with each step. Two mitre gates, facing away from each other, will be in the center of the lock chamber. The size of the actual dimensions of the mitre gates is outside the scope of this thesis but a 2.5 m wide spacing for the lock head will be accounted for on either side of the chamber. Each gate will be 9.5 m long, resulting in the inner width of the center lock head of 20 m, with a height of 16.2 m (NAP +11.0 m). 7 steps will be on the seaside of the chamber along the dike slope until the wall height reaches the lowest wall position (8$^{th}$ step) at NAP +7.0 m. To minimize formwork materials two and two steps will have the same wall slope (tapered wall design). This can be seen on Figure 32 where to the left of the center lock head 8 steps are visible but every 2 steps share the same angle. 14 steps are provided along the dike slope on the riverside with the last step at a height of NAP +4.5 m. A top view of the chamber walls is shown in Figure 33 where the step walls are numbered from 0 to 14 depending on their height.

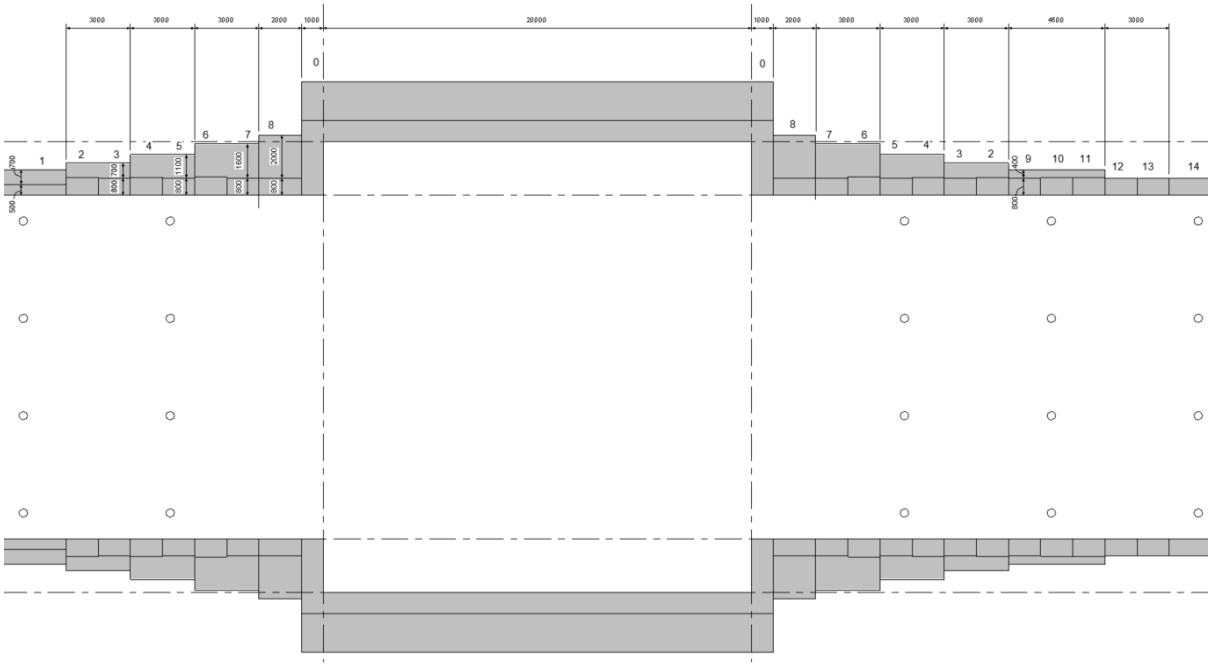


**Figure 33: Top view of the chamber wall in proximity to the center lock head**

In appendix C.2.3 a detailed table is presented with all the rebars in the whole base case concrete chamber design, their position, diameter, spacing, length, quantity and volume. The anchoring and lapping lengths of rebars are also found in appendix C.2.2. The perpendicular lock head chamber walls (2.5 m long perp. To the chamber walls) were not taken into consideration when calculating the material quantities as the will not be detrimental to the LCA comparison of the base case design and the alternative design.

The total rebar volume for the base case design is:

$$V_{s,bc} = 122.37\ m^3$$

The concrete volume for the base case design is:

$$V_{c,bc} = 11{,}083.48\ m^3$$

# 5. Sustainable Design Optimizations

The main goal of this research is to find a sustainable design of the concrete ship lock chamber. To do so they chamber structural typology will be optimised, considering the durability and flexibility of the structure. Sustainability of the concrete structure will be dependent on GHG emissions from the concrete/cement, resource consumption, weight of the structure, and durability, as well as the costs throughout the structures service life.

As was mentioned for the base case, the lock head in the center of the lock will be the first part of the lock that will be constructed and used for the first 50 years of the lifetime of the storm surge barrier. During those first 50 years lifetimes the storm surge barrier will be kept open except for the case of an extreme flood event. Therefore, the center lock head will act as flood gates for those 50 years. It will however be kept closed and only opened when vessels need to navigate through it. This will lower the probability of closing procedure failure in the case of extreme flood events.

## 5.1. Sustainable Concrete Structure

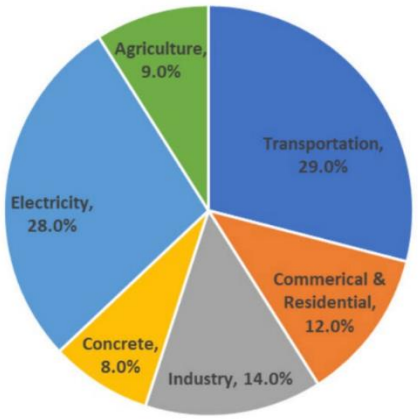


**Figure 34: Categorical contribution to global $CO_2$ emissions (Ramsden, 2020)**

Concrete is the second most consumed material in the world after water. The reason behind this is that concrete is a very durable material that can last for over 100 years, and it is widely available around the world as a construction material. Concrete is a mixture of water, fine and coarse aggregates, cement and some chemical additives. Cement acts as the binder between the other ingredients and gives concrete its durability. 10 to 15% of the concrete mixture is cement. Portland cement is the most widely used cement. To manufacture Portland cement, limestone, silica-alumina and iron are pulverised and mixed in desired proportions. The mixture is then sintered or fired at 1400 – 1650 °C in a rotary kiln to form clinker. To finish off the Portland cement the clinker is cooled and ground into a powder, mixed with a few additives, and a small amount of gypsum is added in order to regulate the initial chemical reaction of the cement (Gagg, 2014). Cement clinker production is the main source of $CO_2$ emission in concrete structures with 8% of the total $CO_2$ emissions globally. The vast majority of this emission comes from the energy used to fire the materials (fuel combustion) and the chemical reaction from the mixture while being heated (Ramsden, 2020). The two main components contributing to $CO_2$ emissions in cement are the clinker-to-cement ratio (a higher ratio emits more $CO_2$) and the fossil fuels used to reach the extreme heat in the kiln. Lowering the clinker-to-cement ratio can be achieved by adoption of supplementary cement materials (Vass, Levi, Gouy, & Mandová, 2021).

Higher concrete strength classes have more cement strength which is achieved by grinding the cement to finer particles and increasing the clinker content. More electric energy is used to achieve the finer grind of the cement which is beneficial for the strength as more of the clinker and other reactive particles can be hydrated after 28 days. More clinker will increase the reactive phases of the cement and therefore allow for higher strength to be achieved.

## 5.2. Structural Wall Type

To minimize the use of material (concrete and steel) an optimum chamber wall type for the lock will be chosen. Four main chamber wall typologies will be investigated and compared; Counterfort wall, anchored wall, wall with relief shelves and a retaining wall with rubble floor. The most sustainable chamber wall type would be the one that requires the least amount of concrete and reinforcement.

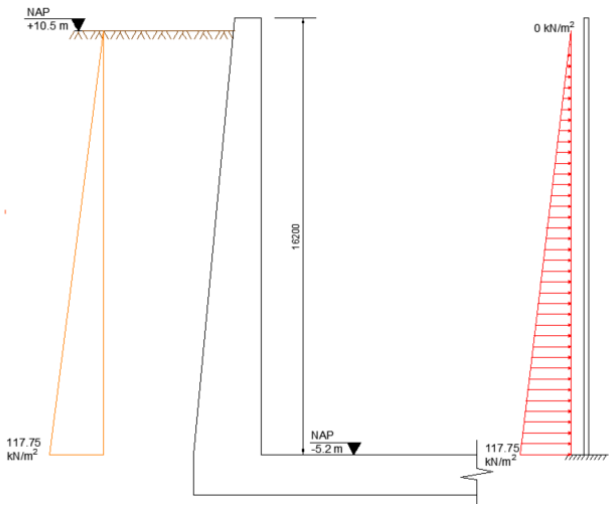


**Figure 35: base case under a simplified load**

To get a better understanding on how each wall typology behaves a simplified load will be applied to the five wall types (including the base case type). The simple load will assume a 13 kN/m$^3$ soil density, empty chamber and no groundwater (a simple triangular distributed uniform load). This load and the resulting moments and shears for each typology are then used to determine which chamber wall type would lead to the optimum lock chamber considering sustainability. A wall with the smallest bending moment will lead to the least amount of reinforcement in the stem and the wall with the lowest shear force will use the least amount of concrete (shear determines the thickness of the stem). An approximation of the concrete volume of other elements of the wall (heal, toe, shelves and counterforts) will be found. The types can hence be compared in a simplified manner concerning concrete volume. After an optimum typology has been determined the optimized lock chamber will be fully designed using the complete load situation for the new Haringvliet lock, as was done for the base case in chapter 4. The simple load situation and the base case is depicted on Figure 35. This load gives a maximum moment of $M_{max} = 6530.44\ kNm$, and a maximum shear of $V_{max} = 1247.86\ kN$.

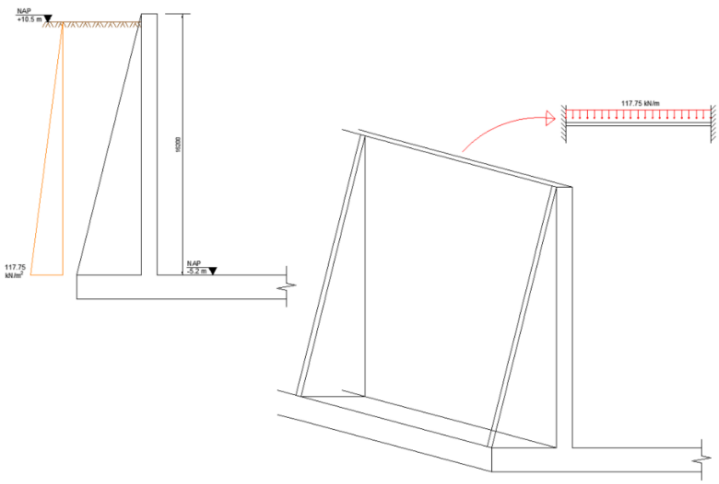

**Figure 37: Type 1; Counterfort wall under a simplified load**

Counterfort walls have a heal (horizontal base) and vertical concrete webs called counterforts. The counterforts join the stem to the base with regular spacing between them (see Figure 37). This design is usually used for tall retaining walls as they significantly reduce the moments and increasing the shear strength. Instead of a cantilever beam design (base case) the wall now behaves like a two-way slab, fixed on three edges under uniformly varying load. The wall stem deflects away from the earth face between the counterforts (see Figure 36). The spacing between Counterforts is normally between ½$H_{wall}$ and ⅔$H_{wall}$ (Brooks & Nielsen, 2013). Therefor a spacing of 9 m is chosen for this preliminary comparison of wall types. The width of the counterforts is chosen as 0.05H = 0.8m (Behera, 2023). Thus,

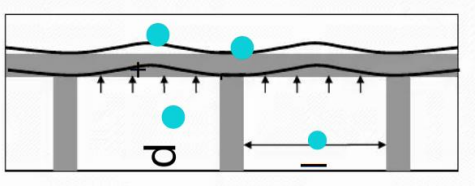


**Figure 36: the way that a counterfort retaining wall deflects**

the clear spacing between counterforts is $l = 8.2\ m$. The maximum positive bending moment occurs at the base of the wall, mid-way between the counterforts. Thus, the main reinforcement is on the outer face along the length of the wall.

$$M_{mid} = \frac{p\gamma l^2}{16} = \frac{117.75\ kN/m \cdot 1.35 \cdot 8.2\ m^2}{16} = 668.04\ kNm$$

A negative bending moment occurs over the counterfort due to the fixity they provide and thus a main reinforcement must be at the inner face near the counterforts.

$$M_{neg} = -\frac{p\gamma l^2}{12} = -\frac{117.75\ kN/m \cdot 1.35 \cdot 8.2\ m^2}{12} = -890.72\ kNm$$

Figure 36 shows how the counterfort wall stem deflects. The maximum shear in the stem is:

$$V = \frac{p\gamma l}{2} = \frac{117.75\ kN/m \cdot 1.35 \cdot 8.2\ m}{2} = 651.75\ kN$$

An anchored concrete wall can be formulated as beam fixed at one end and simply supported higher up on the wall; a statically indetermined beam (see Figure 39). The anchor will work in tension and reduce the maximum moment in the wall by transferring load to the subsoil by means of friction, as well as restrict the outward deformation of the cantilever wall (Voorendt & Molenaar, 2020). Both negative and positive bending moment will occur in the wall stem and thus the position of the main reinforcement will vary between faces over the height of the wall according to the direction of bending moment. The Optimum position of the anchor is where it reduces the moments in the wall stem the most. for this simplified load the optimum position of the anchor will be at NAP +3.3 m. The bending moments and shear are shown in Figure 38. The Thickness of the anchored wall is determined by the moment as it dominates over the shear force. The shear force would lead to a relatively thin wall stem design. However, the moment that must be resisted with flexural reinforcement is so large that with such a thin wall the cross section would be overly reinforced. Therefore, it is more economical to increase the thickness of the wall so the flexural reinforcement can be reduced.

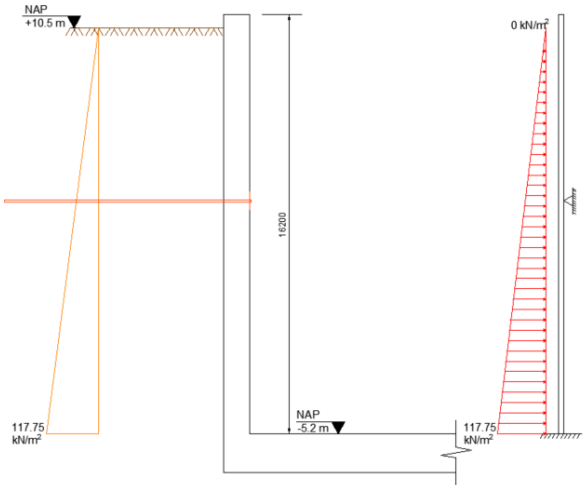


**Figure 39: Type 2; Anchored wall under a simplified load**

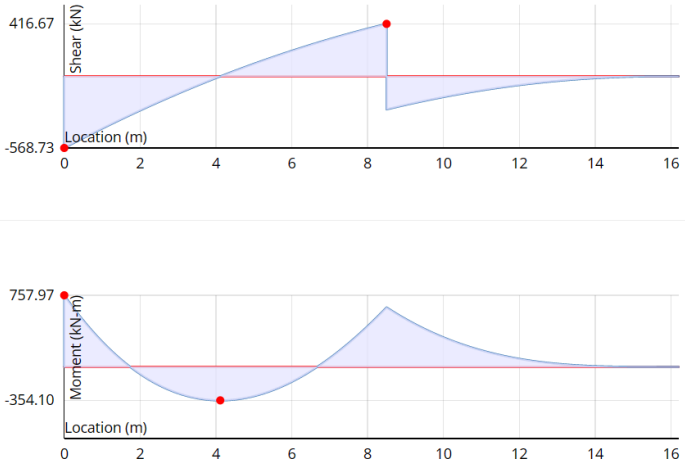


**Figure 38: Moment and shear diagrams for the anchored wall with the anchor positioned at NAP +3.3 m (8.5 m from the bottom slab)**

A relief shelve wall, depicted in Figure 40, has shelves that are added on the backfill side of the wall and reduce the overall bending moments and shear forces by decreasing the active horizontal earth pressure and increasing the stability of the wall (Shehata, 2016). The disadvantage of this wall type is that it is difficult to maintain. Weak cross sections are formed where the shelves attach to the wall but since there is soil above them it is hard to fix if crack forms. If there are multiple shelves the lower shelves are especially hard to maintain as one would have to excavate soil and go under the upper concrete relief shelve. Many theoretical papers were found on retaining walls with multiple relief shelves but only one was found where it was applied in real life. The wall was located in India and for that specific case the retaining wall had failed (Chauhan, Dasaka, & Gade, 2016). After multiplying the horizontal soil pressures with γ = 1.35 the maximum moment and shear, occurring at the bottom of the stem are calculated as:

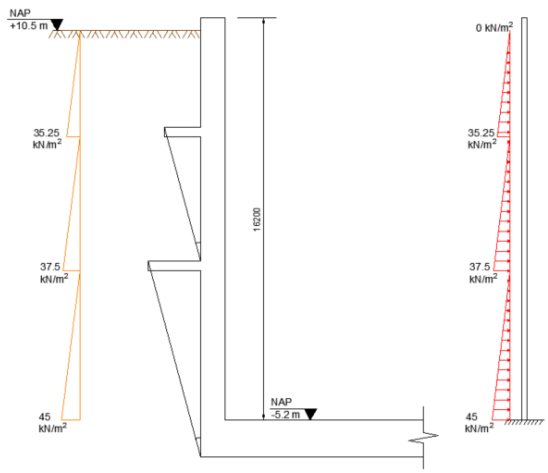


**Figure 40: Type 3; Wall with relief 2 shelves located at NAP +0.8 m and NAP +5.8 m, under a simplified load.**

$$M_{max} = 2740.15\ kNm$$

$$V_{max} = 420.65\ kN$$

The fourth typology that will be considered is a retaining wall with a rubble floor, depicted on Figure 41. A retaining wall of this height will closely resemble a gravity structure and thus will need a great quantity of concrete to resist the overturning moment and sliding. On the other hand, with such structure a rubble flooring could be used instead of concrete and the walls can be constructed on the dry and later submerged, hence there would be no need for a construction pit during the construction face of the lock chamber. The rubble flooring must be safe against outburst from upward hydrostatic pressure. Horizontal stability of the retaining wall needs to be checked where the horizontal force from the soil must be lesser than the friction forces resisting the sliding. Overturning moment must also be resisted by the stabilizing moments from the vertical forces coming from the weight of the soil and the weight of the retaining wall:

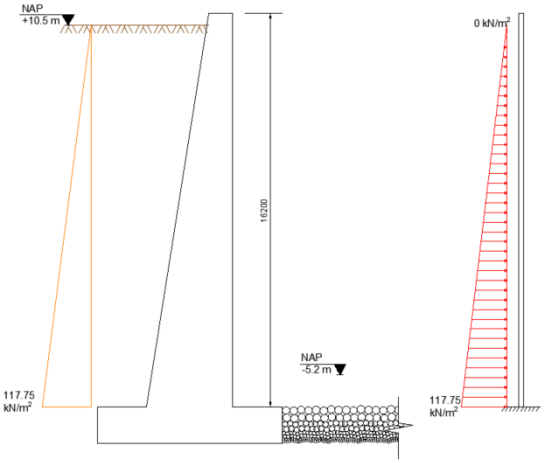


**Figure 41: Type 4; Retaining wall with rubble flooring under a simplified load.**

$$\frac{RM}{OM} \geq 1.5$$

RM = restoring moment. Comes from the weight of the structure and the weight of the soil with a lever arm from the center of gravity of those loads to the toe of the retaining wall. With a width at the base of the stem set to 4 m and a top width of 1 m, a heal length and toe length both 2 m and the base thickness of 1.7 m the restoring moment is:

$$RM = M_{wall} + M_{soil} = 4802.5\ kNm + 5224.5\ kNm = 10027\ kNm$$

Therefore, the criteria becomes:

$$\frac{RM}{OM} = \frac{10027\ kNm}{6530.44\ kNm} = 1.53$$

The vertical effective soil stress that resists the acting loads must be smaller than the maximum bearing capacity of the soil to avoid the collapsing of the soil.

Below are lists stating the advantages and disadvantages of each wall type.

**Counterfort Wall**

Pros:

- Stiffer structure as it is fixed on three edges
- Reduced moments in stem
- Increased shear strength
- Thinner stem design (less concrete)
- Easy in construction
- Easy to maintain
- Reduced reinforcement in floor

Cons:

- Constructed inside a construction pit
- Takes a long time to construct

**Anchored Wall**

Pros:

- Decreased deflection
- Reduced moments in stem
- Thinner stem design (less concrete)
- Easy in construction
- Easy to maintain
- Reduced reinforcement in floor

Cons:

- Constructed inside a construction pit
- Additional punching shear reinforcement necessary in proximity to the anchor

**Relief shelve wall**

Pros:

- Increased stability
- Decreased active horizontal earth pressure
- Reduced moments in stem
- Decreased shear stress in wall stem
- Thinner stem design (less concrete)
- Reduced reinforcement in floor
- Simple in construction

Cons:

- Constructed inside a construction pit
- The connection of shelves to wall is vulnerable (additional moments and shear form there)
- Very difficult to maintain the shelves if cracks form

**Retaining wall with rubble floor**

Pros:

- Pre-cast structure that is submerged
- No Construction pit necessary

Cons:

- Less stable

- No concrete flooring
- Easy to maintain
- Easy to construct
- Can be constructed in parts
- More failure modes (sliding, overturning…)
- Concrete heavy structure (thick stem)

**Table 19: The maximum moments and shear force for each wall along with the estimated wall thickness for the simplified load, assuming no shear reinforcement**

| | M [kNm] | V [kN] | $t_{wall}$ (base/top thickness) [m] |
|---|---|---|---|
| **Base Case** | 6530.44 | 1247.86 | *2.8 / 1.0 |
| **1. Counterfort Wall** | 890.72 | 651.75 | 1.6 / 0.8 |
| **2. Anchored Wall** | 757.97 | 568.73 | 1.3 / 0.8 |
| **3. Relief shelves** | 2740.15 | 420.64 | **1.0 / 1.0 |
| **4. Retaining wall w/o floor** | 6530.44 | 1247.86 | 4.0 / 1.0 |

* Due to the large shear force in the base case the longitudinal flexural reinforcement must be locally increased or shear reinforcement must be added for the wall to be able to resist the shear and not be excessively wide. The value given in the table is for a wall stem without any shear reinforcement. Shear reinforcement will be added later in the optimised sustainable design.

** Due to the low shear for the relief shelve wall alternative the wall stem thickness, is relatively narrow compared to the other alternatives. It does however have a much higher moment than alternatives 1 and 2 and thus requires more flexural reinforcement.

## 5.3. Durability and Flexibility

Durability and flexibility of the structure are crucial factors when it comes to the sustainability of the structure. A durable concrete structure should maintain its form and strength throughout its lifetime by resisting weathering actions, chemical attacks, abrasion and other forms of deterioration. The service life of a structure is increased as the durability gets higher. With higher durability and thus longer lifetime, there will be less need for maintenance and the structure will not have to be rebuilt for a long time. On the other hand, very durable structures are often not very flexible. Therefore, durability can result in less material consumption in relation to the structures lifetime as it would need less maintenance over its lifetime. A structure with a service life of 50 years might need to be rebuilt after that time and thus would use much more concrete than a structure that already lasts 100 years. Concrete is however a very durable material and many building have a much longer life span than the actual service life. Therefore, most concrete structures are demolished at the end of their service life due to there being no use for them anymore rather than deterioration (PCA, 2022).

There is however much to be considered here. A more durable concrete structure will most likely use a lot of concrete compared to a less durable structure, leading to a more rigid design. for a structure such as the one in this study, which is designed with a lifetime of over 150 years, a lack of flexibility might be negative. The design parameters are highly dependent on forecasted environmental scenarios (SLR) and marine traffic forecasts which may change in the future and thus change the whole loading situation and the dimensions of the structure. A durable ship lock complex that has a service life of 100 years has to take into account marine traffic forecast 100 years in the future which is difficult to predict with accuracy. It also must take into account SLR, so at the start of the service life of the structure, much of its strength will not be utilized at all. A possibility to compensate for this is to split the construction over its lifetime. Some of the elements of the lock chamber must last 200 years. However, the full height of the lock chamber is not needed over its whole lifetime and therefore flexibility is of importance too. The full chamber wall height on the seaside of the lock is not necessary for 150 years. For the first 50 years the walls can be constructed

up to a certain height that is necessary for the sea level in the year 2150. In the year 2150 the walls can then be raised to the standard of the sea level in the year 2250. This would mean that the lower part of the wall must have a more durable concrete design with a lifetime of 150 years but the upper part of the wall, which is later constructed, can be designed with concrete of lower strength as it will have a lifetime of only 75 years. This will be beneficial for the overall sustainability of the ship lock chamber. This is also beneficial as future sea level rise is a forecast based on many assumptions. It is easier to make a forecast for the close future and thus in the year 2150 a more detailed forecast of the sea level rise in the year 2250 can be made.

## 5.4. Construction Methods

Two different construction methods are considered; In-situ construction in a construction pit or (as in the case of the retaining wall with a rubble flooring) a pre-cast structure that is later submerged, not needing a construction pit. To include the entirety of these two construction methods in the LCA can be of a complicated nature as it would need transport information, as well as labour needed and excavation volumes. For the design of this sustainable concrete lock chamber only the materials that would be needed in a construction pit (steel and concrete) will be included. This will provide some idea of the environmental footprint of a construction pit but is it should be noted that it will in no way the full picture of the affect.

## 5.5. New Optimized Design

From the information provided above a new structural typology will be chosen. Type 3; the relief shelve wall, will not be chosen due to the difficult maintainability and risk of cracking of the shelves, as well as a larger volume of reinforcement due to a larger moment compared to type 1 and 2. Type 1 and 2 both have low moments compared to the base case. Type 1; Counterfort wall will not be chosen as it will require much more concrete compared to type 2; anchored wall, as it has the counterforts and heal slabs. The counterforts themselves are also pure tension elements and therefore will require a lot of reinforcement. Therefore type 2; the anchored wall type will be chosen for the new optimized design.

To decide if type 4 is preferable, the material savings on not having a construction pit must be evaluated against the increased amount of concrete that is needed for the retaining wall structure with rubble flooring. If the absence of a construction pit and concrete flooring shows through LCA to be beneficial enough to compete with type 1 or type 2 in overall sustainability, Further calculations will be performed to fully design the wall and ensure that outburst of the rubble flooring can be avoided.

# 6. Design Results: Anchored Wall Lock Chamber

Using the insight given in chapter 5 the chosen wall typology for the new sustainable optimisation of the ship lock chamber is an anchored concrete chamber wall. In this chapter a preliminary design of the anchored concrete lock chamber will be made.

## 6.1. Sizing of the Lock Chamber

For the LCA's of both design cases to be comparable all major dimensions for the lock size must be kept the same for both designs. Therefore, the total length of the chamber is $L_{ch} = 144$ m and the width of the chamber that must be provided must have the same minimum side clearance. For the base case the width of the chambers was 16 m. However, for the anchored concrete wall design some additional width must be provided in order to ensure that the chamber width of 16 m is provided everywhere across the of the lock. The ends of the anchors will protrude into the chamber due to the end plate that distributes the force on the concrete wall and some bolts and nuts to secure said plate to the tie rod. The inner chamber width for the anchored chamber wall will thus be designed to be $B_{ch} = 16.5$ m, allowing for a 250 mm width for anchor fastenings on either side of the chamber.

The lock head around the center flood gates will have the same width as the dike crest which is 22 m wide. It has the same height of as the base case of NAP +11.0 m resulting in a 16.2 m high wall around the flood gates. It will allow for an additional width of 2.5 m for the lock metre gates. Assuming that the rotating mechanism positioned 1.5 m away from the chamber wall the gates must be able to close an 18.5 m wide opening. The extra 1.5 m behind the gates will be used for maintenance of the gates. Two mitre gates (4 "gates" in total) are provided at the crest of the dike. Assuming the optimum angle of around 18.4° for load transfer, the total length of a single gate is:

$$L_{gate} = \frac{18.5\ m/2}{\cos(18.4°)} \approx 9.8\ m$$

Allowing for 0.8 m space between the two mitre gates for rotating mechanisms the total width of the lock head will be:

$$L_{center,head} = 2t_{wall,center} + L_{gate} \cdot 2 + 0.8\ m = 2t_{wall,center} + 20.4\ m$$

After the center lock head, the wall will gradually decrease in height following the dikes slope of 1:3 until it reached its minimum wall height. The minimum wall height for the base case was chosen as NAP +7.0 m, accounting for the maximum locking level of NAP +5.55 m in the year 2250. A recreational harbour is situated at the seaward side of the lock complex. The land surrounding the harbour will be at NAP +6.5 m. This is fairly high as it is in accordance with the water level of the year 2250. Therefore, the wall at the seaward side of the chamber will first be constructed with the year 2150 in mind and then later raised in accordance with water level predictions for the year 2250. Therefore, for the 1st 100 years of the use phase of the lock the level of the surrounding harbour will be NAP +4.50 m, e.g. 1.28 m higher than the maximum locking level of NAP +3.22 m for the year 2150 (1.55 m SLR). The wall that will be constructed and used until the year 2150 will have the same amount of reinforcement and thickness as it would have after the increased height in 2250. That way no concrete will be demolished in 2150, but instead the increased height can be added on top of the old wall. On the riverside of the lock the minimum wall height can be kept at NAP +4.5 m as the maximum locking level on that side is lower than at the seaside of the lock.

## 6.2. Governing Load Case

The new optimized concrete chamber will be designed for the same load case as was presented for the base case. The assumed soil type is sand with a dry unit weight of $\gamma_s = 19$ kN/m$^2$ and a saturated weight of $\gamma_{s,sat} = 21$ kN/m$^2$. The water within the chamber will provide resistance to the horizontal load from the soil. On top of the surrounding soil an allowance for a distributed load, $q = 20$ kN/m$^2$, due to machinery, roads, and trucks will be considered. The top of the soil will be 0.5 m lower than the chamber wall. Using equations 4.13 to 4.15 the effective horizontal soil pressure is found. The horizontal soil pressure for the chamber wall at the center lock head and the horizontal soil pressure at the low wall on the seaside are presented in Figure 42 below. The low wall at the seaside has a height of 9.7 m until the year 2150 (NAP +4.5 m). It will however need to resist the same critical load as the 12.2 m high wall, as it will be raised to that level in 2150. Therefore the 9.7 m wall is presented with the critical load that will act on the increased wall height in the year 2250. The critical load for the 12.2 m high wall will include the minimum locking level for the year 2150 as in that year the wall will be the highest, but the minimum locking level will be the lowest. From the year 2100 until 2150 the sea level will have risen by 0.68 m (see Table 6) resulting in a minimum locking level of NAP +0.5 m. The walls have different wall thickness as the resulting load for the lower wall type allows for a reduction in thickness.

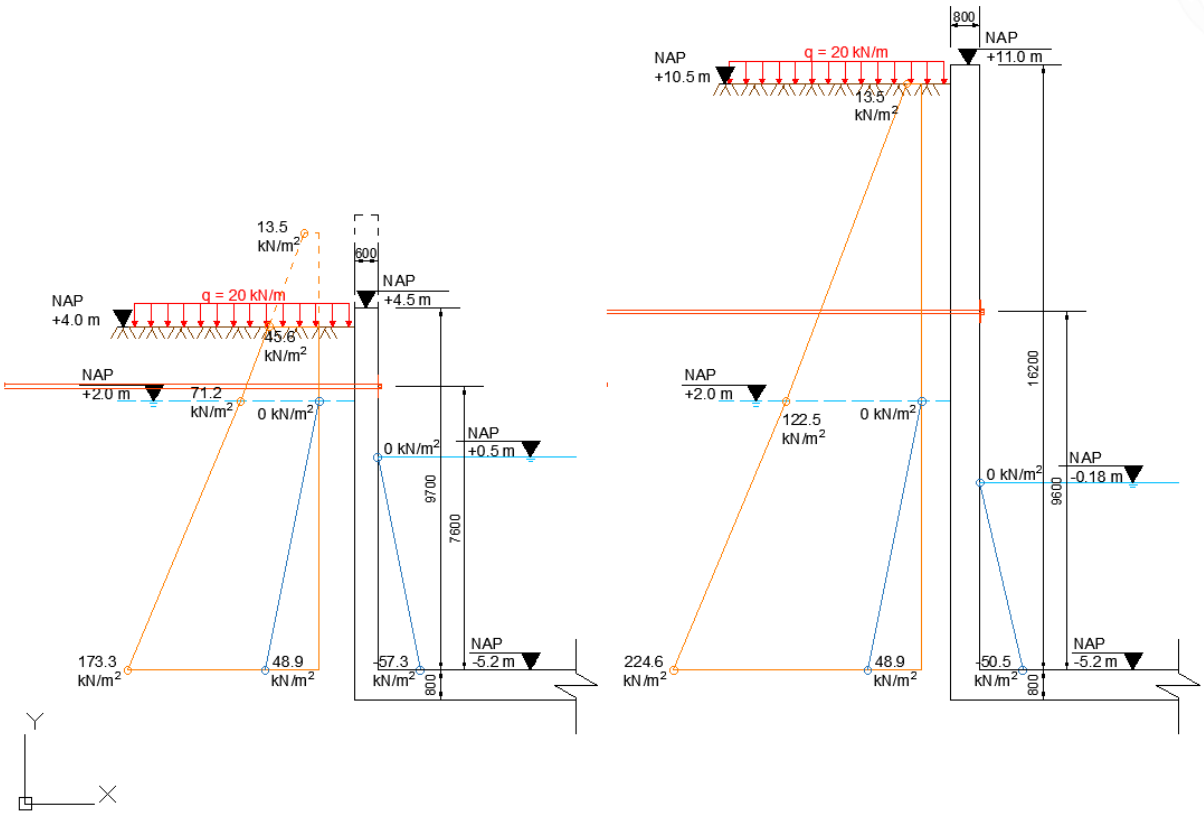


**Figure 42: Active horizontal loads for the chamber wall around the center flood gates (right) and the low chamber wall on the sea and riverside of the lock (left). The dotted lines on the left figure are representative for the wall in the year 2150 after the 2.5 m increment of the chamber wall.**

The due to the presence of anchors, the chamber walls will now behave like a 2-way slab and will therefore be modelled in Diana FEA as a 3D plate element fixed along the bottom and simply supported at the locations of the anchors. Three different wall segments are modelled in Diana FEA to calculate the resulting moments $M_{xx}$ and $M_{yy}$ along with the shear and reaction forces. The wall segments modelled are the 16.2 meter high wall around the center lock head, the wall on the seaside, and the riverside wall including the low wall segment and the sloped wall following the dike slope. The optimum placements of the anchors

are found iteratively by varying the anchor position in Diana FEA so that minimum moments are reached. For the high wall at the dike crest it was found to be at 9.5 m above the bottom of the camber, e.g. NAP +4.3 m, for the low wall on the seaside the anchors are placed 7.5 m above the bottom of the chamber, e.g. NAP +2.3 m, and for the low wall on the riverside they are placed at 6.4 m above the bottom of the chamber, e.g. NAP +1.2. For the sloped wall segment the height of the anchors was chosen such that they followed a linear line from NAP +2.3 m to NAP +4.3 m. Note that this optimum height of the anchors will be different under different soil conditions. The anchors have a center-to-center distance of three meters for the wall at the center lock head and for the sloped wall segment. For the lowest part of the wall the anchors will have a center-to-center distance of 3.5 m. The loads are inserted as linear function in Diana, varying over the height of the wall. For the sloped wall segment the soil pressure will change both over the length, and the height of the wall as the soil profile height is also decreasing along the slope. As the ground water level is always lower than the wall the soil pressure will be split into two parts: a dry soil pressure depending on x and y and an additional pressure of $\gamma_s - \gamma_{s,sat} = 2$ kN/m$^2$ starting from the ground water level down to the bottom to take into account the additional pressure from the saturated soil $\gamma_{s,sat}$. The function describing the load from the dry soil is formulated as follows:

$$\sigma_{h,act,dry} = \gamma_s (H(x) - y) K_0 \gamma_{G,uf} \tag{5.01}$$

Where:

| | | |
|---|---|---|
| $\gamma_s$ | [kN/m$^2$] | Unit weight of dry sand, $\gamma_s = 19$ kN/m$^2$ |
| $H(x)$ | [m] | Top height of the wall depending on x coordinate. |
| $y$ | [m] | y coordinate |
| $K_0$ | [-] | Neutral soil pressure calculated as 0.5 in chapter 4.2.1 |
| $\gamma_{G,uf}$ | [-] | Permanent load safety factor for an unfavourable load; $\gamma_{Q,unf} = 1.35$ |

The change in height H(x) can be formulated as a line with a 1:3 slope. The model for the low wall + the sloped wall starts at x=0 and ends at x= 70.6 (top of slope). Hence the sloped segment of the wall ends at x = 58.4 m where the wall height is 12.2 m, and the soil height is 11.7 m (this height represents the more critical load case for the low wall that will be increased to this height in 2150). H(x) can then be formulated as:

$$H(x) = {}^1\!/_3\,(x - 58.4\ m) + 11.7\ m \tag{5.02}$$

The function for the load originating from the dry soil pressure can now be formulated using equation 5.01 and 5.02:

$$\sigma_{h,act,dry} = 12.825\ kN/m^2 \left({}^1\!/_3\,(x - 58.4\ m) + 11.7\ m - y\right)$$

The ends of the modelled walls are connected to a 2.5 m long perpendicular wall connecting the chamber to the lock heads. This results in a boundary condition at either end of the wall segment that allows for some flexibility, e.g. the ends are neither free nor fixed. Hence the wall segments are modelled in two ways; Free unsupported edges and simply supported edges hindering displacement in perpendicular direction to the wall. The true situation will be closer to that of a simply supported edge as the ends of the wall segment will be fairly stiff due to the supporting wall in the perpendicular direction. Therefore, it is assumed the true values for the moments and shear forces are the equal to a weighed value giving 60% importance to the simply supported edge and 40% importance to the free edge. This 60/40 ratio is a conservative estimate based on engineering experience but could perhaps be a bit stiffer.

$$Value = 0.4 \cdot Value_{free} + 0.6 \cdot Value_{fixed} \tag{5.03}$$

Figure 43 and Figure 44 below show the 2 different modelled wall segments with simply supported edges.

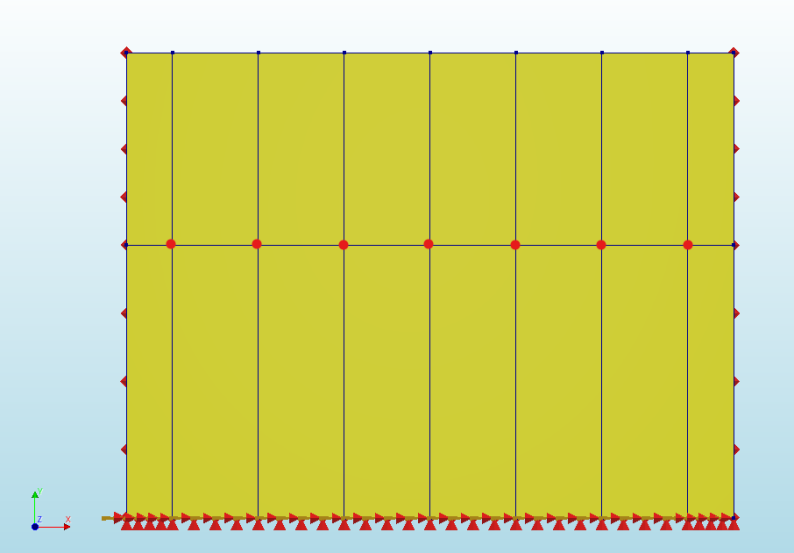

**Figure 43: 16.2 m high wall around the center flood gates modelled in Diana FEA with simply supported edges, fixed bottom and simply supported at locations of anchors.**

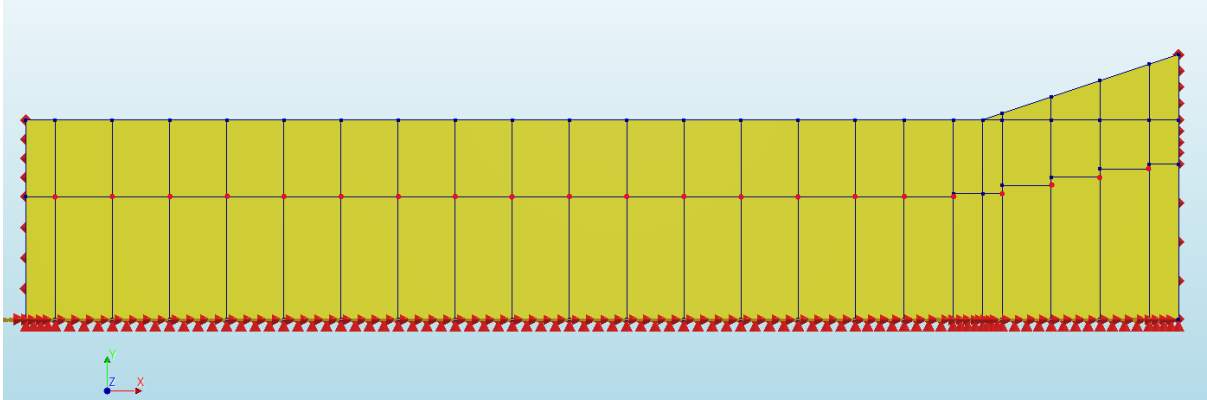

**Figure 44: Wall along the seaside chamber with the height of 12.2 m and the highest point at 16.2 m, modelled in Diana FEA with simply supported edges, fixed bottom and simply supported at locations of anchors.**

The loads were split into 4 and applied as functions to the model:

- Soil pressure: $\sigma_{v,act,soil}(y) \cdot \gamma_{G,unf} \cdot K_0$
- Imposed vertical load: $q \cdot \gamma_{G,unf} \cdot K_0$
- Ground water pressure: $-p_{act}(y) \cdot \gamma_{G,unf} \cdot K_0$
- Water pressure from within the chamber: $-p_{pas}(y) \cdot \gamma_{G,f} \cdot K_0$

Where

| | | |
|---|---|---|
| $\sigma_{v,act,soil}(y)$ | [kN/m²] | Active vertical soil pressure only from the soil dependant on the soil depth, y (distributed load on top of soil not included). |
| $q$ | [kN/m²] | Imposed vertical load on top of soil due to equipment and traffic $q = 20\ kN/m^2$. |
| $-p_{act}(y)$ | [kN/m²] | Active ground water pressure releasing some of the soil pressure, hence the negative sign. Dependant on the ground water depth, y. |
| $-p_{pas}(y)$ | [kN/m²] | Passive water pressure from within the chamber acting favourably hence the negative sign. Dependant on water depth, y. |

$K_0$ [-] Neutral soil pressure calculated as 0.5

The element size for all models was set to 0.1 m. The results from Diana for the 16.2 m high wall segment around the center lock head are presented in Table 20 below where "Value" is the equated value for the moments, shear and reaction forces using equation 5.03 that will be used when designing the chamber resistance. Similar table for the other wall segment is given in Appendix D. Figure 45 to Figure 50 show the moments in y and x and the displacements of the wall around the center flood gates for both the free side edges scenario and the simply supported side edges scenario.

In the model a stress singularity occurs at the anchors modelled as a simple support. The location where the values of moments and shear forces are taken are chosen at the edge of the anchor plate. Three plate sizes are considered for the anchor support at the concrete wall; 400 x 400 mm, 600 x 600 mm, and 800 x 800 mm plates. The plate size that is used in the design for different anchors was chosen such that the shear forces would not be extremely large. For the chamber wall at the center lock head and the sloped walls, the plate sizes chosen are 600 x 600 mm and for the low chamber walls at the sea- and riverside the plate sizes are 400 x400 mm.

**Table 20: Moment in x and y direction, shear forces and reaction forces for the 16.2 m high wall segment around the center flood gates. Values are displayed for the free edge case, supported edge case and the estimated averaged value that is used in the design.**

| **Moment $M_{xx}$** | **X [m]** | **Y [m]** | **Free [kNm]** | **Supported [kNm]** | **Value [kNm]** |
|---|---|---|---|---|---|
| *Bottom edge* | 1.6 | 0 | 1120.50 | 502.68 | 749.8 |
| *Bottom middle* | 10.6 | 0 | 1055.65 | 1086.62 | 1074.2 |
| *Anchor middle 800* | 10.6 | 9.5 | 834.89 | 822.83 | 827.7 |
| *Anchor edge 800* | 1.6 | 9.5 | 855.24 | 381.54 | 571.0 |
| ***Anchor middle 600*** | 10.6 | 9.5 | 908.71 | 898.78 | 902.8 |
| ***Anchor edge 600*** | 1.6 | 9.5 | 932.59 | 414.74 | 621.9 |
| *Center middle* | 10.6 | 4.9 | -541.24 | -557.99 | -551.3 |
| *Center edge* | 1.6 | 4.9 | -547.06 | -259.16 | -374.3 |
| | | | | | |
| **Moment $M_{yy}$** | **X [m]** | **Y [m]** | **Free [kNm]** | **Supported [kNm]** | **Value [kNm]** |
| *Bottom edge* | 2.2 | 0 | 328.11 | 179.75 | 239.1 |
| *Bottom middle* | 10.6 | 0 | 316.59 | 325.57 | 322.0 |
| *Anchor middle 800* | 10.6 | 9.5 | 493.88 | 444.63 | 464.3 |
| ***Anchor middle 600*** | 10.6 | 9.5 | 584.25 | 519.36 | 545.3 |
| *Center edge* | 1.6 | 4.9 | -86.77 | -244.07 | -181.2 |
| *Center middle* | 10.6 | 4.9 | -163.57 | -181.36 | -174.2 |
| | | | | | |
| **Shear V** | **X [m]** | **Y [m]** | **Free [kN]** | **Supported [kN]** | **Value [kN]** |
| *Bottom middle* | 10.6 | 0 | 643.76 | 668.87 | 658.8 |
| *Bottom edge* | 1 | 0 | 797.86 | 299.19 | 498.7 |
| *Anchor middle 800* | 10.6 | 9.5 | 1304.20 | 1335.18 | 1322.8 |
| *Anchor edge 800* | 1.6 | 9.5 | 1346.80 | 725.48 | 974.0 |
| ***Anchor middle 600*** | 10.6 | 9.5 | 1776.20 | 1820.26 | 1802.6 |
| ***Anchor edge 600*** | 1.6 | 9.5 | 1842.70 | 993.76 | 1333.3 |
| | | | | | |
| **Reaction forces R** | **X [m]** | **Y [m]** | **Free [kN]** | **Supported [kN]** | **Value [kN]** |
| *Anchor middle* | 10.6 | 9.5 | 2623.31 | 2695.87 | 2666.9 |
| *Anchor edge* | 1.6 | 9.5 | 2749.94 | 1483.17 | 1989.9 |

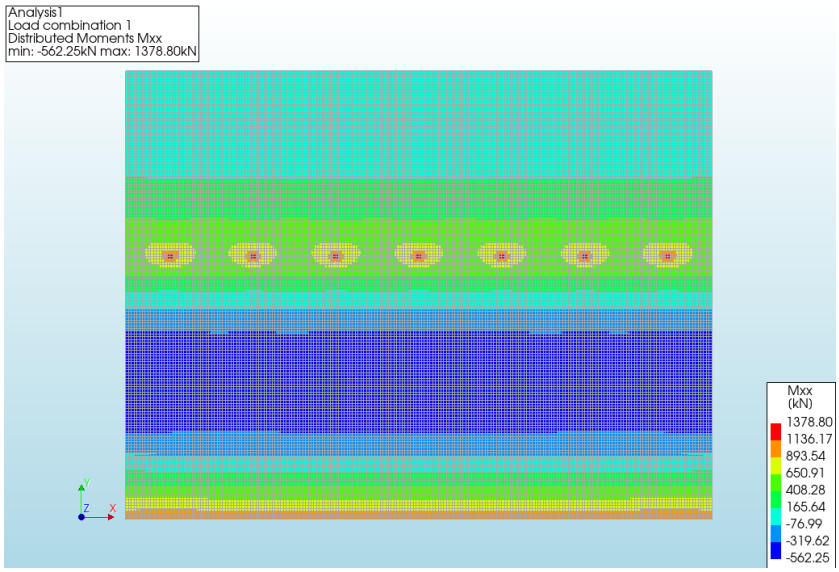


**Figure 45: $M_{xx}$ moments [kNm/m] on the chamber wall along the center flood gates, free edges.**

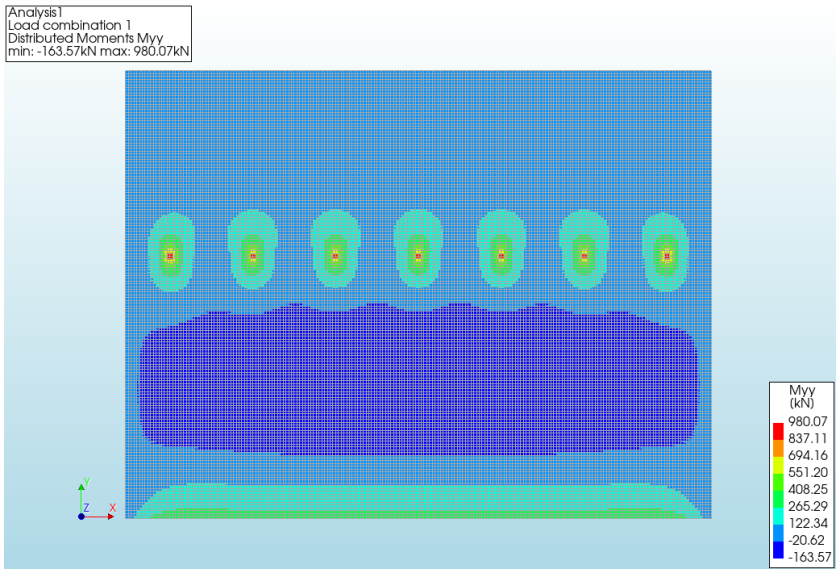


**Figure 46: $M_{yy}$ moments [kNm/m] on the chamber wall along the center flood gates, free edges.**

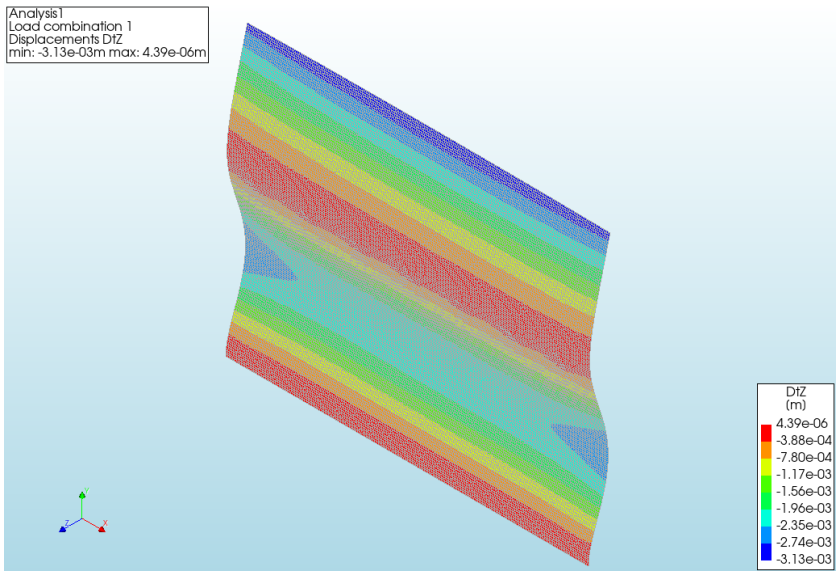


**Figure 47: displacements [m] of the chamber wall along the center flood gates in z-direction with free edges.**

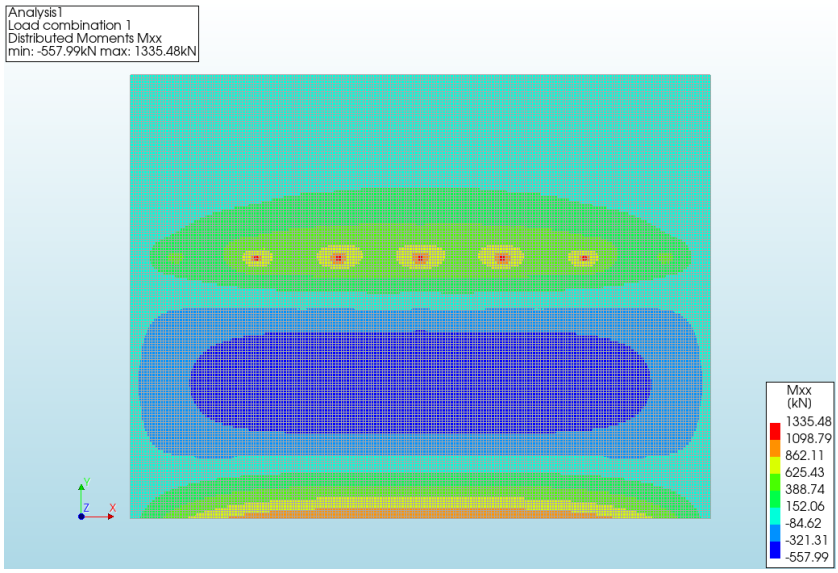


**Figure 48: $M_{xx}$ moments [kNm/m] on the chamber wall along the center flood gates, simply supported edges.**

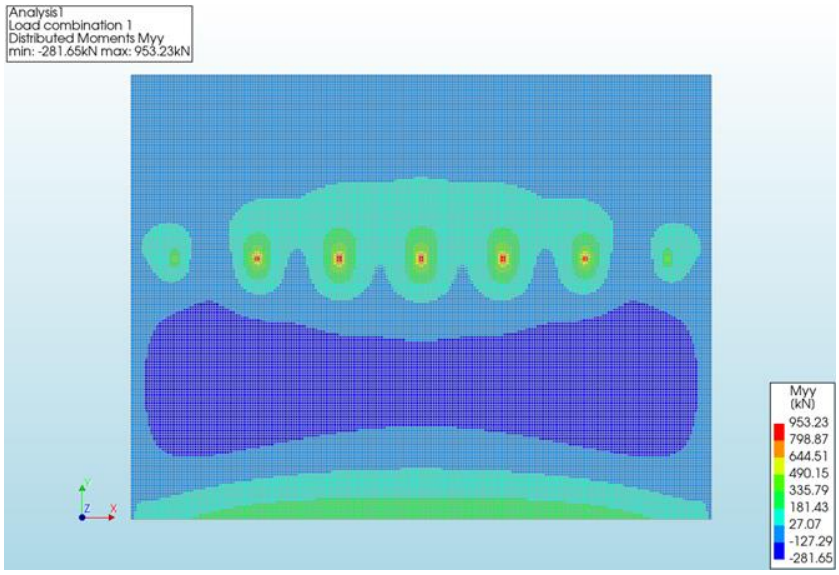


**Figure 49: $M_{yy}$ moments [kNm/m] on the chamber wall along the center flood gates, simply supported edges.**

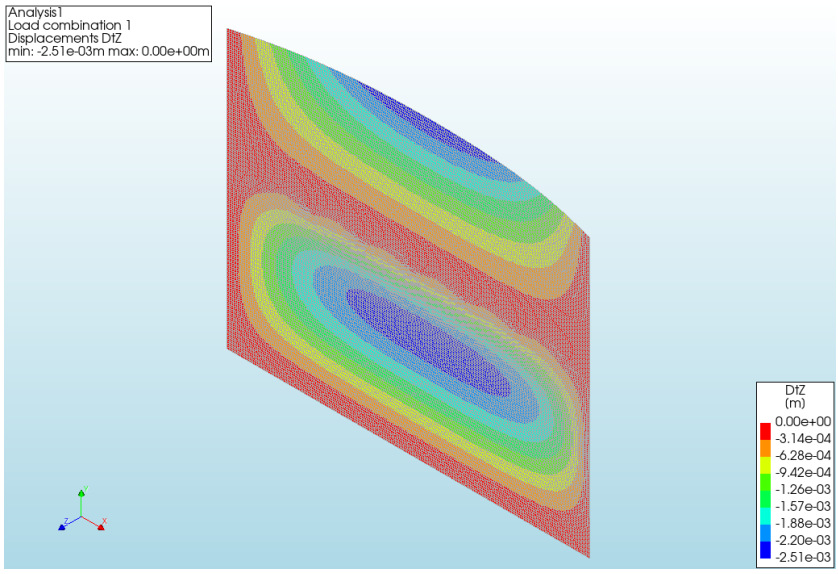


**Figure 50: displacement [m] of the chamber wall along the center flood gates in z-direction with simply supported edges.**

## 6.3. Structural Design of the Anchored Wall Concrete Chamber

All formulas presented in chapter 4.2.2 will be used for the reinforcement design of the anchored wall chamber design. Shear links will be provided in the alternative design to minimize the wall thickness. Calculations and results for the wall around the center flood gates will be explained and presented in this chapter. The resulting reinforcement volumes for the other wall segments will be presented in Appendix D:.

Due to the reduced moments and shear forces and the use of shear links the wall thickness and concrete class can be reduced. The concrete class used for the new optimised design is C35/45. For the 2.5 m wall height increment on the seaside of the lock the concrete class can be further reduced to C25/30 as it does not need to be as durable as the lower part of the wall. The chamber wall around the center flood gates and along the dike slopes until the wall height reaches the level of NAP +4.5 m will have a thickness of 0.8 m. For the low chamber wall on the sea and riverside chamber (NAP +4.5 m) the wall will have a thickness on 0.6 m. The floor has a thickness of 0.8 m everywhere. The material factors for the concrete used in the optimized chamber design are presented in Table 21

**Table 21: Material factors of concrete strength classes C35/45 and C25/30**

| **Concrete class C35/45** | | | |
|---|---|---|---|
| *Characteristic cylinder compressive strength* | $f_{ck}$ | 35.00 | MPa |
| *Mean cylinder compressive strength* | $f_{cm}$ | 43.00 | MPa |
| *Mean tensile strength* | $f_{ctm}$ | 3.21 | MPa |
| *Elastic modulus* | $E_{cm}$ | 34077 | MPa |
| *Design compressive strength* | $f_{cd}$ | 23.33 | MPa |
| *Design tensile strength* | $f_{ctd}$ | 1.50 | MPa |
| *Minimum longitudinal tension reinf. ratio* | $\rho_{min}$ | 0.167 | % |
| *Minimum shear reinf. ratio* | $\rho_{w,min}$ | 0.095 | % |

| **Concrete class C25/30** | | | |
|---|---|---|---|
| *Characteristic cylinder compressive strength* | $f_{ck}$ | 25.00 | MPa |
| *Mean cylinder compressive strength* | $f_{cm}$ | 33.00 | MPa |
| *Mean tensile strength* | $f_{ctm}$ | 2.56 | MPa |
| *Elastic modulus* | $E_{cm}$ | 31476 | MPa |
| *Design compressive strength* | $f_{cd}$ | 16.67 | MPa |
| *Design tensile strength* | $f_{ctd}$ | 1.20 | MPa |
| *Minimum longitudinal tension reinf. ratio* | $\rho_{min}$ | 0.133 | % |
| *Minimum shear reinf. ratio* | $\rho_{w,min}$ | 0.08 | % |

### *Underwater concrete floor*

Similarly to the base case, the optimized chamber will be constructed in a construction pit with an UWCF (See chapter 4.1.4). Circular prefabricated concrete foundation piles are also used for the optimized design. Assuming a chamber floor thickness of 0.6 m (see section about floor reinforcement below) the bottom of the chamber is at a level of NAP -5.8 m. Allowing for a 1.2 m margin on either side of the chamber the UWCF width for the optimized design is:

$$B_{uwc} = B_{ch} + 2t_{wall} + 2 \cdot 1.2\ m = 20.5\ m$$

An UWCF thickness of $t_{uwc} = 0.5$ m was chosen for the construction pit of the optimised design. The hydrostatic uplift force was calculated with equation 4.1 as:

$$P_{hydro} = \left(h_{gwl} - h_{bot,uw}\right) \cdot \gamma_w = 83.46\ kN/m^2$$

The bottom of the UWCF slab is at -6.3 m NAP. The piles for the optimized design will reach to the same depth as the ones for the base case, e.g. they will reach down to NAP -20.5 m. with a 0.3 m anchoring length into the UWCF the total pile length is 14.5 m. the pile diameter is kept the same as $D_{pile}$ = 500 mm.

The total uplift force that the tension piles will have to resist is calculated with equation 4.2 as:

$$F_{uplift} = 106{,}210.9\ kN - 36.1 n_p$$

Where $n_p$ is the total number of piles in the UWCF for one chamber.

The representative value for the cone resistant at depth z is calculated in Appendix C.1: for the base case. It was adjusted for the optimized design so that zone 1 starts at a higher level of NAP -6.3 m, and therefore $\Delta z_I = 3.7$ m and $L = 14.2$ m. Therefore $q_{c,z,rep} = 10.28$ MPa. The design value for the tensile strength of the soil was then calculated with equation 4.4 as:

$$q_{c,z,d} = 5.08\ MPa$$

With $L = 14.2$ m the maximum tensile force that a single pile can resist was determined through equation 4.3 as:

$$F_{r,tension,d} = 792.77\ kN$$

The number of tension piles necessary to resist the uplift is found iteratively using equation 4.2 and 4.3

$$n_{p,tens} = \frac{F_{uplift}}{F_{r,tension,d}} = \frac{106{,}210.9\ kN - 36.1 n_{p,tens}}{792.77\ kN} \approx 129\ piles$$

The tension pile resistance is also checked for the clump criterion using equation 4.5 and 4.6 with $L_{cil} = 12.95$ m and $L = 14.2$ m:

$$F_{clump} = 1051.52\ kN$$

Since $F_{clump} > F_{r,tension,d}$ the cone resistance of the pile is the determining factor for the number of piles needed and thus a minimum of 129 tension piles are necessary. With an underwater concrete floor area of a single chamber of $A_{uw} = 1476$ m² (length of 72 m and width of 20.5 m) the piles will be distributed in 22 rows over the length of the chamber and 6 rows of the width of the chamber giving a total number of 132 piles. This also fulfils the spacing requirements for the piles in the clump criterion as a minimum spacing between piles is over 3 m.

It is also necessary to check if extra compression piles will be necessary. The critical load condition for the compression piles is when the ship lock chamber is at maximum locking level of NAP +5.55 m e.g., 10.75 m chamber water depth. The weight of water within the chamber was calculated similarly to chapter 4.1.4 with a 16.5 m chamber width as:

$$W_{water} = 192{,}623.4\ kN$$

The weight of the chamber itself is (on the seaside):

$$W_{ch} = \gamma_{G,unf}\left(V_f + 2V_w\right)\rho_{cc} = 1.35 \cdot (1026.02\ m^3 + 2 \cdot 513.28\ m^3) \cdot 25\frac{kN}{m^3} = 69{,}274.6\ kN$$

Where:

| | | |
|---|---|---|
| $V_f$ | [m] | Floor volume for the seaside chamber |
| $V_w$ | [m] | Wall volume for the seaside chamber before the height increment |
| $\rho_{cc}$ | [kN/m³] | Unit weight of reinforced concrete |

$\gamma_{G,unf}$ [-] Permanent load safety factor for an unfavourable load

The total compressive force is therefore:

$$F_{comp} = W_{water} + W_{ch} = 261{,}898.0\ kN$$

The Koppejan method is used to determine the bearing capacity of a compression pile. The maximum tip resistance, $p_{r;max;tip}$, and the maximum tip resistance force, $F_{r;max;tip}$, is the same as for the base case determined by eq's 4.9 and 4.10 as:

$$p_{r;max;tip} = 10.59\ MPa$$

$$F_{r;max;tip} = 2078.9\ kN$$

The maximum pile shaft friction at depth z, $p_{r;max;shaft,z}$, is determined with eq. 4.11 with the cone resistance calculated in the same as $q_{c,z,rep}$ is calculated, but the value in zone V is now limited to 15 MN/m$^2$:

$$p_{r;max;shaft,z} = \alpha_s q_{c;z;a} = 0.01 \cdot 8.06 = 0.0806\ MPa$$

The maximum shaft friction is calculated using eq. 4.12:

$$F_{r;max;shaft} = O_{p;avg} \cdot p_{r;max;shaft,z} \cdot \Delta L = 1798.6\ kN$$

The bearing capacity of a pile is found with equation 4.8;

$$F_{r;max} = F_{r;max;tip} + F_{r;max;shaft} = 3877.4\ kN$$

The number of compression needed is therefore:

$$n_{comp} = \frac{F_{comp}}{F_{r;max}} = \frac{261{,}898.0\ kN}{3877.4\ kN} = 68\ piles$$

The required number of compression piles are fewer than the required number of tension piles (132 piles) therefore no additional piles need to be added to resist compression.

## *Shear reinforcement in walls and floors*

Concrete has a fair amount of shear capacity without shear reinforcement but only up to a certain limit. Beyond that limit, shear links must be provided. To find this limit it is first assumed that the chamber wall has no shear reinforcement. From the flexural reinforcement calculations (see below) it was found that the bottom part of the wall requires a vertical flexural (tensile) reinforcement of a single row of K32 bars with c/c = 220 mm. With the require concrete cover of 42 mm, the effective depth of the 0.8 m thick wall is $d_e = 742$ mm (see Appendix C.2.2: for information on concrete covers). The shear resistance capacity of the concrete wall without shear reinforcement is found by applying equation 4.17 (repeated here below) with $f_{ck} = 35$ MPa (C35/45 concrete):

$$V_{Rd,c} = \left[C_{Rd,c} k (100 \rho_l f_{ck})^{1/3} + k_1 \sigma_{cp}\right] b_w d_e \geq \left(v_{min} + k_1 \sigma_{cp}\right) b_w d_e = \mathbf{391.0\ kN} < V_{Ed}$$

$$\sigma_{cp} = \frac{N_{Ed}}{A_c} = \frac{t_{wall,cent} \cdot H_{wall,cent} \cdot 1\ m \cdot 25 \frac{kN}{m^3} \cdot \gamma_{G,f}}{t_{wall,cent} \cdot 1\ m} \cdot 10^{-3} = 0.405$$

$$\rho_l = \frac{A_{sl}}{b_w d_e} = 0.0050$$

$$v_{min} = 0.035 k^{3/2} f_{ck}^{1/2} = 0.39$$

The design shear that needs to be resisted by the wall is presented in Table 22.

**Table 22: Design shear forces for the chamber wall at the center lock head.**

| Location | $V_{Ed}$ [kN] |
|---|---|
| *Bottom of the wall, center* | 658.8 |
| *Bottom of the wall, edge* | 498.7 |
| *Inner anchors (600x600 anchor plate)* | 1802.3 |
| *Anchors at the edge (600x600 anchor plate)* | 1333.3 |

These shear forces all surpass the 391 kN shear resistance of the concrete and therefore shear links will be provided at the bottom of the wall and around the anchors in order to resist the additional shear.

The shear resistance without shear reinforcement for the 0.6 m thick floor was found similarly. The reinforcement at the edge of the floor at the center flood gates is a single row of K32 c/c = 110 mm. With a concrete cover of 50 mm the effective depth is: $d_e = 534$ mm. The shear resistance capacity of the floor without shear reinforcement is:

$$V_{Rd,c} = 463.2 > V_{Ed} = 437.4\ kN$$

The normal force for at the floor is taken as equal to the shear force at the bottom of the wall.

$$\sigma_{cp} = \frac{N_{Ed}}{A_c} = \frac{658.8}{t_{floor} \cdot 1\ m} \cdot 10^{-3} = 1.098$$

$$\rho_l = \frac{A_{sl}}{b_w d_e} = 0.013$$

$$v_{min} = 0.035 k^{3/2} f_{ck}^{1/2} = 0.42$$

Therefore, no shear reinforcement is required in the floor slab of the chamber.

As mentioned above, shear links will be provided at the bottom of the walls and around the anchors to resist the additional shear. Without shear reinforcement shear cracks will form near these supports (see Figure 52). Shear reinforcement is placed to avoid this. Both inclined and vertical shear links can be used. In the chamber design vertical shear links will be provided (or in this case horizontal as this is a wall and not a beam).

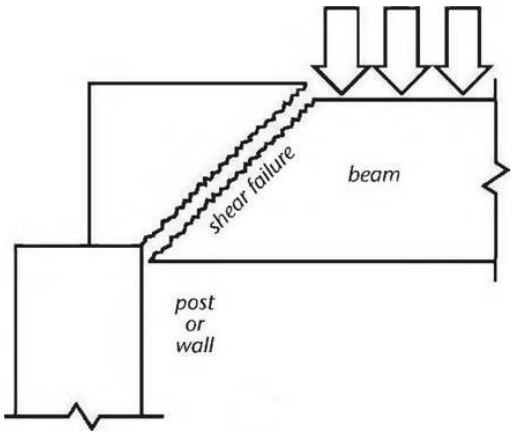


**Figure 52: shear failure of a concrete beam or wall near a support**

Shear reinforcement design is based on a truss model; a method called the variable strut inclination method according to EN 1992-1-1:2004 6.2.3. The maximum shear resistance of a member with shear reinforcement is equal to the concrete compression strut capacity:

$$V_{Rd,max} = \frac{\alpha_{cw} b z \nu_1 f_{cd}}{\cot\theta + \tan\theta} \qquad (5.04)$$

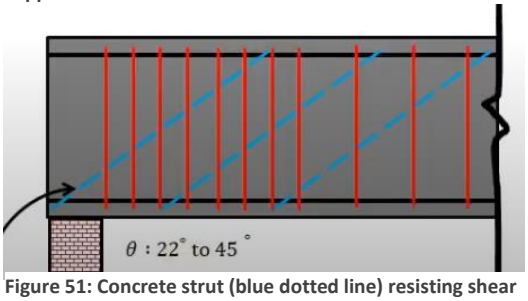


**Figure 51: Concrete strut (blue dotted line) resisting shear in compression.**

Where:

| | | |
|---|---|---|
| $\alpha_{cw}$ | [-] | Coefficient considering the shear reinforcement strength |
| $b$ | [mm] | Width of the wall segment considered, $b = 1000$ mm |
| $z$ | [mm] | lever arm between the tension and compression stresses within the element, $z = 0.9d_e = 666\,mm$ |
| $\nu_1$ | [-] | Strength reduction factor for concrete cracked in shear. $\nu_1 = \nu = 0.6\left[1 - \frac{f_{ck}}{250}\right] = 0.516$ |
| $f_{ck}$ | [MPa] | Characteristic compressive cylinder strength of concrete, $f_{ck} = 35$ MPa |
| $f_{cd}$ | [MPa] | Design value for concrete compressive strength, $f_{cd} = 23.333$ MPa |
| $\theta$ | [°] | Angle of a concrete strut. Varies from 22° to 45° |

The $\alpha_{cw}$ coefficient is dependant on the mean compressive stress in the concrete due to the design axial force, but is taken as $\alpha_{cw}$ = 1 for non-prestressed structures.

The shear resistance of a member with shear reinforcement is:

$$V_{Rd,s} = \frac{A_{sw}}{s} z f_{ywd} \cot\theta \tag{5.05}$$

Where:

| | | |
|---|---|---|
| $A_{sw}$ | [mm$^2$] | Area of shear reinforcement. Taken as the area of a single bar multiplied with the number of links over the breadth of the section, b. |
| $s$ | [mm] | Spacing of shear links |
| $f_{ywd}$ | [MPa] | Design value for the shear reinforcement yield strength, $f_{ywd} = 435$ MPa |

First the angle of the concrete strut is found by first assuming $\theta = 22°$ and calculating the concrete compressive strut capacity, $V_{Rd,max}$ using equation 5.04. If $V_{Rd,max} > V_{Ed}$ the assumption is valid, and calculations can proceed using $\theta = 22°$.

$$V_{Rd,max} = \frac{1 \cdot 1000\,mm \cdot 666\,mm \cdot 0.516 \cdot 23.333\,MPa}{\cot 22° + \tan 22°} = 2765\,kN > V_{Ed}$$

Therefore $\theta = 22°$ and $\cot\theta = 2.5$. To find the required shear reinforcement, $V_{Ed}$ is substituted for $V_{Rd,s}$ in equation 5.05 and the equation is solved for $A_{sw}/s$ (see eq. 5.06). Results of eq. 5.06 are shown in Table 23 along with information about the chosen shear reinforcement for the chamber wall around the center flood gates. As a rule of thumb, the spacing, s, shall never exceed 0.75d = 555 mm for vertical stirrups (Beeby, Narayanan, & Gulvanessian, 2015).

$$\frac{A_{sw}}{s} = \frac{V_{Ed}}{z f_{ywd} \cot\theta} \tag{5.06}$$

**Table 23: results of the equation 5.06, along with the chosen shear reinforcement for the design that fulfils the requirement.**

| ***Location*** | **$A_{sw}/s$ [mm]** | **s [mm]** | **$\emptyset_{bar}$ [mm]** | **No. arms** | **$A_{sw}$ [mm$^2$]** |
|---|---|---|---|---|---|
| *Bottom of the wall, center* | 0.91 | 360 | K10 | 5 | 392.7 |
| *Bottom of the wall, edge* | 0.69 | 360 | K8 | 5 | 251.3 |
| *Inner anchors* | 2.48 | 210 | K12 | 5 | 565.5 |
| *Anchors at the edge* | 1.84 | 210 | K10 | 5 | 392.7 |

The shear reinforcement will be from the bottom of the wall reaching over a height of 4 meters (NAP -1.2 m), 2 meters above from where the $V_{Ed} < V_{Rd,c}$ (2 m is the length of the concrete compressive strut). It will also be around the anchors over a height of 7.5 meters starting 5.5 m from the bottom of the chamber (NAP +0.3 m). The bars will overlap each other in a similar manner as depicted in Figure 53 and Figure 54.

On either end of the wall the shear will be lower due to the perpendicular lock head wall providing extra support. The same holds for the shear links around the anchors.

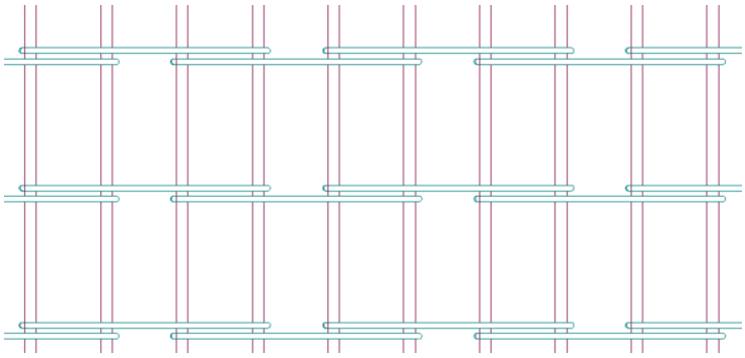

**Figure 53: depiction of how bars will overlap each other in the wall. View is of the longitudinal vertical bars and shear link spaced over the vertical**

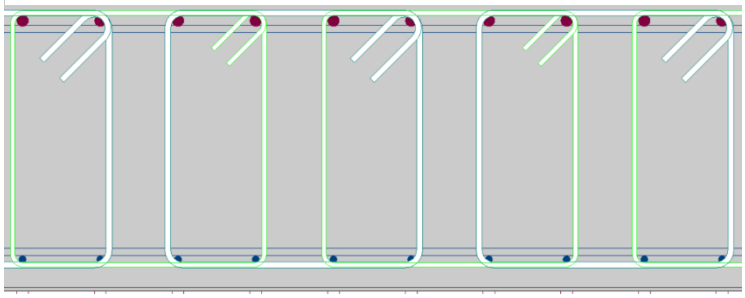

**Figure 54: top view of the shear link bars. One meter width has a minimum of 5 shear link arms within that width. The shear links loop around the vertical flexural reinforcement bars**

## *Flexural wall reinforcement*

Due to the presence of the anchors, the wall will now act as a two-way slab subjected to out-of-plane bending and will therefore have bending in x and y. Therefore, the rule of thumb to use 20% of the flexural reinforcement area in the transverse direction no longer valid. Flexural reinforcement will be designed according to EN 1992-1-1:2004, 9.6.1.

Vertical flexural reinforcement (resisting $M_{xx}$) that surpasses the minimum required reinforcement must be provided in three places over the height of the wall; at the bottom of the wall on the outer side of the chamber wall (touching the soil), around the anchors on the outer side of the chamber wall, and on the inner side of the chamber wall (wall facing inside chamber) where $M_{xx}$ is negative (see the blue region on Figure 45 and Figure 48). At other locations minimum reinforcement in the vertical direction will be provided. Horizontal flexural reinforcement (resisting $M_{yy}$) that surpasses the minimum required reinforcement must only be provided around the anchors. At other locations minimum reinforcement in the horizontal will be provided.

The effective depth of the flexural reinforcement is affected by the presence of the shear links. The effective depth for the vertical reinforcement $d_{e,y,o}$ and the horizontal reinforcement $d_{e,x,o}$ on the outer side of the wall are calculated with equation 5.07 below:

$$d_{e,y,o} = B_w - c - \emptyset_{shear} - \frac{\emptyset_y}{2} = 730\ mm$$
$$d_{e,x,o} = B_w - c - \emptyset_{shear} - \emptyset_y - \frac{\emptyset_x}{2} = 704\ mm \quad (5.07)$$

Where:

$B_w$ [mm] Width of the wall; $B_w = 800$ mm

| | | |
|---|---|---|
| $c$ | [mm] | Concrete cover. Here, $c = 42$ mm for the outer side of the wall and $c = 65$ mm for the inner side of the wall |
| $\emptyset_{shear}$ | [mm] | Largest shear reinforcement diameter, 12 mm |
| $\emptyset_y$ | [mm] | Vertical rebar diameter; $\emptyset_y = 32$ mm |
| $\emptyset_x$ | [mm] | Horizontal rebar diameter; $\emptyset_x = 20$ mm |

The effective depth for the inner side of the wall is calculated in a similar manner except for different bar diameters; $\emptyset_y$ and $\emptyset_x$, and a different concrete cover; c = 65 mm.

The reinforcement was calculated using equations 4.24, 4.25, and 4.27 with a minimum reinforcement of

$$A_{s,min} = 0.26\frac{f_{ctm}}{f_{yk}} b_t d = \mathbf{1218.5\ mm^2} \geq 0.0013 b_t d = 949\ mm^2$$

Equation 4.24 for the required reinforcement area is repeated here below:

$$A_{s1} = \frac{M_{Ed}}{f_{yd} z}$$

The results of the calculations and the chosen flexural reinforcement detailing for the optimized design that fulfils the flexural reinforcement requirement are presented in Table 24.

**Table 24: Flexural reinforcement required to resist the moments and the design reinforcement for the chamber wall around the center flood gates.**

| **Vertical reinforcement** | **$M_{xx}$ [kNm]** | **$A_{s1}$ [mm²]** | **$\emptyset_{bar}$ [mm]** | **c/c [mm]** |
|---|---|---|---|---|
| *Bottom middle; NAP -5.2 m to -3.0 m* | 1074.2 | 3560.8 | 32 | 220 |
| *Bottom edge; NAP -5.2 m to -3.0 m* | 749.8 | 2465.2 | 20 | 110 |
| *Anchor middle; NAP +3.3 m to 6.0 m* | 902.8 | 2992.6 | 32 | 220 |
| *Anchor edge; NAP +3.3 m to 6.0 m* | 621.9 | 2051.7 | 25 | 220 |
| *-$M_{xx}$ inner side of wall, middle; NAP -1.9 m to +1.9 m* | -551.3 | 1877.6 | 25 | 220 |
| *-$M_{xx}$ inner side of wall, edge; NAP -1.9 m to +1.9 m* | -374.3 | 1270.3 | 20 | 220 |
| *Minimum reinforcement* | [-] | 1218.5 | 20 | 220 |

| **Horizontal reinforcement** | **$M_{xx}$ [kNm]** | **$A_{s1}$ [mm²]** | **$\emptyset_{bar}$ [mm]** | **c/c [mm]** |
|---|---|---|---|---|
| *Around anchors; NAP* | 545.3 | 1802.6 | 20 | 170 |
| *Minimum reinforcement* | [-] | 1175.2 | 20 | 260 |

## *Floor reinforcement*

The floor slab was checked against shear to determine its thickness. The chamber lays on top of a soil and the reaction of the chamber floor is calculated via MATLAB. Like for the base case, the floor for the optimized design is modelled with the Winkler – Pasternak model; as a beam on a continuous spring support with a shear layer. Pasternak adds shear deformation in the elastic support to create horizontal linkage between the Winkler springs. The thickness of the underwater concrete floor will again represent the height of the shear layer; 0.5 m thick. the shear modulus of the sub layer is:

$$k_s = G \cdot d_{eff} = 5 \cdot 10^6 \frac{kN}{m^2} \cdot 0.5\ m = 2.5 \cdot 10^6 \frac{kN}{m}$$

The soil modulus of subgrade reaction is kept the same as for the base case where it is assumed to be similar to that of crushed stone, $k_0$ = k = 200,000 kN/m²/m. The distributed load on the floor slab of the alternative chamber design is:

$$q = -(78.43 - 50.47) = -27.96\ kN/m^2$$

The moment of inertia for the chamber slab in the optimized design is:

$$I = \frac{bt^3}{12} = \frac{1 \cdot 0.6^3}{12} = 0.018\ m^4$$

Symmetry condition is applied for the floor slab and hence only half of the slab is modelled. Four boundary conditions are applied. The floor slab is connected to the chamber wall. Therefore, the two boundary conditions at the end of the slab are an applied moment and an applied shear force from the weight of the wall. In the center of the chamber (x = 11.15) the shear force and the curvature will be 0. The boundary conditions for the floor slab at the lock head around the center flood gates are:

$$M(0) = 1074.2\ kNm$$

$$V(0) = 437.4\ kN$$

$$\varphi(L/2) = 0$$

$$V(L/2) = 0\ kN$$

The ODE presented in equation 4.18 is solved via MATLAB. The length of the whole beam (width of floor) is taken as the length between the center of gravity of the walls at the center lock head, considering the additional 2.5 m on either side of the chamber at the lock heads;

$$L = B_{ch} + 2 \cdot 2.5 + 2 \cdot \frac{t_{wall}}{2} = 22.3\ m$$

After the ODE is solved the moment and shear force can be calculated through:

$$M = EI\frac{d^2w}{dx^2}$$

$$V = EI\frac{d^3w}{dx^3}$$

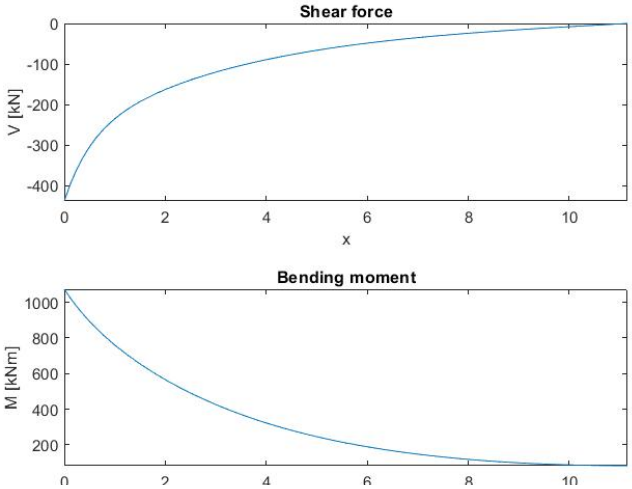


**Figure 55: Shear and moment diagrams over half of the floor at the center lock head**

The MATLAB script is shown in appendix D.1:. The resulting bending moment and shear force diagrams over half of the beam are shown in Figure 55. x = 0 is the center of gravity of the wall and therefore x=0.4 is located at the inner side of the wall. Due to length limitations of rebars and to save material, the floor will be split into 3 zones; the 1st zone is where the maximum moment occurs, from the outer edge of the wall until 2.3 meters inside the chamber measured from the inner side of the wall (x=2.7 on Figure 55), the 2nd zone is from 2.3 meters inside the chamber (x = 2.7) until 5.8 m inside the chamber (x = 6.2), and the 3rd zone spans the middle part of the chamber floor where 9800 m long bars will be placed. The maximum shear and moment for each of the zones are taken from Figure 55 and presented in Table 25:

Table 25: maximum moments and shear forces for the floor design at the center lock head of the optimized concrete chamber design

| Zone | Coordinate on Figure 55 | Maximum moment $M_{max}$ [kNm/m] | Maximum shear force $V_{max}$ [kN/m] |
|---|---|---|---|
| **1 (edges)** | 0 | 1074.2 | 437.4 |
| **2** | 2.7 | 463.7 | 130.8 |
| **3 (center)** | 6.2 | 176.5 | 44.9 |

The flexural, compression and transverse reinforcement were found in the same manner as for the walls using equations 4.24 to 4.27. The compression reinforcement at the upper edge of the slab will need three 8.58 m long bars to span the whole width of the chamber. The floor is assumed to behave in as a one-way slab and therefore the required secondary transverse reinforcement can be taken as 20% of the provided flexural reinforcement. Results of the calculations and the chosen flexural reinforcement detailing for the optimized design that fulfils the flexural reinforcement requirement are presented in Table 26 below:

Table 26: Flexural, compression and secondary transverse reinforcement required to resist the moments in the floor, and the design reinforcement for the floor at the center flood gates

| Floor reinforcement | $M_{xx}$ [kNm] | $A_{s1}$ [mm²] | $Ø_{bar}$ [mm] | c/c [mm] |
|---|---|---|---|---|
| *Flexural, bottom, zone 1 (edge)* | 1074.2 | 5274.9 | 32 | 110 |
| *Flexural, bottom, zone 2* | 463.7 | 2231.2 | 25 | 220 |
| *Flexural, bottom, zone 3 (center)* | 176.5 | 1001.5 | 20 | 220 |
| *Secondary transverse, bottom, zone 1 (edge)* | 1074.2 | 1462.3 | 16 | 130 |
| *Secondary transverse, bottom, zone 2* | 463.7 | 467.5 | 10 | 130 |
| *Secondary transverse, bottom, zone 3 (center)* | 176.5 | 299.2 | 8 | 130 |
| *Compression, top* | [-] | 1001.5 | 20 | 220 |
| *Secondary transverse, top* | [-] | 285.6 | 10 | 260 |

## *All reinforcement volumes for the optimised design*

Total reinforcement for chamber floor and walls at the center flood gates is presented in Table 27. L-bars and U-loops were provided at wall-floor connection and wall ends. The lap and anchorage lengths for C35/45 concrete is given in appendix C.2.2:. The reinforcement detailing and quantities for the whole alternative anchor design is given in appendix D.2:.

Table 27: Total reinforcement for the chamber walls and floor at the lock head around the center flood gates. The table depicts the length of each bar, diameter, volume of a single bar, number of bars in the horizontal direction, number of bars in the vertical direction, center-to-center distance of the bars, number of walls, total number of bars in the whole chamber design and total volume of bars.

| ***Shear reinforcement*** | ***L [mm]*** | ***Ø [mm]*** | ***volume [m³]*** | ***no. bars horiz.*** | ***no. bars y*** | ***c/c [mm]*** | **no. Walls** | ***tot bars*** | ***tot volume [m³]*** |
|---|---|---|---|---|---|---|---|---|---|
| *Shear bot middle 690x690* | 2975 | 10 | 0.0002 | 39 | 12 | 360 | 2 | 936 | 0.22 |
| *Shear bot edge 675x690* | 2925 | 8 | 0.0001 | 12 | 12 | 360 | 2 | 288 | 0.04 |
| *Shear anch. Middle 690x690* | 3025 | 12 | 0.0003 | 39 | 36 | 210 | 2 | 2808 | 0.96 |
| *Shear anch edge 675x690* | 2950 | 10 | 0.0002 | 12 | 36 | 210 | 2 | 864 | 0.20 |
| ***Vertical bars (Mxx)*** | | | | | | | | | |
| *tension bottom L-bar 3000x1720, S* | 4650 | 32 | 0.0037 | 75 | 1 | 220 | 2 | 150 | 0.56 |
| *tension anchor, S* | 2800 | 32 | 0.0023 | 75 | 1 | 220 | 2 | 150 | 0.34 |
| *tens cent. (-Mxx), C* | 3800 | 25 | 0.0019 | 75 | 1 | 220 | 2 | 150 | 0.28 |
| *betw. bottom & anchor S* | 8300 | 20 | 0.0026 | 75 | 1 | 220 | 2 | 150 | 0.39 |
| *from anchor to top S* | 5700 | 20 | 0.0018 | 75 | 1 | 220 | 2 | 150 | 0.27 |
| *from bottom to center, C* | 4200 | 20 | 0.0013 | 75 | 1 | 220 | 2 | 150 | 0.20 |
| *from center to top, C* | 10000 | 20 | 0.0031 | 75 | 1 | 220 | 2 | 150 | 0.47 |

| | | | | | | | | | |
|---|---|---|---|---|---|---|---|---|---|
| *tension bottom edges, S* | 2200 | 20 | 0.0007 | 50 | 1 | 110 | 2 | 100 | 0.07 |
| *tension anchor edges, S* | 2800 | 25 | 0.0014 | 25 | 1 | 220 | 2 | 50 | 0.07 |
| *betw. bottom & anchor edges, S* | 8100 | 20 | 0.0025 | 25 | 1 | 220 | 2 | 50 | 0.13 |
| *from anchor to top edges, S* | 5550 | 20 | 0.0017 | 25 | 1 | 220 | 2 | 50 | 0.09 |
| *from bottom to center, C* | 7050 | 20 | 0.0022 | 19 | 1 | 220 | 2 | 38 | 0.08 |
| *from center to top, C* | 10000 | 20 | 0.0031 | 19 | 1 | 220 | 2 | 38 | 0.12 |
| ***Horizontal bars (Myy)*** | | | | | | | | | |
| *tension anchor, S* | 7950 | 20 | 0.0025 | 3 | 11 | 170 | 2 | 66 | 0.16 |
| *from bottom to anchor, S* | 7950 | 20 | 0.0025 | 3 | 34 | 260 | 2 | 204 | 0.51 |
| *from anchor to top S* | 7950 | 20 | 0.0025 | 3 | 22 | 260 | 2 | 132 | 0.33 |
| *from bottom to top, C* | 7460 | 20 | 0.0023 | 3 | 62 | 260 | 2 | 372 | 0.87 |
| ***Floor*** | ***L [mm]*** | ***Ø [mm]*** | ***volume [m³]*** | ***no. bars z*** | ***no. bars x*** | ***c/c [mm]*** | **no. walls/ floors** | ***tot bars*** | ***tot volume [m³]*** |
| *tension bottom edge* | 4400 | 32 | 0.0035 | 2 | 201 | 110 | 1 | 402 | 1.42 |
| *tens. bottom betw. edge & center* | 4400 | 25 | 0.0022 | 2 | 101 | 220 | 1 | 202 | 0.44 |
| *tension bottom center* | 9800 | 20 | 0.0031 | 1 | 101 | 220 | 1 | 101 | 0.31 |
| *transverse Bottom edge* | 7680 | 12 | 0.0009 | 42 | 3 | 130 | 1 | 126 | 0.11 |
| *transv. bottom betw. edge & center* | 7610 | 10 | 0.0006 | 74 | 3 | 130 | 1 | 222 | 0.13 |
| *transverse bottom center* | 7550 | 8 | 0.0004 | 61 | 3 | 130 | 1 | 183 | 0.07 |
| *compression top* | 8580 | 20 | 0.0027 | 3 | 101 | 220 | 1 | 303 | 0.82 |
| *compression top transverse* | 7610 | 10 | 0.0006 | 89 | 3 | 260 | 1 | 267 | 0.16 |
| ***U-bars, L bars and anchor bars*** | | | | | | | | | |
| *U-loops top 1100x670x1100* | 2800 | 20 | 0.0009 | 1 | 94 | 220 | 2 | 188 | 0.17 |
| *U-loops top - anchors* | 8100 | 25 | 0.0040 | 2 | 3 | [-] | 2 | 12 | 0.05 |
| *U-loop floor 1490x684x1070* | 3150 | 20 | 0.0010 | 1 | 100 | 220 | 2 | 200 | 0.20 |
| *L-bar bottom edges 1760x180* | 2800 | 20 | 0.0009 | 1 | 25 | 220 | 2 | 50 | 0.04 |
| *J-bar bottom-C 1800x664x290* | 2650 | 20 | 0.0008 | 1 | 94 | 220 | 2 | 188 | 0.16 |
| *K32 anchor bottom* | 8110 | 32 | 0.0065 | 1 | 3 | [-] | 2 | 6 | 0.04 |
| *K25 anchor bottom* | 8100 | 25 | 0.0040 | 2 | 3 | [-] | 2 | 12 | 0.05 |

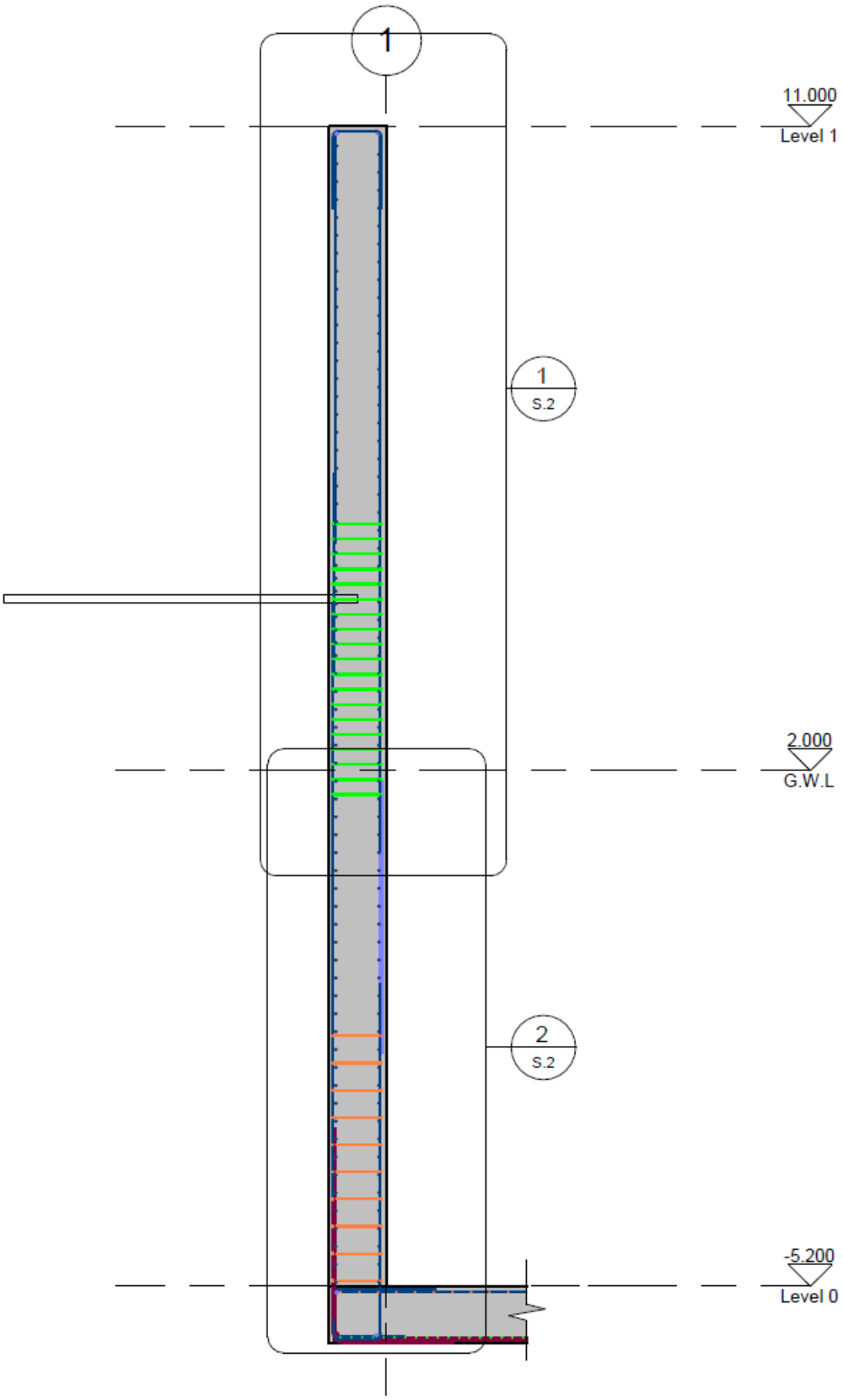


0 Chamber wall flood gates

1 : 75

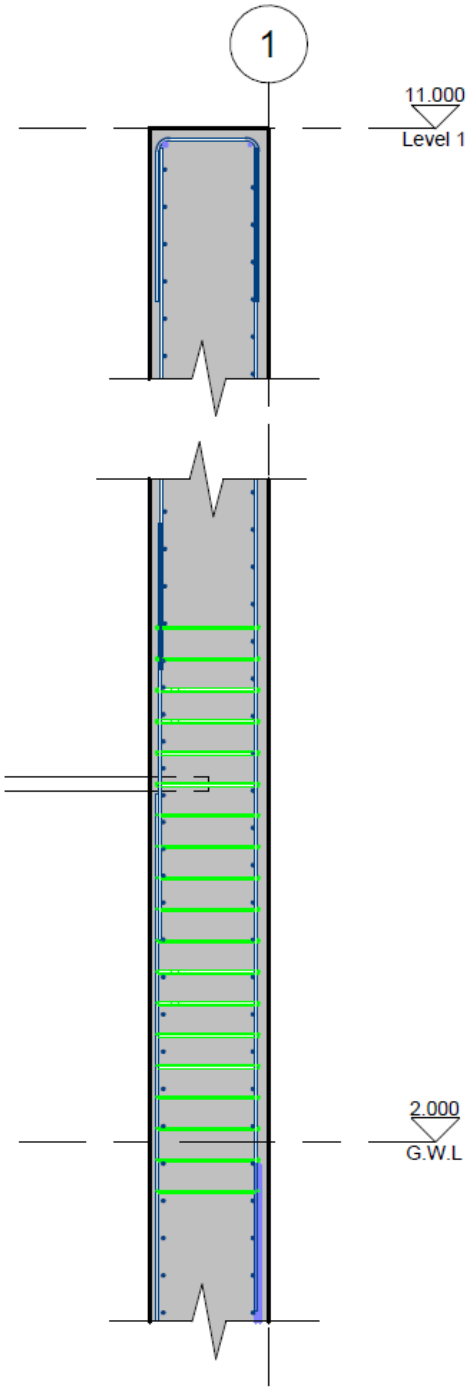


1 Magnified 1
1 : 40

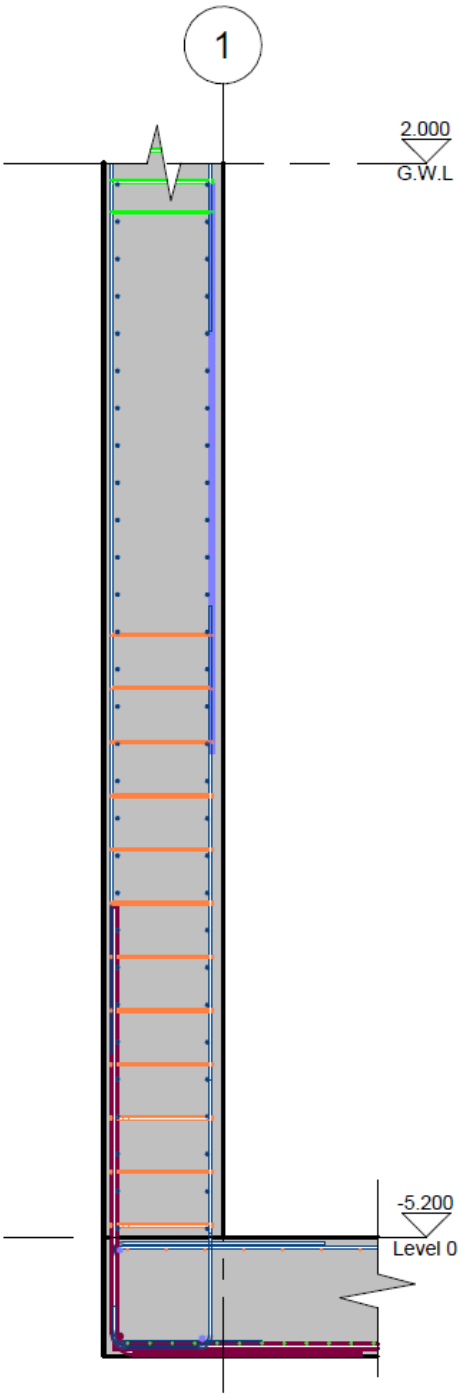


2 Magnified 2
1 : 40

## *Anchors*

To reduce the maximum moments and shear forces the concrete wall in the optimized design will be anchored with plated steel rod anchors. The anchors must provide sufficient design resistance to satisfy the design load; the reaction force. In reality the design load will be a bit lower than the reaction force gotten from the Diana models. This is because in the Diana models the anchors are modelled as supports restricting out-of-plane movement, but in reality, the soil will compress and settle a bit and therefore the design load will be a bit smaller.

An anchors length is split into three parts; the anchor head, unbonded length and bond length. The unbonded anchor length is determined by the potential failure plane. The potential failure plane of soil is determined with the angle of internal friction of the soil, $\varphi'$. In the design for the lock chamber wall, it is $\varphi' = 30°$. The angle of internal friction is an empirical shear strength parameter. The unbonded length transfers the loads behind the predicted failure plane of the soil and helps minimize the load loss due to movement at the anchor head (Sabatini, Pass, & Bachus, 1999). Figure 56 shows a grout anchor where the dotted line is the potential failure surface. The angle between the dotted line and the retaining wall is:

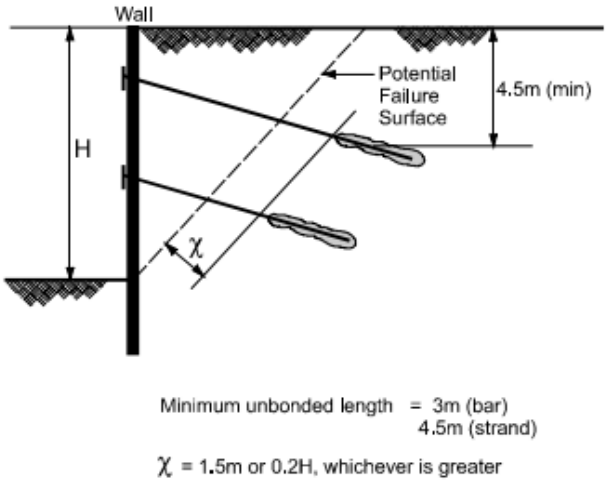


**Figure 56: grout anchor reaching past the potential failure surface**

$$\alpha = 45° - \varphi'/2$$

The unbonded length is extended a minimum distance of $\chi = \min(1.5m, 0.2H)$ beyond the critical potential failure plane. This extra length is provided to accommodate minor load transfer to the anchor above the top of the anchor bond zone. The minimum height of 4.5 m to the surface, shown on the figure, is not required for a plated anchor. This height must be provided for a grouted anchor to prevent grout leakage and is therefore not relevant here.

For the design of the concrete chamber wall, a vertical plate anchor will be installed, consisting of a tie rod and an end plate resisting pull out. These type of anchors can be split into two types; a deep anchor where H/D > 5 and a shallow anchor where H/D ≤ 5. Here H is the depth of the anchor measured from above and D is the height of the end blade on the anchor. At the center lock head, the anchors are positioned 6.1 m below the soil surface and the anchor blade is assumed to have D = 900 mm resulting in $H/D = 6.8$. The length of a deep anchor can be found by using the figure above as a reference for the unbonded length:

$$L_{anchor} = \frac{H_{anchor}}{\cos(45° - \varphi'/2)} + t_{wall} + t_{blade} + t_{fast.plate} + 2h_{nut} \approx 9800\ mm \qquad (5.08)$$

Where:

| | | |
|---|---|---|
| $H_{anchor}$ | [mm] | Height from the bottom of the chamber up to the anchor positioning. 9.6 m for the anchors at the center lock head |
| $t_{wall}$ | [mm] | Thickness of the wall, here $t_{wall} = 0.8$ m |
| $t_{blade}$ | [mm] | Thickness of the end blade on the anchor. Here assumed to be 12 mm |
| $t_{fast.plate}$ | [mm] | Thickness of the fastening plate at the concrete wall. Here assumed to be 20 mm |
| $h_{nut}$ | [mm] | Height of a fastening nut |

The fastening plate will be vulnerable as it is subjected to a very aggressive environment. Therefore, its thickness is taken as 20 mm. $h_{nut}$ is the height of the fastening nut here taken as 90 mm (fitting a M110 nut profile).

The end plate size is chosen using Hergarden's research on the grip force of a deep screw anchor in sandy ground (Voorendt & Molenaar, 2020). He found a relation between the anchor force and the cone resistance in the area of the anchor:

$$F_{r,A,scr,min} = 0.4 \cdot A \cdot q_{c,avg} \geq F_{s,A,d} \quad (5.09)$$

Where:

| | | |
|---|---|---|
| $F_{r,A,scr,min}$ | [kN] | Minimum grip force of the anchor |
| $A$ | [m²] | Anchor blade area |
| $q_{c,avg}$ | [kPa] | Average cone resistance in the area of influence, 3D above and below the anchor's axis |
| $F_{s,A,d}$ | [kN] | Design value for the maximum anchor force that can be resisted |

The average cone resistance has to be chosen here as the earth surrounding the chamber will be made from landfill. It is chosen using Schmertmann's soil profiling chart, as a densely packed sand with a cone resistance of 10000 kPa (see Figure 57Figure 57) (Schmertmann, 1978). Therefore $q_{c,avg}$ is taken as 10000 kPa. The minimum grip force of the anchor must be equal to or larger than the reaction force that the anchor must resist. At the center lock head two different reaction forces occur; at the edge anchors and for the inner anchors. The end blade minimum area for both anchor types are:

$$A_{min,edge} = \frac{1815.8\ kN}{0.4 \cdot 10000\ kPa} = 0.454\ m^2$$

$$A_{min,inner} = \frac{2612.4\ kN}{0.4 \cdot 10000\ kPa} = 0.653\ m^2$$

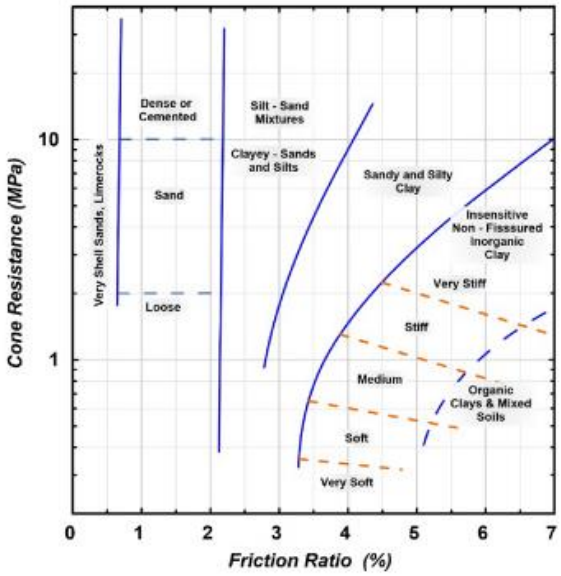


**Figure 57: Schmertmann's soil profiling chart**

ASDO anchors for marine structures were chosen for the optimized chamber design. They are round steel bars with forged or threaded ends with diameters that range from M64 to M170 and they are supplied in four different steel grades; S355, S460, S500 and S700 (ASDO, 2015).

Chemical composition and processing procedure determine the strength and toughness of steel. Easiest way to improve steel strength is to increase carbon content. However, increasing the carbon content reduces toughness (stiffness), formability and weldability. With increasing steel strength, the ratio of ultimate strength to yield strength decreases. High strength steel will produce a lighter product but might not be suitable for stiffness requirements and on-site welding. The stiffness of an anchor is also of importance in SLS especially if large vertical loads are applied on top of the soil. It is a function of the shaft diameter and therefore the higher strength steel might result in a diameter that is not stiff enough. In this design no large vertical loads are expected on top of the soil other than the 20 kN/m². Therefore, the higher strength steels will be permitted for the anchors as long as it will have approximately the same diameter as the anchors that have a smaller design load such as those along the lowest wall segment on the seaside of the lock. The anchor diameters were gotten from table 2 in the ASDO Anchors for marine structures manual. This table is repeated here below as Table 28.

**Table 28: Anchors with upset forged threads**

**ASDO460 – Tensile resistance (EN1993-5)**

| | | | | | | | | | | | | | | | |
|---|---|---|---|---|---|---|---|---|---|---|---|---|---|---|---|
| ASDO460 | $k_t$ = 0.6 | Anchor code | | ASDO460 - | M64/48 | M68/52 | M72/52 | M76/56 | M80/60 | M85/64 | M90/68 | M95/72 | M100/76 | M105/80 | M110/85 | M115/90 |
| | | Optimum shaft diameter | $Ød_s$ | mm | 48 | 52 | 52 | 56 | 60 | 64 | 68 | 72 | 76 | 80 | 85 | 90 |
| | | Shaft gross area | $A_s$ | mm² | 1,810 | 2,124 | 2,124 | 2,463 | 2,827 | 3,217 | 3,632 | 4,072 | 4,536 | 5,027 | 5,675 | 6,362 |
| | | Shaft yield capacity | $F_y$ | kN | 832 | 977 | 977 | 1,133 | 1,301 | 1,480 | 1,671 | 1,873 | 2,087 | 2,312 | 2,610 | 2,926 |
| | | Shaft ultimate capacity | $F_{us}$ | kN | 1,104 | 1,295 | 1,295 | 1,502 | 1,725 | 1,962 | 2,215 | 2,484 | 2,767 | 3,066 | 3,461 | 3,881 |
| | | Tensile resistance | $F_{t,Rd}$ | kN | 784 | 895 | 977 | 1,133 | 1,272 | 1,449 | 1,637 | 1,837 | 2,048 | 2,271 | 2,505 | 2,751 |
| | $k_t$ = 0.9 | Anchor code | | ASDO460 - | M64/56 | M68/60 | M72/64 | M76/68 | M80/72 | M85/76 | M90/80 | M95/85 | M100/90 | M105/95 | M110/100 | M115/105 |
| | | Optimum shaft diameter | $Ød_s$ | mm | 56 | 60 | 64 | 68 | 72 | 76 | 80 | 85 | 90 | 95 | 100 | 105 |
| | | Shaft gross area | $A_s$ | mm² | 2,463 | 2,827 | 3,217 | 3,632 | 4,072 | 4,536 | 5,027 | 5,675 | 6,362 | 7,088 | 7,854 | 8,659 |
| | | Shaft yield capacity | $F_y$ | kN | 1,133 | 1,301 | 1,480 | 1,671 | 1,873 | 2,087 | 2,312 | 2,610 | 2,926 | 3,261 | 3,613 | 3,983 |
| | | Shaft ultimate capacity | $F_{us}$ | kN | 1,502 | 1,725 | 1,962 | 2,215 | 2,484 | 2,767 | 3,066 | 3,461 | 3,881 | 4,324 | 4,791 | 5,282 |
| | | Tensile resistance | $F_{t,Rd}$ | kN | 1,133 | 1,272 | 1,449 | 1,637 | 1,837 | 2,048 | 2,271 | 2,505 | 2,926 | 3,261 | 3,557 | 3,849 |

**ASDO500 – Tensile resistance (EN1993-5)**

| | | | | | | | | | | | | | | | |
|---|---|---|---|---|---|---|---|---|---|---|---|---|---|---|---|
| ASDO500 | $k_t$ = 0.6 | Anchor code | | ASDO500 - | M64/48 | M68/52 | M72/52 | M76/56 | M80/60 | M85/64 | M90/68 | M95/72 | M100/76 | M105/80 | M110/85 | M115/90 |
| | | Optimum shaft diameter | $Ød_s$ | mm | 48 | 52 | 52 | 56 | 60 | 64 | 68 | 72 | 76 | 80 | 85 | 90 |
| | | Shaft gross area | $A_s$ | mm² | 1,810 | 2,124 | 2,124 | 2,463 | 2,827 | 3,117 | 3,632 | 4,072 | 4,536 | 5,027 | 5,675 | 6,362 |
| | | Shaft yield capacity | $F_y$ | kN | 905 | 1,062 | 1,062 | 1,232 | 1,414 | 1,559 | 1,816 | 2,036 | 2,268 | 2,513 | 2,837 | 3,181 |
| | | Shaft ultimate capacity | $F_{us}$ | kN | 1,194 | 1,402 | 1,402 | 1,626 | 1,866 | 2,057 | 2,397 | 2,687 | 2,994 | 3,318 | 3,745 | 4,199 |
| | | Tensile resistance | $F_{t,Rd}$ | kN | 848 | 968 | 1,062 | 1,232 | 1,376 | 1,559 | 1,771 | 1,987 | 2,216 | 2,457 | 2,710 | 2,976 |
| | $k_t$ = 0.9 | Anchor code | | ASDO500 - | M64/56 | M68/60 | M72/64 | M76/68 | M80/72 | M85/76 | M90/80 | M95/85 | M100/90 | M105/95 | M110/100 | M115/105 |
| | | Optimum shaft diameter | $Ød_s$ | mm | 56 | 60 | 64 | 68 | 72 | 76 | 80 | 85 | 90 | 95 | 100 | 105 |
| | | Shaft gross area | $A_s$ | mm² | 2,463 | 2,827 | 3,217 | 3,632 | 4,072 | 4,536 | 5,027 | 5,675 | 6,362 | 7,088 | 7,854 | 8,659 |
| | | Shaft yield capacity | $F_y$ | kN | 1,232 | 1,414 | 1,608 | 1,816 | 2,036 | 2,268 | 2,513 | 2,837 | 3,181 | 3,544 | 3,927 | 4,330 |
| | | Shaft ultimate capacity | $F_{us}$ | kN | 1,626 | 1,866 | 2,123 | 2,397 | 2,687 | 2,994 | 3,318 | 3,745 | 4,199 | 4,678 | 5,184 | 5,715 |
| | | Tensile resistance | $F_{t,Rd}$ | kN | 1,232 | 1,376 | 1,567 | 1,771 | 1,987 | 2,216 | 2,457 | 2,710 | 3,181 | 3,544 | 3,849 | 4,164 |

**ASDO700 – Tensile resistance (EN1993-5)**

| | | | | | | | | | | | | | | | |
|---|---|---|---|---|---|---|---|---|---|---|---|---|---|---|---|
| ASDO700 | $k_t$ = 0.6 | Anchor code | | ASDO700 - | M64/48 | M68/52 | M72/52 | M76/56 | M80/60 | M85/64 | M90/68 | M95/72 | M100/76 | M105/80 | M110/85 | M115/85 |
| | | Optimum shaft diameter | $Ød_s$ | mm | 48 | 52 | 52 | 56 | 60 | 64 | 68 | 72 | 76 | 80 | 85 | 85 |
| | | Shaft gross area | $A_s$ | mm² | 1,810 | 2,124 | 2,124 | 2,463 | 2,827 | 3,217 | 3,632 | 4,072 | 4,536 | 5,027 | 5,675 | 5,675 |
| | | Shaft yield capacity | $F_y$ | kN | 1,267 | 1,487 | 1,487 | 1,724 | 1,979 | 2,252 | 2,542 | 2,850 | 3,176 | 3,519 | 3,972 | 3,972 |
| | | Shaft ultimate capacity | $F_{us}$ | kN | 1,629 | 1,911 | 1,911 | 2,217 | 2,545 | 2,895 | 3,269 | 3,664 | 4,083 | 4,524 | 5,107 | 5,107 |
| | | Tensile resistance | $F_{t,Rd}$ | kN | 1,156 | 1,320 | 1,487 | 1,680 | 1,877 | 2,137 | 2,415 | 2,710 | 3,022 | 3,350 | 3,696 | 3,972 |
| | $k_t$ = 0.9 | Anchor code | | ASDO700 - | M64/56 | M68/60 | M72/64 | M76/68 | M80/72 | M85/76 | M90/80 | M95/85 | M100/90 | M105/95 | M110/100 | M115/105 |
| | | Optimum shaft diameter | $Ød_s$ | mm | 56 | 60 | 64 | 68 | 72 | 76 | 80 | 85 | 90 | 95 | 100 | 105 |
| | | Shaft gross area | $A_s$ | mm² | 2,463 | 2,827 | 3,217 | 3,632 | 4,072 | 4,536 | 5,027 | 5,675 | 6,362 | 7,088 | 7,854 | 8,659 |
| | | Shaft yield capacity | $F_y$ | kN | 1,724 | 1,979 | 2,252 | 2,542 | 2,850 | 3,176 | 3,519 | 3,972 | 4,453 | 4,962 | 5,498 | 6,061 |
| | | Shaft ultimate capacity | $F_{us}$ | kN | 2,217 | 2,545 | 2,895 | 3,269 | 3,664 | 4,083 | 4,524 | 5,107 | 5,726 | 6,379 | 7,069 | 7,793 |
| | | Tensile resistance | $F_{t,Rd}$ | kN | 1,680 | 1,877 | 2,137 | 2,415 | 2,710 | 3,022 | 3,350 | 3,972 | 4,438 | 4,835 | 5,248 | 6,061 |

A conservative $k_t$ reduction factor of 0.6 should be used when determining the anchor diameter unless structural detailing at the connection eliminated any possible bending. To fully eliminate bending is very difficult to achieve at typical site conditions (ASDO, 2015). Therefore, the chosen anchors refer to the rows where $k_t = 0.6$.

The concrete lock chamber is a marine structure and therefore it operates in an aggressive environment where protection against corrosion is of a high importance. Therefore, a robust protection system for the anchors is key to their longevity. Corrosion protection can be provided in Three different ways;

- Sacrificial steel: The corrosion estimate in mm of steel over the lifetime of the structure is added to the anchor shaft and thread size diameters this increase in diameter is not considered when calculating the resistance of the steel anchor as it is expected to corrode away over the lifetime of the structure. ASDO provides a table giving corrosion allowances for steel anchors for up to a 100-year lifetime. The increment between different life longevities is linear and therefore the corrosion allowance for steel anchors with a 150 year lifetime will be the values given in the table for 100 year lifetime and a 50 year lifetime, e.g. 7.5 mm + 3.75 mm ≈ 12 mm. this sacrificial steel is in accordance to an environment with sea water in temperate climate in the zone of high attack.
- Wrapping systems: The anchors are protected by wrapping them in a protective barrier such as petrolatum tape. The downside to this corrosion protection is that the connections cannot be wrapped until being installed at site, e.g. it cannot be fully protected until installation, and this can often be difficult to achieve in site conditions and can increase installation time considerably. Therefore, this corrosion protection will not be chosen for the design as it is difficult to guarantee a correctly wrapped anchor head.
- Galvanising: S355, S460 and S500 bars can be hot dip galvanised. Since a few anchors in the design are from S700 steel, this corrosion protection will not be chosen for the design.

The anchors for the whole chamber were chosen through Table 28 and are presented in Table 29 below. 12 mm have been added to the shaft diameter for corrosion protection:

**Table 29: Details about the anchors chosen for the optimized chamber design showing the total volume of each anchor type.**

| position | no. | no. Walls | Length [mm] | strength grade | Type | $Ø_{shaft}$ [mm] | $A_{s,gross}$ [mm2] | $F_{Ed}$ [kN] | $F_{t,Rd}$ [kN] | total volume [m3] |
|---|---|---|---|---|---|---|---|---|---|---|
| *Inner anchors center lock head* | 5 | 2 | 9800 | S700 | M95/72 | 84 | 5542 | 2612.4 | 2710 | 0.543 |
| *edge anchors center lock head* | 2 | 2 | 9800 | S460 | M95/72 | 84 | 5542 | 1815.8 | 1837 | 0.217 |
| *1st anchor top of slope* | 1 | 4 | 10000 | S500 | M105/80 | 92 | 6648 | 2299.1 | 2457 | 0.266 |
| *2nd anchor slope* | 1 | 4 | 9600 | S700 | M115/85 | 97 | 7390 | 3702.3 | 3972 | 0.284 |
| *3rd anchor slope* | 1 | 4 | 9200 | S700 | M110/85 | 97 | 7390 | 3401.4 | 3696 | 0.272 |
| *4th anchor slope* | 1 | 4 | 8800 | S460 | M110/85 | 97 | 7390 | 2465.2 | 2502 | 0.260 |
| *5th anchor slope* | 1 | 4 | 8500 | S460 | M90/68 | 80 | 5027 | 1466.1 | 1637 | 0.171 |
| *6th anchor slope* | 1 | 4 | 8400 | S460 | M85/64 | 76 | 4537 | 1274.6 | 1449 | 0.152 |
| *7th anchor bottom of slope* | 1 | 4 | 9000 | S460 | M90/68 | 80 | 5027 | 1532.3 | 1637 | 0.181 |
| *Low wall on river and seaside* | 18 | 4 | 8200 | S460 | M95/72 | 84 | 5542 | 1659.2 | 1837 | 3.272 |

## 6.4. Design Results

In this sub chapter design results of the two concrete chamber alternatives are compared.

For the base case design the concrete chamber was designed as a semi-gravity u-basin structure with a tapered wall design and no shear reinforcement. To minimise material use, the height of the chamber wall along the slope of the dike was decreased in steps of 0.5 m.

The alternative anchored wall chamber design of the concrete chamber was designed as a shear reinforced anchored wall u-basin structure. The wall height decreased gradually along the dike slope at a 1:3 angle. The chamber width was 16.5 m; 0.5 m greater than for the base case chamber width. This was to ensure the same ship-wall clearance for both structures as the anchors will protrude into the chamber to be fastened. For the first 50 year of the lifetime of the structure, the wall height of the seaside chamber for the optimised design will be equal to the riverside chamber wall height of 9.7 m. the wall height will be increased by 2.5 m in the year 2150, making it the same height as the base case chamber wall on the seaside. This was done to allow for more flexibility of the design. The full wall height of 12.2 m is not necessary for the entire lifetime of the structure. Constructing it in parts will therefore minimise material use and allow for more flexibility in the design and more detail as the SLR will be better predicted in the year 2150 for the year 2250.

For the base case chamber wall at the center lock head the maximum moment and shear force at the bottom of the wall was:

$$M_{max,b} = 9385.5\ kNm$$

$$V_{max,b} = 1524.9\ kN$$

For the alternative chamber wall design at the center lock head the maximum moment and shear force at the bottom of the wall was:

$$M_{max,a} = 1074.2\ kNm$$

$$V_{max,a} = 658.8\ kN$$

The subscripts b and o represent the base case design and the optimised design respectively. This is a reduction in maximum moment of 88% and a reduction in maximum shear force at the bottom of the structure of 56%

Concrete and reinforcement volumes along with the reinforcement-concrete ratio for both design alternatives are presented in Table 30.

**Table 30: Concrete and reinforcement volumes for the two design alternatives**

| | $V_{concrete}$ [$m^3$] | $V_{rebar}$ [$m^3$] | Rebar-reinf. Ratio [%] |
|---|---|---|---|
| **Base case structure** | 11083.48 | 122.32 | 1.1 |
| **Optimised structure** | 6145.75 | 56.32 | 1.1 |

The concrete volume in the optimised structure was reduced by 47% compared to the base case and the reinforcement volume was reduced by 46%.

# 7. Results: Life Cycle Assessment of the Two Chamber Designs

As mentioned in Chapter 2.2.1, a partial LCA for the concrete ship lock includes life cycle stages A1 – A4 ("cradle to gate"), C1-C4 and D (end of life). The first step of an LCA is to conduct an inventory analysis which is presented in chapter 7.1. This includes both a bill of materials and research into suitable environmental product declarations (EPDs). To estimate the carbon footprint of the two chamber alternatives, the global warming potential (GWP)of each material type used in the structures is acquired from the EPDs. Using this information along with all material quantities, the total GWP is calculated. The results are presented in chapter 7.2.

Stages A1 – A4 represent the product stage and include manufacturing of the raw material used in the production and fuels used by machines at the manufacturing facilities as well as transport of the raw material to the manufacturing facilities. Stage A4 is the transport of the product to the site. Stage 4 must be included to make an informed decision for the choice of EPD. Stages C1 – C4 and D will also be investigated as this has to do with the end of life of the construction. Life cycle stages C1 to C4 are the end-of-life stages; Demolition of construction, transport, waste processing and disposal of materials. Stage D represents the re-use, recovery and recycling potential. Stage C1: Dismantling of reinforced concrete structures, is usually carried out with a long-front excavator with attachments like concrete crushers, multi jaw demolition tool and more. They crush the concrete by applying compressive force. Stage C2: transport, includes the transport of coarse concrete demolition material to the concrete crushing plant. Stage C3: waste processing, includes the pre-screening of the concrete and metal separation. By doing so the material that is disposed of into landfills can be minimized. In 2010 only 4.1% of mineral construction waste ended up in landfills. Therefore, Stage C4 is not included for the concrete used in the chamber designs. For stage D the demolished crushed concrete can replace primary materials in concrete mixes (sand/gravel and crushed stone) as secondary materials. Crushed concrete is mainly re-used in road constructions. Life-cycle stages B1-B5 (use-stage) were not included in the study as its aim was to find a structural design path that minimizes the carbon footprint of the structure. For the use stages more information about the number of lock operations and damages that could occur during use stage needs to be known. This will have an effect on the total GWP over the whole life cycle of structure, however as both design alternatives will serve the same purpose the GWP for the use stage of the structures will be the same.

The LCA will provide a $CO_2$-eq/year value (amount of carbon dioxide released over the considered life cycle stages, divided by the lifecycle of the relating structural component) using the total global warming potential ($GWP_{tot}$) indicators measured in kg $CO_2$-eq/100 years (eq = equivalent). Global warming impact is due to many contributors. Greenhouse gasses (GHG's) are transparent towards short-wave radiation but not towards long-wave radiation. This results in them allowing sun radiation to penetrate through the atmosphere but blocking infrared radiation from leaving the atmosphere, e.g. it acts like an insulating blanket, trapping heat on Earth. GWP measures the amount of energy that will be absorbed over a period of time with the emission of 1 ton of gas. This time period is usually 100 years. The unit of measure for GWP is $CO_2$-eq and can therefore be used to easily compare the global warming impacts of different GHGs. A large GWP value for a certain GHG indicates how much more that specific gas has contributed to global warming compared to $CO_2$. For example, as $CO_2$ is the gas that is used as a reference and thus it always has a GWP of 1. On the other hand, nitrous oxide ($N_2O$) has a GWP of 296 times that of $CO_2$ for a 100 year timescale, meaning that a kilo of $N_2O$ emissions absorbs the same amount of energy as 296 kilos of $CO_2$ emissions do. The total global warming potential is the added-up emission estimates of all the different GHGs (US EPA, 2023). The equivalent $CO_2$ emissions for different GHG's are presented in Table 31 below:

Table 31: Equivalent $CO_2$ emissions for different greenhouse gas emissions

| Greenhouse gas | GWP indicators/ 100 years |
|---|---|
| *Carbon dioxide [$CO_2$]* | 1 |
| *Methane [$CH_4$]* | 23 |
| *Nitrous oxide [$N_2O$]* | 296 |
| *Hydrofluorocarbons [HFC-23]* | 12000 |
| *Perfluoromethane [$CF_4$]* | 5700 |
| *Sulphur hexafluoride [$SF_6$]* | 22200 |

In this study the structure as a whole (initial ship passage and the later ship lock) has a design lifetime of 200 years. Therefore, the $GWP_{tot}$ gotten from EPDs used in this study must be multiplied with a factor if it goes over the 100-year time period that the GWP is measured over. E.g. the center lock head and the sloped walls on either side of it must be multiplied with 2 (lifetime of 200 years), and the low chamber walls before (before the increment in 2150) must be multiplied with the factor of 1.5 (lifetime of 150 years, 2100-2250)

The volume of concrete for each concrete class used in the two designs and the weight of steel have been quantified in Chapter 5.1 and 6.1.4 and are used in the inventory analysis. Product emissions are calculated from life cycle inventory data extracted from concrete and steel manufacturers reports from a life cycle inventory (LCI) database called EnvironDec and other data bases. Environmental product declaration (EPD) can be accessed through the LCI databases. It is a third-party verified document by the manufacturers that shows the environmental impact of their product using LCA (Ecomatters, 2024). Stages

## 7.1. Inventory Analysis

Results from the inventory analysis for both chamber designs are presented in this section. This includes EPDs for different materials for life cycle stages A1-A3 and elements that are used in the designed concrete chambers and a bill of materials.

### 7.1.1. Environmental Product Declarations

**Concrete**

Three different types of concrete were used in the designs. The base case is a semi-gravity structure constructed out of C50/60 concrete. Four different EPDs from different manufacturers were investigated and the results are presented in Table 32. All of the EPDs for concrete had the declared unit of 1 $m^3$. The table includes the manufacturers name and location to be able to calculate the total GWP for the concrete. For A4 the EPD's assume that the transport distance is 10 km with an 8 $m^3$ truck, and $GWP_{tot,A4,site}$ represents the total GWP for transporting 1 $m^3$ of concrete to the construction site. For the GWP for stage A4 for the concrete manufactured by KP Betong AB the value given in the EPD report is for trucks with a capacity of 6 $m^3$ and the value given in Table 32 has been adjusted for trucks with 8 $m^3$ capacity.

Table 32: Environmental impact data on the GWP for C50/60 concrete including the total energy use for life cycle stages A1 – A3. Declared unit of 1 $m^3$ unless otherwise specified and GWP for a 100 year time period.

| | location | Distance [km] | $GWP_{tot,A1-A3}$ [kg $CO_2$-eq] | Total energy use [kWh] | $GWP_{tot,A4}$ [kg $CO_2$-eq/8 $m^3$] | $GWP_{tot,A4,site}$ [kg $CO_2$-eq/$m^3$] |
|---|---|---|---|---|---|---|
| *London Concrete Pumping (Dear & Dalipi, 2022)* | London, UK | 435 | $3.73 \cdot 10^2$ | 529.0 | 3.98 | $2.16 \cdot 10^1$ |
| *Interbeton (Martha, 2022)* | Athenes, GR | 2911 | $3.09 \cdot 10^2$ | 330.6 | 2.07 | $7.53 \cdot 10^1$ |
| *KP Betong AB (Rinse & During, 2022)* | Arlöv, SE | 923 | $4.02 \cdot 10^2$ | 559.2 | 2.54 | $2.94 \cdot 10^1$ |
| ***InformationsZentrum Beton** (InformationsZentrum Beton GmbH, 2023)* | Düsseldorf, DE | 267 | $3.44 \cdot 10^2$ | 470.55 | 7.38 | $2.47 \cdot 10^1$ |

The GWP for life cycle stage A4 is used as an indicator of how the distance from the manufacturing plant to the construction site might affect the overall results. From the data in Table 32 it is clear that the C50/60 concrete from KP Betong AB is the least sustainable as it has the highest GWP for stages A1-A3 of the four manufacturers and a higher GWP for stage A4 than Interbeton. Interbeton has a fairly low GWP for both stages A1-A3 and stage A4 for a 10 km distance, but as it is located much farther away from the Netherlands than the other three manufacturers the total GWP for the overall transport in stage A4 is much higher than for the others. The opposite holds for InformationsZentrum Beton; they have a high GWP for stage A4 for 10 km distance but as they are located in Germany the GWP for the overall transport in stage A4 is fairly low. InformationsZentrum Beton also performs well when it comes to the total GWP for stages A1-A3, with the second lowest GWP out of the four manufacturers. Therefore the information from the EPD from InformationsZentrum Beton for C50/60 concrete is used in the LCA for this study.

The majority of the structure for the optimized concrete chamber design is constructed out of C35/C45 concrete. The 2.5 m increment of the lower wall on the seaside of the chamber will be constructed out of C25/30 concrete. Three EPDs from different manufacturers were investigated and the results are presented in Table 33 and Table 34 below, structured the same way as Table 32.

**Table 33 Environmental impact data on the GWP for C35/45 concrete including the total energy use for life cycle stages A1 – A3. Declared unit of 1 m³ and GWP for a 100 year time period.**

| *Manufacturer* | location | Distance [km] | $GWP_{tot,A1-A3}$ [kg $CO_2$-eq] | Total energy use [kWh] | $GWP_{tot,A4}$ [kg $CO_2$-eq/8 m³] | $GWP_{tot,A4,site}$ [kg $CO_2$-eq/m³] |
|---|---|---|---|---|---|---|
| ***InformationsZentrum Beton*** *(InformationsZentrum Beton GmbH, 2023)* | Düsseldorf, DE | 265 | $3.09 \cdot 10^2$ | 376.7 | 4.65 | $1.55 \cdot 10^1$ |
| *Interbeton (Martha, 2022)* | Athenes, GR | 2911 | $2.65 \cdot 10^2$ | 272.72 | 2.07 | $7.53 \cdot 10^1$ |
| *Unicon A/S (Unicon A/S, 2023)* | Vejle, DK | 826 | $3.16 \cdot 10^2$ | 842.5 | 2.25 | $2.32 \cdot 10^1$ |

**Table 34 Environmental impact data on the GWP for C25/30 concrete including the total energy use for life cycle stages A1 – A3. Declared unit of 1 m³ and GWP for a 100 year time period.**

| *Manufacturer* | Location | Distance [km] | $GWP_{tot,A1-A3}$ [kg $CO_2$-eq] | Total energy use [kWh] | $GWP_{tot,A4}$ [kg $CO_2$-eq/8 m³] | $GWP_{tot,A4,site}$ [kg $CO_2$-eq/m³] |
|---|---|---|---|---|---|---|
| ***InformationsZentrum Beton*** *(InformationsZentrum Beton GmbH, 2023)* | Düsseldorf, DE | 267 | $2.23 \cdot 10^2$ | 317.8 | 2.24 | 7.49 |
| *Interbeton (Martha, 2021)* | Athenes, GR | 2911 | $2.34 \cdot 10^2$ | 271.1 | 3.92 | $1.43 \cdot 10^2$ |
| *Unicon A/S (Unicon A/S, 2024)* | Vejle, DK | 826 | $2.22 \cdot 10^2$ | 356.2 | 2.16 | $2.23 \cdot 10^1$ |

For the C35/45 concrete, Unicon A/S has the highest total GWP for stages A1-A3 out of the three manufacturers. InformationsZentrum Beton has a higher GWP for stages A1-A3 than Interbeton, however, as it is located in Germany the total GWP is the lowest out of the three manufacturers. Therefore, InformationsZentrum Beton is the most sustainable choice for C35/45 concrete. For the C25/30 concrete, all manufacturers have relatively similar GWP for stages A1-A3. Therefore, the choice of a manufacturers EPD for this study is made based on the GWP for the overall transport in stage A4, which means that all EPD's chosen for C50/60, C35/45 and C25/30 concrete is from InformationsZentrum Beton GmbH.

**Reinforcement**

Both concrete chamber designs are constructed from reinforced concrete with S500 reinforcing bars. The base case design has a reinforcing volume of 131.75 m³ and the optimised design has a reinforcing volume of 56.32 m³. Given that the density of steel is 7850 kg/m³ the total weight of reinforcing steel for each design is:

$$W_{rs,base\ case} = 7850\frac{kg}{m^3} \cdot 131.75\ m^3 * 10^{-3}\frac{ton}{kg} = 1034.2\ tons$$

$$W_{rs,optimized} = 7850\frac{kg}{m^3} \cdot 56.32\ m^3 * 10^{-3}\frac{ton}{kg} = 442.2\ tons$$

Different EPDs from different manufacturers were investigated and the results from the three best performing EPDs are presented in Table 35, based on the declared unit of 1 ton. The table gives the manufacturers name, location of manufacturer, distance from the construction site, as well as the GWP for A1-A3 and A4. For the EPD's assume a 10 km transport distance for 1 ton of steel, and $GWP_{tot,A4,site}$ for stage A4 represents the total GWP for transporting 1 ton of steel to the construction site.

**Table 35 Environmental impact data on the GWP for S500 reinforcing steel bars including the total energy use for life cycle stages A1 – A3. Declared unit of 1 ton and GWP for a 100 year time period.**

| ***Manufacturer*** | **Location** | **Distance [km]** | **$GWP_{tot,A1-A3}$ [kg $CO_2$-eq]** | **Total energy use [kWh]** | **$GWP_{tot,A4,10km}$ [kg $CO_2$-eq/ton]** | **$GWP_{tot,A4,site}$ [kg $CO_2$-eq/ton]** |
|---|---|---|---|---|---|---|
| ***SERFAS, Ltd*** *(SERFAS, Ltd, 2023)* | Kaunas, LT | 1681 | $2.53 * 10^2$ | 1586.1 | $4.57 \cdot 10^{-2}$ | $7.69 \cdot 10^1$ |
| *Celsa Steel Service AS (Celsa Steel Service AS, 2021)* | Kristiansand, NO | 1225 | $3.58 \cdot 10^2$ | 1839.7 | $4.22 \cdot 10^{-2}$ | $5.17 \cdot 10^1$ |
| *BE Group (BE Group Sverige AB, 2021)* | Malmö, SE | 908 | $3.57 \cdot 10^2$ | 2869.4 | $1.03 \cdot 10^{-1}$ | $9.40 \cdot 10^1$ |

In the EPDs the $GWP_{tot,A4}$ is given for an average transport distance; for SERFAS that distance is 486 km, 119 km for Celsa, and 400 km for BE Group. The value given in the table has been adjusted for a 10 km transport distance. Nearly 50% of the total energy use for SERFAS is from renewable energy and over 60% of the total energy usage of Celsa Steel is from renewable energy. It is clear from Table 35 that SERFAS is has the best performing product when it comes to the total GWP even though they are located the furthest away from the construction site. This is due to the fact that they use 100% renewable energy when producing raw materials in an electric arc furnace.

**Anchors**

Anchored concrete walls are used for the optimised chamber design. The anchors chosen for the design are ASDO marine anchors and vary in strength classes depending on the reaction force (S355, S460, S500 & S700). They are manufactured from round steel bar with forged or threaded ends that allow a variety of connections. ASDO do not offer an EPD open to the public. Therefore, this study will rely on an EPD for round steel bars from other manufacturers.

Three different EPDs from different manufacturers were investigated. All of the EPDs had the declared unit of 1 ton. The density of steel is 7850 kg/m$^3$. Given the total anchor volume of 5.025 m$^3$ the total weight of steel for the anchors is:

$$W_{a,s} = 7850\frac{kg}{m^3} \cdot 5.025 m^3 * 10^{-3}\frac{ton}{kg} = 40\ tons$$

Table 36 gives the manufacturers name, location of manufacturer, distance from the construction site, as well as the GWP for A1-A3 and A4. For the EPD's assume a 10 km transport distance, and $GWP_{tot,A4,site}$ for stage A4 represents the total GWP for transporting 1 ton of steel to the construction site. The steel from SeAH Besteel would have to be transported via. cargo ship. The GWP of stage A4 for the SeAH Besteel steel was found through the website routescanner.com as 1691 kg $CO_2$-eq/TEU where TEU is the unit for one 20 feet (6.10 m) container. Since all the anchors are longer than a 6.10 m a 40 ft container with a maximum capacity of 29 tons must be used. The total weight of all the anchors surpasses that

of 29 tons and therefore two 40 ft containers equivalent to 4 TEU's are needed for the transport of anchors from Gunsan to Rotterdam. Therefore the total GWP for stage A4 for a ton of steel is:

$$GWP_{tot,A4,site} = \frac{1691 \frac{kg\ CO_2eq}{TEU} \cdot 4\ TEU}{W_{a,s}} = 169.1\ kg\ CO_2eq/ton$$

The other two manufacturers are within Europe in Italy and Romania and therefore the anchors will be transported via road to the construction site. Routescanner.com was again used to find an approximate estimation of the total GWP for A4. For Marcegaglia specialties it was found to be 1115 kg $CO_2$-eq/TEU and for AFV Beltrame Group it was found to be 2290 kg $CO_2$-eq/TEU

**Table 36: Environmental impact data on the GWP for S355, S460, S500 and S700 steel anchor rods including the total energy use for life cycle stages A1 – A3. Declared unit of 1 ton and GWP for a 100 year time period.**

| ***Manufacturer*** | **Location** | **Distance [km]** | **$GWP_{tot,A1-A3}$ [kg $CO_2$-eq]** | **Total energy use [kWh]** | **$GWP_{tot,A4,site}$ [kg $CO_2$-eq/ton]** |
|---|---|---|---|---|---|
| ***SeAH Besteel*** *(Baek, 2024)* | Gunsan, KR | 27107 | $1.10 * 10^3$ | 5148.3 | $1.69 \cdot 10^2$ |
| *Marcegaglia specialties (Marcegaglia Specialties S.p.A, 2023)* | Volta Mantovana, IT | 1167 | $1.80 \cdot 10^3$ | 8125.0 | $1.12 \cdot 10^2$ |
| *Donalam AFV Beltrame Group (AFV Beltrame Group, 2021)* | Calarasi, ROU | 2397 | $1.88 \cdot 10^3$ | 6969.4 | $2.29 \cdot 10^2$ |

The EPD of SeAH Besteel steel manufacturer is chosen for the LCA. As can be seen from Table 36. steel anchors from the steel manufacturer SeAH Besteel have the lowest overall GWP for stages A1-A3 and the second lowest GWP for A4. Gunsan is by far the greatest distance away from the construction site but as the steel bars will be transported via a cargo ship it will have a relatively low GWP for A4 because cargo ship transport has a much lower $GWP_{tot,A4}$/km for a ton of steel than road transport. This is due to the cargo carrying capacity of cargo ships.

### Steel plates and nuts

The head of the anchor is secured to the concrete wall with a bolted steel plate. Another plate is at the end of the anchors, that will be the anchor blade resisting pullout of the anchor. These plates will all be constructed from a S460 steel.

Different EPDs from different manufacturers were investigated and the results from the three best performing EPDs are presented in Table 37. The declared unit is 1kg of steel plates. The table gives the manufacturers name, location of manufacturer, distance from the construction site, as well as the GWP for A1-A3 and A4, and total energy use during life cycle stages A1 – A3, GWP for A4 is given per 10 km transport distance in the EPD's, and $GWP_{tot,A4,site}$ representing the total GWP for transport to the construction site.

**Table 37: Environmental impact data on the GWP for S460 steel plates including the total energy use for life cycle stages A1 – A3. Declared unit of 1 kg and GWP for a 100 year time period**

| ***Manufacturer*** | **Location** | **Distance [km]** | **$GWP_{tot,A1-A3}$ [kg $CO_2$-eq]** | **Total energy use [kWh]** | **$GWP_{tot,A4,10km}$ [kg $CO_2$-eq/kg]** | **$GWP_{tot,A4,site}$ [kg $CO_2$-eq/kg]** |
|---|---|---|---|---|---|---|
| ***BE Group*** *(BE Group Sverige AB, 2021)* | Malmö, SE | 908 | 2.07 | 6.58 | $2.40 \cdot 10^{-4}$ | $2.18 \cdot 10^{-1}$ |
| *METINVEST (METINVEST TRAMETAL S.p.A., 2023)* | San Giorgio di Nogaro, IT | 1348 | 2.81 | 34.36 | $5.11 \cdot 10^{-5}$ | $6.89 \cdot 10^{-2}$ |
| *Spartan UK (Ltd, Spartan UK, 2021)* | Gateshead, UK | 858 | 2.10 | 31.57 | $2.40 \cdot 10^{-4}$ | $2.06 \cdot 10^{-1}$ |

A4 was not included in the EPD from Spartan UK LTd and therefore an estimation had to be made. It was assumed that the $GWP_{tot,A4,10km}$ is equal to the higher value from the other two manufacturers. Comparing the total GWP for stages A1-A4 it is clear that METNVEST has the highest value. BE Group and Spartan UK

have very similar values for $GWP_{tot,A1-A4}$, 2.29 and 2.31 kg $CO_2$-eq/kg steel respectively, with BE Group performing slightly better. But as an assumption had to be made for Spartan UK for the total GWP for A4, it could be lower, which would make Spartan UK the best performing manufacturer out of the three. Spartan UK will still not be chosen for the LCA for this study both to lower the uncertainty for the $GWP_{tot,A4}$ and because they are not located within the European Union (EU) which might result in extra fees to be added for the import of the product and as economy is a part of the LCA of a product this would not be beneficial. Therefore, BE Group will be chosen for the LCA in this study as they still perform well with the $GWP_{tot}$ and as they are within the EU.

No Specific EPD was found for the bolt nuts to secure the plates to the anchor and concrete chamber wall. therefore, the same EPD and $GWP_{tot,A1-A3}$ will be used for the nuts as for the steel plates.

**Under water concrete**

Underwater concrete has a low water-cement ratio meaning the cement content in UWC is high, making it a generally high-strength concrete. Therefore, the EPD is assumed to be the same as for the C50/60 concrete.

**Tension piles**

The $GWP_{tot,A4,100km}$ is given for a meter of tension pile transported 100 km.

**Table 38: Environmental impact data on the GWP for S460 steel plates including the total energy use for life cycle stages A1 – A3. Declared unit of 1 m and GWP for a 100 year time period**

| ***Manufacturer*** | **Location** | **Distance [km]** | **$GWP_{tot,A1-A3}$ [kg $CO_2$-eq/m]** | **$GWP_{tot,A4,100km}$ [kg $CO_2$-eq/m]** | **$GWP_{tot,A4,site}$ [kg $CO_2$-eq/m]** |
|---|---|---|---|---|---|
| *Peab Grundläggning (Peab Grundläggning AB, 2019)* | Tollarp, SE | 986 | $1.66 \cdot 10^{2}$ | $4.02 \cdot 10^{-2}$ | $3.96 \cdot 10^{-1}$ |

The total EPDs for each material type is presented in Table 39:

**Table 39: Total global warming potential for all material used in the two design alternatives for life cycle stages A1 – A4, C1 – C4 and D**

| ***Material*** | **Manufacturer** | **Dseclared unit** | **$GWP_{tot,A1-A3}$ [kg $CO_2$-eq/m]** | **$GWP_{tot,A4,site}$ [kg $CO_2$-eq/m]** | **$GWP_{tot,C1-C4}$ [kg $CO_2$-eq/m]** | **$GWP_{tot,D}$ [kg $CO_2$-eq/m]** |
|---|---|---|---|---|---|---|
| *Concrete C50/60* | InformationsZentrum Beton | $m^3$ | 344 | 24.7 | 18.7 | −12.1 |
| *Concrete C35/45* | InformationsZentrum Beton | $m^3$ | 309 | 15.51 | 18.7 | −12.1 |
| *Concrete C25/30* | InformationsZentrum Beton | $m^3$ | 223 | 7.49 | 18.7 | −12.1 |
| *Reinforcement* | SERFAS, Ltd | $ton$ | 253 | 76.9 | 28.3 | 0 |
| *Anchors* | SeAH Besteel | $ton$ | 1100 | 169 | 102.4 | −94.4 |
| *Steel plates and bolts* | BE Group | $kg$ | 2.07 | 0.218 | 0.034 | −0.54 |
| *Tension piles* | Peab Grundläggning | $m$ | *166.17* | 0.396 | 0 | 0 |

The values for life-cycle stage D for the anchors, steel plates and bolt have been reduced as much of the steel will be lost to corrosion over the 150 year lifetime of the product (sacrificial steel was considered in the design). Tension piles are rarely extracted from the earth after the end of life of the structure and hence the 0 GWP for C1-C4 and D. A 20 % reduction of the value given in the EPD for life cycle stage D for the anchor rods and a 50% reduction of the value for life cycle stage D given in the EPD for the steel plates was applied

## 7.1.2. Bill of Materials

The bill of materials is a list of all the materials used in the two chamber designs with information on the strength classes and weight or volume. The base case design has C50/60 concrete, S500 steel reinforcement, underwater concrete floor and tension piles. The bill of materials for the base case is presented in Table 40

**Table 40: bill of materials for the base case chamber design**

| Material | Quantity | Unit |
|---|---|---|
| *C50/60 concrete* | 11794.74 | $m^3$ |
| *Reinforcement S500* | 1034.27 | tons |
| *Underwater concrete floor* | 4788.76 | $m^3$ |
| *Tension piles* | 4108.00 | m |

To get a better overview the reinforcement quantity for each rebar diameter is shown in Table 41 below along with the total length for each rebar type.

**Table 41: Total length and weight of each rebar diameter used in the base case design**

| Ø [mm] | L [m] | Weight [ton] |
|---|---|---|
| **32** | 100652.50 | 635.45 |
| 25 | 35142.56 | 135.42 |
| 20 | 58476.38 | 144.21 |
| 16 | 48495.22 | 76.54 |
| 12 | 19484.21 | 17.30 |
| 10 | 41107.38 | 25.34 |

The optimized chamber design has C35/45 concrete and C25/30 concrete reinforced with S500 steel rebars. The walls are anchored with plated steel anchor rods from S460, S500 and S700 steel. Plates and nuts are from S460 steel. The bill of materials for the optimised chamber design is given in Table 42. Table 43 to Table 46 show an aggregated bill of material for every rebar size, anchor diameter, plate size and nut size.

**Table 42: bill of materials for the optimized chamber design**

| Material | Quantity | Unit |
|---|---|---|
| *C35/45 concrete* | 5949.90 | $m^3$ |
| *C25/30 concrete* | 195.84 | $m^3$ |
| *Reinforcement S500* | 441.15 | tons |
| *Anchors S460, S500 & S700* | 45.53 | tons |
| *Steel plates S460* | 9149.96 | kg |
| *Steel nuts S460* | 1581.36 | kg |
| *Underwater concrete floor* | 1749.84 | $m^3$ |
| *Tension piles* | 3889.60 | m |

**Table 43: Total length and weight of each rebar diameter used in the optimized chamber design**

| $Ø_{rebar}$ [mm] | L [m] | Weight [ton] |
|---|---|---|
| **32** | 7955.10 | 50.22 |
| 25 | 13672.74 | 52.69 |
| 20 | 67799.35 | 167.20 |
| 16 | 50165.56 | 79.18 |
| 12 | 46285.67 | 41.09 |
| 10 | 25504.87 | 15.72 |
| 8 | 19745.10 | 7.79 |

| | | |
|---|---|---|
| 6 | 6746.50 | 1.50 |

Table 44: Total length and weight of each anchor diameter used in the optimized chamber design

| $Ø_{anchor}$ [mm] | L [m] | Weight [ton] |
|---|---|---|
| **97** | 208.4 | 12.09 |
| **92** | 40.0 | 2.09 |
| **84** | 629.6 | 27.39 |
| **80** | 70.0 | 2.76 |
| **76** | 33.6 | 1.20 |

Table 45: Area, quantity and total weight of all plate types used for the optimized chamber design.

| Plate [mm x mm] | A [m2] | Quantity | Weight [kg] |
|---|---|---|---|
| **1000x1000 t= 10 mm** | 1.00 | 8 | 628.00 |
| 900x900 t= 10 mm | 0.81 | 10 | 635.85 |
| 800x800 t= 10 mm | 0.64 | 8 | 401.92 |
| 700x700 t= 10 mm | 0.49 | 76 | 2923.34 |
| 650x650 t= 10 mm | 0.42 | 8 | 265.33 |
| 600x600 t= 10 mm | 0.36 | 4 | 113.04 |
| 600x600 t= 20 mm | 0.36 | 42 | 2373.84 |
| 400x400 t= 20 mm | 0.16 | 72 | 1808.64 |

Table 46: Quantity and total weight of all nut types used in the optimized chamber design.

| Nut type [mm] | Quantity | Weight [kg] |
|---|---|---|
| **M110** | 52 | 426.40 |
| M100 | 152 | 1036.64 |
| M90 | 24 | 118.32 |

## 7.2. Results

The functional unit for the LCA is for the structure as a whole. For the LCA of the construction pit only the underwater concrete floor and tension piles are included. The amount sheet-piles needed for the construction pit will be the same for both design alternatives.

The global warming potential for the structures for life cycle stages A1-A3 is found by using the information from the environmental product declarations and applying it to the bill of materials.

$$GWP_{product} = \sum GWP_{tot,A1-A3} \cdot Quntaity$$

The results are shown in Table 47 with the total GWP of each structure underlined:

Table 47: Global warming potential for stages A1-A4 and stages C1-D for both chamber designs with the total GWP of the structure underlined

| Base design materials | Material Quantity | $GWP_{A1-A4}$ [ton $CO_2$-eq] | $GWP_{C1-D}$ [ton $CO_2$-eq] | $GWP_{total}$ [ton $CO_2$-eq] |
|---|---|---|---|---|
| C50/60 | 11083.48 $m^3$ | 4083.73 | 72.82 | 4156.55 |
| Reinforcement total | 960.19 tons | 316.77 | 27.21 | 343.98 |
| UWCF | 4788.76 $m^3$ | 1764.43 | 31.46 | 1795.89 |
| Tension piles | 4108 m | 684.24 | 0.00 | 684.24 |
| | | | | **6980.657** |

| Optimized design materials | Material Quantity | $GWP_{A1-A4}$ [ton $CO_2$-eq] | $GWP_{C1-D}$ [ton $CO_2$-eq] | $GWP_{total}$ [ton $CO_2$-eq] |
|---|---|---|---|---|
| C35/45 | 5020.64 $m^3$ | 1627.75 | 32.99 | 1660.74 |
| C25/30 | 199.84 $m^3$ | 46.06 | 1.31 | 47.38 |
| Reinforcement total | 438.12 tons | 144.54 | 12.42 | 156.95 |
| Anchors | 44.10 tons | 55.97 | 0.35 | 56.32 |
| Plates | 9149.96 kg | 20.94 | -4.63 | 16.30 |
| nuts | 1581.36 kg | 3.62 | -0.80 | 2.82 |
| UWCF | 1455.265 $m^3$ | 536.20 | 9.56 | 545.76 |
| Tension piles | 3828.00 m | 637.60 | 0 | 637.60 |
| | | | | **3123.87** |

This results in a reduction for the overall GWP between the structures of 55.25% for A1-A4, C1-C4 & D. The total global warming potential for A1-A4 for both design alternatives are shown on a graph on Figure 58.

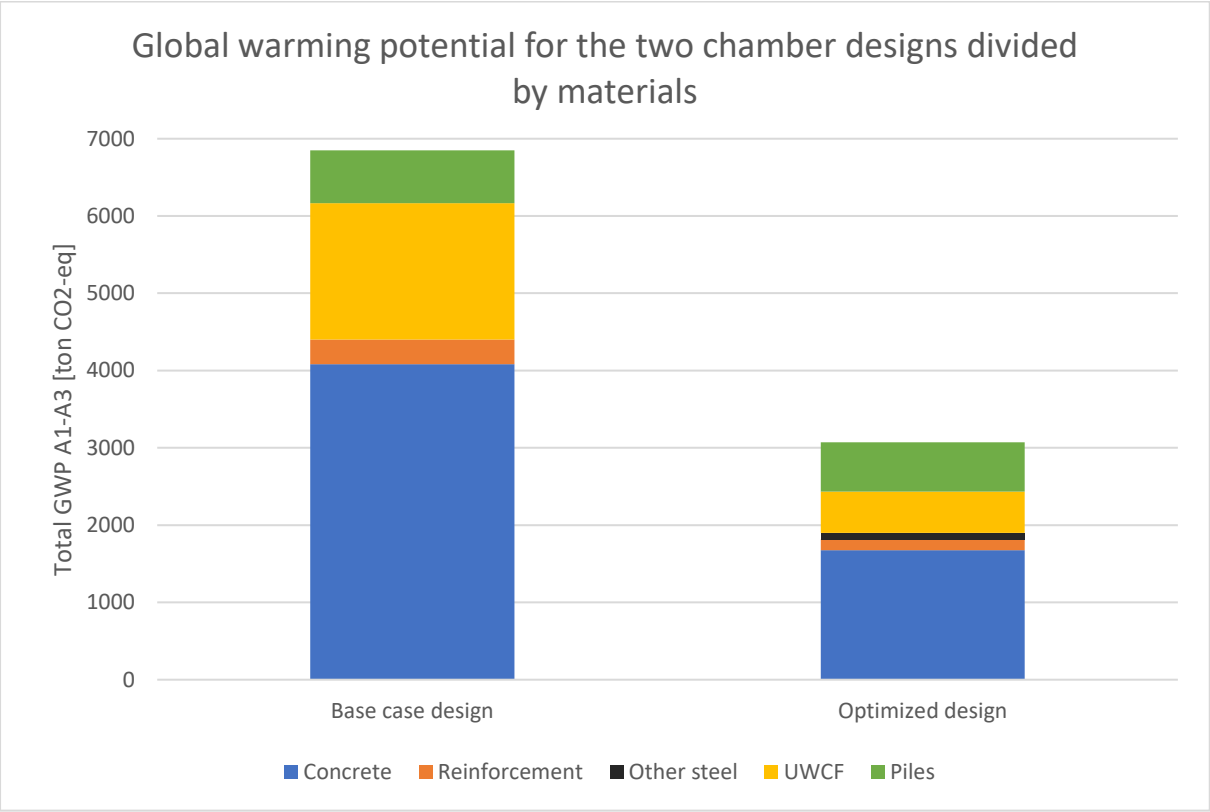


**Figure 58: Total global warming potential for life-cycle stages A1-A4 for the two chamber design alternatives divided by materials**

Figure 59 shows a chart comparing the two designs by depicting in percentages the contribution of each material to the total GWP.

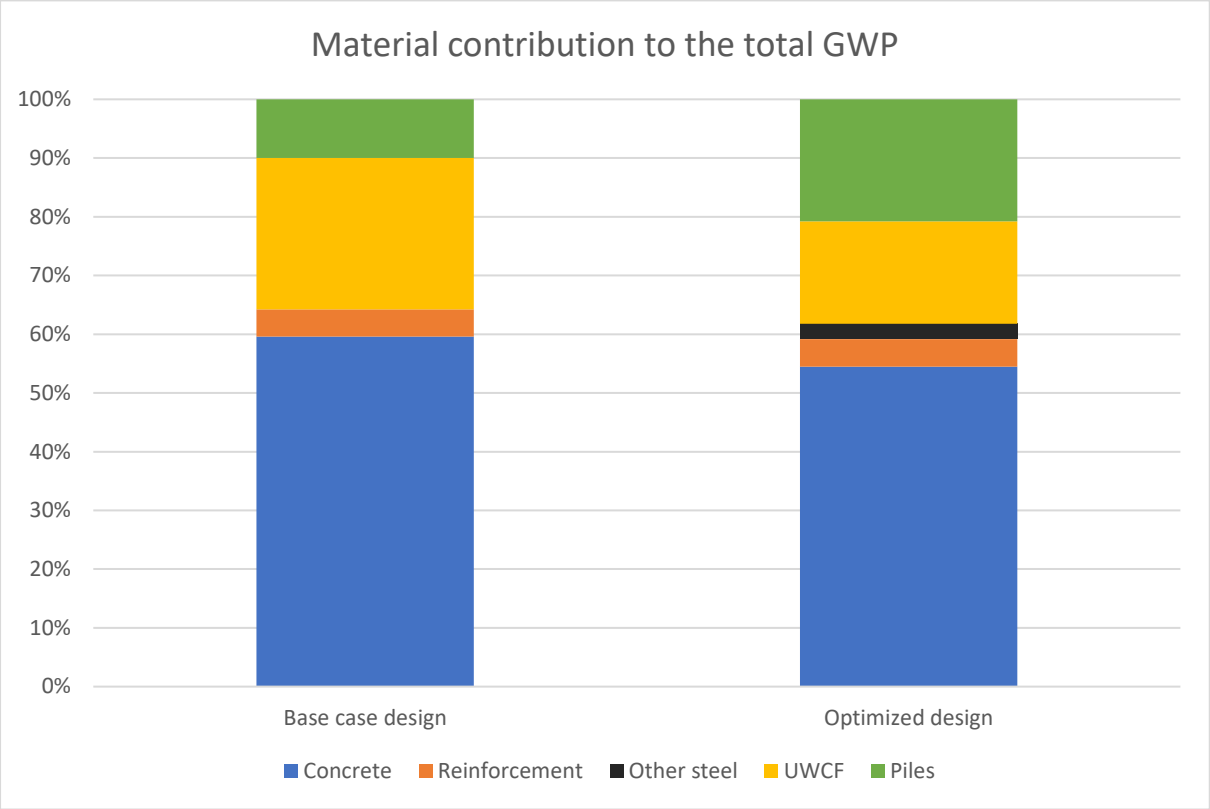


**Figure 59: 100% stacked column chart comparing the percentage that each material contributes to the total GWP for stages A1-A4**

Figure 60 shows the contribution of the underwater concrete floor system (uwc and piles) to the total GWP of the two chamber designs.

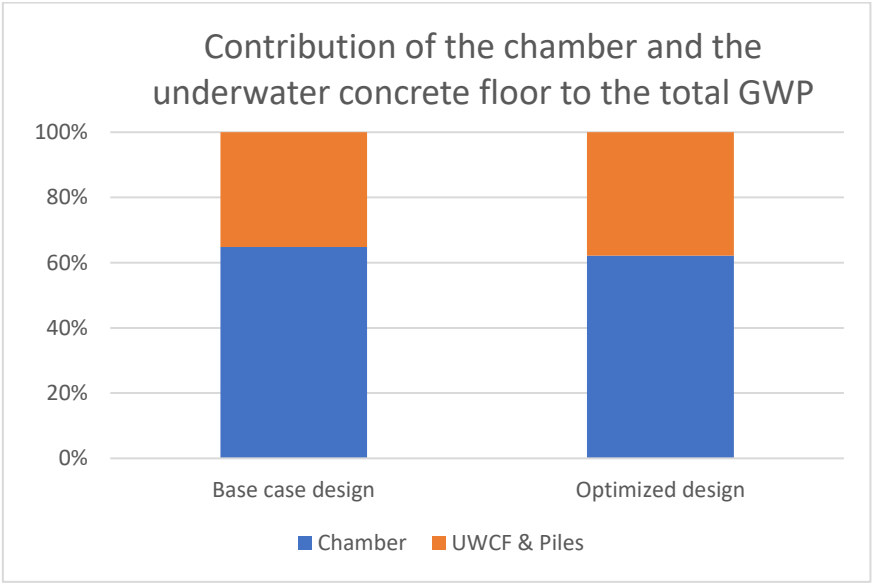


**Figure 60: 100% stacked column chart comparing the percentage that the concrete chamber vs the UWCF system contributes to the total GWP**

The reinforcement in the anchored chamber wall around the center lock head is calculated for different wall thicknesses, and the total GWP that wall and the material cost was calculated. The cost for concrete C35/45 was taken from a price list from UNICON A/S as 271.96 €/m$^3$ and the price for a ton of reinforcement was found as 678 €/ton steel according to Europe Steel Prices – MEPS International. The

reinforcement-concrete ratio for each wall thickness is presented in Table 48Table 1 along with the GWP and cost of the two materials. Figure 61 presents the results on a graph.

**Table 48: GWP and Cost of the anchored chamber wall around the center lock for varying wall thickness. cc stands for concrete and s stands for steel. The unit for GWP is in ton $CO_2$-eq.**

| $t_{wall}$ [m] | $V_{cc}$ [$m^3$] | $W_s$ [ton] | $GWP_{cc}$ | $GWP_s$ | $Cost_{cc}$ [€] | $Cost_s$ [€] | $GWP_{tot}$ | $Cost_{tot}$ [€· $10^{-3}$] | reinf/cc |
|---|---|---|---|---|---|---|---|---|---|
| **0.42** | 144.69 | 39.26 | 47.86 | 14.06 | 39349.0 | 31408.5 | 61.9 | 70.8 | 3.46 |
| **0.43** | 148.58 | 36.69 | 49.15 | 13.14 | 40407.5 | 29348.5 | 62.3 | 69.8 | 3.15 |
| **0.44** | 152.43 | 34.43 | 50.42 | 12.34 | 41454.8 | 27546.5 | 62.8 | 69.0 | 2.88 |
| **0.45** | 156.18 | 33.00 | 51.66 | 11.82 | 42473.6 | 26401.7 | 63.5 | 68.9 | 2.69 |
| **0.46** | 159.93 | 31.54 | 52.90 | 11.30 | 43493.4 | 25235.7 | 64.2 | 68.7 | 2.51 |
| **0.47** | 163.68 | 30.07 | 54.14 | 10.77 | 44513.8 | 24053.4 | 64.9 | 68.6 | 2.34 |
| **0.48** | 167.32 | 29.42 | 55.35 | 10.54 | 45505.6 | 23532.9 | 65.9 | 69.0 | 2.24 |
| **0.49** | 170.95 | 28.96 | 56.55 | 10.37 | 46490.8 | 23165.7 | 66.9 | 69.7 | 2.16 |
| **0.5** | 174.61 | 28.19 | 57.76 | 10.10 | 47486.7 | 22551.5 | 67.9 | 70.0 | 2.06 |
| **0.51** | 178.31 | 27.11 | 58.98 | 9.71 | 48493.34 | 21687.50 | 68.69 | 70.18 | 1.94 |
| **0.52** | 182.04 | 25.81 | 60.22 | 9.25 | 49507.63 | 20648.01 | 69.46 | 70.16 | 1.81 |

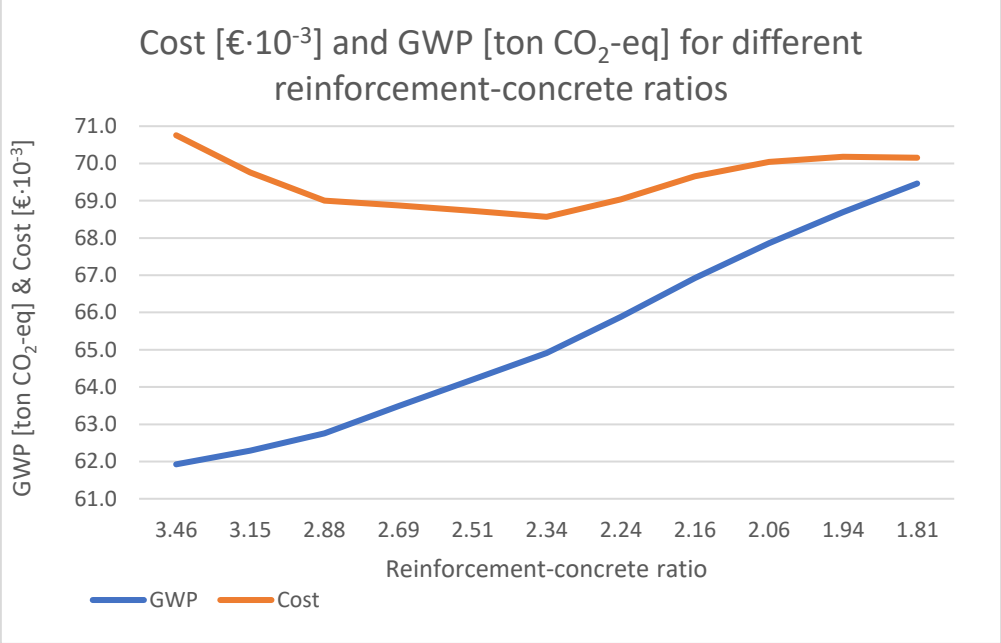


**Figure 61: Cost and GWP of concrete and reinforcement for different reinforcement-concrete ratios of the anchored wall at the center lock head**

# 8. Discussions

The chamber dimensions for the navigation lock in this study were chosen to be equal to those of Goereese Sluis. This may however not accurately fit future navigational needs. Further studies must be carried out to consider navigational volumes, and forecasts for fisheries (If fish quota permanently increases then fishing vessel will also increase in size). This is however not detrimental to the comparison of the sustainability of the two lock chambers.

The dike and landfill designs are out of the scope of this thesis, nor has it been designed for the Delta21 Project. Therefore, an assumption was made that the soil surrounding the structure would be the same everywhere with a dry unit weight of 19 kN/m$^2$ and a saturated unit weight of 21 kN/m$^2$. This has an effect on the design of the two chamber alternatives, but it would however not affect the comparison between the two designs; a similar reduction of moments and shear forces can be achieved between the two design even under different soil conditions. When this ship lock will be designed further the design must be adjusted to fit the actual land fill and dike composition that will be constructed for the Delta21 project in the future. For this thesis a change in soil type will not have a great effect on the comparison of the sustainability of the two structures.

Maximising rebar lengths can lower the GWP of the structure. Where long spans of the same reinforcement are required, it is beneficial to use long rebar lengths as the necessary lapping of bars is minimized (bars wont lap as often). If all bars are bent at the manufacturers and the manufacturer provides large diameter rebars, then limitations to the rebar diameter can be disregarded. K40 bars could be used, and the wall thickness can be minimised.

For the anchors, the GWP reduction due to re-use or recycling of the product at the end-of-life was taken as 80% of the value given in the EPD. This is because the anchors are a part of a marine structure and will be in an aggressive environment. As mentioned in chapter 6.1.3 the anchors will need a 12 mm increment of the diameter just to resist corrosion. After 150-year lifetime there will be damage and a lot of steel will have been lost due to corrosion. The same holds for the plates and bolts, especially for the plate and bolt connecting the anchor to the concrete wall as it will be completely exposed to weather. Therefore, the GWP reduction for stage D for the plates and bolts was taken as 50% of the value given in the EPD. The EPD for the Reinforcement from SERFAS does not give a value for the GWP of life cycle stage D. This was done to avoid double counting. Only the mass of primary steel in the product provides the benefit.

A lot of pressure is being put on the concrete industry to lower the carbon footprint of their products. Therefore, the EPD might be lower than what is given in the chapters above as the chambers will not be constructed until the year 2100.

The results on Figure 58 show that the GWP of the alternative anchored chamber design can be reduced by 55.25% compared to the base case design. This was achieved through the change of the chamber wall structural type which resulted in a significant decrease of the design moments and shear. This in return allowed for a reduced wall and floor thickness, reduction in concrete classes as the required shear resistance is lower, and reduction of reinforcement volumes. The reinforcement-concrete volume ratio is 1.1% for both designs. As a rule of thumb in civil engineering, this ration should be between 1% - 2%. Having the same reinforcement concrete ratio gives a clear view of how effective changing the structural type of the chamber wall was in reducing the GWP. The concrete volume could be further reduced but special care must be taken to avoid floating of the structure by designing the structure too light.

In both design alternatives, the percentage of the total GWP due to reinforcement is similar, around 8%, not considering the UWCF and piles (see Figure 59). This is similar for both designs as the reinforcement-concrete ratio was kept the same.

The concrete in the UWCF system accounts for a much larger part of the total GWP for the base case design than for the optimized design (see Figure 59). This is due to a limit to the number of tension piles. Every pile affects a volume of soil around it with a diameter of 6D. A single pile for both designs have a diameter of D = 500 mm. therefore a 3 m spacing is necessary between piles for them to be as effective as possible. The area of the underwater concrete floor therefore limits the number of piles that can be placed affectively under it. For the base case design, the chamber floor thickness is 1.7 m, and this limiting number of piles is 161. For the optimised chamber design the floor thickness is reduced by 65% resulting in a much thinner UWCF with 132 piles. If the chamber floor thickness is reduced, it raises the bottom of the floor and consequently the UWCF as well. Therefore, a floor thickness reduction is not only beneficial for the reduction of GWP for the chamber structure, but it will also reduce the GWP for the UWCF system as the UWCF thickness and/or number of tension piles can be reduced as the uplift water pressure decreases.

The results showed that the underwater concrete floor (UWCF) system accounts for over 30% of the total GWP for both chamber design alternatives (see Figure 60). As of now UWCFs are primarily utilized in construction pits as a water retaining element, rather than an integral part of the structure later to be built. In this study, impermeability of the chamber floor is not a requirement for the chamber design as the lock chamber was designed to be never fully emptied. Therefore, the UWCF could potentially be used as the primary floor of the lock chamber. By utilizing the UWCF as the primary chamber flooring, material volumes of the structure could be substantially reduced.

The walls would be cast directly on top of the UWCF and secured to the floor with reinforcement bolts. The interface between the floor and the wall would be weaker than if it were to be cast as one whole structure. Special consideration must be given to the wall-floor connection, particularly regarding vulnerability to corrosion from saltwater exposure. This is both because the wall and floor would no longer be cast as a whole and because the underwater concrete floor is expected to crack. To mitigate corrosion risk, additional corrosion measures such as sacrificial steel can be implemented.

Furthermore, adjustment of the wall thickness might be necessary to compensate for a reduced lateral support, as the connection becomes more flexible for this alternative. To increase the stiffness of the floor-wall connection a slight local increment of the UWCF thickness of 0.1 – 0.2 m between the chamber walls could be implemented. This would provide additional lateral support at the bottom of the chamber wall.

Upon implementing these modifications, a new assessment of the GWP can be conducted. As can be seen from Figure 62 below, preliminary calculations suggest that replacing the conventional concrete chamber floor with the UWCF system and increasing its thickness locally by 0.2 m between the walls could result in a GWP reduction of approximately 680 tons $CO_2$-eq for the alternative anchored wall chamber (14% GWP reduction). This results in the total GWP reduction of 65% between the base case design and the alternative anchored wall chamber design with an UWCF as the primary flooring.

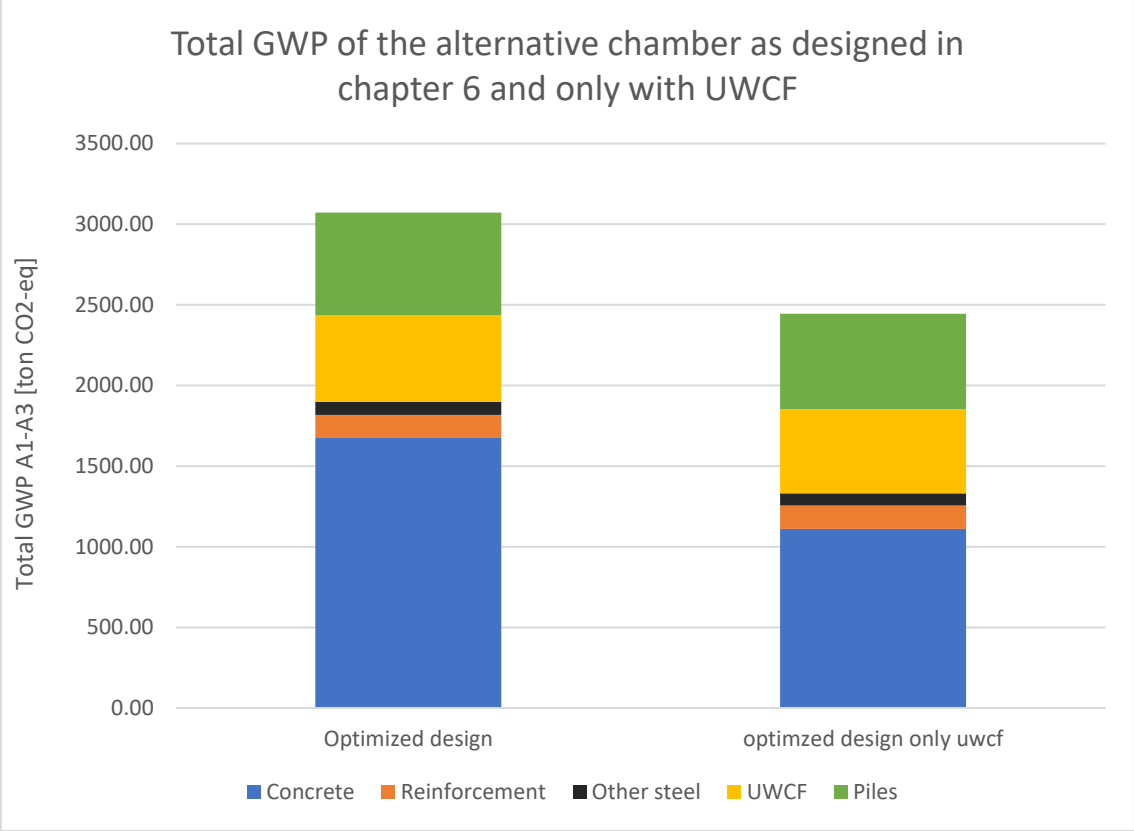


**Figure 62: comparison between the total GWP of the optimized design as designed in chapter 6.1 an optimized design using the UWCF of the construction pit as the permanent floor of the ship lock chamber.**

Looking at the moment, the results showed that the moment at the intersection of the +4.5 wall and the +7.0 wall increment is $M_{xx}$ = 26 kNm, and the shear is V = 51 kN. This moment is very low compared to the moments at lower levels of the wall and therefore, not a lot of flexural reinforcement is needed to reach structural integrity of the 2.5 m high wall segment. The shear is also low and therefore the wall increment above NAP +4.5 m may have less width than the wall below. This can also be constructed from a lower concrete class. Furthermore, there is an option to do this 2.5 m high wall segment as a lego-block construction as the shear forces that would cause sliding are very low. By doing so, the wall height doesn't need to be raised from NAP +4.5 m to NAP +7.0 instantaneously in the year 2150, but can be increased in parts by adding for example 0.5 m high blocks when the sea-level rise calls for it. SLR is better predicted when forecasting for the near future. Therefore, materials could be saved and minimized using the lego-block design as the SLR that is currently predicted for the year 2250 in this thesis might not be as extreme when the time actually comes. This will therefore result in a more detailed design when it comes to the final height of the chamber wall at the seaside of the lock. The option of lego-block construction also contributes to a delay in the emissions, and as the immediate, near future reduction is more important than a distant reduction this can be a very beneficial option.

The recommended concrete-rebar ratio was found to be between 1%-2%. An optimum concrete-rebar ratio would be such that the structure would have a minimum total GWP without the cost increasing. This ratio is found by looking at the effect that the reinforcement-concrete ratio for the anchored wall at the center lock head has on the total GWP and costs of the two materials combined. The optimum ratio results in the lowest total GWP without the costs starting to increase due to the increased reinforcement ratio. This point is found for a wall thickness of 0.47 m which resulted in a reinforcement-concrete ratio of 2.34% (See Figure 61). This ratio is rather high which is due to the fact that this wall includes shear reinforcement. The determination of an optimum reinforcement-to-concrete ratio indicates a trade-off between structural

performance and environmental sustainability. By finding the right balance, the structure achieves adequate strength and durability while minimizing its carbon footprint.

The alternative design in this study had anchored concrete walls using plated steel rod anchors. This design might be difficult to install in many countries that do don't have a great access to specialist for the installation of anchors. Therefore, in those situations, a better alternative might be the counterfort concrete wall as the only materials used in for that structure would be concrete and reinforcement.

# 9. Conclusion

The goal of this thesis was then to find an improved design of a concrete ship lock chamber with regards to sustainability and reduce the overall carbon footprint of the structure by at least 50%. As a base case, a concrete lock chamber was designed as a semi-gravity u-basin structure with tapered walls according to NEN-EN 1992-1-1, and by following the design norms for such a structure, i.e. not including any shear reinforcement in a concrete chamber design as that is not usual.

The introduction of structural elements, specifically plated steel anchors, in the alternative design of the concrete chamber proved beneficial in transferring loads to the subsoil. It effectively reduced both the maximum moments and shear forces within the structure by 88% and 56% respectively. This reduction allowed for a decrease in the volume of concrete and rebar steel required, as well as the lowering of strength classes. The concrete volume could be reduced by 47% compared to the base case and the reinforcement volume was reduced by 46%.

Changing the chamber wall type was not only found to enhance structural performance but also significantly reduces the carbon footprint of the concrete structure by over 55%. This reduction is primarily due to the decreased shear forces at the bottom of the wall, shear reinforcement implementation, and moment reduction, which collectively reduce the concrete volume in the structure. This is most influential for the lowering of the GWP, accounting for around 60% of the total reduction of GWP between the two designs. This highlights the potential for integrating sustainability goals into structural design by prioritizing optimization strategies that minimize material use, energy consumption, and enhances structural efficiency. The application of LCA methodologies, covering stages A1-A4 and end-of-life stages, provides a comprehensive understanding of environmental implications associated with design choices. This approach enables informed decision-making aimed at achieving sustainability targets while maintaining structural integrity and performance.

An optimum reinforcement-concrete ratio for the anchored chamber wall was identified (2.34%) that minimizes the structure's GWP without increasing it material costs. The fact that the optimum ratio does not increase the material cost of the structure implies that sustainable design solutions can be economically viable. This ratio serves as a reference for other concrete walls with shear reinforcement. However, the ratio doesn't incorporate labour cost, which could influence the ratio, considering that highly reinforced walls require more construction hours, potentially raising the costs. Nevertheless, identification of this optimal reinforcement-concrete ratio represents a significant advancement in sustainable designs, demonstrating the potential for achieving environmentally responsible solutions without compromising structural integrity or incurring additional costs.

# 10. Recommendations

While the specific conclusions above are tailored to the u-basin concrete chamber design and its soil retaining walls, the principles underlying the optimisation process can be applied to other concrete structures, particularly structures involving soil retention or similar load-bearing requirements. The general principles that can be applied to other structures are:

- Optimisation through structural elements: Adding or modifying structural elements to minimize maximum moments and shear forces within a concrete structure can be applied broadly. This may involve various techniques such as introducing anchors, braces, shear reinforcement, tension elements (i.e. counterforts), or relieving elements (i.e. relief shelves) to distribute loads more efficiently.
- Reduction of material volumes: By effectively reducing moments and shear forces, it becomes possible to optimize the use of materials such as concrete and rebar steel. This reduction can lead to potential cost savings and allows for the adjustment of strength classes, optimizing the structural design further.
- Comparative analysis: Conducting comparative analyses between a base case design and an optimized designs allows for the quantification of improvements achieved through optimization strategies. This approach provides valuable insights into the effectiveness of specific design modifications and their potential applicability to other concrete structures.

Further research and studies on optimizing the sustainability of concrete structures can explore several avenues to enhance understanding and improve design methodologies. The development of integrated design frameworks that consider sustainability principles from the early stages of conceptualization through construction and operation is recommended for further research. This could for example include an optimum reinforcement-to-concrete ratio as discussed above for multiple different concrete elements. This optimum ratio would vary depending on the element; shear reinforced walls, beam, floor, slabs on soil, columns and more.

Furthermore, research on the feasibility of using an underwater concrete floor as a primary flooring in a structure such as this where impermeability of the floor is not a requirement could be performed. This entails evaluating its potential implementation, including the behaviour of the wall-floor connection, designing it with sufficient stiffness and strength against corrosion, and assessing the impact of the floor cracking on the overall integrity of the chamber structure. Researching this could allow for an UWCF to be used in certain constructions as an integral part of the main structure, instead of only being used as an element in a construction pit with a very short service life that accounts for a large part of the total GWP over the structure’s lifetime.

# References


abg. (2022, August 11). *Soil properties | Soil unit weight technical note*. Retrieved from abg | Creative Geosynthetic engineering: https://www.abg-geosynthetics.com/technical/soil-properties/unit-weight/

AFV Beltrame Group. (2021). *Environmetnal Product Declaration; Special Steel - SBQ Bars.* Stockholm, SE: The International EPD System.

Alonso, A. C. (2018). *Morphodynamics of the Haringvliet ebb-tidal delta; Unravelling the mechanisms behind its Unravelling the mechanisms behind its.* Delft: Delft University of Technology.

Alonso, C. A. (2018). *Morphodynamics of the Haringvliet ebb-tidal delta.* Delft, NL: Delft University of Technology.

Andrew, R. M. (2018). Global CO2 emissions from cement production. *Earth System Science Data, 10*, 195-217.

Apriyono, A., & et al. (2018). *Soil classification based on cone penetration test (CPT) data in Western Central Java.* Purwokerto: Jenderal Soedirman University. Retrieved from https://doi.org/10.1063/1.5028062

ASDO. (2015). *Anchors for Marine Structures; M64 - M170 in accordance with EN1993-5.* Dortmund: Anker Schroeder ASDO GmbH.

Autodesk Support. (2019, 08 22). *New Rebar to Rebar Constraint Types in Revit 2020.1*. Retrieved from autodesk.com: https://www.autodesk.com/support/technical/article/caas/tsarticles/ts/7w0Il3YfMsRadUrwJvpyyA.html

Baek, J. (2024). *Environmental Product Decleration; Round Bar from SeAH Besteel.* Stockholm, SE: The International EPD® System.

BaltMetExport SIA. (2023). *Environmental Product Declaration; Steel reinforcement products from baltMetExport SIA.* Stockholm, SE: The International EPD® System.

BE Group Sverige AB. (2021). *Environmental Product declaration; Hot Rolled Steel Plates and Sheets BE Group Sverige AB.* Stockholm, SE: The International EPD®.

BE Group Sverige AB. (2021). *Environmental Product Declaration; Reinforcing Steel Bar BE Group Svergie AB.* Stockholm, SE: The International EPD System.

Beeby, A., Narayanan, R., & Gulvanessian, H. (2015). *Designers' Guide to Eurocode 2: Design of Concrete Structures.* London, UK: Thomas Telford Ltd.

Beem, R., Boogaard, A., Glerum, A., de Graaf, M., Henneberque, S., Hiddinga, P., . . . Weijers, J. (2000). *Design of Locks 1.* Utrecht, NL: The Civil Engineering Division of the Directorate General of Public Works.

Behera, G. (2023, November 19). *Retainng Wall Structure.* Retrieved from Government College of Engineering, Kalahandi: https://gcekbpatna.ac.in/assets/documents/lecturenotes/1671874900_4b7c4a492b6b254c7625.pdf

Brooks, H., & Nielsen, J. P. (2013). *Basics of Rtaining Wall Design; A Design Guide for Earth Retaining Structures* (10th ed.). Newport Beach, California: HBAPublications.

Celsa Steel Service AS. (2021). *Environmental Product Declaration; Steel reinforcement products for concrete – Norwegian production from Celsa Steel Service AS.* Stockholm, SE: The International EPD® System.

CEN. (2011). *Sustainability of construction works - Assessment of environmental performance of buildings - Calculation methods.* Brussels: NEN.

Chauhan, V. B., Dasaka, S. M., & Gade, V. K. (2016). Investigation of failure of a rigid retaining wall with relief shelves. *apanese Geotechnical Society Special Publication, 2*(73), 2492-2497. doi:10.3208/jgssp.TC302-02

CRDG University of Hawaii. (2023, 10 03). *Tide Patterns and Currents*. Retrieved from manoa.hawaii.edu: https://manoa.hawaii.edu/exploringourfluidearth/physical/tides/tide-patterns-and-currents#:~:text=A%20semidiurnal%20tidal%20cycle%20is,6.17).

Dear, A., & Dalipi, D. (2022). *Environmental Product Decleration C50/60 F5 CEM1 10MM Slip-Form Ready-Mix Concrete London Concrete Pumping.* London, UK: EPD Hub.

Delta21. (2021). *Delta21: An adaptive and robust solution for the southwest delta.* Delft: Delta21.

Deltares. (2018). *Mogelijke gevolgen van versnelde zeespiegelstijging voor het Deltaprogramma; Een verkenning.* Delft: Deltares.

DONGKUK STEEL MILL CO., LTD. (2024). *Environmental Product Declaration; Reinforcing Bar.* Stockholm, SE: The International EPD® System.

Ecomatters. (2024, 03 01). *LCA, EPD & PEF*. Retrieved from Ecomatters - Sustainability consultancy: https://www.ecomatters.nl/services/lca-epd/

Fernando, J. (2022, 06 29). *What Are Stakeholders: Definition, Types, and Examples*. Retrieved from Investopedia: https://www.investopedia.com/terms/s/stakeholder.asp

Fine. (2022, August 18). *Table of Ultimate Friction Factors for Dissimilar Materials*. Retrieved from Fine Software: https://www.finesoftware.eu/help/geo5/en/table-of-ultimate-friction-factors-for-dissimilar-materials-01/

Gagg, C. R. (2014). Cement and concrete as an engineering material:. *Engineering Failure Analysis, 40*, 114-140.

Golsteijn, L. (2022, 07 11). *Life Cycle Assessment (LCA) explained*. Retrieved from PRé Sustainability: https://pre-sustainability.com/articles/life-cycle-assessment-lca-basics/

Google. (2022, 12 05). *Haringvliet Estuary.* Retrieved from Google: https://www.google.com/maps/place/51%C2%B054'08.0%22N+3%C2%B058'02.0%22E/@51.9053546,3.9148811,20209m/data=!3m1!1e3!4m6!3m5!1s0x0:0x36ac0858a8f95313!7e2!8m2!3d51.9022094!4d3.9672232!5m1!1e4

Gupta, A. (2017, March 19). *Steel Structures Vs Concrete Structures | Complete Comparison of Steel & Concrete*. Retrieved February 07, 2023, from CivilDigital: https://civildigital.com/steel-structures-vs-concrete-structures-complete-comparison-of-steel-concrete/

Hansen, M. (2022, July 8). *Goereese sluis, Haringvliet*. Retrieved from Binnenvaart in Beeld: https://www.binnenvaartinbeeld.com/nl/haringvliet/goereese_sluis

Hasanbeigi, A., Arens, M., Cardenas, J. C., Price, L., & Triolo, R. (2016). Comparison of carbon dioxide emissions intensity of steel production in China, Germany, Mexico, and the United States. *Resources Conservation and Recycling, 113*(4), 127-139.

Huizer, T. (2022). *Onderzoek aanzanding kust Haringvlietmonding; Achtergrondrapport. Toekomstige morfologische ontwikkelingen. Effecten waterveiligheid, ecologie, economie en leefbaarheid.* Rotterdam: Arcadis.

InformationsZentrum Beton GmbH. (2023). *UMWELT-PRODUKTDEKLARATION; Beton der Druckfestigkeitsklasse C25/30.* Berlin, DE: Institut Bauen und Umwelt e.V. (IBU).

InformationsZentrum Beton GmbH. (2023). *UMWELT-PRODUKTDEKLARATION; Beton der Druckfestigkeitsklasse C35/45 InformationsZentrum Beton GmbH.* Berlin, DE: IBU – Institut Bauen und Umwelt e.V.

InformationsZentrum Beton GmbH. (2023). *UMWELT-PRODUKTDEKLARATION; Beton der Druckfestigkeitsklasse C50/60, InformationsZentrum Beton GmbH.* Berlin, DE: Institut Bauen und Umwelt e.V. (IBU.

Jonkers, H. M. (2019). *Reader CIE4100; Materials and Ecological Engineering.* Delft, NL: TU Delft Faculty of Civil Engineering & Geosciences.

KC, S., & Gautam, D. (2021). Progress in sustainable structural engineering: a review. *Innovative Infrastructure Solutions, 6*, 1-23.

KNMI. (2021). *KNMI Klimaatsignaal'21: Hoe het klimaat in Nederland snel verandert.* De Bilt: KNMI.

KNMI. (2022, July 5). *Satellite observations*. Retrieved from KNMI: https://www.knmi.nl/research/satellite-observations

Le Cozannet , G., Lawrence, J., Schoeman, D. S., Adelekan, I., Cooley, S. R., Glavovic, B., . . . Supratid, S. (2022). *Cross-Chapter Box SLR | Sea Level Rise. In: Climate Change 2022: Impacts, Adaptation and Vulnerability.* Working Group II to the Sixth Assessment Report of the Intergovernmental Panel on Climate Change. Cambridge, UK and New York: Cambridge University Press.

Lehne, J., & Preston, F. (2018). *Making Concrete Change; Innovative in Low-carbon Cement and Concrete.* London: Chatham House.

Levinson, M. (2018). *Standardization of mitre gates; Standardizing steel mitre gates within existing navigation locks in the Netherlands.* Delft: Delft University of Technology.

Ltd, Spartan UK. (2021). *Environmental Product Declaration; Spartan UK Ltd, Hot Rolled Reversing Mill Steel Plates.* Stockholm, SE: The International EPD®.

Maduka, N., Greenwood, D., Osborne, A., & Udeaja, C. (2016). *Implementing Sustainable Construction Principles and Practices by Key Stakeholders.* Edmonton: Modular and Offsite Construction Summit.

Marcegaglia Specialties S.p.A. (2023). *Environmental Product Declaration; Carbon Steel Bars Drawn, Peeled or Ground.* Stockholm, SE: The International EPD®System.

Martha, K. (2021). *EPD, Environmental Product Declaration for Ready Mixed Concrete C25/30 XC3, S2.* Stockholm, SE: The International EPD® System.

Martha, K. (2022). *Environmenta Product Decloration for Ready Mixed Concrete Antaeus HPC C50/60 & Antaeus HPC C70/85.* Stockholm, SE: The International EPD System.

Martha, K. (2022). *EPD; Environmental Product Declaration for Ready Mixed Concrete C35/45.* Stockholm, SE: Programme The International EPD® System.

METINVEST TRAMETAL S.p.A. (2023). *Environmental Product Declaration; Hot rolled steel plate from METINVEST TRAMETAL S.p.A.* Stockholm, SE: The International EPD® System.

Molenaar, W. F. (2020). *Hydraylic Structures: Locks.* Delft: TU Delft.

MPA the Concrete Center. (2022, 12 01). *CO2 Emissions - Production*. Retrieved from Sustainable Concrete: https://www.sustainableconcrete.org.uk/Sustainable-Concrete/Performance-Indicators/CO2-Emissions-Production.aspx

mpa The Concrete Centre. (2023, 12 26). *Microsoft PowerPoint - Lecture 3 Bending and Shear in Beams - PHG - A8 - 2Oct16 - Print version.* Retrieved from concretecentre.com: https://www.concretecentre.com/TCC/media/TCCMediaLibrary/Presentations/Lecture-3-Bending-and-Shear-in-Beams-PHG-A8-2Oct16.pdf?fbclid=IwAR0IISyhGsy3UJyQ67fd0jNZaG4i90biB2Lkls26pC5RvijHN0iFTQwg1Gw

Olivier, J., & Peters, J. (2020). *Trends in global CO2 and total greenhouse gas emissions: 2020 Report.* The Hague: PBL Netherlands Environmental Assessment Agency.

Paasman, Y. (2020). *Design for the in- and outlet structure of the Energy Storage Lake within the Delta21 plan.* Delft: TU Delft.

Pathak, M., Slade, R., Shukla, P., Skea, J., Pichs-Madruga, R., & Ürge-Vorsatz, D. (2022). *Climate Change 2022: Mitigation of Climate Change. Contribution of Working Group III to the Sixth Assessment Report of the Intergovernmental Panel on Climate Change.* Cambridge, UK and New York, NY, USA: Cambridge University Press. doi:10.1017/9781009157926.002

PCA. (2022, 09 02). *Durability*. Retrieved from PCA cement.org: https://www.cement.org/learn/concrete-technology/durability

Peab Grundläggning AB. (2019). *Environmental Product Declaration; PRECAST CONCRETE FOUNDATION PILES FOR PEAB GRUNDLÄGGNING AB.* Stockholm, SE: The International EPD® System.

Ramsden, K. (2020, 11 03). *Cement and Concrete: The Environmental Impact*. Retrieved from PSCI Princeton: https://psci.princeton.edu/tips/2020/11/3/cement-and-concrete-the-environmental-impact

Rijkswaterstaat. (2020). *Waterway Guidlines 2020.* BNSV. Rijswijk: Rijkswaterstaat.

Rijkswaterstaat. (2022, August 9). *Hellevoetsluis Waterhoogte Oppervlaktewater*. Retrieved from Rijkswaterstaat Waterinfo: https://waterinfo.rws.nl/#!/details/themakaarten/Waterkwantiteit/Hellevoetsluis(HELL)/Waterhoogte___20Oppervlaktewater___20t.o.v.___20Normaal___20Amsterdams___20Peil___20in___20cm

Rinse, J., & During, O. (2022). *Environmental Product decleration Fabriksbetong C50/60 VCT 0,38; KP Betong AB.* Oslo, NO: EPD-Norge.

Sabatini, P., Pass, D., & Bachus, R. (1999). *Geotechnical Engineering Circular No. 4; Ground Anchors and Anchored Systems.* U.S. Department of Transportation. Washington, DC: Federal Highway Administration.

Schiermeier, Q. (2010, July 8). Few fishy facts found in climate report. *Nature, 466*, 170.

Schmertmann, J. (1978). *Guidelines for Cone Penetration Test; Performace and Design.* Washington, DC: Federal Highway administration.

SERFAS, Ltd. (2023). *Environmental Product Declaration; Green steel rebars (steel proceeding from an electric arc furnace using 100% renewable energy).* Stockholm, SE: The International EPD® System.

Shehata, H. F. (2016). Retaining walls with relief shelves. *innovative infrastructure solutions, 1*, 4. Retrieved from https://doi.org/10.1007/s41062-016-0007-x

Sundseth, K. (2008). *Natura 2000: Protecting Europe's biodiversity.* (S. Wegefelt, Ed.) Oxford: European Comission, Directorate-General for Environment.

UN. (2022, 08 31). *Sustainability*. Retrieved from United Nations: https://www.un.org/en/academic-impact/sustainability

UN. (2022, 08 31). *Take Action for the Sustainable Development Goals*. Retrieved from United Nations: https://www.un.org/sustainabledevelopment/sustainable-development-goals/

Unicon A/S. (2023). *Environmental product declaration; STANDARDBETON (C35/45 Slump Concrete in Moderate Environmental Exposure Class).* Oslo, NO: The Norwegian EPD Foundation.

Unicon A/S. (2024). *Environmental product declaration; STANDARDBETON (C25/30 Lava Concrete in Passive Environmental Exposure Class).* Oslo, NO: The Norwegian EPD Foundation.

US EPA. (2023, 04 18). *Understanding Global Warming Potentials*. Retrieved from United States Environmental Protection Agency: https://www.epa.gov/ghgemissions/understanding-global-warming-potentials

US Geological Survey. (2023, January 31). *Cement production worldwide from 1995 to 2022 (in billion metric tons)*. Retrieved February 07, 2023, from Statista: https://www.statista.com/statistics/1087115/global-cement-production-volume/

van Eeden, E. (2021). *A new dynamic landscape for the Haringvliet.* Delft: TU Delft.

Van Heel, D. D., Maas, T., De Gijt, J., & Said, M. (2011). Comparison of infrastructure designs for quay wall and small bridges in concrete, steel, wood and composites with regard to the co2-emission and the life cycle analysis. *Oikos*, 161-167.

Varen, V. d. (2022, June 27). *6.4 Goereese Sluis (Noordzee - Haringvliet)*. Retrieved from Varen doe je Samen: https://varendoejesamen.nl/kenniscentrum/artikel/knooppunt-6-4

Vass, T., Levi, P., Gouy, A., & Mandová, H. (2021). *Cement.* Paris: IEA. Retrieved from https://www.iea.org/reports/cement

Verschoor, B. (2023). *The Delta Barrier; A climate robust preliminary design of the Delta21 storm surge barrier.* Delft: Delft University of Technology.

Voorendt, D., & Molenaar, I. (2020). *Manual: Hydraulic Structures.* Delft: Delft University of Technology.

Vrijburcht, A., Beem, R., Boogaard, A., Glerum, A., de Graaf, M., Henneberque, S., . . . Weijers, J. (2000). *Ontwerp van Schutsluizen: Deel 1 + 2.*

Waterkaart. (2022, June 27). *Goereesesluis, in Stellendam: openingstijden en contact*. Retrieved from Waterkaart Live | Gids: https://waterkaart.net/gids/sluis.php?naam=Goereesesluis

Windy Weather World Inc. (2023, 01 17). *Oudorp uitloop: Weather statistics and wind history*. Retrieved from Windy.app: https://windy.app/forecast2/spot/4399915/Oudorp+uitloop+/statistics

# Appendix A: Soil properties

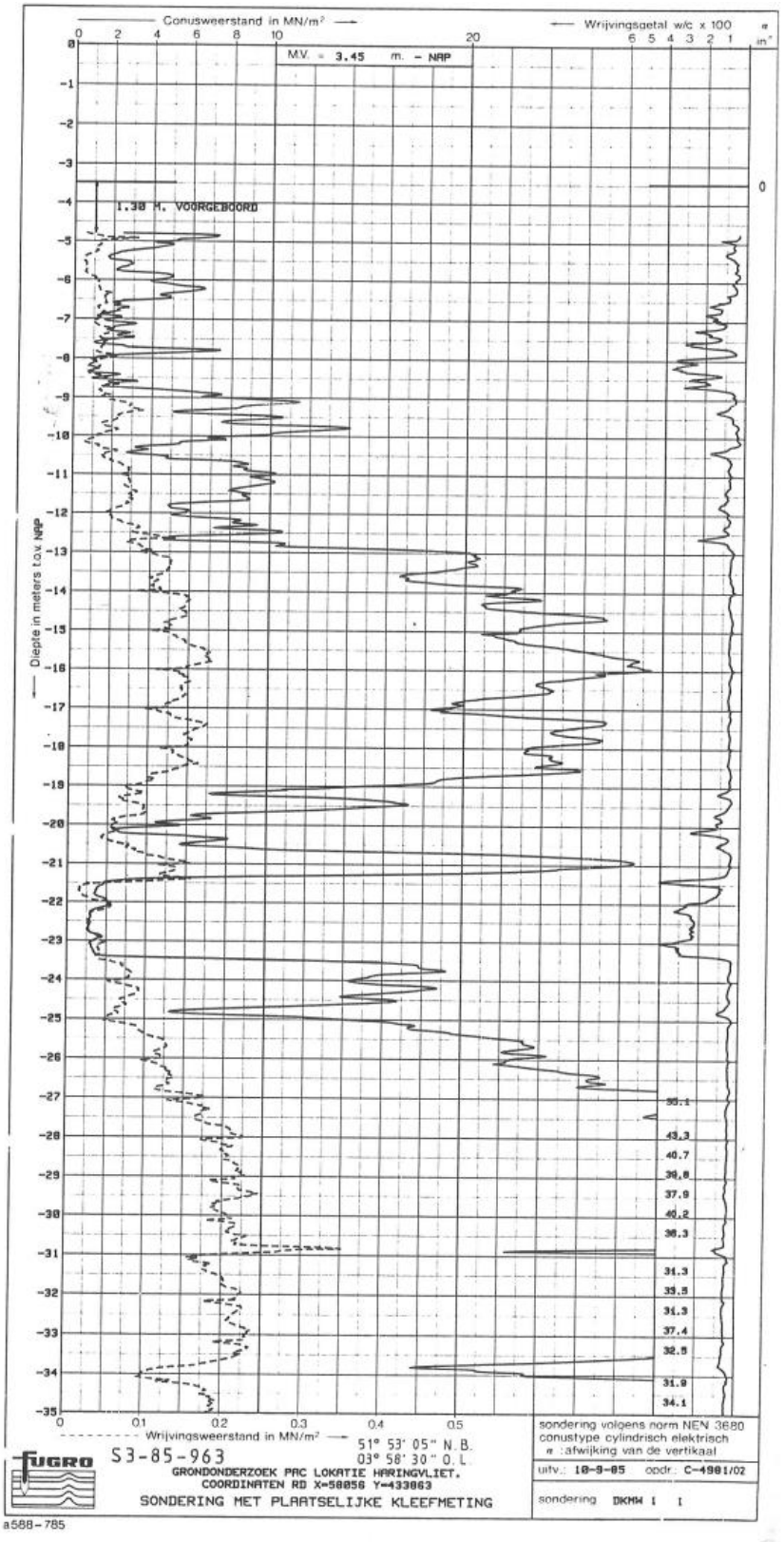


**Figure 63: CPT test from 0 to -35 m NAP. For the location of the ship lock each depth is lowered by 3.5m e.g., -5 m NAP on the graph is at -8.5 at the structures site.**

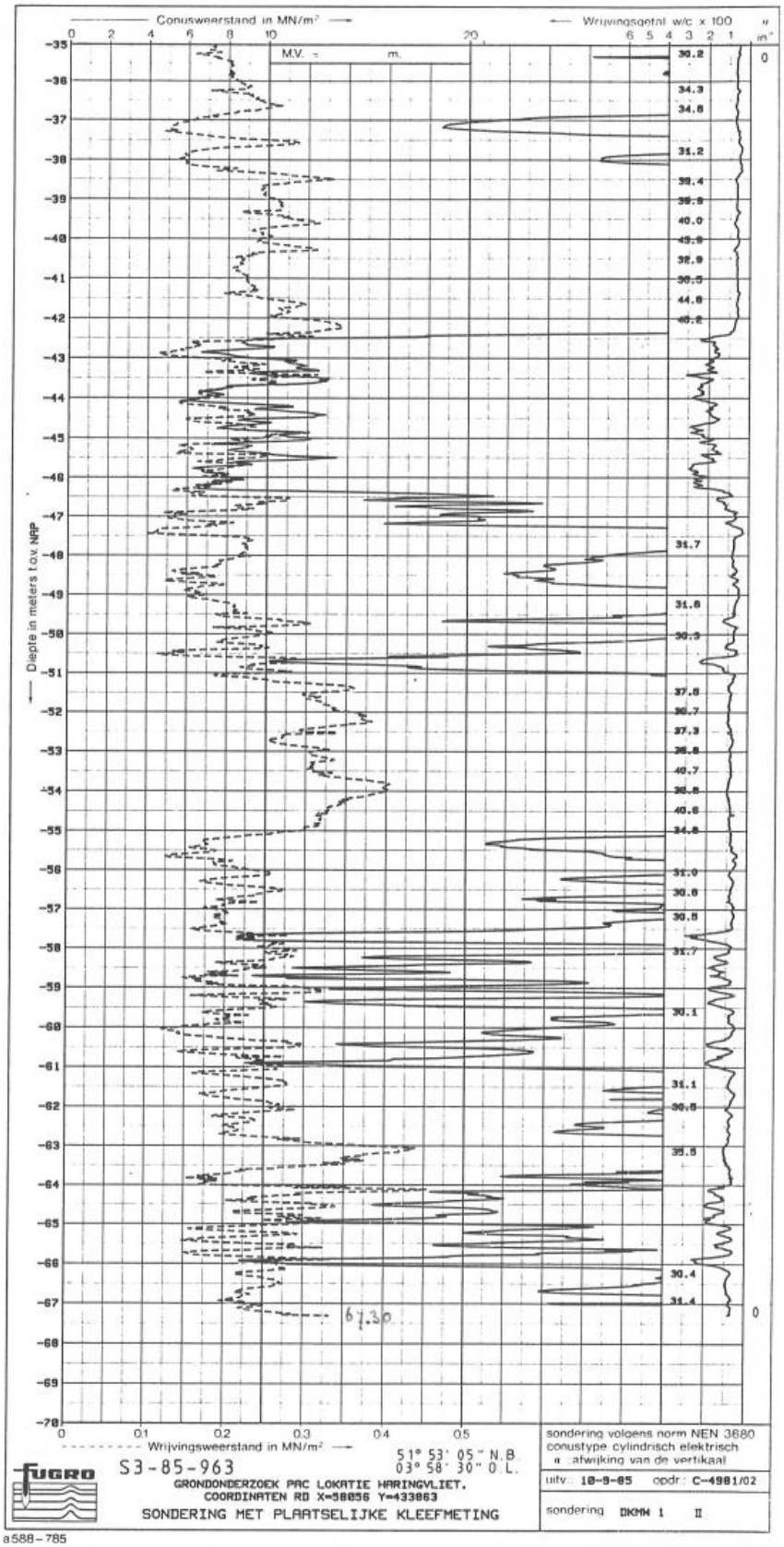


**Figure 64: CPT test from -35 to -70 m NAP**

# Appendix B: Dimensioning of the lock complex

A schematic representation of a lock chamber in a water way is depicted in figure below. The chamber length, $L_k$, is the distance between the stop lines. The run-out zone is the area length necessary to slow down the vessel. As the lock that is being designed in this report is not in a narrow & straight water way but connecting the sea and a river, this are does not need to be in line with the rest of the approach channel. The dimensioning of the lock complex for the Delta21 project will be done in accordance to Rijkswaterstaats Waterway Guidelines 2020 (Rijkswaterstaat, Waterway Guidlines 2020, 2020)

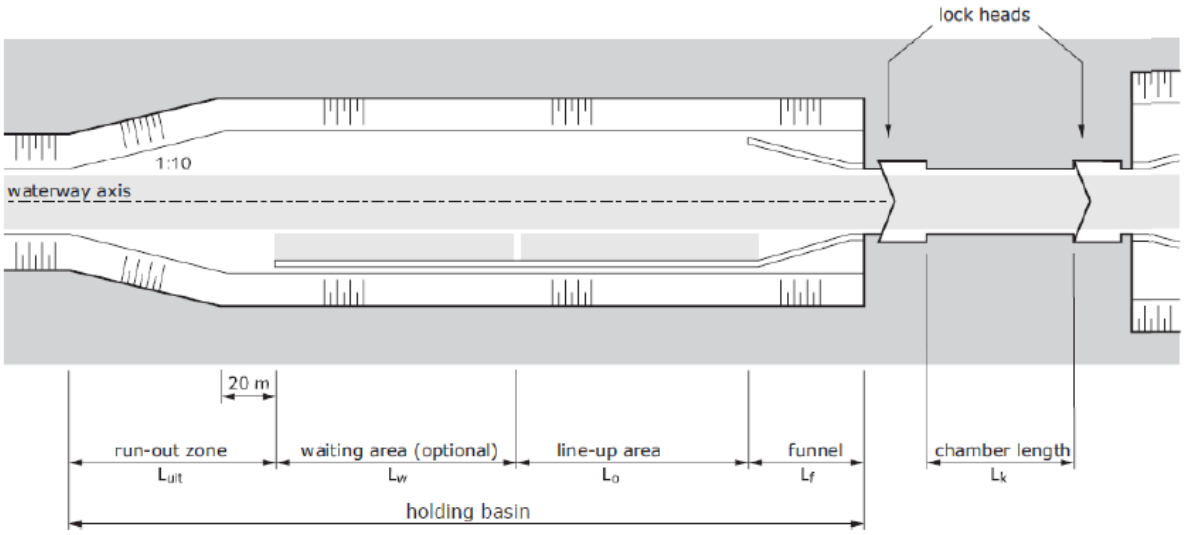


**Figure 65: Approach area of a lock**

The dimensions of the lock chambers will be the same as for goereese sluis lock; L = 145 m, $B_{ch}$ = 16 m, and D = 5 m. To decrease waiting and use time for smaller ships and boats the lock will be split into two chambers (This is also the case for Goereese sluis), giving a chamber length of 2x $L_k$ = 72.5 m. Splitting the lock into two chambers is also favourable for the flood defence function of the lock as the chamber between the high and low water level can be filled with water to a hight in between the extremes, lowering the forces on the gates. Four gates will separate the waterways and chambers; one at the seaward end, one at the landward end, and two in the middle separating the chambers. Mitre gates will be used as they take less space compared to sliding gates and since the lock is relatively narrow (16 m). The two gates in the middle will serve as the main flood defence gates. Having two gates reduces the failure probability of the flood defence in the case of a ship collision; if one gate is damaged the second gate can still function in case of an extreme flood.

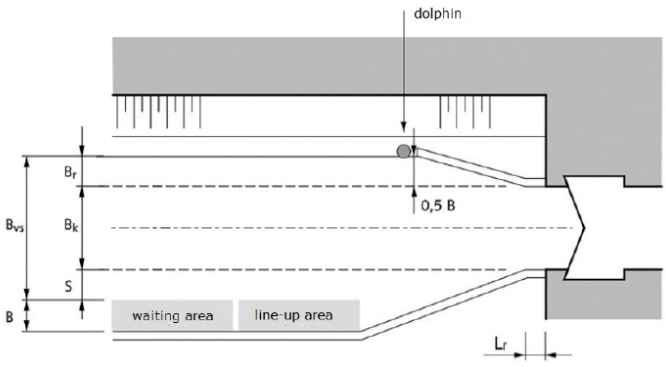


B = width of reference vessel
$B_k$ = chamber width
S = safety strip: distance measured perpendicular to the lock axis between the line of the chamber wall and the line-up area
$B_r$ = distance between the line of the chamber wall and the depth in the keel plane of a laden vessel, measured perpendicular to the lock axis
$B_{vs}$ =traffic lane width in holding basin = $B_r$ + $B_k$ + S
$L_r$ = length of the straight connection of the funnel to the lock head

**Figure 66: Outer port with a line-up area on one side**

A lock approach in necessary to connect the lock chambers to the sea/river. Since the chamber length is 72.5 m that gives CEMT class between II and III allowing maximum ship length of approximately 65 m in one

chamber. This would give a minimum length of $L_{k,min} = 1.1 \times L = 71.5\,m$. Class II and III give a beam width of B = 6.6 – 8.2 m. Given that the chamber width is $B_k = 16\,m$, the maximum beam allowed is approximately 7 m. this will leave 0.5 m on either side of the vessels and 1 m between them when passing, and is in accordance to the minimum chamber width given in Hydraulic structures: Locks as $B_{k,min} = B + B \times 1.25 = 15.75\,m$ (Molenaar, 2020).

Figure 66 shows a layout of the outer port with berths on one side. The straight connection to the funnel of the lock head is taken as $L_r$ = 3 m. The lead-in jetty has a slope of 1:6 and a width $B_r = 8$. This value was chosen from Table 49 as it fits within the range for a vessel of type II and III. That gives jetty length on the dolphin side of:

$$L_{f,short,S} = 8\,m \cdot 6 + 3\,m = 51\,m$$

On the line-up/berthing side, the width of the lead in jetty will be the beam width of the design vessel + a safety strip $S_S$ = 3.75 m taken from Table 49 as the median value between class II and III:

$$L_{f,long,S} = (7 + 3.75)\,m \cdot 6 + 3\,m = 67.5\,m$$

The length of the line-up area is a minimum of 1.1 x chamber length:

$$L_{0,S} = 1.1 \cdot 72.5\,m = 79.75\,m \approx 80\,m$$

**Table 49: Dimensions of outer ports with berths on one side.**

| class | B | $B_k$ | S | $B_r$(narrow) | $B_r$ (normal) |
|---|---|---|---|---|---|
| I | 5.1 | 6.0 | 3.0 | 5.0 | 6.3 |
| II | 6.6 | 7.5 | 3.5 | 6.0 | 8.8 |
| III | 8.2 | 9.0 | 4.0 | 7.5 | 11.1 |
| IV | 9.5 | 10.5 | 5.0 | 8.5 | 13.0 |
| Va | 11.4 | 12.5 | 6.0 | 10.5 | 16.1 |
| Vb | 11.4 | 12.5 | 7.0 | 11.5 | 15.1 |
| VIa | 22.8 | 23.8 | 12.0 | not advised | 32.2 |
| VIb | 22.8 | 23.8 | 12.0 | not advised | 32.2 |

A waiting area is a space designated to vessels waiting for the next locking cycle. On the seaward end of the lock a small part of the recreational harbour can be used as a waiting area when the wait time for vessels is over 15 minutes. Hence the straight approach channel on the seaward end of the lock need not be longer than $L_{tot,S} = L_{f,long} + L_0 = 147.5$ m.

There will not be a port on the riverside of the lock and thus the waiting area is necessary. As there are more than 2000 passages per year (over 5000 operations per year; ch. 4.4.2) a two-sided line-up/waiting area with alternating functions will be used. Since the chamber width is over 8 m the line up area on the riverside of the lock should be

$$L_{0,R} = 1.5L_k \approx 109\,m$$

It is assumed that it is enough to have this length on either side and thus functioning both as a line-up and a waiting area. The safety strip $S_R$ is taken as 2 m wide, and for a yacht holding basin the line-up area should be wide enough to allow for quick mooring with two abreast. Considering that the design vessel has a beam width of 7 m it is very likely that that is a barge or a small fishing boat. Most yachts that will

pass through the lock will have a beam width under 5 m. Therefore, the width of the line-up/waiting area can be taken as 11 m + the safety margin to allow for mooring of two vessels abreast:

$$11\ m + S_R = 13\ m$$

The funnel length on the riverside with a slope of 1:6 is therefore:

$$L_{f,R} = 13\ m \cdot 6 + L_r = 81\ m$$

The total approach length on the riverside of the lock is:

$$L_{tot,river} = L_{f,R} + L_0 = 190\ m$$

The horizontal dimensions of the lock complex are presented in the table below;

| **Chamber** | | **Dimension [m]** |
|---|---|---|
| Chamber length | $L_k$ | 72.5 |
| Chamber width | $B_k$ | 16 |
| Design vessel beam | B | 7 |
| **Seaward end** | | |
| Funnel length land side | $L_{f,long,S}$ | 67.5 |
| Funnel length SSB side | $L_{f,short,S}$ | 51 |
| Line-up length | $L_{0,S}$ | 80 |
| Total length seaward | $L_{tot,S}$ | 147.5 |
| Waiting/line-up width | B + $S_S$ | 10.75 |
| Keel-wall distance | $B_r$ | 8 |
| **River end** | | |
| Funnel length | $L_{f,R}$ | 81 |
| Line-up/Waiting length | $L_{0,R}$ | 109 |
| Total length riverside | $L_{tot,river}$ | 190 |
| Waiting/line-up width | 11 + $S_R$ | 13 |

# Appendix C: Base Case Design

## C.1: Underwater concrete floor

Before designing an underwater concrete floor (UWCF) calculations for a mass concrete floor will be carried out to check if such floor would be feasible for the ship lock instead of the UWCF. A mass concrete floor resists the upward water pressure from the hydrostatic loads by the weight of the floor alone. Therefore, the required thickness of the mass concrete floor to resist uplift must be determined. The uplift force acting on the floor is:

$$Q_{uplift} = p_{bottom} \cdot b_{floor} \cdot \gamma_{G,uf}$$

Where:

| | | |
|---|---|---|
| $b_{floor}$ | [m] | Width of the chamber; $b_{floor} = 16\ m$ |
| $\gamma_{G,uf}$ | [-] | Partial factor for unfavourable steady load; $\gamma_{G,uf} = 1.35$ |
| $p_{bottom}$ | [kN/m$^2$] | Water pressure acting on the bottom of the floor: $p_{bottom} = -(d_{chamber} - d_{gwl} - t_{floor}) \cdot \gamma_{sw} = -(-10.1\ m - (-2.5\ m) - t_{floor}) \cdot 10.06 kN/m^2$. |

If the top of the soil surrounding the chambre is set as zero, $d_{gwl}$ is the groundwater level relative to that and $c_{hamber}$ is the level of the bottom of the chamber (top of the mass concrete floor). The weight of the mass concrete floor has to be enough to counter act the uplift pressure, e.g.

$$W_{floor} \geq Q_{uplift}$$

$$W_{floor} = t_{floor} \cdot b_{floor} \cdot \gamma_{cc} \cdot \gamma_{G,f}$$

Where $\gamma_{cc}$ is the unit weight of reinforced concrete taken as 25 kN/m$^3$ and as the weight of the concrete floor is a permanent favourable load it is multiplied with the partial factor $\gamma_{G,f}$. Solving this iteratively results in the required floor thickness of:

$$t_{floor} \geq 5.3\ m$$

A concrete floor of this thickness requires a lot of concrete and reinforcement as the chamber is 144.5 m long. This would be very unpractical and not a feasible solution. Therefore, a piled and anchored underwater concrete floor will be opted for instead.

To Ensure water tightness of the construction pit, an underwater concrete floor (uwc) will be constructed. hydrostatic water loads will cause loading on the floor in the form of uplift force from an upward water pressure. After the lock chamber is constructed there will also be compression on the floor. Therefore, prefabricated concrete foundation piles will be used as they can perform in both tension and compression. These piles can reach a length of maximum 35 m (see Figure 67) and are suitable for both tension and compression forces. They can be driven down using vibrations. As the ship lock is not located near older buildings or any industry the driving of the piles should not lead to any damages to nearby structures.

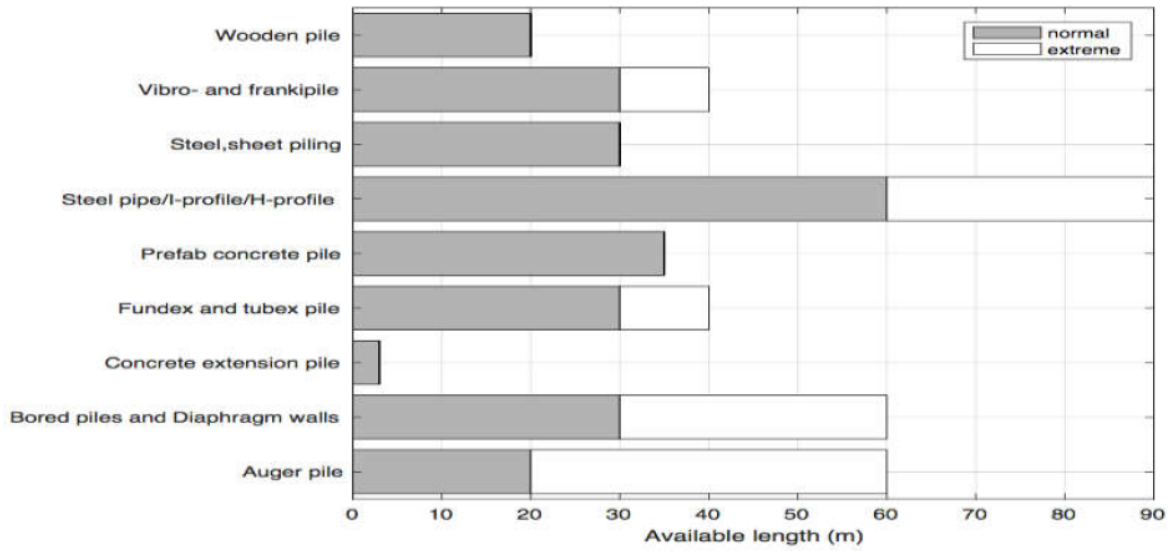


Figure 67: available pile lengths

The bottom of the chamber is at -6.9 m NAP and assuming 1.7 meter thick chamber floor and with a 1.4 m thick underwater concrete floor the bottom of the uwc floor will be at -8.3 m NAP. The construction pit will allow for 1.7 m margin on either side of the Chamber. Therefore, the width of the floor will be

$$B_{uw} = B_{ch} + 2 \cdot B_{wall} + 2 \cdot 1.7\ m = 25\ m$$

Where

| | | |
|---|---|---|
| $B_{ch}$ | [m] | Internal Width of the chamber; $B_{ch}$ = 16 m |
| $B_{wall}$ | [m] | Bottom width of the wall; $B_{wall}$ = 2.8 m |

The hydrostatic uplift force at NAP -8.3 m is calculated as

$$P_{hydro} = \left(h_{gwl} - h_{bot,uw}\right) \cdot \gamma_w = 103.57 \frac{kN}{m^2}$$

Where:

| | | |
|---|---|---|
| $h_{gwl} = +2$ | [m NAP] | Ground water level |
| $h_{bot,uw} = -8.3$ | [m NAP] | UWCF bottom level |
| $\gamma_w = 10.06$ | [kN/m$^2$] | Specific weigh of salt water, saltwater density of 1025 kg/m$^3$. |

Forces that will counteract this uplift force to avoid floatation of the floor are the weight of the UWCF, the weight of the piles and the attached clump weight pulled up by the piles. The UWCF is made out of unreinforced concrete with a unit weight of $\gamma_{uwc} = 23\ kN/m^3$. Hence, the weight of the UWCF is:

$$W_{uw} = 23 \frac{kN}{m^3} \cdot 1.4\ m\ = 31.60\ kN/m^2$$

The bottom of the chambre is at -5.2 m NAP and the floor thickness will be 1.7 m. the piles will reach 0.8 m into the 1.4 m thick underwater concrete floor for anchoring purposes. Therefore, the top of the piles that is not within the slab is at -8.3 m NAP. The CPT test in appendix A (offset by 3.5 m for the chosen location) shows that from -8.3 m NAP to -16.2 m NAP is a sand layer. From -16.2 m NAP to -22.5 m NAP is a gravely sand layer. Therefore, the Piles should reach at least 7.9 m below the floor so that they reach through the sand layers. With a 1 m anchoring length into the UWCF the minimum length of the piles will

be 8.9 m. This length might not provide enough resistance and thus the pile might have to reach into the sand-gravel layer. For a first estimation a pile length of 15.0 m will be assumed. Therefore, the pile tip will reach to a depth of -22.5 m.

As it is harder to drive a prefabricated concrete pile in a sand gravel layer than in a sand layer, a circular pile will be chosen as the best option for drivability. The slenderness of the pile may not go above 80 due to drivability requirements. The minimum width of the pile is thus:

$$D_{pile,min} = \frac{L_{pile}}{80} = \frac{15000}{80} = 187.5\ mm$$

For further calculations a pile diameter of $D_{pile}$ = 500 mm is assumed, and hence, the slenderness requirement is fulfilled.

## *Tension piles – Cone resistance*

During construction the ship lock the chamber will be completely empty and will thus be subjected to a buoyancy (uplift) force under its floor causing tensile loads on the foundation piles. The total uplift force causing tensile loads is the upwards buoyancy force counteracted by the weight of the 1 m thick uwc slab:

$$F_{uplift} = A_{uw}\left(P_{hydro} - \gamma_{uwc} \cdot t_{uw}\right) - n_{piles} \cdot V_{pile} \cdot \gamma_{cc}$$

$$= (25\ m\ \cdot 72.25\ m) \cdot \left(103.57\frac{kN}{m^2} - 23\frac{kN}{m^3} \cdot 1.4\ m\right) - n_{piles} \cdot 2.94\ m^3 \cdot 25\frac{kN}{m^3}$$

$$= 128{,}910.4\ kN - 73.63 n_{piles}$$

Where:

| | | |
|---|---|---|
| $A_{uw}$ | [m²] | Area of the underwater concrete floor |
| $\gamma_{cc}$ | [kN/m³] | Unit weight of reinforced concrete; $\gamma_{cc} = 25\ kN/m^3$ |
| $\gamma_{uwc}$ | [kN/m³] | Unit weight of concrete; $\gamma_{uwc} = 23\ kN/m^3$ |
| $P_{hydro}$ | [kN/m²] | Hydrostatic uplift force at NAP -8.3 m |
| $t_{uw}$ | [m] | Thickness of UWCF |
| $n_{piles}$ | [-] | Total number of piles in the UWCF |
| $V_{pile}$ | [m³] | Volume of a single pile; $V_{pile} = \frac{\pi D_{pile}^2}{4} h_{pile} = \frac{\pi \cdot (0.5m)^2}{4} \cdot 15\ m = 2.94\ m^3$ |

The required number of tension piles can be determined using the cone resistance method which checks for failure due to sliding. The maximum tensile forces that a pile can resist can be determined through the following equation:

$$F_{r,tension,d} = \int_{z=0}^{L} q_{c,z,d} \cdot f_1 \cdot f_2 \cdot O_{p,mean} \cdot \alpha_t\ dz$$

Where:

$q_{c,z,d}$: Design value for the tensile strength of the soil

$f_1$: Pile installation factor $\geq 1$. Here taken as $f_1 = 1$

$f_2$: Cone resistance reduction factor $\leq 1$. Hare taken as $f_2 = 1$

$O_{p,mean}$: Average circumference of the pile shaft. $O_{p,mean} = \frac{2\pi D}{2} = 1.57$

$\alpha_t$: Pile class factor depending on soil type. Table 50 gives values for different piles driven in sand. $\alpha_t = 0.007$

**Table 50: Maximum values for the pile class factor in sand and sand containing gravel (Voorendt & Molenaar, 2020)**

| Pile class/type | $\alpha_t$ |
|---|---|
| • Ground displacing installing methods: | |
| ○ driven smooth prefab concrete pile and steel tube pile with closed tip[1)] | 0,007 |
| ○ pile made in the soil, whereby the concrete column directly presses onto the ground and the tube is driven back (*teruggeheid*) out of the soil[2)] | 0,012 |
| ○ ditto, in case the tube is removed by vibration | 0,010 |
| ○ tapered wooden pile | 0,012 |
| • Screwed piles: | |
| ○ with grout injection or mixing | 0,009 |
| • Piles with little ground displacement: | |
| ○ driven steel profiles | 0,004 |
| • Soil removing piles: | |
| ○ drilled piles (and auger piles) | 0,0045 |
| [1)] The base of a tube pile with a closed tip shall not exceed 10 mm beyond the tube protruding. [2)] For this type of pile the diameter of the base may in principle be 30-50 mm larger than the outside diameter of the casing. | |

Representative value for the cone resistance at depth z, $q_{c,z,rep}$, is determined per layer using the CPT test from appendix A. Too get a better estimation of the weighted resistance, the CPT results are split into 5 zones depicted in Figure 68 below; Space I starts at -8.3 m NAP (on picture –4.8 m NAP as it is offset by 3.5 m) and has Δz = 1.7 m and q = 4.0 MPa

| Space | Δz [m] | $\mathbf{q_{c,z,rep,i}}$ [MPa] |
|---|---|---|
| **I** | 1.7 | 4.0 |
| **II** | 2.2 | 2.1 |
| **III** | 1.7 | 8.0 |
| **IV** | 2.4 | 7.7 |
| **V** | 4.2 | 22.5 |

$$q_{c,z,rep} = \frac{1}{L}\sum_{i=1}^{5} q_{c,z,rep,i} \cdot \Delta z_i = \frac{1}{12.2}(4.0 \cdot 1.7 + 2.1 \cdot 2.2 + 8 \cdot 1.7 + 7.7 \cdot 2.4 + 22.5 \cdot 4.2)$$
$$= 11.31\ MPa$$

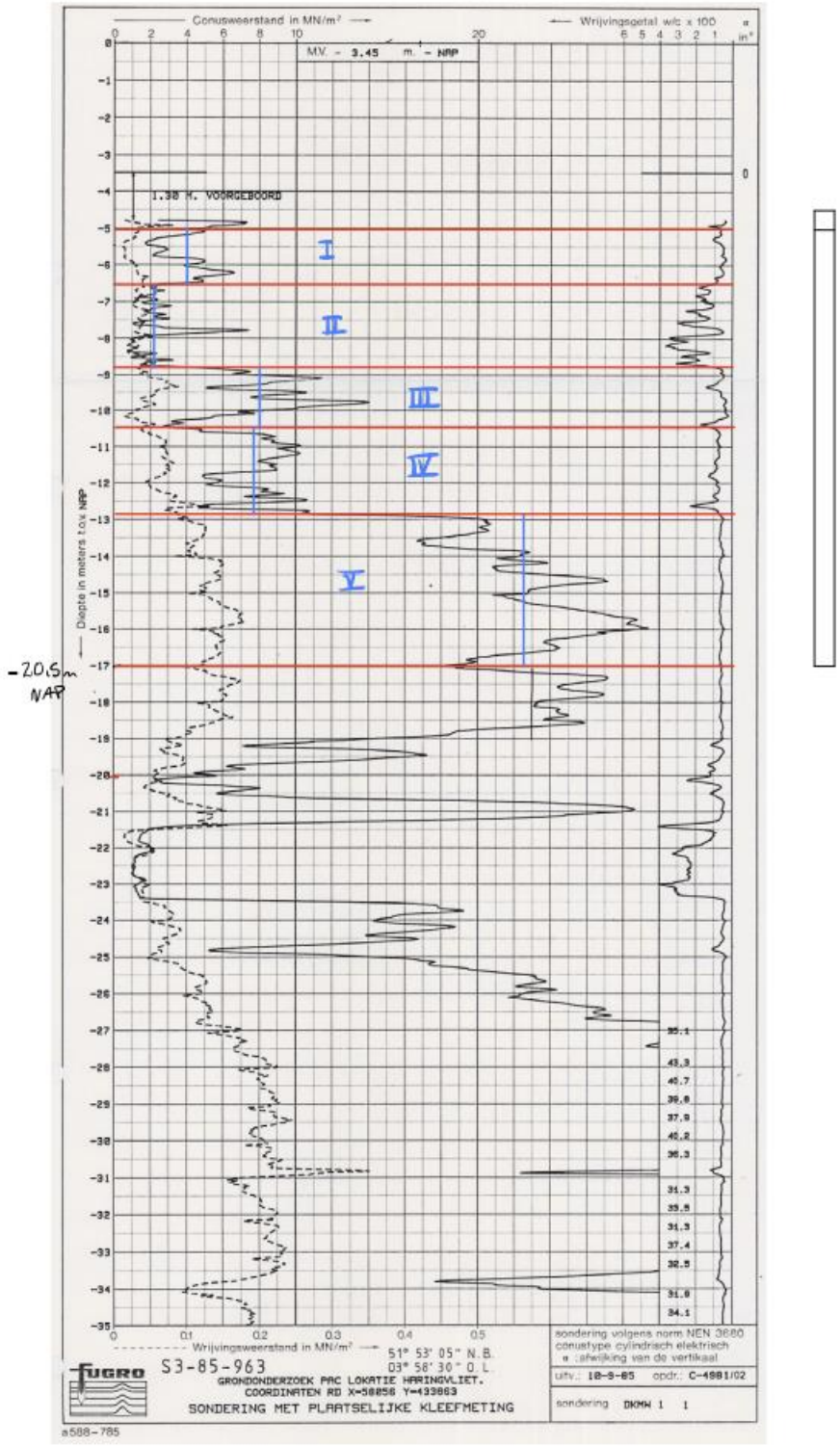


**Figure 68: CPT test split into 5 zones over the depth of the pile (depicted on the right). The CPT test is offset by 3.5 m.**

The design value for the cone resistance is then:

$$q_{c,z,d} = \frac{q_{c,z,rep}}{\gamma_{m,b,4} \cdot \gamma_{m,var,qc}} = 5.47\ MPa$$

Where $\gamma_{m,b,4} = 1.35$ is the resistance factor for tension piles and $\gamma_{m,var,qc} = 1.5$ is the factor for variable loads, taken as the maximum value of the material factor to be on the safe side. The maximum tensile force that a single pile can resist can now be calculated using eq. xxx:

$$F_{r,tension,d} = \int_{z=0}^{L} q_{c,z,d} \cdot f_1 \cdot f_2 \cdot O_{p,mean} \cdot \alpha_t \, dz = q_{c,z,d} \cdot O_{p,mean} \cdot \alpha_t \cdot L$$

$$F_{r,tension,d} = 5.47 \cdot 10^3 \ kN/m^2 \cdot 1.57 \, m \cdot 0.007 \cdot 12.6 \, m = 758.01 \, kN$$

The tension piles need to resist the uplift force, but the uplift is also counter acted by the weight of the piles. The submerged weight of a single pile is:

$$W_{pile} = \frac{\pi D_{pile}^2}{4} \cdot L_{pile} \cdot \left(\frac{\gamma_{cc}}{1.1} - \gamma_w\right) = \frac{\pi \cdot 0.5m^2}{4} \cdot 13.1m \cdot \left(\frac{25 \ kN/m^3}{1.1} - 10.06 \ kN/m^3\right) = 32.59 \, kN$$

The number of tension piles necessary to resist the uplift force is therefore found iteratively as:

$$n_{tension} = \frac{F_{uplift} - n_{tension} \cdot W_{pile}}{F_{r,tension,d}} = \frac{129{,}954.22 \, kN - 165 \cdot 32.59 \, kN}{758.01 \, kN} \approx 165$$

## *Tension piles – clump criterion*

The second check for the tension piles is the clump criterion, considering the surrounding soil. It indicates that the tensile force on a pile cannot surpass the weight of the pile and the wight of the clump of soil effected by the pile, hence $F_{tension} < F_{clump}$. The resisting clump force is computed using the following equation:

$$F_{clump} = V_{clump}\gamma_{d,soil} + V_{pile}\gamma_{d,cc} = \left(V_{cone} + V_{cilinder} - V_{pile}\right)\gamma_{d,soil} + V_{pile}\gamma_{d,cc}$$

Where:

$F_{clump}$ $[kN]$: Maximum tensile force the soil can absorb

$V_{clump}$ $[m^3]$: Volume of the clump of soil affected by the pile

$V_{cone}$ $[m^3]$: Volume of the cone-shaped soil at the tip of the pile

$V_{cilinder}$ $[m^3]$: Volume of the cylinder-shaped soil above the cone

$V_{pile}$ $[m^3]$: Volume of the pile shaft that is underground

$\gamma_{d,soil}$ $[kN/m^3]$: Design value for the effective specific weight of the soil;
$\gamma_{d,soil} = \gamma_{s,sat} - \gamma_w = 21 - 10.05 = 10.94 \, kN/m^3$

$\gamma_{d,cc}$ $[kN/m^3]$: Design value for the underwater weight of the pile. $\gamma_{d,cc} = 25 \, kN/m^3$

The zones of each pile cannot overlap as the soil can only absorb tensile load once. The maximum influence area of a pile is a cylindrical area with R = 3D

## *Compression piles*

The maximum locking level will be during high astronomical tide with +2.1 m NAP water level + an additional 1.5m to consider sea level rise e.g., +3.6 m NAP. The total weight of the water in the chamber that will cause maximum compression is thus:

$$W_{lock,full} = \gamma_{sw} \cdot$$

# C.2: U-Chamber, conceptual design

## C.2.1: Floor MATLAB script

```
clc;
clear variables;
close all;

%% Values
M1 = 9385.452; %[kNm]
V1 = 1038.83; %[kN]
N = 1;
E = 37*10^6; %[kN/m2]
G = 5000000; %[kN/m2] shear modulus concrete
Gp = G*1.4 %[kN/m] 1.5 uwcf thickness (shear layer)
q = -(89.49-50.47); %[kN/m]
L = 18.04; %[m]
t = 1.7; %[m]
b = 1; %[m]
I = (b*t^3)/12 %[m4]
EI = E*I;
k = 200000*b; %[kN/m2/m}
beta = (k/(4*EI))^(1/4);
%% Differential equation, kinematic and constitutive relations
syms w(x)
ODE = diff(w,x,4)-(Gp/EI)*diff(w,x,2)+4*beta^4*w == q/EI;
phi = diff(w,x); M = EI*diff(w,x,2) ; V = EI*diff(w,x,3);
%% Boundary conditions
cond1 =  M(0) == M1;
cond2 = V(0) == -V1;
cond3 = phi(L/2) == 0;
cond4 = V(L/2) == 0;
conds = [cond1,cond2,cond3,cond4];
wSol(x) = dsolve(ODE,conds);
Msol =@(x) EI*diff(wSol,x,2);
Vsol =@(x) EI*diff(wSol,x,3);

tiledlayout(2,1)
nexttile
fplot(Vsol(x),[0 L/2])
title('Shear force')
xlabel('x')
ylabel('V [kN]')

nexttile
fplot(Msol(x),[0 L/2])
title('Bending moment')
xlabel('x')
ylabel('M [kNm]')
```

**Soil**

It is necessary to verify that no tension forces are acting on the soil. In order to have no tension acting on the soil the minimum load acting on the subsoil ($\sigma_{k,min}$) needs to be larger than 0 and the maximum load acting on the subsoil ($\sigma_{k,max}$) needs to be less than the bearing capacity of the soil:

$$\sigma_{k,min} = \frac{F}{A} - \frac{M}{W} = \frac{\sum V}{b \cdot l} - \frac{\sum M}{{}^{1}/_{6} \cdot l \cdot b^2} > 0$$

$$\sigma_{k,max} = \frac{F}{A} + \frac{M}{W} = \frac{\sum V}{b \cdot l} + \frac{\sum M}{{}^{1}/_{6} \cdot l \cdot b^2} < Bearing\ capacity$$

Assuming that the U-shaped chamber is a rigid structure the bearing capacity of the soil is calculated for the width of the whole chamber, and the moment is disregarded as it is fully transmitted to the bottom slab of the chamber via reinforcement. It is assumed that the underwater concrete floor is cracked. Therefore, the uplift water pressure lifting the structure up is taken at a depth of NAP -7.1 m. the outer width of the chamber is:

$$B = B_{ch} + 2 \cdot b_{bot} = 16\ m + 2 \cdot 2.8\ m = 21.6\ m$$

As the moment can be neglected (rigid structure) the minimum load acting on the subsoil, $\sigma_{k,min}$, will always be greater than zero. The vertical force is the weight of the whole chamber, full of water. The water level within the chamber is thus taken as +10.5 m NAP as the SSB is designed to resist this water height. The sum of vertical forces is thus:

$$\sum V = \left(V_{wall} + V_{soil} + V_q\right) \cdot 2 + V_{floor} + V_{uwcf} + V_{w,ch} + V_{up} = 6589.17\ kN/m$$

Where:

| | | | |
|---|---|---|---|
| $\boldsymbol{V_{wall}}$ | [kN/m] | $= \boldsymbol{W_{wall} \cdot \gamma_{G,uf}} = \mathbf{1038.83}$ kN/m | Self-weight of one wall |
| $\boldsymbol{V_{soil}}$ | [kN/m] | $= W_{soil} \cdot \gamma_{G,uf} = 319.93$ kN/m | vertical soil force acting on an inclined wall |
| $\boldsymbol{V_q}$ | [kN/m] | $= q\left(b_{bot} - b_{top}\right)\gamma_{Q,uf} = 54$ kN/m | Vertical load from surcharge |
| $\boldsymbol{V_{floor}}$ | [kN/m] | $= B \cdot t_{floor}\gamma_{cc}\gamma_{G,uf} = 1385.10$ kN/m | Self-weight of the chamber floor |
| $\boldsymbol{V_{uwcf}}$ | [kN/m] | $= B \cdot t_{uwc}(\gamma_{uwc} - \gamma_w)\gamma_{G,uf} = 566.20$ kN/m | Self-weight of the uwc floor over the width of the chamber |
| $\boldsymbol{\gamma_{uwc}}$ | [kN/m$^3$] | = 23 kN/m$^3$ | Underwater concrete density |
| $\boldsymbol{V_{w,ch}}$ | [kN/m] | $= \left(+10.5 - (-5.2)\right)m\ NAP \cdot B_{ch}\gamma_w\gamma_{Q,uf} = 3788.82\ kN/m$ | Weight of the water inside the chamber |
| $\boldsymbol{V_{up}}$ | [kN/m] | $= -\gamma_{Q,f}\left(h_{gwl} - d - t_{floor}\right)\gamma_w B = -1976.46\ kN/m$ | Uplift force under the chamber floor |

Therefore,

$$\sigma_{k,max} = \frac{\sum V}{b \cdot l} = \frac{6589.17\ kN/m}{21.6\ m\ \cdot 1\ m} = 305.05\ kN/m^2/m$$

To guarantee that there will be no tension force acting on the soil the maximum load acting on the subsoil ($\sigma_{k,max}$) should be smaller than the bearing resistance of the soil. EN 1997-1 is used to determine the bearing capacity of the soil. To compute the bearing resistance of the subsoil, Equation D.2 from EN 1997-1 for drained conditions is used as the subsoil consists of sand:

$$R/A' = c'N_c b_c s_c i_c + q'N_q b_q s_q i_q + 0.5\gamma' B' N_\gamma b_\gamma s_\gamma i_\gamma$$

The bearing resistance depends on cohesion (c), the surcharge pressure at the level of the foundation (q) and the specific weight of the soil below the foundation (γ). Form table 31-4 in *Manual: hydraulic structures 2020*, the cohesion factor c' is zero for sand. Thus, the bearing resistance only depends on the surcharge pressure and the specific weight of the soil. The bearing resistances are determined as:

$$N_q = e^{\pi \cdot tan\varphi'} \tan^2(45 + \frac{\varphi'}{2}) = 18.40$$

$$N_\gamma = 2\big(N_q - 1\big)\tan(\varphi') = 20.09$$

Where ϕ' is the internal friction angle for sand taken as 30°. The inclination angle of the foundation of the gravity wall is α=0°:

$$b_q = b_\gamma = (1 - \alpha \cdot \tan\varphi')^2 = 1$$

To determine the shape factors for the foundation the effective width and length needs to be determined. As the gravity wall is a solid rectangular block the effective width and length are equal to the actual width and length:

$$B' = B = 21.6\, m$$

$$L' = L = 72.25\, m$$

The shape factors for a rectangular shape are therefore:

$$s_q = 1 + (B'/L')sin\varphi' = 1.15$$

$$s_\gamma = 1 - 0.3(B'/L') = 0.91$$

The inclination of the load, caused by a horizontal load H is:

$$i_q = [1 - H/(V + A'c'cot\varphi')]^m = 1$$

$$i_\gamma = [1 - H/(V + A'c'cot\varphi')]^{m+1} = 1$$

Where H is the total horizontal loads( The global structure is being considered and therefore H is taken as 0), V is the total vertical load calculated above (ΣV), and as the load H acts in parallel direction to the width B, $m = m_B = \frac{2+(B'/L')}{1+(B'/L')} = 1.77$.

The surcharge on top of the soil is q' = 20 kN/m$^2$ and the design effective weight density of the soil is:

$$\gamma' = \gamma_{s,sat} - \gamma_w = 21 - 10.06 = 10.94\, kN/m^2$$

With all the factors determined, the bearing resistance of the soil is calculated as:

$$R/A' = 2585.09\ kN/m^2 < \sigma_{k,max} = 305.05\, kN/m^2$$

The bearing resistance of the soil is greater than the maximum load acting on the subsoil. Therefore, no tension forces will be acting on the soil.

## C.2.2: Reinforcement

In order to determine the necessary reinforcement in the U-chamber all concrete covers must be known. Concrete covers, $c_{nom}$, were calculated according to EN 1992-1-1:2004.

$$c_{nom} = c_{min} + \Delta c_{dev}$$

Where $\Delta c_{dev}$ is the allowance in design for deviation and $c_{min}$ is the minimum concrete cover to be provided. The recommended value for $\Delta c_{dev}$ is 10 mm. The minimum concrete cover ensures safe transmission of bond forces, protects the reinforcement from corrosion, and provides fire resistance.

$$c_{min} = \max\{c_{min,b};\ c_{min,dur} + \Delta c_{dur,\gamma} - \Delta c_{dur,st} - \Delta c_{dur,add};\ 10\ mm\}$$

Where:

| | | |
|---|---|---|
| $\boldsymbol{c_{min,b}}$ | [mm] | Minimum cover for bond |
| $\boldsymbol{c_{min,dur}}$ | [mm] | Minimum cover for reinforcement due to the environment (durability requirement) |
| $\boldsymbol{\Delta c_{dur,\gamma}}$ | [mm] | Additive safety element, recommended as 0 mm |
| $\boldsymbol{\Delta c_{dur,st}}$ | [mm] | Reduction of minimum cover if stainless steel is used, recommended as 0 mm |
| $\boldsymbol{\Delta c_{dur,add}}$ | [mm] | Reduction of minimum cover if additional protection is used, recommended as 0 mm |

The minimum cover for bond is taken from EN 1992-1-1:2004, Table 4.2: $c_{min,b} = \emptyset$ (bar diameter). The minimum cover for durability depends on the structural class and the exposure class. Table 4.3N in EN 1992-1-1:2004 shown here below is used to determine the structural class. This Table only allows for a maximum lifetime of 100 years where the structural class is increased by two compared to the base structural class S4 for a structure with a 50 year lifetime. Since the Lock chamber will have a 150 year lifetime it is assumed that the structural class may be increased by three. The member will not be considered to have slab geometry as the position of reinforcement is likely to be affected by the construction process as it is cast in situ. Special quality control can be ensured during the concrete production and thus the structural class can be reduced by a further 1. For C50/60 concrete this results in a final structural class of S5 for all chamber elements.

| **Structural Class** | | | | | | | |
|---|---|---|---|---|---|---|---|
| **Criterion** | **Exposure Class according to Table 4.1** | | | | | | |
| | X0 | XC1 | XC2 / XC3 | XC4 | XD1 | XD2 / XS1 | XD3 / XS2 / XS3 |
| Design Working Life of 100 years | increase class by 2 | increase class by 2 | increase class by 2 | increase class by 2 | increase class by 2 | increase class by 2 | increase class by 2 |
| Strength Class [1) 2)] | ≥ C30/37 reduce class by 1 | ≥ C30/37 reduce class by 1 | ≥ C35/45 reduce class by 1 | ≥ C40/50 reduce class by 1 | ≥ C40/50 reduce class by 1 | ≥ C40/50 reduce class by 1 | ≥ C45/55 reduce class by 1 |
| Member with slab geometry (position of reinforcement not affected by construction process) | reduce class by 1 | reduce class by 1 | reduce class by 1 | reduce class by 1 | reduce class by 1 | reduce class by 1 | reduce class by 1 |
| Special Quality Control of the concrete production ensured | reduce class by 1 | reduce class by 1 | reduce class by 1 | reduce class by 1 | reduce class by 1 | reduce class by 1 | reduce class by 1 |

The minimum cover due to environmental conditions can then be found using table 4.4N in EN 1992-1-1:2004 shown here below:

Table 4.4N: Values of minimum cover, $c_{min,dur}$, requirements with regard to durability for reinforcement steel in accordance with EN 10080.

| Environmental Requirement for $c_{min,dur}$ (mm) | | | | | | | |
|---|---|---|---|---|---|---|---|
| Structural Class | Exposure Class according to Table 4.1 | | | | | | |
| | X0 | XC1 | XC2 / XC3 | XC4 | XD1 / XS1 | XD2 / XS2 | XD3 / XS3 |
| S1 | 10 | 10 | 10 | 15 | 20 | 25 | 30 |
| S2 | 10 | 10 | 15 | 20 | 25 | 30 | 35 |
| S3 | 10 | 10 | 20 | 25 | 30 | 35 | 40 |
| S4 | 10 | 15 | 25 | 30 | 35 | 40 | 45 |
| S5 | 15 | 20 | 30 | 35 | 40 | 45 | 50 |
| S6 | 20 | 25 | 35 | 40 | 45 | 50 | 55 |

The bottom of the floor slab will be cast against and uneven surface (UWCF) and thus the minimum cover is increased by at least 5 mm there and $c_{min}$ must be at least 40 mm when the concrete is cast against prepared ground (UWCF). Exposure classes and concrete covers for different parts of the ship lock chamber and different concrete classes are presented in Table 51, and 52 below

Table 51: concrete covers for different parts of the ship lock chamber C50/60

| Chamber part | Conditions | Exposure class | Concrete cover; c [mm] |
|---|---|---|---|
| *Wall outside of the chamber (soil contact)* | Wet, rarely dry | XC2 | 42 |
| *Wall, inside chamber, submerged* | Sea water, permanently submerged | XS2 | 55 |
| *Wall, inside chamber, above minimum locking level* | Sea water, tidal splash zone | XS3 | 60 |
| *Top of wall* | Carbonation, cyclic wet & dry | XC4 | 45 |
| *Top of floor slab* | Sea water, permanently submerged | XS2 | 55 |
| *Bottom of floor slab* | Wet, rarely dry, cast on uneven | XC2 | 45 |

Table 52 concrete covers for different parts of the ship lock chamber C35/45

| Chamber part | Conditions | Exposure/ structural class | Concrete cover; c [mm] |
|---|---|---|---|
| *Wall outside of the chamber (soil contact)* | Wet, rarely dry | XC2 / S5 | 42 |
| *Wall, inside chamber, submerged* | Sea water, permanently submerged | XS2 / S6 | 60 |
| *Wall, inside chamber, above minimum locking level* | Sea water, tidal splash zone | XS3 / S6 | 65 |
| *Top of wall* | Carbonation, cyclic wet & dry | XC4 / S6 | 50 |
| *Top of floor slab* | Sea water, permanently submerged | XS2 / S6 | 60 |
| *Bottom of floor slab* | Wet, rarely dry, cast on uneven | XC2 / S5 | 50 |

| Chamber part | Conditions | Exposure/ structural class | Concrete cover; c [mm] |
|---|---|---|---|
| *Wall outside of the chamber (soil contact)* | Wet, rarely dry | XC2 / S5 | 45 |
| *Wall, inside chamber, submerged* | Sea water, permanently submerged | XS2 / S6 | 60 |
| *Wall, inside chamber, above minimum locking level* | Sea water, tidal splash zone | XS3 / S6 | 65 |

| | | | |
|---|---|---|---|
| *Top of wall* | Carbonation, cyclic wet & dry | XC4 / S6 | 50 |
| *Top of floor slab* | Sea water, permanently submerged | XS2 / S6 | 60 |
| *Bottom of floor slab* | Wet, rarely dry, cast on uneven | XC2 / S5 | 50 |

**Lap- and anchorage lengths**

Anchorage length is provided so that the bond forces are safely transmitted to the concrete, avoiding longitudinal cracking or spalling. To prevent bond failure the ultimate bond strength must be sufficient. The design value of the ultimate bond stress for ribbed bars can be calculated according to EN1992-1-1 8.4.2(2):

$$f_{bd} = 2.25\eta_1\eta_2 f_{ctd}$$

Where:

| | | |
|---|---|---|
| $\eta_1$ | [-] | Coefficient related to the quality of the bond condition and the position of the bar during concreting. $\eta_1 = 1$ for good conditions and $\eta_1 = 0.7$ for all other cases. |
| $\eta_2$ | [-] | Coefficient related to the bar diameter. $\eta_2 = 1$ for $\emptyset \leq 32\ mm$ and $\eta_2 = \frac{132-\emptyset}{100}$ for $\emptyset > 32\ mm$ |
| $f_{ctd}$ | [MPa] | Design value of concrete tensile strength, $f_{ctd} = 1.64$ for 40/50 concrete |

Assuming Good bond conditions and a bar diameter $\emptyset \leq 32$, $f_{bd} = 3.69$ MPa. The design anchorage length is calculated according to EN1992-1-1 8.4.4(1):

$$l_{bd} = \alpha_1\alpha_2\alpha_3\alpha_4\alpha_5 l_{b,rqd} \geq l_{b,min}$$

Where:

| | | |
|---|---|---|
| $l_{b,rqd}$ | [mm] | Basic required anchorage length: $l_{b,rqd} = \frac{\emptyset}{4}\frac{\sigma_{sd}}{f_{bd}}$ |
| $\sigma_{sd}$ | [MPa] | Design steel stress. Maximum value under USL loads is equal to $f_{yd}$ = 435 MPa |
| $\emptyset$ | [mm] | Bar diameter |
| $f_{bd}$ | [MPa] | Design value of the ultimate bond stress for ribbed bars |
| $\alpha_1$ | [-] | Coefficient accounting for the effect of the shape of the bar |
| $\alpha_2$ | [-] | Coefficient accounting for the effect of minimum concrete cover |
| $\alpha_3$ | [-] | Coefficient accounting for the effect of confinement by transverse reinforcement not welded to main reinforcement |
| $\alpha_4$ | [-] | Coefficient accounting for the influence of one or more welded transverse bars along the design anchorage length |
| $\alpha_5$ | [-] | Coefficient accounting for the effect of confinement by transverse pressure, taken conservatively as $\alpha_5 = 1$ |

The $\alpha$ values can be determined using Table 53. Values for K (to calculate $\alpha_3$) are shown in Figure 69.

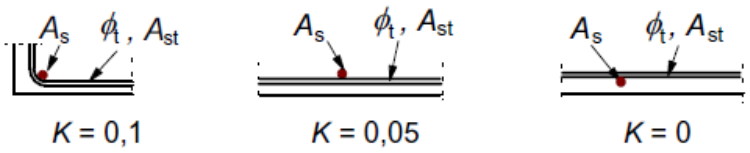


**Figure 69: Values of K for beams and slabs**

Flexural reinforcement in the walls and floor is the outer most bars and therefore K = 0 for those. For the transverse reinforcement K = 0.05. $\Sigma A_{st}$ (explained in Table 53) is determined as:

$$\sum A_{st} = \frac{\pi \emptyset_t^2}{4} \cdot \frac{l_{bd}}{s}$$

Where $\emptyset_t$ is the diameter of the transverse reinforcement and s is the center-to-center distance between the transverse rebars. Both the walls and the floor are modelled as slabs and therefore $\Sigma A_{st,min} = 0$ for the anchorage length. $c_d$ is determined using Figure 70:

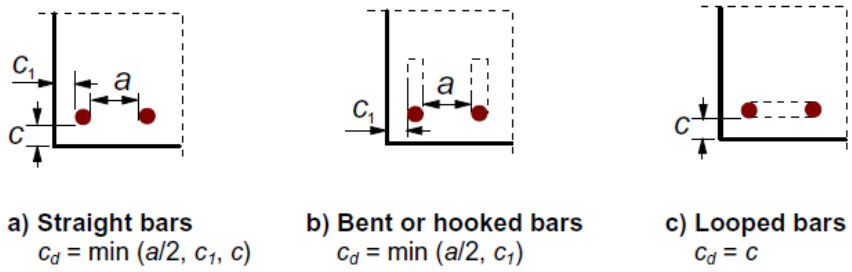


**Figure 70: Values of $c_d$ for beams and slabs**

**Table 53: Values of $\alpha_1$, $\alpha_2$, $\alpha_3$, $\alpha_4$, and $\alpha_5$ coefficients**

| Influencing factor | Type of anchorage | Reinforcement bar | |
|---|---|---|---|
| | | In tension | In compression |
| Shape of bars | Straight | $\alpha_1 = 1,0$ | $\alpha_1 = 1,0$ |
| | Other than straight (see Figure 8.1 (b), (c) and (d) | $\alpha_1 = 0,7$ if $c_d > 3\phi$ otherwise $\alpha_1 = 1,0$ (see Figure 8.3 for values of $c_d$) | $\alpha_1 = 1,0$ |
| Concrete cover | Straight | $\alpha_2 = 1 - 0,15\,(c_d - \phi)/\phi$ $\geq 0,7$ $\leq 1,0$ | $\alpha_2 = 1,0$ |
| | Other than straight (see Figure 8.1 (b), (c) and (d)) | $\alpha_2 = 1 - 0,15\,(c_d - 3\phi)/\phi$ $\geq 0,7$ $\leq 1,0$ (see Figure 8.3 for values of $c_d$) | $\alpha_2 = 1,0$ |
| Confinement by transverse reinforcement not welded to main reinforcement | All types | $\alpha_3 = 1 - K\lambda$ $\geq 0,7$ $\leq 1,0$ | $\alpha_3 = 1,0$ |
| Confinement by welded transverse reinforcement* | All types, position and size as specified in Figure 8.1 (e) | $\alpha_4 = 0,7$ | $\alpha_4 = 0,7$ |
| Confinement by transverse pressure | All types | $\alpha_5 = 1 - 0,04p$ $\geq 0,7$ $\leq 1,0$ | - |

where:

$\lambda$ = $(\Sigma A_{st} - \Sigma A_{st,min})/ A_s$

$\Sigma A_{st}$ cross-sectional area of the transverse reinforcement along the design anchorage length $l_{bd}$

$\Sigma A_{st,min}$ cross-sectional area of the minimum transverse reinforcement = 0,25 $A_s$ for beams and 0 for slabs

$A_s$ area of a single anchored bar with maximum bar diameter

$p$ transverse pressure [MPa] at ultimate limit state along $l_{bd}$

Production and transport of reinforcement rebars limits the length of the bars. The length is mostly limited by the maximum hauling length for the transport. Usually, the maximum length of rebars is 12 m (Autodesk Support, 2019). As the length of the chamber is 72.25 m and the height of the chamber walls is 16.2 m it is evident that rebars must overlap to span the whole length/height. To ensure safe and efficient transfer of

load from one bar to another a certain lap length needs to be provided for the overlapping of two bars. Design lap length can be calculated according to EN1992-1-1 8.7.3(1):

$$l_0 = \alpha_1\alpha_2\alpha_3\alpha_5\alpha_6 l_{b,rqd} \geq l_{0,min}$$

Where values for $\alpha_1$, $\alpha_2$, $\alpha_3$, and, $\alpha_5$ can be taken from Table 53, except that for the calculation of $\alpha_3$, $\sum A_{st,min}$ should be taken as $A_s(\sigma_{sd}/f_{yd})$, with $A_s$ = area of one lapped bar. $\alpha_6$ accounts for the percentage $\rho_1$ of reinforcement bars lapped within $\pm 0.65 l_0$ from the center of the lap length considered. Table 8.3 in EN1992-1-1 8.7.3(1) gives values for the coefficient $\alpha_6$. Assuming 50% lapped bars relative to the total cross section area gives $\alpha_6 = 1.4$. $l_{b,rqd}$ is calculated and $l_{0,min} = \max\begin{pmatrix} 0.3\alpha_6 l_{b,rqd}; \\ 15\emptyset; 200\ mm \end{pmatrix}$. For secondary reinforcement, minimum lap lengths are given in a table in EN1992-1-1 8.7.5.2. The lap lengths are however only given for a 12 mm rebar diameter and smaller (see Table 54). The secondary reinforcement in the base case design ranges from 12 mm to 25 mm and therefore some assumptions have to be made for the larger diameter secondary reinforcement. As can be seen in Table 54, the increment in lap length between groups is 100 mm. It is therefore assumed that this holds for further increment of the bar diameters. Lap lengths of the secondary reinforcement are shown in table below.

**Table 54: Minimum required lap lengths of secondary reinforcement**

| Diameter of secondary wires (mm) | Lap lengths |
|---|---|
| $\phi \leq 6$ | ≥ 150 mm; at least 1 wire pitch within the lap length |
| $6 < \phi \leq 8{,}5$ | ≥ 250 mm; at least 2 wire pitches |
| $8{,}5 < \phi \leq 12$ | ≥ 350 mm; at least 2 wire pitches |

| DIAMETER OF SECONDARY REINFORCEMENT | LAP LENGTH |
|---|---|
| 12 mm | 350 mm |
| 16 mm | 450 mm |
| 20 mm | 550 mm |
| 25 mm | 650 mm |

A design aid is provided by EurocodeApplied.com and will be used here to determine all lap and anchorage lengths. The results are shown in Table 55 to Table 57. Good bond conditions are for all of the bars in the wall as well as the bottom bars in the floor. Top bars in the floor have a poor bond condition (see Figure 71).

**Table 55: Design anchorage length $l_{bd}$ and lap length $l_0$ for ribbed bars Ø ≤ 30 mm according to EN1992-1-1 using EurocodeApplied.com for concrete class C50/60**

| Bar diameter [mm] | Bond condition | Loading | Shape | $l_{bd}$ [mm] | $l_0$ [mm] |
|---|---|---|---|---|---|
| **32** | Good | Tension/compression | Straight & bent in comp. | 832 | 1248 |
| **32** | Good | tension | Bent | 576 | 864 |
| **32** | Poor | Tension/compression | Straight & bent in comp. | 1184 | 1760 |
| **32** | Poor | tension | Bent in tension | 832 | 1248 |
| **25** | Good | Tension/compression | Straight & bent in comp. | 650 | 975 |
| **25** | Good | tension | Bent | 450 | 675 |
| **25** | Poor | Tension/compression | Straight & bent in comp. | 925 | 1375 |
| **25** | Poor | tension | Bent in tension | 650 | 975 |
| **20** | Good | Tension/compression | Straight & bent in comp. | 520 | 780 |
| **20** | Good | tension | Bent | 360 | 540 |
| **20** | Poor | Tension/compression | Straight & bent in comp. | 740 | 1100 |

| | | | | | |
|---|---|---|---|---|---|
| **20** | Poor | tension | Bent in tension | 520 | 780 |
| **16** | Good | Tension/compression | Straight & bent in comp. | 416 | 624 |
| **16** | Good | tension | Bent | 288 | 432 |
| **16** | Poor | Tension/compression | Straight & bent in comp. | 592 | 880 |
| **16** | Poor | tension | Bent in tension | 416 | 624 |
| **12** | Good | Tension/compression | Straight & bent in comp. | 312 | 468 |
| **12** | Good | tension | Bent | 216 | 324 |
| **12** | Poor | Tension/compression | Straight & bent in comp. | 444 | 660 |
| **12** | Poor | tension | Bent in tension | 312 | 468 |
| **10** | Good | Tension/compression | Straight & bent in comp. | 260 | 390 |
| **10** | Good | tension | Bent | 180 | 270 |
| **10** | Poor | Tension/compression | Straight & bent in comp. | 370 | 550 |
| **10** | Poor | tension | Bent in tension | 260 | 390 |
| **8** | Good | Tension/compression | Straight & bent in comp. | 208 | 312 |
| **8** | Good | tension | Bent | 144 | 216 |
| **8** | Poor | Tension/compression | Straight & bent in comp. | 296 | 424 |
| **8** | Poor | tension | Bent in tension | 208 | 312 |

**Table 56: Design anchorage length $l_{bd}$ and lap length $l_0$ for ribbed bars Ø ≤ 30 mm according to EN1992-1-1 using EurocodeApplied.com for concrete class C35/45**

| Bar diameter [mm] | Bond condition | loading | shape | $l_{bd}$ [mm] | $l_0$ [mm] |
|---|---|---|---|---|---|
| **32** | Good | Tension/compression | Straight & bent in comp. | 1056 | 1568 |
| **32** | Good | tension | Bent | 736 | 1088 |
| **32** | Poor | Tension/compression | Straight & bent in comp. | 1504 | 2240 |
| **32** | Poor | tension | Bent in tension | 1056 | 1568 |
| **25** | Good | Tension/compression | Straight & bent in comp. | 825 | 1225 |
| **25** | Good | tension | Bent | 575 | 850 |
| **25** | Poor | Tension/compression | Straight & bent in comp. | 1175 | 1750 |
| **25** | Poor | tension | Bent in tension | 825 | 1225 |
| **20** | Good | Tension/compression | Straight & bent in comp. | 660 | 980 |
| **20** | Good | tension | Bent | 460 | 680 |
| **20** | Poor | Tension/compression | Straight & bent in comp. | 940 | 1400 |
| **20** | Poor | tension | Bent in tension | 660 | 980 |
| **16** | Good | Tension/compression | Straight & bent in comp. | 528 | 784 |
| **16** | Good | tension | Bent | 368 | 544 |
| **16** | Poor | Tension/compression | Straight & bent in comp. | 752 | 1120 |
| **16** | Poor | tension | Bent in tension | 528 | 784 |
| **12** | Good | Tension/compression | Straight & bent in comp. | 396 | 588 |
| **12** | Good | tension | Bent | 276 | 408 |
| **12** | Poor | Tension/compression | Straight & bent in comp. | 564 | 840 |
| **12** | Poor | tension | Bent in tension | 396 | 588 |
| **10** | Good | Tension/compression | Straight & bent in comp. | 330 | 490 |
| **10** | Good | tension | Bent | 230 | 340 |
| **10** | Poor | Tension/compression | Straight & bent in comp. | 470 | 700 |
| **10** | Poor | tension | Bent in tension | 330 | 490 |
| **8** | Good | Tension/compression | Straight & bent in comp. | 264 | 392 |
| **8** | Good | tension | Bent | 184 | 272 |
| **8** | Poor | Tension/compression | Straight & bent in comp. | 376 | 560 |
| **8** | Poor | tension | Bent in tension | 264 | 392 |

**Table 57: Design anchorage length $l_{bd}$ and lap length $l_0$ for ribbed bars Ø ≤ 30 mm according to EN1992-1-1 using EurocodeApplied.com for concrete class C25/30**

| Bar diameter [mm] | Bond condition | loading | shape | $l_{bd}$ [mm] | $l_0$ [mm] |
|---|---|---|---|---|---|

| | | | | | |
|---|---|---|---|---|---|
| **32** | Good | Tension/compression | Straight & bent in comp. | 1312 | 1952 |
| **32** | Good | tension | Bent | 928 | 1376 |
| **32** | Poor | Tension/compression | Straight & bent in comp. | 1856 | 2784 |
| **32** | Poor | tension | Bent in tension | 1312 | 1952 |
| **25** | Good | Tension/compression | Straight & bent in comp. | 1025 | 1525 |
| **25** | Good | tension | Bent | 725 | 1075 |
| **25** | Poor | Tension/compression | Straight & bent in comp. | 1450 | 2175 |
| **25** | Poor | tension | Bent in tension | 1025 | 1525 |
| **20** | Good | Tension/compression | Straight & bent in comp. | 820 | 1220 |
| **20** | Good | tension | Bent | 580 | 860 |
| **20** | Poor | Tension/compression | Straight & bent in comp. | 1160 | 1740 |
| **20** | Poor | tension | Bent in tension | 820 | 1220 |
| **16** | Good | Tension/compression | Straight & bent in comp. | 656 | 976 |
| **16** | Good | tension | Bent | 464 | 688 |
| **16** | Poor | Tension/compression | Straight & bent in comp. | 928 | 1392 |
| **16** | Poor | tension | Bent in tension | 656 | 976 |
| **12** | Good | Tension/compression | Straight & bent in comp. | 492 | 732 |
| **12** | Good | tension | Bent | 348 | 516 |
| **12** | Poor | Tension/compression | Straight & bent in comp. | 696 | 1044 |
| **12** | Poor | tension | Bent in tension | 492 | 732 |
| **10** | Good | Tension/compression | Straight & bent in comp. | 410 | 610 |
| **10** | Good | tension | Bent | 290 | 430 |
| **10** | Poor | Tension/compression | Straight & bent in comp. | 580 | 870 |
| **10** | Poor | tension | Bent in tension | 410 | 610 |
| **8** | Good | Tension/compression | Straight & bent in comp. | 328 | 488 |
| **8** | Good | tension | Bent | 232 | 344 |
| **8** | Poor | Tension/compression | Straight & bent in comp. | 464 | 696 |
| **8** | Poor | tension | Bent in tension | 328 | 488 |

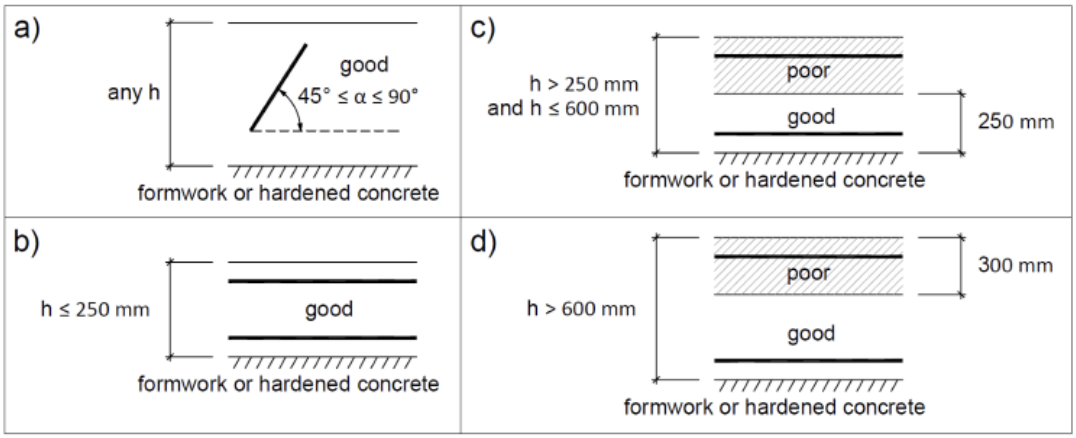


**Figure 71: Definition of good and poor bond conditions according to EN1992-1-1**

Reinforcement detailing for the base case chamber is presented in the tables below

**Table 58: Required reinforcement area for a given moment and its resulting bar diameter and c/c distance for the center lock head**

| **Vertical wall reinforcement** | **M [kNm]** | **$A_{s1}$ [mm²]** | **$Ø_{bar}$ [mm]** | **c/c [mm]** | **No. rows** |
|---|---|---|---|---|---|
| *Tension bottom primary* | 9385.5 | 8606.0 | 32 | 170 | 2 |
| *Tension bottom transverse* | [-] | 1721.2 | 16 | 220 | 2 |
| *Tension NAP +0.8 m primary* | 2590 | 4515.0 | 25 | 210 | 2 |
| *Tension NAP +0.8 m primary* | [-] | 935.0 | 12 | 220 | 2 |
| *Compression bottom primary* | 9385.5 | 5585.2 | 32 | 140 | 1 |
| *Compression bottom transverse* | [-] | 1117.0 | 16 | 180 | 1 |

| | | | | | |
|---|---|---|---|---|---|
| *Compression NAP +0.8 m primary* | 2590 | 3873.0 | 25 | 120 | 1 |
| *Compression NAP +0.8 m primary* | [-] | 774.6 | 16 | 260 | 1 |

| **Floor bottom reinforcement** | **M [kNm]** | **$A_{s1}$ [mm²]** | **$Ø_{bar}$ [mm]** | **c/c [mm]** | **No. rows** |
|---|---|---|---|---|---|
| *Edges primary* | 9385.5 | 13575.8 | 32 | 110 | 2 |
| *Edges transvers* | [-] | 2924.5 | 20 | 200 | 2 |
| *X = 3 primary* | 6446.6 | 10329.5 | 32 | 110 | 2 |
| *X = 3 transverse* | [-] | 2065.9 | 12 | 100 | 2 |
| *Center primary* | 4656.4 | 7325.5 | 25 | 110 | 2 |
| *Center transverse* | [-] | 1465.1 | 16 | 200 | 2 |

| **Floor top reinforcement** | **M [kNm]** | **$A_{s1}$ [mm²]** | **$Ø_{bar}$ [mm]** | **c/c [mm]** | |
|---|---|---|---|---|---|
| *Compression top* | [-] | 3597.9 | 32 | 220 | 1 |
| *Transverse top* | [-] | 719.6 | 16 | 270 | 1 |

**Table 59: Required reinforcement area for a given moment and its resulting bar diameter and c/c distance for wall 8**

| **Vertical wall reinforcement** | **M [kNm]** | **$A_{s1}$ [mm²]** | **$Ø_{bar}$ [mm]** | **c/c [mm]** | **No. rows** |
|---|---|---|---|---|---|
| *Tension bottom primary* | 8515.8 | 8042.5 | 32 | 200 | 2 |
| *Tension bottom transverse* | [-] | 1543.3 | 16 | 260 | 2 |
| *Tension NAP +0.8 m primary* | 2200.0 | 4308.3 | 25 | 200 | 2 |
| *Tension NAP +0.8 m primary* | [-] | 861.7 | 12 | 260 | 2 |
| *Compression bottom primary* | 8515.8 | 5369.3 | 32 | 140 | 1 |
| *Compression bottom transverse* | [-] | 1073.9 | 16 | 180 | 1 |
| *Compression NAP +0.8 m primary* | 2200.0 | 3499.5 | 25 | 140 | 1 |
| *Compression NAP +0.8 m primary* | [-] | 699.9 | 12 | 160 | 1 |

| **Floor bottom reinforcement** | **M [kNm]** | **$A_{s1}$ [mm²]** | **$Ø_{bar}$ [mm]** | **c/c [mm]** | **No. rows** |
|---|---|---|---|---|---|
| *Edges primary* | 8515.8 | 11414.7 | 32 | 120 | 2 |
| *Edges transvers* | [-] | 2282.9 | 20 | 200 | 2 |
| *X = 3 primary* | 5500.0 | 8141.5 | 25 | 120 | 2 |
| *X = 3 transverse* | [-] | 1628.3 | 12 | 100 | 2 |
| *Center primary* | 3500.0 | 5096.0 | 20 | 120 | 2 |
| *Center transverse* | [-] | 1019.2 | 12 | 200 | 2 |

| **Floor top reinforcement** | **M [kNm]** | **$A_{s1}$ [mm²]** | **$Ø_{bar}$ [mm]** | **c/c [mm]** | |
|---|---|---|---|---|---|
| *Compression top* | [-] | 3597.9 | 32 | 220 | 1 |
| *Transverse top* | [-] | 719.6 | 16 | 270 | 1 |

**Table 60: Required reinforcement area for a given moment and its resulting bar diameter and c/c distance for wall 6 & 7**

| **Vertical wall reinforcement** | **M [kNm]** | **$A_{s1}$ [mm²]** | **$Ø_{bar}$ [mm]** | **c/c [mm]** | **No. rows** |
|---|---|---|---|---|---|
| *Tension bottom primary* | 7308.4 | 7861.9 | 32 | 200 | 2 |
| *Tension bottom transverse* | [-] | 1572.4 | 16 | 250 | 2 |
| *Tension NAP +0.8 m primary* | 1690.0 | 3752.6 | 20 | 160 | 2 |
| *Tension NAP +0.8 m primary* | [-] | 750.5 | 12 | 300 | 2 |

| | | | | | |
|---|---|---|---|---|---|
| *Compression bottom primary* | 7308.4 | 4522.7 | 32 | 170 | 1 |
| *Compression bottom transverse* | [-] | 904.5 | 16 | 220 | 1 |
| *Compression NAP +0.8 m primary* | 1690.0 | 2857.1 | 25 | 170 | 1 |
| *Compression NAP +0.8 m primary* | [-] | 577.5 | 12 | 190 | 1 |

| **Floor bottom reinforcement** | **M [kNm]** | **$A_{s1}$ [mm²]** | **$Ø_{bar}$ [mm]** | **c/c [mm]** | **No. rows** |
|---|---|---|---|---|---|
| *Edges primary* | 7308.4 | 9909.0 | 32 | 160 | 2 |
| *Edges transvers* | [-] | 1981.8 | 16 | 200 | 2 |
| *X = 3 primary* | 4715.0 | 6926.7 | 20 | 80 | 2 |
| *X = 3 transverse* | [-] | 1385.3 | 10 | 100 | 2 |
| *Center primary* | 3000.0 | 4346.7 | 16 | 80 | 2 |
| *Center transverse* | [-] | 869.3 | 12 | 200 | 2 |

| **Floor top reinforcement** | **M [kNm]** | **$A_{s1}$ [mm²]** | **$Ø_{bar}$ [mm]** | **c/c [mm]** | |
|---|---|---|---|---|---|
| *Compression top* | [-] | | | | 1 |
| *Transverse top* | [-] | | | | 1 |

**Table 61: Required reinforcement area for a given moment and its resulting bar diameter and c/c distance for wall 4 & 5**

| **Vertical wall reinforcement** | **M [kNm]** | **$A_{s1}$ [mm²]** | **$Ø_{bar}$ [mm]** | **c/c [mm]** | **No. rows** |
|---|---|---|---|---|---|
| *Tension bottom primary* | 5871.7 | 8245.6 | 32 | 190 | 2 |
| *Tension bottom transverse* | [-] | 1649.1 | 16 | 240 | 2 |
| *Tension NAP +0.8 m primary* | 1180.0 | 3204.7 | 20 | 190 | 2 |
| *Tension NAP +0.8 m primary* | [-] | 683.0 | 10 | 230 | 2 |
| *Compression bottom primary* | 5871.7 | 3464.5 | 32 | 230 | 1 |
| *Compression bottom transverse* | [-] | 692.9 | 12 | 160 | 1 |
| *Compression NAP +0.8 m primary* | 1180 | 2491.8 | 25 | 190 | 1 |
| *Compression NAP +0.8 m primary* | [-] | 498.4 | 10 | 160 | 1 |

| **Floor bottom reinforcement** | **M [kNm]** | **$A_{s1}$ [mm²]** | **$Ø_{bar}$ [mm]** | **c/c [mm]** | **No. rows** |
|---|---|---|---|---|---|
| *Edges primary* | 5871.7 | 8029.0 | 25 | 110 | 2 |
| *Edges transvers* | [-] | 1605.8 | 16 | 200 | 2 |
| *X = 3 primary* | 3795.0 | 5537.4 | 20 | 110 | 2 |
| *X = 3 transverse* | [-] | 1107.5 | 12 | 200 | 2 |
| *Center primary* | 2435.0 | 3809.5 | 20 | 110 | 2 |
| *Center transverse* | [-] | 761.9 | 10 | 200 | 2 |

| **Floor top reinforcement** | **M [kNm]** | **$A_{s1}$ [mm²]** | **$Ø_{bar}$ [mm]** | **c/c [mm]** | |
|---|---|---|---|---|---|
| *Compression top* | [-] | 3597.9 | 32 | 220 | 1 |
| *Transverse top* | [-] | 719.6 | 16 | 270 | 1 |

**Table 62: Required reinforcement area for a given moment and its resulting bar diameter and c/c distance for wall 2 & 3**

| **Vertical wall reinforcement** | **M [kNm]** | **$A_{s1}$ [mm²]** | **$Ø_{bar}$ [mm]** | **c/c [mm]** | **No. rows** |
|---|---|---|---|---|---|
| *Tension bottom primary* | 4631.3 | 8606.9 | 32 | 180 | 2 |
| *Tension bottom transverse* | [-] | 1721.4 | 16 | 230 | 2 |

| | | | | | |
|---|---|---|---|---|---|
| *Tension NAP +0.8 m primary* | 820.0 | 2094.0 | 16 | 180 | 2 |
| *Tension NAP +0.8 m primary* | [-] | 446.8 | 8 | 220 | 2 |
| *Compression bottom primary* | 4631.3 | 2618.0 | 25 | 180 | 1 |
| *Compression bottom transverse* | [-] | 523.6 | 10 | 140 | 1 |
| *Compression NAP +0.8 m primary* | 820.0 | 2116.4 | 25 | 180 | 1 |
| *Compression NAP +0.8 m primary* | [-] | 423.3 | 10 | 180 | 1 |

| **Floor bottom reinforcement** | **M [kNm]** | **$A_{s1}$ [mm²]** | **$Ø_{bar}$ [mm]** | **c/c [mm]** | **No. rows** |
|---|---|---|---|---|---|
| *Edges primary* | 4631.3 | 6367.3 | 25 | 140 | 2 |
| *Edges transvers* | [-] | 1273.5 | 10 | 100 | 2 |
| *X = 3 primary* | 2995.0 | 4344.9 | 20 | 140 | 2 |
| *X = 3 transverse* | [-] | 869.0 | 12 | 200 | 2 |
| *Center primary* | 1915.0 | 3809.5 | 20 | 140 | 2 |
| *Center transverse* | [-] | 761.9 | 10 | 200 | 2 |

| **Floor top reinforcement** | **M [kNm]** | **$A_{s1}$ [mm²]** | **$Ø_{bar}$ [mm]** | **c/c [mm]** | |
|---|---|---|---|---|---|
| *Compression top* | [-] | 3597.9 | 32 | 220 | 1 |
| *Transverse top* | [-] | 719.6 | 16 | 270 | 1 |

**Table 63: Required reinforcement area for a given moment and its resulting bar diameter and c/c distance for seaside wall 1**

| **Vertical wall reinforcement** | **M [kNm]** | **$A_{s1}$ [mm²]** | **$Ø_{bar}$ [mm]** | **c/c [mm]** | **No. rows** |
|---|---|---|---|---|---|
| *Tension bottom primary* | 3724.0 | 8255.5 | 32 | 180 | 2 |
| *Tension bottom transverse* | [-] | 1651.1 | 16 | 240 | 2 |
| *Tension NAP +0.8 m primary* | 568.0 | 2216.2 | 16 | 180 | 2 |
| *Tension NAP +0.8 m primary* | [-] | 443.2 | 8 | 220 | 2 |
| *Compression bottom primary* | 3724.0 | 2194.7 | 25 | 220 | 1 |
| *Compression bottom transverse* | [-] | 438.9 | 12 | 250 | 1 |
| *Compression NAP +0.8 m primary* | 568.0 | 1689.7 | 20 | 180 | 1 |
| *Compression NAP +0.8 m primary* | [-] | 337.9 | 10 | 230 | 1 |

| **Floor bottom reinforcement** | **M [kNm]** | **$A_{s1}$ [mm²]** | **$Ø_{bar}$ [mm]** | **c/c [mm]** | **No. rows** |
|---|---|---|---|---|---|
| *Edges primary* | 3724.0 | 5812.9 | 25 | 180 | 2 |
| *Edges transvers* | [-] | 1162.6 | 12 | 200 | 2 |
| *X = 3 primary* | 2450.0 | 3782.6 | 20 | 170 | 2 |
| *X = 3 transverse* | [-] | 756.5 | 10 | 200 | 2 |
| *Center primary* | 1580.0 | 3597.9 | 20 | 170 | 2 |
| *Center transverse* | [-] | 719.6 | 10 | 200 | 2 |

| **Floor top reinforcement** | **M [kNm]** | **$A_{s1}$ [mm²]** | **$Ø_{bar}$ [mm]** | **c/c [mm]** | |
|---|---|---|---|---|---|
| *Compression top* | [-] | 3597.9 | 32 | 220 | 1 |
| *Transverse top* | [-] | 719.6 | 16 | 270 | 1 |

**Table 64: Required reinforcement area for a given moment and its resulting bar diameter and c/c distance for wall 9, 10, & 11**

| **Vertical wall reinforcement** | **M [kNm]** | **$A_{s1}$ [mm²]** | **$Ø_{bar}$ [mm]** | **c/c [mm]** | **No. rows** |
|---|---|---|---|---|---|

| | | | | | |
|---|---|---|---|---|---|
| *Tension bottom primary* | 3310.3 | 6693.0 | 32 | 110 | 1 |
| *Tension bottom transverse* | [-] | 1338.6 | 20 | 220 | 1 |
| *Tension NAP +0.8 m primary* | 434.0 | 1133.9 | 20 | 140 | 1 |
| *Tension NAP +0.8 m primary* | [-] | 424.7 | 12 | 260 | 1 |
| *Compression bottom primary* | 3310.3 | 2406.3 | 25 | 200 | 1 |
| *Compression bottom transverse* | [-] | 481.3 | 12 | 230 | 1 |
| *Compression NAP +0.8 m primary* | 434.0 | 2123.3 | 20 | 140 | 1 |
| *Compression NAP +0.8 m primary* | [-] | 424.7 | 10 | 180 | 1 |

| **Floor bottom reinforcement** | **M [kNm]** | **$A_{s1}$ [mm²]** | **$Ø_{bar}$ [mm]** | **c/c [mm]** | **No. rows** |
|---|---|---|---|---|---|
| *Edges primary* | 3310.3 | 5147.2 | 25 | 170 | 2 |
| *Edges transvers* | [-] | 1029.4 | 8 | 100 | 2 |
| *X = 3 primary* | 2250.0 | 3468.2 | 20 | 170 | 2 |
| *X = 3 transverse* | [-] | 719.6 | 10 | 200 | 2 |
| *Center primary* | 1400.0 | 2143.4 | 20 | 170 | 2 |
| *Center transverse* | [-] | 719.6 | 10 | 200 | 2 |

| **Floor top reinforcement** | **M [kNm]** | **$A_{s1}$ [mm²]** | **$Ø_{bar}$ [mm]** | **c/c [mm]** | |
|---|---|---|---|---|---|
| *Compression top* | [-] | 3597.9 | 32 | 220 | 1 |
| *Transverse top* | [-] | 719.6 | 16 | 270 | 1 |

**Table 65: Required reinforcement area for a given moment and its resulting bar diameter and c/c distance for wall 12 & 13**

| **Vertical wall reinforcement** | **M [kNm]** | **$A_{s1}$ [mm²]** | **$Ø_{bar}$ [mm]** | **c/c [mm]** | **No. rows** |
|---|---|---|---|---|---|
| *Tension bottom primary* | 2231.0 | 6958.9 | 32 | 110 | 1 |
| *Tension bottom transverse* | [-] | 1391.8 | 20 | 220 | 1 |
| *Tension NAP +0.8 m primary* | 375.0 | 1262.5 | 25 | 180 | 1 |
| *Tension NAP +0.8 m primary* | [-] | 338.6 | 10 | 230 | 1 |
| *Compression bottom primary* | 2231.0 | 1262.5 | 20 | 200 | 1 |
| *Compression bottom transverse* | [-] | 338.6 | 10 | 240 | 1 |
| *Compression NAP +0.8 m primary* | 375.0 | 1559.8 | 20 | 200 | 1 |
| *Compression NAP +0.8 m primary* | [-] | 312.0 | 10 | 230 | 1 |

| **Floor bottom reinforcement** | **M [kNm]** | **$A_{s1}$ [mm²]** | **$Ø_{bar}$ [mm]** | **c/c [mm]** | **No. rows** |
|---|---|---|---|---|---|
| *primary* | 2231.0 | 3435.3 | 20 | 170 | 2 |
| *transvers* | [-] | 687.1 | 16 | 210 | 2 |

| **Floor top reinforcement** | **M [kNm]** | **$A_{s1}$ [mm²]** | **$Ø_{bar}$ [mm]** | **c/c [mm]** | |
|---|---|---|---|---|---|
| *Compression top* | [-] | 3597.9 | 32 | 220 | 1 |
| *Transverse top* | [-] | 719.6 | 16 | 270 | 1 |

**Table 66: Required reinforcement area for a given moment and its resulting bar diameter and c/c distance for wall 14**

| **Vertical wall reinforcement** | **M [kNm]** | **$A_{s1}$ [mm²]** | **$Ø_{bar}$ [mm]** | **c/c [mm]** | **No. rows** |
|---|---|---|---|---|---|
| *Tension bottom primary* | 1699.3 | 5300.5 | 32 | 150 | 1 |
| *Tension bottom transverse* | [-] | 1060.1 | 20 | 290 | 1 |

| | | | | | |
|---|---|---|---|---|---|
| *Tension NAP +0.8 m primary* | 220.0 | 1693.1 | 20 | 180 | 1 |
| *Tension NAP +0.8 m primary* | [-] | 338.6 | 10 | 230 | 1 |
| *Compression bottom primary* | 1699.3 | 1559.8 | 20 | 200 | 1 |
| *Compression bottom transverse* | [-] | 312.0 | 10 | 240 | 1 |
| *Compression NAP +0.8 m primary* | 220.0 | 1693.1 | 20 | 230 | 1 |
| *Compression NAP +0.8 m primary* | [-] | 338.6 | 10 | 180 | 1 |

| **Floor bottom reinforcement** | **M [kNm]** | **$A_{s1}$ [mm²]** | **$Ø_{bar}$ [mm]** | **c/c [mm]** | **No. rows** |
|---|---|---|---|---|---|
| *primary* | 1699.3 | 2605.7 | 20 | 170 | 2 |
| *transvers* | [-] | 687.1 | 16 | 210 | 2 |

| **Floor top reinforcement** | **M [kNm]** | **$A_{s1}$ [mm²]** | **$Ø_{bar}$ [mm]** | **c/c [mm]** | |
|---|---|---|---|---|---|
| *Compression top* | [-] | 3597.9 | 32 | 220 | 1 |
| *Transverse top* | [-] | 719.6 | 16 | 270 | 1 |

## C.2.3: Base case volumes

The reinforcement volumes for the base case design are presented in the tables below. Figure 72 shows the wall types in proximity to the center lock head.

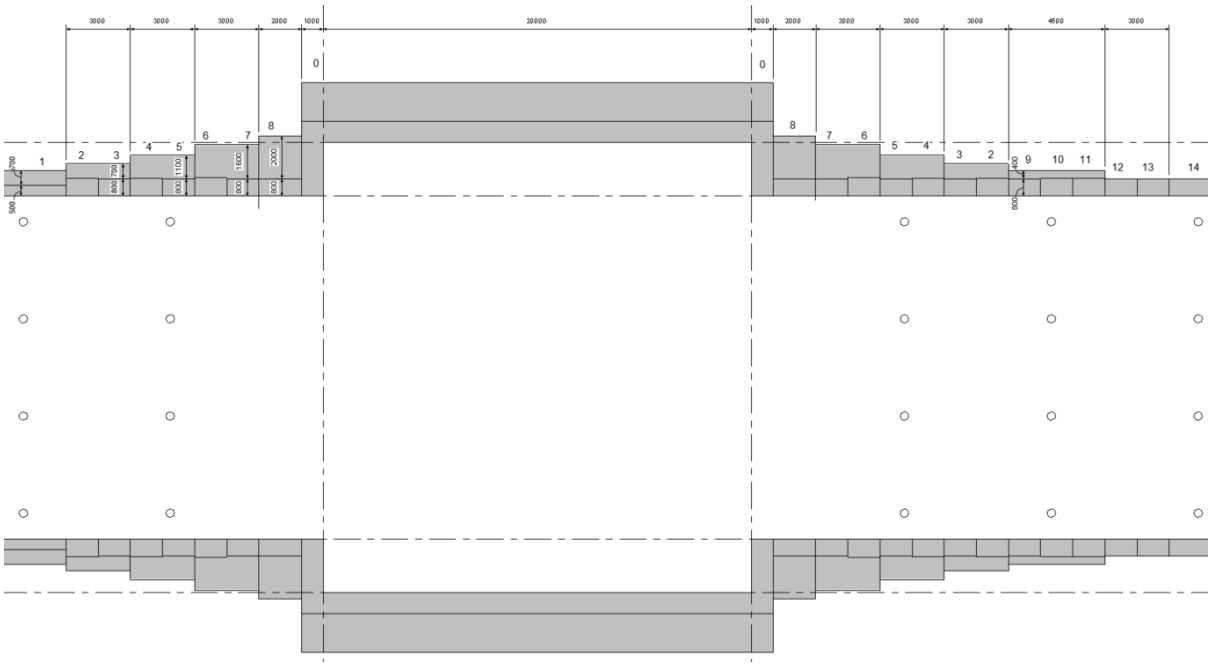

**Figure 72: Top view of the chamber in proximity to the center lock head. The wall types are numbered 0 – 14.**

Wall reinforcement is presented in Table 52 to Table 77 and floor reinforcement is presented in Table 78 and Table 79.

**Table 67: Reinforcement Wall 0; Center flood gates, NAP +11.0 m**

| | *L [mm]* | *Ø [mm]* | *Volume [m³]* | *no. Rows* | *c/c [mm]* | *no bars long* | no. Walls | *Total no. bars* | *Total length [m]* |
|---|---|---|---|---|---|---|---|---|---|
| ***Addition flex. reinf. for shear*** | 2825 | 32 | 0.0023 | 1 | 100 | 219 | 2 | 438 | 1237.35 |
| | 2300 | 32 | 0.0018 | 1 | 100 | 219 | 2 | 438 | 1007.4 |

| | | | | | | | | | |
|---|---|---|---|---|---|---|---|---|---|
| | 4225 | 32 | 0.0034 | 1 | 100 | 219 | 2 | 438 | 1850.55 |
| ***tension bottom*** | 7100 | 32 | 0.0057 | 2 | 170 | 129 | 2 | 516 | 3663.6 |
| ***tension top*** | 10000 | 25 | 0.0049 | 2 | 200 | 110 | 2 | 440 | 4400 |
| ***transv. Tens. Bottom*** | 7730 | 16 | 0.0016 | 2 | 220 | 84 | 2 | 336 | 2597.28 |
| ***transv. Tens. Top*** | 7200 | 12 | 0.0008 | 2 | 320 | 96 | 2 | 384 | 2764.8 |
| ***comp. Long. Bottom*** | 9000 | 32 | 0.0072 | 1 | 140 | 139 | 2 | 278 | 2502 |
| ***comp. Long. Top*** | 8000 | 25 | 0.0039 | 1 | 100 | 199 | 2 | 398 | 3184 |
| ***transv. comp. Bottom*** | 7380 | 16 | 0.0015 | 1 | 180 | 153 | 2 | 306 | 2258.28 |
| ***transv. comp. Top*** | 7380 | 16 | 0.0015 | 1 | 260 | 81 | 2 | 162 | 1195.56 |
| ***U-loops top*** | 2975 | 25 | 0.0015 | 1 | 100 | 199 | 2 | 398 | 1184.05 |
| | 2775 | 25 | 0.0014 | 1 | 100 | 199 | 2 | 398 | 1104.45 |
| ***anchorage bar*** | 8060 | 32 | 0.0065 | 3 | [-] | 3 | 2 | 18 | 145.08 |
| ***U-loop floor*** | 4725 | 32 | 0.0038 | 1 | 120 | 183 | 2 | 366 | 1729.35 |
| ***anchor bars*** | 8060 | 32 | 0.0065 | 3 | [-] | 3 | 2 | 18 | 145.08 |
| ***anchor bars*** | 8480 | 32 | 0.0068 | 2 | [-] | 3 | 2 | 12 | 101.76 |
| ***L-bar bottom*** | 5200 | 32 | 0.0042 | 1 | 140 | 139 | 2 | 278 | 1445.6 |

**Table 68: Reinforcement Wall 8; NAP +10.5 m**

| | *L [mm]* | *Ø [mm]* | *volume [m³]* | *no. Rows* | *c/c [mm]* | *no bars long* | no. Walls | *Total no. bars* | *total length [m³]* |
|---|---|---|---|---|---|---|---|---|---|
| ***Addition flex. reinf. for shear*** | 2850 | 32 | 0.0023 | 1 | 130 | 15 | 4 | 60 | 171 |
| | 2400 | 32 | 0.0019 | 1 | 130 | 15 | 4 | 60 | 144 |
| | 4225 | 32 | 0.0034 | 1 | 130 | 15 | 4 | 60 | 253.5 |
| ***tension bottom*** | 6620 | 32 | 0.0053 | 2 | 200 | 10 | 4 | 80 | 529.6 |
| ***tension top*** | 10000 | 25 | 0.0049 | 2 | 200 | 10 | 4 | 80 | 800 |
| ***transv. Tens. Bottom*** | 2420 | 16 | 0.0005 | 2 | 260 | 23 | 4 | 184 | 445.28 |
| ***transv. Tens. Top*** | 2320 | 12 | 0.0003 | 2 | 260 | 38 | 4 | 304 | 705.28 |
| ***comp. Long. Bottom*** | 9000 | 32 | 0.0072 | 1 | 140 | 21 | 4 | 84 | 756 |
| ***comp. Long. Top*** | 7500 | 25 | 0.0037 | 1 | 140 | 21 | 4 | 84 | 630 |
| ***transv. comp. Bottom*** | 2900 | 16 | 0.0006 | 1 | 180 | 50 | 4 | 200 | 580 |
| ***transv. comp. Top*** | 2900 | 12 | 0.0003 | 1 | 160 | 41 | 4 | 164 | 475.6 |
| ***U-loops top*** | 2775 | 25 | 0.0014 | 1 | 140 | 14 | 4 | 56 | 155.4 |
| | 2575 | 25 | 0.0013 | 1 | 140 | 14 | 4 | 56 | 144.2 |
| ***anchor bar comp.*** | 2900 | 32 | 0.0023 | 3 | [-] | 1 | 4 | 12 | 34.8 |
| ***U-loop floor*** | 4950 | 32 | 0.0040 | 1 | 120 | 16 | 4 | 64 | 316.8 |
| ***anchor bars*** | 3840 | 32 | 0.0031 | 3 | [-] | 1 | 4 | 12 | 46.08 |
| ***L-bar bottom*** | 5200 | 32 | 0.0042 | 1 | 140 | 21 | 4 | 84 | 436.8 |

**Table 69: Reinforcement wall 6&7; NAP +9.5 m & +10 m**

| | *L [mm]* | *Ø [mm]* | *volume [m³]* | *no. Rows* | *c/c [mm]* | *no bars long* | no. Walls | *Total no. bars* | *total length [m³]* |
|---|---|---|---|---|---|---|---|---|---|

| | | | | | | | | | |
|---|---|---|---|---|---|---|---|---|---|
| ***Addition flex. reinf. for shear*** | 2850 | 32 | 0.0023 | 1 | 130 | 23 | 4 | 92 | 262.2 |
| | 2400 | 32 | 0.0019 | 1 | 130 | 23 | 4 | 92 | 220.8 |
| | 4175 | 32 | 0.0034 | 1 | 130 | 23 | 4 | 92 | 384.1 |
| ***tension bottom*** | 5900 | 32 | 0.0047 | 2 | 200 | 15 | 4 | 120 | 708 |
| ***tension top 7*** | 10000 | 20 | 0.0031 | 2 | 160 | 10 | 4 | 80 | 800 |
| ***tension top 6*** | 9500 | 20 | 0.0030 | 2 | 160 | 9 | 4 | 72 | 684 |
| ***transv. Tens. Bottom*** | 3420 | 16 | 0.0007 | 2 | 250 | 24 | 4 | 192 | 656.64 |
| ***transv. Tens. Top 7*** | 1820 | 12 | 0.0002 | 2 | 300 | 2 | 4 | 16 | 29.12 |
| ***transv. Tens. Top 6*** | 3320 | 12 | 0.0004 | 2 | 300 | 29 | 4 | 232 | 770.24 |
| ***comp. Long. Bottom*** | 9200 | 32 | 0.0074 | 1 | 170 | 18 | 4 | 72 | 662.4 |
| ***comp. Long. Top 7*** | 6820 | 25 | 0.0033 | 1 | 170 | 9 | 4 | 36 | 245.52 |
| ***comp. Long. Top 6*** | 6320 | 25 | 0.0031 | 1 | 170 | 9 | 4 | 36 | 227.52 |
| ***transv. comp. Bottom*** | 3420 | 16 | 0.0007 | 1 | 220 | 42 | 4 | 168 | 574.56 |
| ***transv. comp. Top 7*** | 1820 | 12 | 0.0002 | 1 | 190 | 2 | 4 | 8 | 14.56 |
| ***transv. comp. Top 6*** | 3320 | 12 | 0.0004 | 1 | 190 | 29 | 4 | 116 | 385.12 |
| ***U-loops top 7*** | 2350 | 20 | 0.0007 | 1 | 160 | 10 | 4 | 40 | 94 |
| | 2150 | 20 | 0.0007 | 1 | 160 | 10 | 4 | 40 | 86 |
| ***U-loops top 6*** | 2400 | 20 | 0.0008 | 1 | 160 | 9 | 4 | 36 | 86.4 |
| | 2200 | 20 | 0.0007 | 1 | 160 | 9 | 4 | 36 | 79.2 |
| ***anchor bar*** | 2150 | 25 | 0.0011 | 3 | [-] | 2 | 4 | 24 | 51.6 |
| ***U-loop floor*** | 4950 | 32 | 0.0040 | 1 | 160 | 19 | 4 | 76 | 376.2 |
| ***anchor bars*** | 3840 | 32 | 0.0031 | 3 | [-] | 1 | 4 | 12 | 46.08 |
| ***L-bar bottom*** | 4800 | 32 | 0.0039 | 1 | 170 | 18 | 4 | 72 | 345.6 |

**Table 70: Reinforcement wall 4&5; NAP +8.5 m & +9 m**

| | *L [mm]* | *Ø [mm]* | *volume [m³]* | *no. Rows* | *c/c [mm]* | *no bars long* | no. Walls | *Total no. bars* | *total length [m³]* |
|---|---|---|---|---|---|---|---|---|---|
| ***Addition flex. reinf. for shear*** | 2850 | 32 | 0.0023 | 1 | 130 | 23 | 4 | 92 | 262.2 |
| | 2400 | 32 | 0.0019 | 1 | 130 | 23 | 4 | 92 | 220.8 |
| | 4200 | 32 | 0.0034 | 1 | 130 | 23 | 4 | 92 | 386.4 |
| ***tension bottom*** | 5990 | 32 | 0.0048 | 2 | 190 | 16 | 4 | 128 | 766.72 |
| ***tension top 5*** | 8370 | 20 | 0.0026 | 2 | 190 | 8 | 4 | 64 | 535.68 |
| ***tension top 4*** | 8870 | 20 | 0.0028 | 2 | 190 | 8 | 4 | 64 | 567.68 |
| ***transv. Tens. Bottom*** | 3420 | 16 | 0.0007 | 2 | 240 | 25 | 4 | 200 | 684 |
| ***transv. Tens. Top 5*** | 1760 | 10 | 0.0001 | 2 | 230 | 2 | 4 | 16 | 28.16 |
| ***transv. Tens. Top 4*** | 3260 | 10 | 0.0003 | 2 | 230 | 34 | 4 | 272 | 886.72 |
| ***comp. Long. Bottom*** | 9000 | 32 | 0.0072 | 1 | 230 | 13 | 4 | 52 | 468 |
| ***comp. Long. Top 5*** | 6020 | 25 | 0.0030 | 1 | 190 | 8 | 4 | 32 | 192.64 |

| | | | | | | | | | |
|---|---|---|---|---|---|---|---|---|---|
| ***comp. Long. Top 4*** | 5520 | 25 | 0.0027 | 1 | 190 | 8 | 4 | 32 | 176.64 |
| ***transv. comp. Bottom*** | 3320 | 12 | 0.0004 | 1 | 160 | 57 | 4 | 228 | 756.96 |
| ***transv. comp. Top 5*** | 1760 | 10 | 0.0001 | 1 | 160 | 3 | 4 | 12 | 21.12 |
| ***transv. comp. Top 4*** | 3260 | 10 | 0.0003 | 1 | 160 | 28 | 4 | 112 | 365.12 |
| ***U-loops top 5*** | 2325 | 20 | 0.0007 | 1 | 190 | 8 | 4 | 32 | 74.4 |
| | 2125 | 20 | 0.0007 | 1 | 190 | 8 | 4 | 32 | 68 |
| ***U-loops top 4*** | 2375 | 20 | 0.0007 | 1 | 190 | 8 | 4 | 32 | 76 |
| | 2175 | 20 | 0.0007 | 1 | 190 | 8 | 4 | 32 | 69.6 |
| ***anchor bar*** | 2150 | 25 | 0.0011 | 3 | [-] | 2 | 4 | 24 | 51.6 |
| ***U-loop floor*** | 4700 | 32 | 0.0038 | 1 | 110 | 26 | 4 | 104 | 488.8 |
| ***anchor bars*** | 3840 | 32 | 0.0031 | 3 | [-] | 1 | 4 | 12 | 46.08 |
| ***L-bar bottom*** | 4525 | 32 | 0.0036 | 1 | 230 | 13 | 4 | 52 | 235.3 |
| ***anchor (4-8)*** | 10000 | 32 | 0.0080 | 2 | [-] | 1 | 4 | 8 | 80 |

**Table 71: Reinforcement wall 2&3; NAP +7.5 m & +8 m**

| | *L [mm]* | *Ø [mm]* | *volume [m³]* | *no. Rows* | *c/c [mm]* | *no bars long* | no. Walls | *Total no. bars* | *total length [m³]* |
|---|---|---|---|---|---|---|---|---|---|
| ***Addition flex. reinf. for shear*** | 2850 | 32 | 0.0023 | 1 | 140 | 21 | 4 | 84 | 239.4 |
| | 2400 | 32 | 0.0019 | 1 | 140 | 21 | 4 | 84 | 201.6 |
| | 3925 | 32 | 0.0032 | 1 | 140 | 21 | 4 | 84 | 329.7 |
| ***tension bottom*** | 5990 | 32 | 0.0048 | 2 | 180 | 17 | 4 | 136 | 814.64 |
| ***tension top 3*** | 7720 | 16 | 0.0016 | 2 | 180 | 8 | 4 | 64 | 494.08 |
| ***tension top 2*** | 7220 | 16 | 0.0015 | 2 | 180 | 9 | 4 | 72 | 519.84 |
| ***transv. Tens. Bottom*** | 3420 | 16 | 0.0007 | 2 | 230 | 26 | 4 | 208 | 711.36 |
| ***transv. Tens. Top 3*** | 1710 | 8 | 0.0001 | 2 | 220 | 3 | 4 | 24 | 41.04 |
| ***transv. Tens. Top 2*** | 3210 | 8 | 0.0002 | 2 | 220 | 30 | 4 | 240 | 770.4 |
| ***comp. Long. Bottom*** | 9000 | 25 | 0.0044 | 1 | 180 | 17 | 4 | 68 | 612 |
| ***comp. Long. Top 3*** | 5030 | 25 | 0.0025 | 1 | 180 | 8 | 4 | 32 | 160.96 |
| ***comp. Long. Top 2*** | 4530 | 25 | 0.0022 | 1 | 180 | 9 | 4 | 36 | 163.08 |
| ***transv. comp. Bottom*** | 3260 | 10 | 0.0003 | 1 | 140 | 65 | 4 | 260 | 847.6 |
| ***transv. comp. Top 3*** | 1760 | 10 | 0.0001 | 1 | 180 | 3 | 4 | 12 | 21.12 |
| ***transv. comp. Top 2*** | 3260 | 10 | 0.0003 | 1 | 180 | 19 | 4 | 76 | 247.76 |
| ***U-loops top 3*** | 2000 | 16 | 0.0004 | 1 | 180 | 8 | 4 | 32 | 64 |
| | 1800 | 16 | 0.0004 | 1 | 180 | 8 | 4 | 32 | 57.6 |
| ***U-loops top 2*** | 2025 | 16 | 0.0004 | 1 | 180 | 9 | 4 | 36 | 72.9 |
| | 1825 | 16 | 0.0004 | 1 | 180 | 9 | 4 | 36 | 65.7 |
| ***anchor bar*** | 2020 | 20 | 0.0006 | 3 | [-] | 2 | 4 | 24 | 48.48 |
| ***U-loop floor*** | 4575 | 32 | 0.0037 | 1 | 140 | 21 | 4 | 84 | 384.3 |
| ***anchor bars*** | 3840 | 32 | 0.0031 | 3 | [-] | 1 | 4 | 12 | 46.08 |
| ***L-bar bottom*** | 3750 | 25 | 0.0018 | 1 | 180 | 17 | 4 | 68 | 255 |

| | | | | | | | | | |
|---|---|---|---|---|---|---|---|---|---|
| ***anchor (2-3 & into 1 & 9-10-11)*** | 10000 | 32 | 0.0080 | 2 | [-] | 1 | 4 | 8 | 80 |

**Table 72: Reinforcement lowest wall (1), seaside chamber; NAP +7.0 m**

| | *L [mm]* | *Ø [mm]* | *volume [m³]* | *no. Rows* | *c/c [mm]* | *no bars long* | no. Walls | *Total no. bars* | *total length [m³]* |
|---|---|---|---|---|---|---|---|---|---|
| ***Addition flex. reinf. for shear*** | 2850 | 32 | 0.0023 | 1 | 130 | 452 | 2 | 904 | 2576.4 |
| | 4025 | 32 | 0.0032 | 1 | 130 | 452 | 2 | 904 | 3638.6 |
| ***tension bottom*** | 5380 | 32 | 0.0043 | 2 | 180 | 327 | 2 | 1308 | 7037.04 |
| ***tension top*** | 7330 | 16 | 0.0015 | 2 | 180 | 329 | 2 | 1316 | 9646.28 |
| ***transv. Tens. Bottom*** | 64000 | 16 | 0.0129 | 2 | 240 | 23 | 2 | 92 | 5888 |
| ***transv. Tens. Top*** | 62000 | 8 | 0.0031 | 2 | 220 | 30 | 2 | 120 | 7440 |
| ***comp. Long. Bottom*** | 7000 | 25 | 0.0034 | 1 | 220 | 273 | 2 | 546 | 3822 |
| ***comp. Long. Top*** | 6035 | 20 | 0.0019 | 1 | 180 | 333 | 2 | 666 | 4019.31 |
| ***transv. comp. Bottom*** | 63150 | 12 | 0.0071 | 1 | 250 | 28 | 2 | 56 | 3536.4 |
| ***transv. comp. Top*** | 62600 | 10 | 0.0049 | 1 | 230 | 22 | 2 | 44 | 2754.4 |
| ***U-loops top 4*** | 1700 | 16 | 0.0003 | 1 | 180 | 331 | 2 | 662 | 1125.4 |
| | 1600 | 16 | 0.0003 | 1 | 180 | 331 | 2 | 662 | 1059.2 |
| ***anchor bar*** | 10000 | 20 | 0.0031 | 3 | [-] | 6 | 2 | 36 | 360 |
| | 5200 | 20 | 0.0016 | 3 | [-] | 1 | 2 | 6 | 31.2 |
| ***U-loop floor*** | 4650 | 32 | 0.0037 | 1 | 180 | 327 | 2 | 654 | 3041.1 |
| ***anchor bars*** | 68300 | 32 | 0.0549 | 3 | [-] | 1 | 2 | 6 | 409.8 |
| ***L-bar bottom*** | 4025 | 25 | 0.0020 | 1 | 220 | 273 | 2 | 546 | 2197.65 |
| ***anchor*** | 67200 | 32 | 0.0540 | 2 | [-] | 1 | 2 | 4 | 268.8 |

**Table 73: Reinforcement wall 9-10-11; NAP +6 m, +6.5 m & +7 m**

| | *L [mm]* | *Ø [mm]* | *volume [m³]* | *no. Rows* | *c/c [mm]* | *no bars long* | no. Walls | *Total no. bars* | *total length [m³]* |
|---|---|---|---|---|---|---|---|---|---|
| ***Addition flex. reinf. for shear*** | 2850 | 32 | 0.0023 | 1 | 90 | 49 | 2 | 98 | 279.3 |
| ***tension bottom*** | 6000 | 32 | 0.0048 | 1 | 110 | 41 | 2 | 82 | 492 |
| ***tension top 11*** | 6800 | 20 | 0.0021 | 1 | 140 | 11 | 2 | 22 | 149.6 |
| ***tension top 10*** | 6300 | 20 | 0.0020 | 1 | 140 | 11 | 2 | 22 | 138.6 |
| ***tension top 9*** | 5800 | 20 | 0.0018 | 1 | 140 | 11 | 2 | 22 | 127.6 |
| ***transv. Tens. Bottom*** | 5020 | 20 | 0.0016 | 1 | 220 | 28 | 2 | 56 | 281.12 |
| ***transv. Tens. Top 11*** | 1820 | 12 | 0.0002 | 1 | 260 | 2 | 2 | 4 | 7.28 |
| ***transv. Tens. Top 10*** | 3320 | 12 | 0.0004 | 1 | 260 | 2 | 2 | 4 | 13.28 |
| ***transv. Tens. Top 9*** | 4820 | 12 | 0.0005 | 1 | 260 | 19 | 2 | 38 | 183.16 |
| ***comp. Long. Bottom*** | 6000 | 25 | 0.0029 | 1 | 200 | 23 | 2 | 46 | 276 |
| ***comp. Long. Top 11*** | 6790 | 20 | 0.0021 | 1 | 140 | 11 | 2 | 22 | 149.38 |
| ***comp. Long. Top 10*** | 6290 | 20 | 0.0020 | 1 | 140 | 11 | 2 | 22 | 138.38 |
| ***comp. Long. Top 9*** | 5790 | 20 | 0.0018 | 1 | 140 | 11 | 2 | 22 | 127.38 |

| | | | | | | | | | |
|---|---|---|---|---|---|---|---|---|---|
| ***transv. comp. Bottom*** | 4820 | 12 | 0.0005 | 1 | 230 | 26 | 2 | 52 | 250.64 |
| ***transv. comp. Top 11*** | 1760 | 10 | 0.0001 | 1 | 180 | 2 | 2 | 4 | 7.04 |
| ***transv. comp. Top 10*** | 3260 | 10 | 0.0003 | 1 | 180 | 3 | 2 | 6 | 19.56 |
| ***transv. comp. Top 9*** | 4760 | 10 | 0.0004 | 1 | 180 | 29 | 2 | 58 | 276.08 |
| ***U-loop top 11*** | 2325 | 20 | 0.0007 | 1 | 140 | 11 | 2 | 22 | 51.15 |
| ***U-loop top 10*** | 2350 | 20 | 0.0007 | 1 | 140 | 11 | 2 | 22 | 51.7 |
| ***U-loop top 9*** | 2350 | 20 | 0.0007 | 1 | 140 | 11 | 2 | 22 | 51.7 |
| ***anchor bar*** | 2150 | 25 | 0.0011 | 3 | [-] | 3 | 2 | 18 | 38.7 |
| ***U-loop floor*** | 4650 | 32 | 0.0037 | 1 | 170 | 27 | 2 | 54 | 251.1 |
| ***anchor bars*** | 5340 | 32 | 0.0043 | 2 | [-] | 1 | 2 | 4 | 21.36 |
| ***L-bar bottom*** | 4625 | 25 | 0.0023 | 1 | 200 | 23 | 2 | 46 | 212.75 |
| ***anchor 9-13*** | 5690 | 32 | 0.0046 | 1 | [-] | 1 | 2 | 2 | 11.38 |

**Table 74: Reinforcement wall 12 & 13; NAP +5 m & +5.5 m**

| | *L [mm]* | *Ø [mm]* | *volume [m³]* | *no. Rows* | *c/c [mm]* | *no bars long* | no. Walls | *Total no. bars* | *total length [m³]* |
|---|---|---|---|---|---|---|---|---|---|
| ***Addition flex. reinf. for shear*** | 2800 | 32 | 0.0023 | 1 | 110 | 27 | 2 | 54 | 151.2 |
| ***tension bottom*** | 4000 | 32 | 0.0032 | 1 | 110 | 27 | 2 | 54 | 216 |
| ***tension top 13*** | 7300 | 20 | 0.0023 | 1 | 180 | 9 | 2 | 18 | 131.4 |
| ***tension top 12*** | 6800 | 20 | 0.0021 | 1 | 180 | 9 | 2 | 18 | 122.4 |
| ***transv. Tens. Bottom*** | 3520 | 20 | 0.0011 | 1 | 220 | 19 | 2 | 38 | 133.76 |
| ***transv. Tens. Top 13*** | 1760 | 10 | 0.0001 | 1 | 220 | 2 | 2 | 4 | 7.04 |
| ***transv. Tens. Top 12*** | 3260 | 10 | 0.0003 | 1 | 220 | 26 | 2 | 52 | 169.52 |
| ***comp. Long. 13*** | 5650 | 20 | 0.0018 | 2 | 200 | 8 | 2 | 32 | 180.8 |
| ***comp. Long. 12*** | 5400 | 20 | 0.0017 | 2 | 200 | 8 | 2 | 32 | 172.8 |
| ***transv. comp. Top 13*** | 1760 | 10 | 0.0001 | 1 | 240 | 2 | 2 | 4 | 7.04 |
| ***transv. comp. Top 12*** | 3260 | 10 | 0.0003 | 1 | 240 | 42 | 2 | 84 | 273.84 |
| ***U-loops top 13*** | 2325 | 20 | 0.0007 | 1 | 180 | 9 | 2 | 18 | 41.85 |
| ***U-loops top 12*** | 2325 | 20 | 0.0007 | 1 | 180 | 9 | 2 | 18 | 41.85 |
| ***anchor bar*** | 2150 | 25 | 0.0011 | 2 | [-] | 2 | 2 | 8 | 17.2 |

**Table 75: Reinforcement lowest wall on the riverside chamber (14); NAP +4.5 m**

| | *L [mm]* | *Ø [mm]* | *volume [m³]* | *no. Rows* | *c/c [mm]* | *no bars long* | no. Walls | *Total no. bars* | *total length [m³]* |
|---|---|---|---|---|---|---|---|---|---|
| ***Addition flex. reinf. for shear*** | 2800 | 32 | 0.0023 | 1 | 150 | 345 | 2 | 690 | 1932 |
| ***tension bottom*** | 4000 | 32 | 0.0032 | 1 | 150 | 345 | 2 | 690 | 2760 |
| ***tension top*** | 6330 | 20 | 0.0020 | 1 | 180 | 288 | 2 | 576 | 3646.08 |
| ***transv. Tens. Bottom*** | 57000 | 20 | 0.0179 | 1 | 290 | 14 | 2 | 28 | 1596 |
| ***transv. Tens. Top*** | 54600 | 10 | 0.0043 | 1 | 230 | 24 | 2 | 48 | 2620.8 |
| ***comp. Long.*** | 9550 | 20 | 0.0030 | 1 | 200 | 263 | 2 | 526 | 5023.3 |

| | | | | | | | | | |
|---|---|---|---|---|---|---|---|---|---|
| ***transv. comp.*** | 54600 | 10 | 0.0043 | 1 | 240 | 40 | 2 | 80 | 4368 |
| ***U-loop top*** | 2325 | 20 | 0.0007 | 1 | 180 | 288 | 2 | 576 | 1339.2 |
| ***anchor bar*** | 58000 | 25 | 0.0285 | 2 | [-] | 1 | 2 | 4 | 232 |
| ***U-loop floor*** | 4375 | 32 | 0.0035 | 1 | 170 | 322 | 2 | 644 | 2817.5 |
| ***anchor bars*** | 64000 | 32 | 0.0515 | 1 | [-] | 1 | 2 | 2 | 128 |
| | 67400 | 32 | 0.0542 | 1 | [-] | 1 | 2 | 2 | 134.8 |
| ***L-bar bottom*** | 3900 | 20 | 0.0012 | 1 | 200 | 278 | 2 | 556 | 2168.4 |
| ***anchor*** | 10000 | 32 | 0.0080 | 3 | [-] | 6 | 2 | 36 | 360 |
| | 4000 | 32 | 0.0032 | 2 | [-] | 1 | 2 | 4 | 16 |
| | 7400 | 32 | 0.0060 | 1 | [-] | 1 | 2 | 2 | 14.8 |

**Table 76: Reinforcement wall lock head seaside chamber, NAP +7 m**

| | ***L [mm]*** | ***Ø [mm]*** | ***volume [m³]*** | ***no. Rows*** | ***c/c [mm]*** | ***no bars long*** | **no. Walls** | ***Total no. bars*** | ***total length [m³]*** |
|---|---|---|---|---|---|---|---|---|---|
| *Addition flex. reinf. for shear* | 2850 | 32 | 0.0023 | 1 | 130 | 95 | 2 | 190 | 541.5 |
| | 4025 | 32 | 0.0032 | 1 | 130 | 95 | 2 | 190 | 764.75 |
| *tension bottom* | 5380 | 32 | 0.0043 | 2 | 180 | 63 | 2 | 252 | 1355.76 |
| *tension top* | 7330 | 16 | 0.0015 | 2 | 180 | 61 | 2 | 244 | 1788.52 |
| *transv. Tens. Bottom* | 6250 | 16 | 0.0013 | 2 | 240 | 46 | 2 | 184 | 1150 |
| *transv. Tens. Top* | 5820 | 8 | 0.0003 | 2 | 220 | 60 | 2 | 240 | 1396.8 |
| *comp. Long. Bottom* | 7000 | 25 | 0.0034 | 1 | 220 | 47 | 2 | 94 | 658 |
| *comp. Long. Top* | 6035 | 20 | 0.0019 | 1 | 180 | 57 | 2 | 114 | 687.99 |
| *transv. comp. Bottom* | 5680 | 12 | 0.0006 | 1 | 250 | 56 | 2 | 112 | 636.16 |
| *transv. comp. Top* | 5640 | 10 | 0.0004 | 1 | 230 | 44 | 2 | 88 | 496.32 |
| *U-loops top* | 1700 | 16 | 0.0003 | 1 | 180 | 57 | 2 | 114 | 193.8 |
| | 1600 | 16 | 0.0003 | 1 | 180 | 57 | 2 | 114 | 182.4 |
| *anchor bar* | 5830 | 20 | 0.0018 | 3 | [-] | 2 | 2 | 12 | 69.96 |
| *U-loop floor* | 4650 | 32 | 0.0037 | 1 | 180 | 69 | 2 | 138 | 641.7 |
| *anchor bars* | 6780 | 32 | 0.0055 | 3 | [-] | 2 | 2 | 12 | 81.36 |
| *L-bar bottom* | 4025 | 25 | 0.0020 | 1 | 220 | 47 | 2 | 94 | 378.35 |
| *anchor* | 7030 | 32 | 0.0057 | 2 | [-] | 2 | 2 | 8 | 56.24 |

**Table 77: Reinforcement wall lock head riverside chamber, NAP +4.5 m**

| | ***L [mm]*** | ***Ø [mm]*** | ***volume [m³]*** | ***no. Rows*** | ***c/c [mm]*** | ***no bars long*** | **no. Walls** | ***Total no. bars*** | ***total length [m³]*** |
|---|---|---|---|---|---|---|---|---|---|
| ***Addition flex. reinf. for shear*** | 2800 | 32 | 0.0023 | 1 | 150 | 77 | 2 | 154 | 431.2 |
| ***tension bottom*** | 4000 | 32 | 0.0032 | 1 | 150 | 77 | 2 | 154 | 616 |
| ***tension top*** | 6330 | 20 | 0.0020 | 1 | 180 | 64 | 2 | 128 | 810.24 |
| ***transv. Tens. Bottom*** | 6140 | 20 | 0.0019 | 2 | 290 | 14 | 2 | 56 | 343.84 |
| ***transv. Tens. Top*** | 5945 | 10 | 0.0005 | 2 | 230 | 24 | 2 | 96 | 570.72 |
| ***comp. Long.*** | 9550 | 20 | 0.0030 | 1 | 200 | 51 | 2 | 102 | 974.1 |
| ***transv. comp.*** | 5455 | 10 | 0.0004 | 2 | 240 | 40 | 2 | 160 | 872.8 |

| | | | | | | | | | |
|---|---|---|---|---|---|---|---|---|---|
| ***U-loop top*** | 2325 | 20 | 0.0007 | 1 | 180 | 57 | 2 | 114 | 265.05 |
| ***anchor bar*** | 6220 | 25 | 0.0031 | 2 | [-] | 2 | 2 | 8 | 49.76 |
| ***U-loop floor*** | 4375 | 32 | 0.0035 | 1 | 67 | 322 | 2 | 644 | 2817.5 |
| ***anchor bars*** | 6375 | 32 | 0.0051 | 1 | [-] | 2 | 2 | 4 | 25.5 |
| | 6630 | 32 | 0.0053 | 1 | [-] | 2 | 2 | 4 | 26.52 |
| ***L-bar bottom*** | 3900 | 20 | 0.0012 | 1 | 200 | 57 | 2 | 114 | 444.6 |
| ***anchor*** | 6374 | 32 | 0.0051 | 2 | [-] | 2 | 2 | 8 | 50.992 |
| | 6630 | 32 | 0.0053 | 1 | [-] | 2 | 2 | 4 | 26.52 |

**Table 78: Floor; top compression reinforcement**

| **Compression** | ***L [mm]*** | ***Ø [mm]*** | ***volume [m^3]*** | ***c/c [mm]*** | ***no. bars Y*** | ***no. bars X*** | ***no. walls*** | ***tot bars*** | ***total length [m³]*** |
|---|---|---|---|---|---|---|---|---|---|
| *Center lock head* | 10000 | 32 | 0.0080 | 220 | 3 | 100 | 1 | 300 | 3000 |
| *wall 8; edge* | 7500 | 32 | 0.0060 | 220 | 2 | 9 | 2 | 36 | 270 |
| *wall 6-7; edge* | 7100 | 32 | 0.0057 | 220 | 2 | 13 | 2 | 52 | 369.2 |
| *wall 4-5; edge* | 6600 | 32 | 0.0053 | 220 | 2 | 14 | 2 | 56 | 369.6 |
| *wall 2-3; edge* | 6200 | 32 | 0.0050 | 220 | 2 | 14 | 2 | 56 | 347.2 |
| *wall 2-8; middle* | 10000 | 32 | 0.0080 | 220 | 1 | 50 | 1 | 50 | 500 |
| *wall 1* | 10000 | 32 | 0.0080 | 220 | 2 | 268 | 1 | 536 | 5360 |
| *sea lock head* | 8940 | 32 | 0.0072 | 220 | 3 | 55 | 1 | 165 | 1475.1 |
| *wall 9-10-11* | 5900 | 32 | 0.0047 | 220 | 2 | 20 | 1 | 40 | 236 |
| *wall 2-8 & 9-11* | 10000 | 32 | 0.0080 | 220 | 1 | 70 | 1 | 70 | 700 |
| *wall 12-13-14* | 9620 | 32 | 0.0077 | 220 | 2 | 249 | 1 | 498 | 4790.76 |
| *river lock head* | 8670 | 32 | 0.0070 | 220 | 3 | 53 | 1 | 159 | 1378.53 |
| **Transverse** | | | | | | | | | |
| *Center lock head* | 7890 | 16 | 0.0016 | 270 | 97 | 3 | 1 | 291 | 2295.99 |
| *wall 8* | 2880 | 16 | 0.0006 | 270 | 4 | 1 | 2 | 8 | 23.04 |
| *wall 6-7* | 5880 | 16 | 0.0012 | 270 | 4 | 1 | 2 | 8 | 47.04 |
| *wall 4-5* | 8880 | 16 | 0.0018 | 270 | 4 | 1 | 2 | 8 | 71.04 |
| *wall 4-8* | 8880 | 16 | 0.0018 | 270 | 67 | 1 | 2 | 134 | 1189.92 |
| *wall 2-3, sea&river* | 3880 | 16 | 0.0008 | 270 | 2 | 1 | 2 | 4 | 15.52 |
| *wall 1-3* | 10000 | 16 | 0.0020 | 270 | 67 | 7 | 1 | 469 | 4690 |
| *sea lock head; edge* | 6590 | 16 | 0.0013 | 270 | 18 | 2 | 1 | 36 | 237.24 |
| *sea lock head; middle* | 6060 | 16 | 0.0012 | 270 | 67 | 2 | 1 | 134 | 812.04 |
| *wall 2-3 & 9-10-11, river* | 8380 | 16 | 0.0017 | 270 | 4 | 1 | 1 | 4 | 33.52 |
| *wall 9-14* | 10000 | 16 | 0.0020 | 270 | 63 | 7 | 1 | 441 | 4410 |
| *river lock head; edge* | 6180 | 16 | 0.0012 | 270 | 18 | 2 | 1 | 36 | 222.48 |
| *river lock head; middle* | 5860 | 16 | 0.0012 | 270 | 63 | 2 | 1 | 126 | 738.36 |

**Table 79: Floor; bottom tension reinforcement**

| **Tension** | ***L [mm]*** | ***Ø [mm]*** | ***volume [m^3]*** | ***c/c [mm]*** | ***no. bars Y*** | ***no. bars X*** | ***no. walls*** | ***tot bars*** | ***total length [m³]*** |
|---|---|---|---|---|---|---|---|---|---|
| *Center lock head; edge* | 8200 | 32 | 0.0066 | 110 | 2 | 200 | 1 | 800 | 6560 |

| | | | | | | | | | |
|---|---|---|---|---|---|---|---|---|---|
| *Center lock head; between* | 4440 | 32 | 0.0036 | 110 | 2 | 200 | 1 | 800 | 3552 |
| *Center lock head; middle* | 6000 | 25 | 0.0029 | 110 | 1 | 200 | 1 | 400 | 2400 |
| *Wall 8; edge* | 5190 | 32 | 0.0042 | 120 | 2 | 17 | 2 | 136 | 705.84 |
| *Wall 8; between* | 3970 | 25 | 0.0019 | 120 | 2 | 17 | 2 | 136 | 539.92 |
| *Wall 8; middle* | 6000 | 20 | 0.0019 | 120 | 1 | 17 | 2 | 68 | 408 |
| *Wall 6&7; edge* | 4610 | 32 | 0.0037 | 160 | 2 | 19 | 2 | 152 | 700.72 |
| *Wall 6&7; between* | 3820 | 20 | 0.0012 | 80 | 2 | 37 | 2 | 296 | 1130.72 |
| *Wall 6&7; middle* | 6000 | 16 | 0.0012 | 80 | 1 | 37 | 2 | 148 | 888 |
| *Wall 4&5; edge* | 4100 | 25 | 0.0020 | 110 | 2 | 27 | 2 | 216 | 885.6 |
| *Wall 4&5; middle* | 6590 | 20 | 0.0021 | 110 | 2 | 27 | 2 | 216 | 1423.44 |
| *Wall 2&3; edge* | 3800 | 25 | 0.0019 | 140 | 2 | 22 | 2 | 176 | 668.8 |
| *Wall 2&3; middle* | 6590 | 20 | 0.0021 | 140 | 2 | 22 | 2 | 176 | 1159.84 |
| *Wall 1; edge* | 3789 | 25 | 0.0019 | 170 | 2 | 346 | 1 | 1384 | 5243.976 |
| *Wall 1; middle* | 6590 | 20 | 0.0021 | 170 | 2 | 346 | 1 | 1384 | 9120.56 |
| *Sea lock head; edge* | 6280 | 25 | 0.0031 | 170 | 2 | 72 | 1 | 288 | 1808.64 |
| *Sea lock head; middle* | 6590 | 20 | 0.0021 | 170 | 2 | 72 | 1 | 288 | 1897.92 |
| *Wall 9-10-11; edge* | 3500 | 25 | 0.0017 | 170 | 2 | 26 | 1 | 104 | 364 |
| *Wall 9-10-11; middle* | 6590 | 20 | 0.0021 | 170 | 2 | 26 | 1 | 104 | 685.36 |
| *Wall 12-13-14* | 8900 | 20 | 0.0028 | 170 | 2 | 322 | 1 | 1288 | 11463.2 |
| *River lock head* | 7860 | 20 | 0.0025 | 170 | 3 | 68 | 1 | 408 | 3206.88 |
| **Transverse** | | | | | | | | | |
| *Center lock head; edge* | 7830 | 20 | 0.0025 | 200 | 14 | 2 | 1 | 56 | 438.48 |
| | 7830 | 20 | 0.0025 | 200 | 23 | 1 | 1 | 46 | 360.18 |
| *Center lock head & wall 8; edge* | 9830 | 20 | 0.0031 | 200 | 22 | 2 | 1 | 88 | 865.04 |
| *Center lock head & wall 8; between* | 8950 | 12 | 0.0010 | 100 | 31 | 3 | 1 | 186 | 1664.7 |
| *Center lock head; middle* | 7720 | 16 | 0.0016 | 200 | 30 | 3 | 1 | 180 | 1389.6 |
| *Wall 6-7-8; middle* | 5790 | 12 | 0.0007 | 200 | 30 | 1 | 2 | 120 | 694.8 |
| *Wall 6&7; edge* | 3630 | 16 | 0.0007 | 200 | 4 | 1 | 2 | 16 | 58.08 |
| *Wall 4-5-6-7; edge* | 6630 | 16 | 0.0013 | 200 | 36 | 1 | 2 | 144 | 954.72 |
| *Wall 6&7; between* | 3710 | 10 | 0.0003 | 100 | 62 | 1 | 2 | 248 | 920.08 |
| *Wall 2-3-4-5 & 9-13; middle* | 10000 | 10 | 0.0008 | 200 | 60 | 1 | 2 | 240 | 2400 |
| *Wall 2-3; edge* | 3390 | 10 | 0.0003 | 100 | 62 | 1 | 2 | 248 | 840.72 |
| *Wall 1; edge* | 2490 | 12 | 0.0003 | 200 | 28 | 1 | 1 | 56 | 139.44 |
| | 10000 | 12 | 0.0011 | 200 | 28 | 6 | 1 | 336 | 3360 |
| *Wall 1; middle* | 10000 | 10 | 0.0008 | 200 | 60 | 6 | 1 | 720 | 7200 |
| *sea lock head; edge* | 6390 | 12 | 0.0007 | 200 | 54 | 2 | 1 | 216 | 1380.24 |
| *sea lock head; middle* | 10000 | 10 | 0.0008 | 200 | 60 | 1 | 1 | 120 | 1200 |
| *Wall 9-10-11; edge* | 4890 | 10 | 0.0004 | 100 | 56 | 1 | 1 | 112 | 547.68 |

| | | | | | | | | | |
|---|---|---|---|---|---|---|---|---|---|
| *Wall-12-13-14* | 10000 | 10 | 0.0008 | 200 | 86 | 6 | 1 | 1032 | 10320 |
| *river lock head; edge* | 5950 | 10 | 0.0005 | 200 | 24 | 2 | 1 | 96 | 571.2 |
| *river lock head; middle* | 9600 | 10 | 0.0008 | 200 | 86 | 1 | 1 | 172 | 1651.2 |

# Appendix D: Anchored Chamber Design

Moments $M_{xx}$ and $M_{yy}$, shear forces and reaction forces for the low wall at the seaside chamber and the sloped wall segment are presented in Table 80 and the shear forces at the bottom of the sloped wall segment can be found in Table 81. Value represents the weighed value where 60% is from the simply supported (s.s.) edge scenario and 40% is from the free edge scenario. Table 82 presents the moments and shear forces for the low wall at the river side chamber.

**Table 80: Moments, shear forces and reaction forces for the low wall at the seaside chamber and the slope wall segment. X = 0 is at the start of the low wall at the seaside lock head. Anchor level at the low seaside wall at NAP +2.3 m.**

| Moment $M_{xx}$ [kNm] | X [m] | Y [m] | Free | s.s. | Value |
|---|---|---|---|---|---|
| ***Bottom edge*** | 0.8 | 0 | 416.1 | 119.5 | 238.1 |
| ***Bottom middle*** | 26.3 | 0 | 387.9 | 387.2 | 387.5 |
| ***Bottom thickness change*** | 50.8 | 0 | 569.2 | 564.2 | 566.2 |
| ***Bottom before slope*** | 58.6 | 0 | 787.1 | 778.2 | 781.8 |
| ***Bottom edge slope*** | 69.8 | 0 | 2178.5 | 491.0 | 1166.0 |
| ***Middle of slope*** | 65.1 | 0 | 1582.7 | 1475.4 | 1518.3 |
| ***Center edge slope*** | 70.3 | 4.7 | -993.7 | -139.2 | -481.0 |
| ***Center middle slope*** | 68.2 | 4.7 | -912.9 | -547.6 | -693.7 |
| ***Center middle slope*** | 65.2 | 4.5 | -788.9 | -720.3 | -747.7 |
| ***Center middle slope*** | 62.2 | 4.4 | -640.4 | -630.0 | -634.1 |
| ***Center middle slope*** | 59.2 | 4.2 | -452.9 | -445.1 | -448.2 |
| ***Center middle slope*** | 56.2 | 4.2 | -278.0 | -270.8 | -273.7 |
| *Anchor 4 slope 600* | 68.8 | 9.2 | 1616.8 | 666.9 | 1046.9 |
| *Anchor 3 slope 600* | 65.8 | 8.7 | 1133.6 | 1142.3 | 1138.8 |
| *Anchor 2 slope 600* | 62.8 | 8.2 | 896.0 | 997.5 | 956.9 |
| *Anchor 1 slope 600* | 59.8 | 7.7 | 653.5 | 713.3 | 689.4 |
| ***Anchor 600*** | 56.8 | 7.5 | 390.9 | 420.7 | 408.8 |
| ***Anchor 600*** | 53.8 | 7.5 | 353.8 | 368.5 | 362.6 |
| ***Anchor edge 600*** | 50.8 | 7.5 | 495.8 | 502.9 | 500.0 |
| ***Anchor edge 600*** | 47.3 | 7.5 | 393.3 | 394.5 | 394.0 |
| ***Inner anchors 600*** | 26.3 | 7.5 | 425.1 | 425.1 | 425.1 |
| ***Anchor edge 600*** | 1.8 | 7.5 | 445.0 | 255.7 | 331.4 |
| ***Anchor 4 slope 400*** | 68.8 | 9.2 | 1881.6 | 789.7 | 1226.5 |
| ***Anchor 3 slope 400*** | 65.8 | 8.7 | 1308.9 | 1341.9 | 1328.7 |
| ***Anchor 2 slope 400*** | 62.8 | 8.2 | 1053.2 | 1174.4 | 1125.9 |
| ***Anchor 1 slope 400*** | 59.8 | 7.7 | 777.7 | 841.3 | 815.8 |
| *Anchor 400* | 56.8 | 7.5 | 459.7 | 490.2 | 478.0 |
| *Anchor 400* | 53.8 | 7.5 | 415.8 | 431.4 | 425.2 |

| | | | | | |
|---|---|---|---|---|---|
| *Anchor edge 400* | 50.8 | 7.5 | 590.2 | 597.1 | 594.4 |
| *Anchor edge 400* | 47.3 | 7.5 | 468.8 | 470.0 | 469.5 |
| *Inner anchors 400* | 26.3 | 7.5 | 504.0 | 504.0 | 504.0 |
| *Anchor edge 400* | 1.8 | 7.5 | 527.8 | 307.8 | 395.8 |

| **Moment $M_{yy}$ [kNm}** | **X [m]** | **Y [m]** | **Free** | **s.s.** | **Value** |
|---|---|---|---|---|---|
| ***Bottom edge slope*** | 68.9 | 0 | 606.1 | 258.4 | 397.5 |
| ***Bottom low slope*** | 58.6 | 0 | 239.6 | 235.6 | 237.2 |
| ***Bottom middle slope*** | 65.1 | 0 | 475.2 | 434.1 | 450.6 |
| *Anchor 4 slope 600* | 68.8 | 9.2 | 1204.2 | 379.4 | 709.3 |
| *Anchor 3 slope 600* | 65.8 | 8.7 | 766.0 | 757.7 | 761.1 |
| *Anchor 2 slope 600* | 62.8 | 8.2 | 643.5 | 699.0 | 676.8 |
| *Anchor 1 slope 600* | 59.8 | 7.7 | 504.7 | 527.7 | 518.5 |
| ***Anchor 600*** | 56.8 | 7.5 | 297.4 | 308.3 | 304.0 |
| ***Anchor 600*** | 53.8 | 7.5 | 251.6 | 257.8 | 255.3 |
| ***Anchor edge 600*** | 50.8 | 7.5 | 267.2 | 268.6 | 268.0 |
| ***Inner anchors 600*** | 26.3 | 7.5 | 315.7 | 315.7 | 315.7 |
| ***Anchor 4 slope 400*** | 68.8 | 9.2 | 1466.7 | 499.2 | 886.2 |
| ***Anchor 3 slope 400*** | 65.8 | 8.7 | 942.0 | 955.7 | 950.2 |
| ***Anchor 2 slope 400*** | 62.8 | 8.2 | 799.2 | 871.0 | 842.3 |
| ***Anchor 1 slope 400*** | 59.8 | 7.7 | 628.4 | 655.8 | 644.8 |
| *Anchor 400* | 56.8 | 7.5 | 367.5 | 379.5 | 374.7 |
| *Anchor 400* | 53.8 | 7.5 | 314.2 | 320.9 | 318.2 |
| *Anchor edge 400* | 50.8 | 7.5 | 339.6 | 340.9 | 340.4 |
| *Inner anchors 400* | 26.3 | 7.5 | 393.5 | 393.5 | 393.5 |
| ***Center slope edge*** | 68.4 | 4.5 | -183.4 | -497.8 | -372.0 |
| ***Center slope middle*** | 66.3 | 4.5 | -226.8 | -454.9 | -363.7 |
| ***Center middle*** | 28.1 | 4.2 | -61.6 | -61.6 | -61.6 |

| **Shear V [kN]** | **X [m]** | **Y [m]** | **Free** | **s.s.** | **Value** |
|---|---|---|---|---|---|
| ***Bottom middle*** | 28.1 | 0 | 287.8 | 287.8 | 287.8 |
| ***Bottom edge*** | 0.6 | 0 | 370.1 | 97.1 | 206.3 |
| *Anchor 4 slope 600* | 68.8 | 9.2 | 3425.0 | 1632.4 | 2349.4 |
| *Anchor 3 slope 600* | 65.8 | 8.7 | 2418.1 | 2669.4 | 2568.9 |
| *Anchor 2 slope 600* | 62.8 | 8.2 | 2138.1 | 2336.4 | 2257.1 |
| *Anchor 1 slope 600* | 59.8 | 7.7 | 1689.0 | 1747.1 | 1723.9 |
| ***Anchor 600*** | 56.8 | 7.5 | 950.3 | 967.5 | 960.6 |
| ***Anchor 600*** | 53.8 | 7.5 | 837.8 | 845.3 | 842.3 |
| ***Anchor edge 600*** | 50.8 | 7.5 | 1143.4 | 1145.3 | 1144.5 |
| ***Anchor edge 600*** | 47.3 | 7.5 | 985.2 | 984.9 | 985.0 |
| ***Inner anchors 600*** | 26.3 | 7.5 | 1021.3 | 1021.3 | 1021.3 |
| ***Anchor edge 600*** | 1.8 | 7.5 | 1063.5 | 699.9 | 845.4 |
| ***Anchor 4 slope 400*** | 68.8 | 9.2 | 4636.7 | 2393.9 | 3291.0 |
| ***Anchor 3 slope 400*** | 65.8 | 8.7 | 3505.9 | 3905.6 | 3745.7 |
| ***Anchor 2 slope 400*** | 62.8 | 8.2 | 3104.8 | 3402.5 | 3283.4 |
| ***Anchor 1 slope 400*** | 59.8 | 7.7 | 2453.4 | 2538.3 | 2504.3 |
| *Anchor 400* | 56.8 | 7.5 | 1378.0 | 1402.6 | 1392.7 |
| *Anchor 400* | 53.8 | 7.5 | 1220.7 | 1231.4 | 1227.1 |
| *Anchor edge 400* | 50.8 | 7.5 | 1639.9 | 1641.0 | 1640.5 |
| *Anchor edge 400* | 47.3 | 7.5 | 1477.2 | 1446.6 | 1458.8 |

| | | | | | |
|---|---|---|---|---|---|
| *Inner anchors 400* | 26.3 | 7.5 | 1498.7 | 1498.7 | 1498.7 |
| *Anchor edge 400* | 1.8 | 7.5 | 1564.0 | 1030.2 | 1243.7 |

| Reaction forces R [kN] | X [m] | Y [m] | Free | s.s. | Value |
|---|---|---|---|---|---|
| *Anchor middle* | 26.3 | 7.5 | 1555.94 | 1555.94 | 1556.0 |
| *Anchor edge* | 1.8 | 7.5 | 1687.45 | 1640.23 | 1659.2 |
| *Anchor 4 slope* | 68.8 | 9.2 | 3398.2 | 1566.26 | 2299.1 |
| *Anchor 3 slope* | 65.8 | 8.7 | 3738.08 | 3678.33 | 3702.3 |
| *Anchor 2 slope* | 62.8 | 8.2 | 3240.6 | 3508.53 | 3401.4 |
| *Anchor 1 slope* | 59.8 | 7.7 | 2379.38 | 2522.35 | 2465.2 |
| *Anchor* | 56.8 | 7.5 | 1447.41 | 1478.49 | 1466.1 |
| *Anchor* | 53.8 | 7.5 | 1270.69 | 1277.08 | 1274.6 |
| *Anchor edge* | 50.8 | 7.5 | 1533.9 | 1531.21 | 1532.3 |

Table 81: shear forces at the bottom of the sloped wall segment

| X | free | s.s. | Value [kN] |
|---|---|---|---|
| **70.5** | 1405.7 | 142.6 | 647.9 |
| **69.5** | 1740.5 | 584.0 | 1046.7 |
| **68** | 1360.4 | 1097.1 | 1202.5 |
| **66.5** | 1231.5 | 1211.5 | 1219.6 |
| **65** | 1162.7 | 1191.2 | 1179.8 |
| **63.5** | 1093.3 | 1121.0 | 1109.9 |
| **62** | 1013.4 | 1030.1 | 1023.4 |
| **60.5** | 910.9 | 917.7 | 915.0 |
| **59** | 743.1 | 743.7 | 743.3 |
| **57.5** | 466.9 | 464.6 | 465.6 |
| **56** | 363.4 | 360.3 | 361.6 |
| **54.5** | 329.4 | 326.5 | 327.7 |
| **52.8** | 341.6 | 339.2 | 340.2 |
| **50.8** | 352.9 | 352.7 | 352.8 |

Table 82: Moments, shear forces and reaction forces for the low wall at the riverside chamber. X = 0 is at the start of the low wall at the riverside lock head. Anchor level at NAP +1.2 m.

| Moment $M_{xx}$ [kNm] | X [m] | Y [m] | Free | s.s. | Value |
|---|---|---|---|---|---|
| Bottom edge | 0.7 | 0 | 218.5 | 59.1 | 122.9 |
| **Bottom middle** | 26.3 | 0 | 197.1 | 204.4 | 201.5 |
| **Inner anchors 400** | 26.3 | 6.4 | 219.4 | 219.4 | 219.4 |
| **Anchor edge 400** | 1.8 | 6.4 | 236.0 | 162.6 | 191.9 |
| **center edge** | 1.8 | 3.6 | -105.8 | -67.1 | -82.6 |
| **center inner** | 26.3 | 3.6 | -107.4 | -107.3 | -107.3 |

| Moment $M_{yy}$ [kNm] | X [m] | Y [m] | Free | s.s. | Value |
|---|---|---|---|---|---|
| **Anchor edge 400** | 1.8 | 6.4 | 225.8 | 137.6 | 172.8 |
| **Inner anchors 400** | 26.3 | 6.4 | 193.6 | 193.6 | 193.6 |

| Shear V [kN] | X [m] | Y [m] | Free | s.s. | Value |
|---|---|---|---|---|---|

| | | | | | |
|---|---|---|---|---|---|
| Bottom middle | 28.1 | 0 | 165.7 | 165.7 | 165.7 |
| **Bottom edge** | 0.6 | 0 | 220.7 | 65.8 | 127.8 |
| **Inner anchors 400** | 26.3 | 7.5 | 783.2 | 783.2 | 783.2 |
| **Anchor edge 400** | 1.8 | 7.5 | 829.0 | 600.3 | 691.8 |

## D.1: MATLAB; Floor moments and shear forces

```
clc;
clear variables;
close all;

%% Values
M1 = 1074.2; %[kNm]
V1 = 437.4; %[kN]
E = 34.07*10^6; %[kN/m2]
G = 5000000; %[kN/m2] shear modulus concrete
Gp = G*0.5 %[kN/m] 1.4 uwcf thickness (shear layer)
q = -(78.43-50.47); %[kN/m]
L = 22.3; %[m]
t = 0.61; %[m]
b = 1; %[m]
I = (b*t^3)/12 %[m4]
EI = E*I;
k = 200000*b; %[kN/m2/m}
beta = (k/(4*EI))^(1/4);
%% Differential equation, kinematic and constitutive relations
syms w(x)
ODE = diff(w,x,4)-(Gp/EI)*diff(w,x,2)+4*beta^4*w == q/EI;
phi = diff(w,x); M = EI*diff(w,x,2) ; V = EI*diff(w,x,3);
%% Boundary conditions
cond1 =  M(0) == M1;
cond2 = V(0) == -V1;
cond3 = phi(L/2) == 0;
cond4 = V(L/2) == 0;
conds = [cond1,cond2,cond3,cond4];
wSol(x) = dsolve(ODE,conds);
Msol =@(x) EI*diff(wSol,x,2);
Vsol =@(x) EI*diff(wSol,x,3);

tiledlayout(2,1)
nexttile
fplot(Vsol(x),[0 L/2])
title('Shear force')
xlabel('x')
ylabel('V [kN]')

nexttile
fplot(Msol(x),[0 L/2])
title('Bending moment')
xlabel('x')
ylabel('M [kNm]')
```

# D.2: Anchored Wall Chamber Reinforcement

The following tables display the reinforcement and information about the detailing.

**Table 83: Required reinforcement area for a given moment and its resulting bar diameter and c/c distance for the sloped wall segments**

| **Vertical wall reinforcement** | **$M_{xx}$ [kNm]** | **$A_{s1}$ [mm²]** | **$Ø_{bar}$ [mm]** | **c/c [mm]** |
|---|---|---|---|---|
| *Bottom 69.8* | 1166.0 | 3879.7 | 25 | 110 |
| *Bottom 65.1* | 1518.3 | 5281.7 | 32 | 110 |
| *Bottom 58.9* | 781.8 | 2580.9 | 20 | 110 |
| ***Bottom 50.8*** | 566.2 | 1865.4 | 25 | 220 |
| *Anchor 68.8, 62.8* | 1046.9 | 3484.6 | 32 | 220 |
| *Anchor 65.8* | 1138.8 | 3800.2 | 25 | 110 |
| ***Anchor 59.8*** | 689.4 | 2283.6 | 20 | 110 |
| ***Anchor 56.8*** | 478.0 | 1583.5 | 16 | 110 |
| ***Anchor 53.8*** | 425.2 | 1408.3 | 20 | 220 |
| ***Anchor 50.8*** | 594.4 | 1968.8 | 25 | 220 |
| *-$M_{xx}$ inner side of wall, 59* | -488.2 | 1647.7 | 16 | 110 |
| *-$M_{xx}$ inner side of wall, 68-70.6* | -693.7 | 2341.3 | 20 | 110 |
| *-$M_{xx}$ inner side of wall, 65* | -747.7 | 2523.6 | 20 | 110 |
| *-$M_{xx}$ inner side of wall, 62* | 634.1 | 2140.1 | 20 | 110 |
| *Minimum reinforcement* | [-] | 1218.5 | 20 | 220 |

| **Horizontal wall reinforcement** | **$M_{yy}$ [kNm]** | **$A_{s1}$ [mm²]** | **$Ø_{bar}$ [mm]** | **c/c [mm]** |
|---|---|---|---|---|
| *Anchor 68.8 65.8, 62.8* | 761.1 | 2629.0 | 25 | 170 |
| *Anchor 59.8* | 518.5 | 1789.9 | 20 | 170 |
| *Anchor 56.8, 53.8, 50.8* | 374.72 | 1273.5 | 12 | 85 |
| *Bottom of wall* | 450.57 | 1540.0 | 20 | 170 |
| *-$M_{yy}$ inner side of wall* | -375.0 | 1298.2 | 12 | 85 |
| *Minimum reinforcement* | [-] | 1218.5 | 12 | 85 |

| **Floor bottom reinforcement** | **M [kNm]** | **$A_{s1}$ [mm²]** | **$Ø_{bar}$ [mm]** | **c/c [mm]** |
|---|---|---|---|---|
| *X = 68.8, edge, primary* | 1166.0 | 5500.5 | 32 | 110 |
| *X = 68.8, edge, transverse* | [-] | 1462.3 | 16 | 130 |
| *X = 68.8, center, primary* | 303.9 | 1329.7 | 20 | 220 |
| *X = 68.8, center, transverse* | [-] | 285.6 | 10 | 260 |
| *X = 64.9, edge, primary* | 1518.3 | 7492.6 | 32 | 110 |
| *X = 64.9, edge, transverse* | [-] | 1462.3 | 16 | 130 |
| *X = 64.9, center, primary* | 428.1 | 1939.8 | 25 | 220 |
| *X = 64.9, center, transverse* | [-] | 446.2 | 10 | 130 |
| *X = 58.4, edge, primary* | 781.8 | 3595.0 | 32 | 220 |
| *X = 58.4, edge, transverse* | [-] | 731.1 | 12 | 130 |
| *X = 58.4, center, primary* | 201.0 | 910.8 | 12 | 110 |
| *X = 58.4, center, transverse* | [-] | 205.6 | 10 | 260 |
| *X = 50.9, edge, primary* | 566.2 | 2565.8 | 20 | 110 |
| *X = 50.9, edge, transverse* | [-] | 571.2 | 10 | 130 |
| *X = 50.9, center, primary* | 132.8 | 891.4 | 12 | 110 |
| *X = 50.9, center, transverse* | [-] | 205.6 | 10 | 260 |
| *Minimum primary* | [-] | 891.4 | 12 | 110 |

| | | | | |
|---|---|---|---|---|
| *Minimum transverse* | [-] | 205.6 | 10 | 260 |

| **Floor top reinforcement** | **M [kNm]** | **$A_{s1}$ [mm²]** | **$Ø_{bar}$ [mm]** | **c/c [mm]** |
|---|---|---|---|---|
| *Compression top* | [-] | 1001.5 | 20 | 220 |
| *Transverse top* | [-] | 285.6 | 10 | 260 |

**Table 84: Reinforcement for the sloped wall segment of the anchored chamber wall, NAP +4.5 m to NAP +11 m, t = 0.8 m**

| ***Shear reinforcement*** | ***L [mm]*** | ***Ø [mm]*** | ***volume [m³]*** | ***no. bars horiz.*** | ***no bars y*** | ***c/c [mm]*** | **no. Walls** | ***tot bars*** | ***Tot. length [m]*** |
|---|---|---|---|---|---|---|---|---|---|
| *Shear bot 56.2-50.8; 710x690* | 3000 | 8 | 0.0002 | 11 | 5 | 380 | 4 | 220 | 660 |
| *Shear bot 58.4 - 56.2 ; 710x690* | 3000 | 8 | 0.0002 | 5 | 12 | 190 | 4 | 240 | 720 |
| *Shear bot 59.2-58.4; 710x690* | 3000 | 8 | 0.0002 | 2 | 14 | 190 | 4 | 112 | 336 |
| *Shear bot 57.9-59.2; 725x690* | 3075 | 12 | 0.0003 | 3 | 9 | 210 | 4 | 108 | 332.1 |
| *Shear bot 70.6-57.9; 725x690* | 3075 | 12 | 0.0003 | 22 | 17 | 190 | 4 | 1496 | 4600.2 |
| *Shear bot edge; 500x690* | 2625 | 12 | 0.0003 | 1 | 17 | 190 | 4 | 68 | 178.5 |
| *Shear anchor 50.8* | 3075 | 12 | 0.0003 | 5 | 13 | 210 | 4 | 260 | 799.5 |
| *Shear anchor 53.8* | 3075 | 12 | 0.0003 | 6 | 10 | 210 | 4 | 240 | 738 |
| *Shear anchor 56.8; 720x690* | 3075 | 12 | 0.0003 | 6 | 12 | 210 | 4 | 288 | 885.6 |
| *Shear anchor 59.8; 715x690* | 3025 | 10 | 0.0002 | 7 | 25 | 130 | 4 | 700 | 2117.5 |
| *Shear anchor 62.8; 720x690* | 3075 | 12 | 0.0003 | 7 | 32 | 130 | 4 | 896 | 2755.2 |
| *Shear anchor 65.8; 725x690* | 3075 | 12 | 0.0003 | 7 | 34 | 130 | 4 | 952 | 2927.4 |
| *Shear anchor 68.8; 710x690* | 3075 | 12 | 0.0003 | 5 | 30 | 130 | 4 | 600 | 1845 |
| *Shear anchor edge; 495x690* | 2575 | 12 | 0.0003 | 1 | 30 | 130 | 4 | 120 | 309 |
| ***Vertical bars (Mxx)*** | | | | | | | | | |
| *tens. Bottom 70.4-67.8, S* | 3000 | 25 | 0.0015 | 24 | 1 | 110 | 4 | 96 | 288 |
| *tens. Bottom 67.8-60.7, S; L-bar 3780x1720* | 5410 | 32 | 0.0044 | 64 | 1 | 110 | 4 | 256 | 1384.96 |
| *tens. Bottom 60.7-58.8, S* | 3000 | 25 | 0.0015 | 17 | 1 | 110 | 4 | 68 | 204 |
| *tens. Bottom 58.8-56.2, S; L-bar 3780x1720* | 5410 | 20 | 0.0017 | 24 | 1 | 110 | 4 | 96 | 519.36 |
| *tens. Bottom 56.2-50.9, S* | 3000 | 25 | 0.0015 | 24 | 1 | 220 | 4 | 96 | 288 |
| *tens. Anchor 68.8, S* | 3500 | 32 | 0.0028 | 17 | 1 | 220 | 4 | 68 | 238 |
| *tens. Anchor 65.8, S* | 3500 | 25 | 0.0017 | 27 | 1 | 110 | 4 | 108 | 378 |
| *tens. Anchor 62.8, S* | 3440 | 32 | 0.0028 | 13 | 1 | 220 | 4 | 52 | 178.88 |
| *tens. Anchor 59.8, S* | 3000 | 20 | 0.0009 | 20 | 1 | 110 | 4 | 80 | 240 |
| *tens. Anchor 56.8, S* | 3000 | 16 | 0.0006 | 28 | 1 | 110 | 4 | 112 | 336 |
| *tens. Anchor 50.8; total bar length ,S* | 27475 | 25 | 0.0135 | 7 | 1 | 220 | 4 | 28 | 769.3 |
| *between bot & anchor 68.8, S* | 6700 | 20 | 0.0021 | 17 | 1 | 220 | 4 | 68 | 455.6 |
| *between bot & anchor 65.8, S* | 6400 | 20 | 0.0020 | 10 | 1 | 220 | 4 | 40 | 256 |
| *between bot & anchor 65.8-62.8, S* | 6200 | 20 | 0.0019 | 4 | 1 | 220 | 4 | 16 | 99.2 |
| *between bot & anchor 62.8 & 59.8, S* | 6000 | 20 | 0.0019 | 23 | 1 | 220 | 4 | 92 | 552 |
| *between bot & anchor 56.8, S* | 4870 | 20 | 0.0015 | 14 | 1 | 220 | 4 | 56 | 272.72 |
| *between bot & anchor 50.8, S* | 6000 | 20 | 0.0019 | 7 | 1 | 220 | 4 | 28 | 168 |
| *above anchor 68.8; total length given, S* | 70050 | 20 | 0.0220 | 13 | 1 | 220 | 4 | 52 | 70.05 |

| | | | | | | | | | |
|---|---|---|---|---|---|---|---|---|---|
| *above anchor 65.8; total length given, S* | 66575 | 20 | 0.0209 | 14 | 1 | 220 | 4 | 56 | 66.575 |
| *above anchor 62.8; total length given, S* | 54400 | 20 | 0.0171 | 13 | 1 | 220 | 4 | 52 | 54.4 |
| *above anchor 59.8; total length given, S* | 59075 | 20 | 0.0186 | 14 | 1 | 220 | 4 | 56 | 59.075 |
| *above bot. Reinf. 56.8-53.8; tot. Length given S* | 164575 | 20 | 0.0517 | 35 | 1 | 220 | 4 | 140 | 164.575 |
| *tens. Center 70.4-65.6, C* | 5850 | 32 | 0.0047 | 22 | 1 | 220 | 4 | 88 | 514.8 |
| *tens. Center 65.6-62.2, C* | 5900 | 25 | 0.0029 | 32 | 1 | 110 | 4 | 128 | 755.2 |
| *tens. Center 62.6-59, C* | 5300 | 32 | 0.0043 | 14 | 1 | 220 | 4 | 56 | 296.8 |
| *tens. Center 59-56, C* | 5200 | 16 | 0.0010 | 24 | 1 | 110 | 4 | 96 | 499.2 |
| *bottom to center 70.4-56, C* | 3200 | 20 | 0.0010 | 66 | 1 | 220 | 4 | 264 | 844.8 |
| *bottom half 56-50.9, C* | 7000 | 20 | 0.0022 | 23 | 1 | 220 | 4 | 92 | 644 |
| *above center 56-50.9; total length given, C* | 551600 | 20 | 0.1733 | 89 | 1 | 220 | 4 | 356 | 551.6 |
| ***Horizontal bars (Myy)*** | | | | | | | | | |
| *tension bottom 70.4-59.4, S* | 6800 | 20 | 0.0021 | 2 | 13 | 170 | 4 | 104 | 707.2 |
| *tension bottom to H= 9.7; 59.4-50.9, S* | 8750 | 12 | 0.0010 | 1 | 113 | 85 | 4 | 452 | 3955 |
| *tens anchor 68.8, S* | 4100 | 25 | 0.0020 | 1 | 21 | 170 | 4 | 84 | 344.4 |
| *tens anchor 65.8 & 62.8, S* | 6400 | 25 | 0.0031 | 1 | 21 | 170 | 4 | 84 | 537.6 |
| *tens anchor 59.8, S* | 3900 | 20 | 0.0012 | 1 | 21 | 115 | 4 | 84 | 327.6 |
| *above anchor 68.8 & 65.8; total length given, S* | 124800 | 12 | 0.0141 | 1 | 58 | 85 | 4 | 232 | 124.8 |
| *above anchor 62.8 & 59.8; total length given, S* | 64175 | 12 | 0.0073 | 1 | 29 | 85 | 4 | 116 | 64.175 |
| *above anchor 56.8 - 50.8; total length given, S* | 51925 | 12 | 0.0059 | 1 | 23 | 85 | 4 | 92 | 51.925 |
| *betw. Bottom & anchor 70.4-59.4, S* | 6700 | 12 | 0.0008 | 2 | 58 | 85 | 4 | 464 | 3108.8 |
| *tens. Center 70.4-59, C* | 6400 | 12 | 0.0007 | 2 | 45 | 85 | 4 | 360 | 2304 |
| *bottom below center 70.4-59, C* | 6700 | 12 | 0.0008 | 2 | 40 | 85 | 4 | 320 | 2144 |
| *bottom to H = 9.7;  59-50.9, C* | 9500 | 12 | 0.0011 | 1 | 113 | 85 | 4 | 452 | 4294 |
| *above anchor 68.8 & 65.8; total length given, C* | 238600 | 12 | 0.0270 | 1 | 102 | 85 | 4 | 408 | 238.6 |
| *above anchor 62.8 & 59.8; total length given, C* | 170025 | 12 | 0.0192 | 1 | 67 | 85 | 4 | 268 | 170.025 |
| *above anchor 56.8 - 50.8; total length given, C* | 45525 | 12 | 0.0051 | 1 | 19 | 85 | 4 | 76 | 45.525 |

| ***Floor*** | ***L [mm]*** | ***Ø [mm]*** | ***volume [m³]*** | ***no. bars z*** | ***no. bars x*** | ***c/c [mm]*** | **no. Floors/ walls** | ***tot bars*** | ***Tot. length [m]*** |
|---|---|---|---|---|---|---|---|---|---|
| *tension bottom edge 70.4-58.2* | 6800 | 32 | 0.0055 | 2 | 112 | 110 | 2 | 448 | 3046.4 |
| *tension bottom middle 70.4-58.2* | 6250 | 20 | 0.0020 | 1 | 56 | 220 | 2 | 112 | 700 |
| *tension bottom edge 58.2-54.2* | 6800 | 32 | 0.0055 | 2 | 16 | 220 | 2 | 64 | 435.2 |
| *tension bottom middle 58.2-54.2* | 6750 | 12 | 0.0008 | 1 | 33 | 110 | 2 | 66 | 445.5 |
| *tension bottom edge 54.2-50.8* | 6800 | 20 | 0.0021 | 2 | 33 | 110 | 2 | 132 | 897.6 |
| *tension bottom middle 54.2-50.8* | 6750 | 12 | 0.0008 | 1 | 33 | 110 | | | |

| | | | | | | | | | |
|---|---|---|---|---|---|---|---|---|---|
| *transverse bottom edge 70.4-58.2* | 6750 | 16 | 0.0014 | 105 | 2 | 130 | 2 | 420 | 2835 |
| *transverse bottom middle 70.4-58.2* | 6650 | 10 | 0.0005 | 17 | 2 | 130 | 2 | 68 | 452.2 |
| *transverse bottom edge 58.2-50.9* | 7900 | 12 | 0.0009 | 105 | 1 | 130 | 2 | 210 | 1659 |
| *transverse bottom middle 58.2-50.9* | 7700 | 10 | 0.0006 | 17 | 1 | 260 | 2 | 34 | 261.8 |
| *compression top* | 9630 | 20 | 0.0030 | 2 | 89 | 220 | 2 | 356 | 3428.28 |
| *transverse top* | 7150 | 10 | 0.0006 | 69 | 3 | 260 | 2 | 414 | 2960.1 |
| ***U-bars, L bars and anchor bars*** | | | | | | | | | |
| *U-loops top 1100x670x1100* | 2800 | 20 | 0.0009 | 1 | 89 | 220 | 4 | 356 | 996.8 |
| *U-loops top - anchors* | 7650 | 25 | 0.0038 | 2 | 3 | [-] | 4 | 24 | 183.6 |
| *U-loop floor 1490x684x1070* | 3150 | 20 | 0.0010 | 1 | 89 | 220 | 4 | 356 | 1121.4 |
| *L-bar Bottom 70.4-67.8, S; 2010x1340* | 3300 | 25 | 0.0016 | 1 | 32 | 110 | 4 | 128 | 422.4 |
| *L-bar Bottom 60.7-58.8, S; 2010x1340* | 3300 | 32 | 0.0027 | 1 | 9 | 110 | 4 | 36 | 118.8 |
| *L-bar Bottom 56.2-50.9, S; 2010x1340* | 3300 | 25 | 0.0016 | 1 | 24 | 220 | 4 | 96 | 316.8 |
| *J-bar bottom-C 1800x664x290* | 2650 | 20 | 0.0008 | 1 | 89 | 220 | 4 | 356 | 943.4 |
| *K32 anchor bottom* | 7900 | 32 | 0.0064 | 1 | 3 | [-] | 4 | 12 | 94.8 |
| *K25 anchor bottom* | 7600 | 25 | 0.0037 | 2 | 3 | [-] | 4 | 24 | 182.4 |

**Table 85: Required reinforcement area for a given moment and its resulting bar diameter and c/c distance for the low seaside wall**

| **Vertical wall reinforcement** | **$M_{xx}$ [kNm]** | **$A_{s1}$ [mm²]** | **$Ø_{bar}$ [mm]** | **c/c [mm]** |
|---|---|---|---|---|
| *Bottom of wall and anchors edge* | 395.8 | 1770.3 | 16 | 110 |
| *Bottom, edge* | 238.1 | 1069.1 | 20 | 220 |
| *Inner anchors* | 504.0 | 2288.1 | 20 | 110 |
| *-$M_{xx}$ inner side of wall* | -217.8 | 1015.5 | 12 | 110 |
| *Minimum reinforcement* | [-] | 903.0 | 16 | 220 |

| **Horizontal wall reinforcement** | **$M_{yy}$ [kNm]** | **$A_{s1}$ [mm²]** | **$Ø_{bar}$ [mm]** | **c/c [mm]** |
|---|---|---|---|---|
| *Anchors* | 393.46 | 1856.0 | 20 | 160 |
| *Minimum reinforcement* | [-] | 903.0 | 16 | 220 |

| **Floor bottom reinforcement** | **M [kNm]** | **$A_{s1}$ [mm²]** | **$Ø_{bar}$ [mm]** | **c/c [mm]** |
|---|---|---|---|---|
| *Edges primary, near slope* | 395.8 | 1884.1 | 25 | 220 |
| *Edges transvers, near slope* | [-] | 446.2 | 10 | 130 |
| *Minimum primary* | [-] | 1001.5 | 20 | 220 |
| *Minimum transverse* | [-] | 285.6 | 10 | 260 |

| **Floor top reinforcement** | **M [kNm]** | **$A_{s1}$ [mm²]** | **$Ø_{bar}$ [mm]** | **c/c [mm]** |
|---|---|---|---|---|
| *Compression top* | [-] | 1001.5 | 20 | 220 |
| *Transverse top* | [-] | 285.6 | 10 | 260 |

Table 86: Reinforcement for the low wall of the seaside chamber of the anchored chamber wall, NAP +4.5 m, t = 0.6 m

| ***Shear reinforcement*** | ***L [mm]*** | ***Ø [mm]*** | ***volume [m³]*** | ***no. bars horiz.*** | ***no bars y*** | ***c/c [mm]*** | ***no. Walls*** | ***tot bars*** | ***tot length [m]*** |
|---|---|---|---|---|---|---|---|---|---|
| *shear bottom 700x490* | 2575 | 6 | 0.0001 | 116 | 5 | 220 | 2 | 1160 | 2987 |
| *link to sloped wall bot. 450x490x680x690* | 2525 | 8 | 0.0001 | 1 | 5 | 280 | 2 | 10 | 25.25 |
| *shear anchor 725x490* | 2675 | 12 | 0.0003 | 116 | 17 | 150 | 2 | 3944 | 10550.2 |
| *link to sloped wall anch. 460x490x694x690* | 2575 | 12 | 0.0003 | 1 | 17 | 150 | 2 | 34 | 87.55 |
| ***Vertical bars (Mxx)*** | | | | | | | | | |
| *tension bottom inner, S* | 2600 | 16 | 0.0005 | 444 | 1 | 110 | 2 | 888 | 2308.8 |
| *tension anchor to top inner, S* | 3250 | 20 | 0.0010 | 444 | 1 | 110 | 2 | 888 | 2886 |
| *tension bottom edge, S* | 2600 | 20 | 0.0008 | 11 | 1 | 220 | 2 | 22 | 57.2 |
| *tension anchor to top edge, S* | 3250 | 16 | 0.0007 | 22 | 1 | 110 | 2 | 44 | 143 |
| *tens cent. (-Mxx), C* | 2300 | 12 | 0.0003 | 469 | 1 | 110 | 2 | 938 | 2157.4 |
| *betw. bottom & anchor S* | 5300 | 16 | 0.0011 | 233 | 1 | 220 | 2 | 466 | 2469.8 |
| *from bottom to center, C* | 3600 | 16 | 0.0007 | 235 | 1 | 220 | 2 | 470 | 1692 |
| *from center to top, C* | 4850 | 16 | 0.0010 | 235 | 1 | 220 | 2 | 470 | 2279.5 |
| ***Horizontal bars (Myy)*** | | | | | | | | | |
| *tension anchor, S* | 10000 | 20 | 0.0031 | 5 | 20 | 160 | 2 | 200 | 2000 |
| *tension anchor edge, S* | 5900 | 20 | 0.0019 | 1 | 20 | 160 | 2 | 40 | 236 |
| *from bottom to anchor, S* | 10000 | 16 | 0.0020 | 5 | 29 | 220 | 2 | 290 | 2900 |
| *from bottom to anchor, S edge* | 5900 | 16 | 0.0012 | 1 | 29 | 220 | 2 | 58 | 342.2 |
| *from bottom to top, C* | 10000 | 16 | 0.0020 | 5 | 44 | 220 | 2 | 440 | 4400 |
| *from bottom to top, C edge* | 6100 | 16 | 0.0012 | 1 | 44 | 220 | 2 | 88 | 536.8 |

| ***Floor*** | *L [mm]* | *Ø [mm]* | *volume [m³]* | *no. bars z* | *no. bars x* | *c/c [mm]* | no. Floors | *Tot bars* | *Tot length [m]* |
|---|---|---|---|---|---|---|---|---|---|
| *tension bottom edge* | 4710 | 25 | 0.0023 | 2 | 228 | 220 | 1 | 456 | 2147.76 |
| *tension bottom middle* | 10000 | 20 | 0.0031 | 1 | 228 | 220 | 1 | 228 | 2280 |
| *tension bottom small lock head* | 8300 | 20 | 0.0026 | 3 | 51 | 220 | 1 | 153 | 1269.9 |
| *transverse Bottom edge near slope* | 9700 | 10 | 0.0008 | 68 | 1 | 130 | 1 | 68 | 708.1 |
| *transv. bottom center near slope* | 9650 | 10 | 0.0005 | 58 | 1 | 260 | 1 | 58 | 299.15 |
| *transverse bottom rest* | 10000 | 10 | 0.0005 | 126 | 4 | 260 | 1 | 504 | 2720 |
| *transv. Bottom small lock head middle* | 7700 | 10 | 0.0004 | 126 | 2 | 260 | 1 | 252 | 1047.2 |
| *transv. Bottom small lock head edges* | 5800 | 10 | 0.0003 | 40 | 2 | 260 | 1 | 80 | 255.2 |
| *compression top* | 9430 | 20 | 0.0030 | 2 | 233 | 220 | 1 | 466 | 4394.38 |
| *compression top small lock head* | 8600 | 20 | 0.0027 | 3 | 50 | 220 | 1 | 150 | 1290 |
| *compression top transverse* | 10000 | 10 | 0.0008 | 67 | 6 | 260 | 1 | 402 | 4020 |
| *compression top transv. Edge lock head* | 5920 | 10 | 0.0005 | 22 | 2 | 260 | 1 | 44 | 260.48 |
| *compression top transv. middle lock head* | 7100 | 10 | 0.0006 | 67 | 1 | 260 | 1 | 67 | 475.7 |
| ***U-bars, L bars and anchor bars*** | | | | | | | | | |
| *U-loops top 840x490x840* | 2125 | 16 | 0.0004 | 1 | 233 | 220 | 2 | 466 | 990.25 |

| | | | | | | | | | |
|---|---|---|---|---|---|---|---|---|---|
| *U-loops top - anchors* | 10000 | 20 | 0.0031 | 2 | 5 | [-] | 2 | 20 | 200 |
| *U-loops top - anchors edge* | 7100 | 20 | 0.0022 | 2 | 1 | [-] | 2 | 4 | 28.4 |
| *U-loop floor 1490x684x1070* | 3150 | 20 | 0.0010 | 1 | 233 | 220 | 2 | 466 | 1467.9 |
| *L-bar bottom 1760x1090* | 2800 | 16 | 0.0006 | 1 | 466 | 110 | 2 | 932 | 2609.6 |
| *J-bar bottom-C 1570x474x300* | 2300 | 16 | 0.0005 | 1 | 233 | 220 | 2 | 466 | 1071.8 |
| *K25 anchor bottom* | 10000 | 25 | 0.0049 | 3 | 5 | [-] | 2 | 30 | 300 |
| *K25 anchor bottom edge* | 8600 | 25 | 0.0042 | 3 | 1 | [-] | 2 | 6 | 51.6 |
| *Anchor shear link to sloped wall* | 9500 | 20 | 0.0030 | 1 | 1 | [-] | 2 | 2 | 19 |

The 2.5 m wall increment on the seaside chamber walls has a minimum reinforcement volume wit K16 bars, c/c = 220 mm, and K16 transverse bars, c/c = 260 mm.

**Table 87: Reinforcement for the seaside lock head of the anchored chamber wall, NAP +4.5 m, t = 0.6 m**

| ***Shear reinforcement*** | ***L [mm]*** | ***Ø [mm]*** | ***volume [m]*** | ***no. bars horiz.*** | ***no bars y*** | ***c/c [mm]*** | ***no. Walls*** | ***tot bars*** | ***tot volume [m³]*** |
|---|---|---|---|---|---|---|---|---|---|
| *shear bottom 700x490* | 2575 | 6 | 0.0001 | 15 | 5 | 220 | 2 | 150 | 386.25 |
| *shear anchor 725x490* | 2675 | 12 | 0.0003 | 15 | 17 | 150 | 2 | 510 | 1364.25 |
| ***Vertical bars (Mxx)*** | | | | | | | | | |
| *tension bottom inner, S* | 2600 | 16 | 0.0005 | 100 | 1 | 110 | 2 | 200 | 520 |
| *tension anchor to top inner, S* | 3250 | 20 | 0.0010 | 100 | 1 | 110 | 2 | 200 | 650 |
| *tens cent. (-Mxx), C* | 2300 | 12 | 0.0003 | 89 | 1 | 110 | 2 | 178 | 409.4 |
| *betw. bottom & anchor S* | 5300 | 16 | 0.0011 | 50 | 1 | 220 | 2 | 100 | 530 |
| *from bottom to center, C* | 3600 | 16 | 0.0007 | 45 | 1 | 220 | 2 | 90 | 324 |
| *from center to top, C* | 4850 | 16 | 0.0010 | 45 | 1 | 220 | 2 | 90 | 436.5 |
| ***Horizontal bars (Myy)*** | | | | | | | | | |
| *tension anchor, S* | 5820 | 20 | 0.0018 | 2 | 20 | 160 | 2 | 80 | 465.6 |
| *from bottom to anchor, S* | 5820 | 16 | 0.0012 | 2 | 29 | 220 | 2 | 116 | 675.12 |
| *from bottom to top, C* | 5820 | 16 | 0.0012 | 2 | 44 | 220 | 2 | 176 | 1024.32 |
| ***U-bars, L bars and anchor bars*** | | | | | | | | | |
| *U-loops top 840x490x840* | 2125 | 16 | 0.0004 | 1 | 45 | 220 | 2 | 90 | 191.25 |
| *U-loops top - anchors* | 5910 | 20 | 0.0019 | 2 | 2 | [-] | 2 | 8 | 47.28 |
| *U-loop floor 1490x684x1070* | 3150 | 20 | 0.0010 | 1 | 50 | 220 | 2 | 100 | 315 |
| *L-bar bottom 1760x1090* | 2800 | 16 | 0.0006 | 1 | 100 | 110 | 2 | 200 | 560 |
| *J-bar bottom-C 1570x474x300* | 2300 | 16 | 0.0005 | 1 | 45 | 220 | 2 | 90 | 207 |
| *K25 anchor bottom* | 6040 | 25 | 0.0030 | 3 | 2 | [-] | 2 | 12 | 72.48 |

**Table 88: Required reinforcement area for a given moment and its resulting bar diameter and c/c distance for the low riverside wall**

| **Vertical wall reinforcement** | **$M_{xx}$ [kNm]** | **$A_{s1}$ [mm²]** | **$Ø_{bar}$ [mm]** | **c/c [mm]** |
|---|---|---|---|---|
| *Bottom of wall and anchors edge* | 201.5 | 1413.1 | 20 | 220 |
| *Bottom, edge* | 122.9 | 857.0 | 16 | 220 |
| *Inner anchors* | 219.4 | 1586.4 | 16 | 110 |
| *-$M_{xx}$ inner side of wall* | - 107.4 | 819.4 | 16 | 220 |
| *Minimum reinforcement* | [-] | 575.9 | 10 | 110 |

| Horizontal wall reinforcement | $M_{yy}$ [kNm] | $A_{s1}$ [mm²] | $Ø_{bar}$ [mm] | c/c [mm] |
|---|---|---|---|---|
| *Anchors* | 193.6 | 1477.9 | 20 | 210 |
| *Minimum reinforcement* | [-] | 575.9 | 10 | 110 |

| Floor bottom reinforcement | M [kNm] | $A_{s1}$ [mm²] | $Ø_{bar}$ [mm] | c/c [mm] |
|---|---|---|---|---|
| *Edges primary, near slope* | 251 | 1205.5 | 20 | 220 |
| *Edges transvers, near slope* | [-] | 285.6 | 8 | 130 |
| *Minimum primary* | [-] | 1001.5 | 12 | 110 |
| *Minimum transverse* | [-] | 285.6 | 8 | 130 |

| Floor top reinforcement | M [kNm] | $A_{s1}$ [mm²] | $Ø_{bar}$ [mm] | c/c [mm] |
|---|---|---|---|---|
| *Compression top* | [-] | 1001.5 | 20 | 220 |
| *Transverse top* | [-] | 285.6 | 10 | 260 |

**Table 89: Reinforcement for the low wall of the riverside chamber of the anchored chamber wall, NAP +4.5 m, t = 0.4 m**

| ***Shear reinforcement*** | ***L [mm]*** | ***Ø [mm]*** | ***volume [m^3]*** | ***no. bars horiz.*** | ***no bars y*** | ***c/c [mm]*** | ***no. Walls*** | ***tot bars*** | ***Tot length*** |
|---|---|---|---|---|---|---|---|---|---|
| *shear anchor edge 700x490* | 2575 | 10 | 0.0002 | 5 | 10 | 180 | 2 | 100 | 257.5 |
| *shear anchor 725x490* | 2675 | 12 | 0.0003 | 112 | 10 | 180 | 2 | 2240 | 5992 |
| *link to sloped wall bot. 460x490x694x690* | 2575 | 12 | 0.0003 | 1 | 15 | 180 | 2 | 30 | 77.25 |
| ***Vertical bars (Mxx)*** | | | | | | | | | |
| *tension bottom inner, S* | 2600 | 20 | 0.0008 | 222 | 1 | 220 | 2 | 444 | 1154.4 |
| *tension anchor to top inner, S* | 3250 | 16 | 0.0007 | 444 | 1 | 110 | 2 | 888 | 2886 |
| *tension bottom edge, S* | 2600 | 16 | 0.0005 | 11 | 1 | 220 | 2 | 22 | 57.2 |
| *tension anchor to top edge, S* | 3250 | 20 | 0.0010 | 11 | 1 | 220 | 2 | 22 | 71.5 |
| *tens cent. (-Mxx), C* | 2300 | 16 | 0.0005 | 235 | 1 | 220 | 2 | 470 | 1081 |
| *betw. bottom & anchor S* | 5300 | 10 | 0.0004 | 466 | 1 | 110 | 2 | 932 | 4939.6 |
| *from bottom to center, C* | 3600 | 10 | 0.0003 | 470 | 1 | 110 | 2 | 940 | 3384 |
| *from center to top, C* | 4850 | 10 | 0.0004 | 470 | 1 | 110 | 2 | 940 | 4559 |
| ***Horizontal bars (Myy)*** | | | | | | | | | |
| *tension anchor, S* | 10000 | 20 | 0.0031 | 5 | 9 | 210 | 2 | 90 | 900 |
| *tension anchor edge, S* | 5900 | 20 | 0.0019 | 1 | 9 | 210 | 2 | 18 | 106.2 |
| *from bottom to anchor&above anch, S* | 10000 | 10 | 0.0008 | 5 | 70 | 110 | 2 | 700 | 7000 |
| *from bottom to anchor, S edge* | 5900 | 10 | 0.0005 | 1 | 70 | 110 | 2 | 140 | 826 |
| *from bottom to top, C* | 10000 | 10 | 0.0008 | 5 | 88 | 110 | 2 | 880 | 8800 |
| *from bottom to top, C edge* | 6100 | 10 | 0.0005 | 1 | 88 | 110 | 2 | 176 | 1073.6 |

| ***Floor*** | *L [mm]* | *Ø [mm]* | *volume [m³]* | *no. bars z* | *no. bars x* | *c/c [mm]* | no. Floors | *tot bars* | Tot length [m] |
|---|---|---|---|---|---|---|---|---|---|
| *tension bottom near slope* | 9020 | 20 | 0.0028 | 2 | 20 | 220 | 1 | 40 | 360.8 |
| *tension bottom rest (48000)* | 8830 | 12 | 0.0010 | 2 | 429 | 110 | 1 | 858 | 7576.14 |

| | | | | | | | | | |
|---|---|---|---|---|---|---|---|---|---|
| *tension bottom river lock head* | 8200 | 12 | 0.0009 | 3 | 101 | 110 | 1 | 303 | 2484.6 |
| *transv. bottom center near slope* | 9650 | 8 | 0.0005 | 136 | 1 | 130 | 1 | 136 | 1312.4 |
| *transverse bottom rest* | 10000 | 8 | 0.0005 | 126 | 4 | 130 | 1 | 504 | 5040 |
| *transv. Bottom river lock head middle* | 7700 | 8 | 0.0004 | 126 | 2 | 130 | 1 | 252 | 1940.4 |
| *transv. Bottom small lock head edges* | 5800 | 8 | 0.0003 | 40 | 2 | 130 | 1 | 80 | 464 |
| *compression top* | 9100 | 20 | 0.0029 | 2 | 233 | 220 | 1 | 466 | 4240.6 |
| *compression top river lock head* | 8500 | 20 | 0.0027 | 3 | 50 | 220 | 1 | 150 | 1275 |
| *compression top transverse* | 10000 | 10 | 0.0008 | 67 | 6 | 260 | 1 | 402 | 4020 |
| *compression top transv. Edge lock head* | 5920 | 10 | 0.0005 | 22 | 2 | 260 | 1 | 44 | 260.48 |
| *compression top transv. middle lock head* | 7100 | 10 | 0.0006 | 67 | 1 | 260 | 1 | 67 | 475.7 |
| ***U-bars, L bars and anchor bars*** | | | | | | | | | |
| *U-loops top 840x490x840* | 2125 | 12 | 0.0002 | 1 | 466 | 110 | 2 | 932 | 1980.5 |
| *U-loops top - anchors* | 10000 | 20 | 0.0031 | 2 | 5 | [-] | 2 | 20 | 200 |
| *U-loops top - anchors edge* | 7100 | 20 | 0.0022 | 2 | 1 | [-] | 2 | 4 | 28.4 |
| *U-loop floor 1490x684x1070* | 3150 | 20 | 0.0010 | 1 | 233 | 220 | 2 | 466 | 1467.9 |
| *L-bar bottom 1760x1090* | 2800 | 20 | 0.0009 | 1 | 233 | 220 | 2 | 466 | 1304.8 |
| *J-bar bottom-C 1570x474x300* | 2300 | 10 | 0.0002 | 1 | 466 | 110 | 2 | 932 | 2143.6 |
| *K25 anchor bottom* | 10000 | 25 | 0.0049 | 3 | 5 | [-] | 2 | 30 | 300 |
| *K25 anchor bottom edge* | 8600 | 25 | 0.0042 | 3 | 1 | [-] | 2 | 6 | 51.6 |
| *Anchor shear link to sloped wall* | 9500 | 20 | 0.0030 | 1 | 1 | [-] | 2 | 2 | 19 |

**Table 90: Reinforcement for the riverside lock head of the anchored chamber wall, NAP +4.5 m, t = 0.4 m**

| ***Shear reinforcement*** | ***L [mm]*** | ***Ø [mm]*** | ***volume [m]*** | ***no. bars horiz.*** | ***no bars y*** | ***c/c [mm]*** | ***no. Walls*** | ***tot bars*** | ***tot volume [m³]*** |
|---|---|---|---|---|---|---|---|---|---|
| *shear bottom 700x490* | 2675 | 12 | 0.0003 | 15 | 10 | 180 | 2 | 300 | 802.5 |
| ***Vertical bars (Mxx)*** | | | | | | | | | |
| *tension bottom inner, S* | 2600 | 20 | 0.0008 | 49 | 1 | 220 | 2 | 98 | 254.8 |
| *tension anchor to top inner, S* | 3250 | 16 | 0.0007 | 98 | 1 | 110 | 2 | 196 | 637 |
| *tens cent. (-Mxx), C* | 2300 | 16 | 0.0005 | 45 | 1 | 220 | 2 | 90 | 207 |
| *betw. bottom & anchor S* | 5300 | 10 | 0.0004 | 98 | 1 | 110 | 2 | 196 | 1038.8 |
| *from bottom to center, C* | 3600 | 10 | 0.0003 | 90 | 1 | 110 | 2 | 180 | 648 |
| *from center to top, C* | 4850 | 10 | 0.0004 | 90 | 1 | 110 | 2 | 180 | 873 |
| ***Horizontal bars (Myy)*** | | | | | | | | | |
| *tension anchor, S* | 5640 | 20 | 0.0018 | 2 | 9 | 210 | 2 | 36 | 203.04 |
| *from bottom to anchor & above anchor, S* | 5500 | 10 | 0.0004 | 2 | 70 | 110 | 2 | 280 | 1540 |
| *from bottom to top, C* | 5500 | 10 | 0.0004 | 2 | 88 | 110 | 2 | 352 | 1936 |
| ***U-bars, L bars and anchor bars*** | | | | | | | | | |
| *U-loops top 840x490x840* | 2125 | 12 | 0.0002 | 1 | 90 | 110 | 2 | 180 | 382.5 |
| *U-loops top - anchors* | 5640 | 20 | 0.0018 | 2 | 2 | [-] | 2 | 8 | 45.12 |

| | | | | | | | | | |
|---|---|---|---|---|---|---|---|---|---|
| *U-loop floor 1490x684x1070* | 3150 | 20 | 0.0010 | 1 | 50 | 220 | 2 | 100 | 315 |
| *L-bar bottom 1760x1090* | 2800 | 20 | 0.0009 | 1 | 50 | 220 | 2 | 100 | 280 |
| *J-bar bottom-C 1570x474x300* | 2300 | 10 | 0.0002 | 1 | 90 | 110 | 2 | 180 | 414 |
| *K25 anchor bottom* | 5880 | 25 | 0.0029 | 3 | 2 | [-] | 2 | 12 | 70.56 |